PEAK STRESS OF COMPOSITE MULTIPLE-HOLE LAMINATES WITH AND WITHOUT PATCH

by

SAKTHIVEL SELVARAJ

Presented to the Faculty of the Graduate School of

The University of Texas at Arlington in Partial Fulfillment

of the Requirements

for the Degree of

MASTER OF SCIENCE IN AEROSPACE ENGINEERING

THE UNIVERSITY OF TEXAS AT ARLINGTON

MAY 2010

ACKNOWLEDGEMENTS

I would like to express my gratitude towards Dr. Wen Chan for being my research advisor and guiding me throughout my MS degree. He has been my strong support towards my research work. He has always inspired me to provide perfect, accurate and efficient work. I would take this opportunity to thank Dr. Kent Lawrence and Dr. B.P. Wang for assisting me and being my committee members. I am very grateful to E. Dan-Jumbo for giving me the opportunity to do a project for their esteemed company-BOEING. I also thank Dr. Chan's former students, Manishkumar Kheradiya and Puneet Saggar for helping me in my research.

March 31,2010

ABSTRACT

PEAK STRESS OF COMPOSITE MULTIPLE-HOLE LAMINATES

WITH AND WITHOUT PATCH

Sakthivel Selvaraj, M.S.

The University of Texas at Arlington, 2010

Supervising Professor: Wen S. Chan

In repairing of composite structures, the damage in the composite laminate is usually removed in the form of circular cutouts. Then a patch laminate is adhesively bonded to the damaged composite laminate. The primary objective of this study is to investigate the high stress of the damaged laminate with different hole patterns and the effect of having single and double patches with various configurations on these hole different patterns.

Five different hole patterns of the parent laminate with $[\pm 45^0/0^0{}_3/90^0]_s$ graphite/epoxy and five different patch configurations with $[\pm 45^0/0^0]_s$ graphite/epoxy were used in this study. An ANSYS 3D finite element model was developed to study the peak stress of each ply in the parent and patch laminates. Experiments were conducted on the specimens without patch.

This thesis presents a detailed finite element study on various hole arrangements on the parent laminate and effect of different patch configurations on these hole arrangements. It will exhibit the peak stress concentrations for all cases and draw important conclusions by comparing the results of no patch, single patch and double patch. Among the different hole pattern laminates without patch, the peak stress of 0^0 ply is obtained in the following order TBH (Top & bottom hole)>SA (square array)>SSH (side by side

hole)>DA (Diamond array)> FH (five hole). This sequence is in agreement with the test indication where TBH has the highest strength and FH has the least strength. Among the different patch configuration, the circular patch bonded on the both sides of the laminate exhibited the lowest peak stress. This study contributes to a better understanding in selecting patch configurations or geometries for both composite bonded repairs in order to restore the laminate structural integrity.

TABLE OF CONTENTS

ACKNOWLEGEMENTS……iii

ABSTRACT……..iv

LIST OF FIGURES……..x

LIST OF TABLES……..xviii

Chapter Page

1.INTRODUCTION..... 1

1.1 Background..... 1

1.2 Objectives of this study..... 3

1.3 General Outline..... 4

2.FINITE ELEMENT MODEL..... 5

2.1 Geometric Description..... 5

2.2 Material used..... 7

2.3 Element Type used..... 8

2.4 Modeling and Meshing in ANSYS 11.0..... 8

2.5 Boundary Conditions..... 14

2.6 Loading condition..... 15

3.PEAK STRESS OF COMPOSITE LAMINATE WITH MULTIPLE HOLES..... 16

3.1 General discussion on stress profiles..... 16

3.2 Results of 0^0 ply 18

3.2.1 In-Plane stresses σ1. σ2, τ12 for 0^0 ply 18

3.2.2 Inter-laminar stresses σ_1, τ_{13}, τ_{23} for 0^0 ply 24

3.6 Results of $\pm 45^0$ plies 25

3.3.1 In-plane stresses σ_1. σ_2, τ_{12} for $\pm 45^0$ ply 25

3.3.2 Inter-laminar stresses σ_1, τ_{13}, τ_{23} for $\pm 45^0$ plies 32

4.EXPERIMENTAL STUDY ON STRENGTH OF COMPOSITE LAMINATE WITH MULTIPLE HOLES 34

4.1 Description of Test coupon 34

4.2 Experimental setup 35

4.3 Test procedure 36

4.4 Test Results 37

4.5 Damage observation 40

4.5.1 Comparison of failures for SH & TBH hole laminates. 41

4.5.2 Comparison of failures for SSH & SA hole laminates. 42

4.5.3 Comparison of failures for SA & DA hole laminates. 42

5.EFFECTS OF SINGLE PATCH CONFIGURATIONS IN COMPOSITE BONDED REPAIR 44

5.1 Cases investigated 44

5.2 General discussion on stress increase due to patch 44

5.4 Effect of patch configurations with SH pattern on parent laminate 45

5.4.1 In-plane stresses σ_1. σ_2, τ_{12} for bottom 0^0 ply 45

5.4.2 In-plane stresses σ_1. σ_2, τ_{12} for bottom $+45^0$ & -45^0 ply 49

5.5.3 Interlaminar stresses σ_3, τ_{23} at the interfaces 51

5.5 Effect of patch configurations with TBH pattern on parent laminate 54

5.5.1 In-plane stresses σ_1. σ_2, τ_{12} for bottom 0^0 ply 54

5.5.2 In-plane stresses σ_1. σ_2, τ_{12} for bottom $+45^0$& -45^0ply 58

5.5.3 Interlaminar stresses σ_3, τ_{23} at the interfaces 60

5.6 Effect of patch configurations with SSH pattern on parent laminate 63

5.6.1 In-plane stresses σ_1. σ_2, τ_{12} for bottom 0^0 ply 63

5.6.2 In-plane stresses σ_1. σ_2, τ_{12} for bottom $+45^0$& -45^0ply 67

5.6.3 Interlaminar stresses σ_3, τ_{23} at the interfaces 69

5.7 Effect of patch configurations with SA pattern on parent laminate 72

5.7.1 In-plane stresses σ_1. σ_2, τ_{12} for bottom 0^0 ply 72

5.7.2 In-plane stresses σ_1. σ_2, τ_{12} for bottom $+45^0$& -45^0ply 76

5.7.3 Interlaminar stresses σ_3, τ_{23} at the interfaces 78

5.8 Effect of patch configurations with DA pattern on parent laminate 81

5.8.1 In-plane stresses σ_1. σ_2, τ_{12} for bottom 0^0 ply 81

5.8.2 In-plane stresses σ_1. σ_2, τ_{12} for bottom $+45^0$& -45^0ply 85

5.8.3 Interlaminar stresses σ_3, τ_{23} at the interfaces 87

5.9 Effect of patch configurations with FH pattern on parent laminate 90

5.9.1 In-plane stresses σ_1. σ_2, τ_{12} for bottom 0^0 ply 90

5.9.2 In-plane stresses σ_1. σ_2, τ_{12} for bottom $+45^0$& -45^0ply 94

5.9.3 Interlaminar stresses σ_3, τ_{23} at the interfaces 96

5.11 Result Summary of Single Patch laminate 99

6.EFFECTS OF DOUBLE PATCH CONFIGURATIONS IN COMPOSITE BONDED REPAIR 100

6.1 Cases investigated 100

6.2 Effect of patch configurations with SH pattern on parent laminate 100

6.2.1 In-plane stresses σ_1. σ_2, τ_{12} for bottom 0^0 ply 100

6.2.2 In-plane stresses σ_1. σ_2, τ_{12} for bottom $+45^0$& -45^0ply 104

6.2.3 Interlaminar stresses σ_3, τ_{23} at the interfaces 106

6.3 Effect of patch configurations with TBH pattern on parent laminate 109
6.3.1 In-plane stresses σ_1. σ_2, τ_{12} for bottom 0^0 ply 109
6.3.2 In-plane stresses σ_1. σ_2, τ_{12} for bottom $+45^0$& -45^0ply 113
6.3.3 Interlaminar stresses σ_3, τ_{23} at the interfaces 115
6.4 Effect of patch configurations with SSH pattern on parent laminate 118
6.4.1 In-plane stresses σ_1. σ_2, τ_{12} for bottom 0^0 ply 118
6.4.2 In-plane stresses σ_1. σ_2, τ_{12} for bottom $+45^0$& -45^0ply 122
6.4.3 Interlaminar stresses σ_3, τ_{23} at the interfaces 124
6.5 Effect of patch configurations with SA pattern on parent laminate 127
6.5.1 In-plane stresses σ_1. σ_2, τ_{12} for bottom 0^0 ply 127
6.5.2 In-plane stresses σ_1. σ_2, τ_{12} for bottom $+45^0$& -45^0ply 131
6.5.3 Interlaminar stresses σ_3, τ_{23} at the interfaces 133
6.6 Effect of patch configurations with DA pattern on parent laminate 136
6.6.1 In-plane stresses σ_1. σ_2, τ_{12} for bottom 0^0 ply 136
6.6.2 In-plane stresses σ_1. σ_2, τ_{12} for bottom $+45^0$& -45^0ply 140
6.6.3 Interlaminar stresses σ_3, τ_{23} at the interfaces 142
6.7 Effect of patch configurations with FH pattern on parent laminate 145
6.7.1 In-plane stresses σ_1. σ_2, τ_{12} for bottom 0^0 ply 145
6.7.2 In-plane stresses σ_1. σ_2, τ_{12} for bottom $+45^0$& -45^0ply 149
6.7.3 Interlaminar stresses σ_3, τ_{23} at the interfaces 151
6.8 Result summary for double patch laminate 154
7.CONCLUSION 157
REFERENCES 159
BIOGRAPHICAL INFORMATION 160

LIST OF FIGURES

Figure Page

2.1 Hole pattern in parent laminates
(a) Single hole (SH) (b) Top & Bottom hole (TBH)(c) Side-by-side hole (SSH)
(d) Square array (SA) (e) Diamond array (DA) (f) Five Hole (FH) 6

2.2 Dimension of the Patch configurations
(a) Square patch (b) Hexagonal Patch (c) Octagonal Patch
(d) Circular patch (e) Elliptical Patch 7

2.3 Areas for different hole patterns grouped as parent and
patch laminate areas for 2D meshing (a) SH (b) TBH (c) SSH (d) SA (e) DA (f) FH 9

2.4 Finer mesh in the hole and gradation of finer mesh near the
hole to coarse mesh away from it. 10

2.7 Close view of the parent laminate with different hole patterns
(a) SH (b) TBH (c) SSH (d) SA (e) DA (f) FH 12

2.8 Mapped mesh of different hole patterns with square patch
(a) SH (b) TBH (c) SSH (d) SA (e) DA (f) FH 13

2.9 Mapped mesh of different patches for single hole pattern
(a) Square patch (b) Hexagonal Patch (c) Octagonal Patch (d) Circular patch (e) Elliptical Patch 14

2.10 Exploded view of the boundary conditions 15

3.1 Force flux lines for a 0^0 ply composite laminate 16

3.2 Force flux lines for a 0^0 ply composite laminate with single hole 17

3.3 Closer view of the stress contour on the periphery of the hole for 0^0 ply 17

3.4 Comparison of Normalized maximum In-plane stress for different hole patterns 19

3.5 Peak stress at Points A&B 19

3.6 Holes in TBH, SSH & SA has same stress concentrations 21

3.7 Different stress concentrations in holes within DA & FH pattern 22

3.8 Comparison of Stress contours for 0^0 ply in different configurations
(a) SH (b) TBH (c) SSH (d) SA (e) DA (f) FH 23

3.9 Comparison of Interlaminar stresses for different hole patterns for 0^0 ply 24

3.10 peak values of σ_3, τ_{13} and τ_{23} at point A&B 25

3.11 Comparison of in-plane stresses for different configuration for 45^0 ply 26

3.12 Comparison of in-plane stresses for different configuration for -45^0 ply 27

3.13 Location of maximum stress for 45^0 ply 28

3.14 Close view for different hole patterns showing peak stress locations for 45^0 ply. 29

3.15 Stress contour comparison of different configuration for 45^0 ply
(a) SH (b) TBH (c) SSH (d) SA (e) DA (f) FH 30

3.16 Stress contour comparison of different configuration for -45^0 ply
(a) SH (b) TBH (c) SSH (d) SA (e) DA (f) FH 31

3.17 Comparison of Inter-laminar stresses for different hole patterns for 45^0 ply 32

3.18 Comparison of Inter-laminar stresses for different hole patterns for -45^0 ply 33

4.1 Test coupons with different hole patterns (a) SH (b) TBH (c) SSH (d) SA (e) DA 34

4.2 MTS machine used for the test 36

4.3 Strength of different hole pattern 38

4.4 Linear stress-strain diagrams for set1 samples 39

4.5 Linear stress-strain diagrams for set2 samples 39

4.6 Linear stress-strain diagrams for set 3 samples 40

4.7 Edge delamination 41

4.8 Failure comparisons of laminates with SH & TBH pattern 41

4.9 Failure comparisons of laminates with SSH & SA pattern 42

4.10 Failure comparisons of laminates with SA & DA pattern 43

5.1 Eccentricity of the Patch laminate. 45

5.2 Bending due to additional moment 45

5.3 Comparison of in-plane stresses (bottom 0^0 layer) for
SH pattern with different patch configurations 46

5.4 Stress contour for 0^0 layer with different patch configuration for SH pattern
(a) no patch (b) square (c) hexagonal (d) octagonal (e) circular (f) elliptical 47

5.5 Stress contour for 45^0 layer with different patch configuration for SH pattern
at parent and patch interface (a) no patch (b) square (c) hexagonal
(d) octagonal (e) circular (f) elliptical 48

5.6 Comparison of in-plane stresses (bottom 45^0 layer) for SH pattern
with different patch configurations 50

5.7 Comparison of in-plane stresses (bottom -45^0 layer) for SH pattern with different patch configurations 50

5.8 Location of stress plot along width of the laminate 51

5.9 σ_3 stress at parent laminate and adhesive interface for all patch configurations 52

5.10 τ_{23} stress at parent laminate and adhesive interface for all patch configurations 52

5.11 σ_3 stress at patch laminate and adhesive interface for all patch configurations 53

5.12 τ_{23} stress at patch laminate and adhesive interface for all patch configurations 53

5.13 Comparison of in-plane stresses (bottom 0^0 layer) for TBH pattern with different patch configurations 55

5.14 Stress contour for 0^0 layer with different patch configuration for TBH pattern (a) no patch (b) square (c) hexagonal (d) octagonal (e) circular (f) elliptical 56

5.15 Stress contour for 45^0 layer with different patch configuration for TBH pattern at parent and patch interface (a) no patch (b) square (c) hexagonal (d) octagonal (e) circular (f) elliptical 57

5.16 Comparison of in-plane stresses (bottom 45^0 layer) for TBH pattern with different patch configurations 59

5.17 Comparison of in-plane stresses (bottom -45^0 layer) for TBH pattern with different patch configurations 59

5.18 Location of stress plot along width of the laminate 60

5.19 σ_3 stress at parent laminate and adhesive interface for all patch configurations 61

5.20 τ_{23} stress at parent laminate and adhesive interface for all patch configurations 61

5.21 σ_3 stress at patch laminate and adhesive interface for all patch configurations 62

5.22 τ_{23} stress at patch laminate and adhesive interface for all patch configurations 62

5.23 Comparison of in-plane stresses (bottom 0^0 layer) for SSH pattern with different patch configurations 64

5.24 Stress contour for 0^0 layer with different patch configuration for SSH pattern (a) no patch (b) square (c) hexagonal (d) octagonal (e) circular (f) elliptical 65

5.25 Stress contour for 45^0 layer with different patch configuration for SSH pattern at parent and patch interface (a) no patch (b) square (c) hexagonal (d) octagonal (e) circular (f) elliptical 66

5.26 Comparison of in-plane stresses (bottom 45^0 layer) for SSH pattern with different patch configurations 68

5.27 Comparison of in-plane stresses (bottom -45^0 layer) for SSH pattern with different patch configurations 68

5.28 Location of stress plot along width of the laminate 69

5.29 σ_3 stress at parent laminate and adhesive interface for all patch configurations 70

5.30 τ_{23} stress at parent laminate and adhesive interface for all patch configurations 70

5.31 σ_3 stress at patch laminate and adhesive interface for all patch configurations 71

5.32 τ_{23} stress at patch laminate and adhesive interface for all patch configurations 71

5.33 Comparison of in-plane stresses (bottom 0^0 layer) for SA pattern with different patchconfigurations 73

5.34 Stress contour for 0^0 layer with different patch configuration for SA pattern (a) no patch (b) square (c) hexagonal (d) octagonal (e) circular (f) elliptical 74

5.35 Stress contour for 45^0 layer with different patch configuration for SSH pattern at parent and patch interface (a) no patch (b) square (c) hexagonal (d) octagonal (e) circular (f) elliptical 75

5.36 Comparison of in-plane stresses (bottom 45^0 layer) for SA pattern with different patch configurations 77

5.37 Comparison of in-plane stresses (bottom -45^0 layer) for SA pattern with different patch configurations 77

5.38 Location of stress plot along width of the laminate 78

5.39 σ_3 stress at parent laminate and adhesive interface for all patch configurations 79

5.40 τ_{23} stress at parent laminate and adhesive interface for all patch configurations 79

5.41 σ_3 stress at patch laminate and adhesive interface for all patch configurations 80

5.42 τ_{23} stress at patch laminate and adhesive interface for all patch configurations 80

5.43 Comparison of in-plane stresses (bottom 0^0 layer) for DA pattern with different patch configurations 82

5.44 Stress contour for 0^0 layer with different patch configuration for DA pattern (a) no patch (b) square (c) hexagonal (d) octagonal (e) circular (f) elliptical 83

5.45 Stress contour for 45^0 layer with different patch configuration for SSH pattern at parent and patch interface (a) no patch (b) square (c) hexagonal (d) octagonal (e) circular (f) elliptical 84

5.46 Comparison of in-plane stresses (bottom 45^0 layer) for DA pattern with different patch configurations 86

5.47 Comparison of in-plane stresses (bottom -45^0 layer) for DA pattern with different patch configurations 86

5.48 Location of stress plot along width of the laminate 87

5.49 σ_3 stress at parent laminate and adhesive interface for all patch configurations 88

5.50 τ_{23} stress at parent laminate and adhesive interface for all patch configurations 88

5.51 σ_3 stress at patch laminate and adhesive interface for all patch configurations 89

5.52 τ_{23} stress at patch laminate and adhesive interface for all patch configurations 89

5.53 Comparison of in-plane stresses (bottom 0^0 layer) for FH pattern
with different patch configurations 91

5.54 Stress contour for 0^0 layer with different patch configuration for FH pattern
(a) no patch (b) square (c) hexagonal (d) octagonal (e) circular (f) elliptical 92

5.55 Stress contour for 45^0 layer with different patch configuration for SSH pattern
at parent and patch interface (a) no patch (b) square (c) hexagonal
(d) octagonal (e) circular (f) elliptical 93

5.56 Comparison of in-plane stresses (bottom 45^0 layer) for FH pattern
with different patch configurations 95

5.57 Comparison of in-plane stresses (bottom -45^0 layer) for FH pattern
with different patch configurations 95

5.58 Location of stress plot along width of the laminate 96

5.59 σ_3 stress at parent laminate and adhesive interface for all patch configurations 97

5.60 τ_{23} stress at parent laminate and adhesive interface for all patch configurations 97

5.61 σ_3 stress at patch laminate and adhesive interface for all patch configurations 98

5.62 τ_{23} stress at patch laminate and adhesive interface for all patch configurations 98

5.63 Comparison of peak stress for various configurations with different hole patterns 99

6.1 Comparison of in-plane stresses (bottom 0^0 layer) for SH pattern
with different patch configurations 101

6.2 Stress contour for 0^0 layer with different patch configuration for SH pattern
(a) no patch (b) square (c) hexagonal (d) octagonal (e) circular (f) elliptical 102

6.3 Stress contour for 45^0 layer with different patch configuration for SH pattern
at parent and patch interface (a) no patch (b) square (c) hexagonal
(d) octagonal (e) circular (f) elliptical 103

6.4 Comparison of in-plane stresses (bottom 45^0 layer) for SH pattern
with different patch configurations 105

6.5 Comparison of in-plane stresses (bottom -45^0 layer) for SH pattern
with different patch configurations 105

6.6 Location of stress plot along width of the laminate 106

6.7 σ_3 stress at parent laminate and adhesive interface for all patch configurations 107

6.8 τ_{23} stress at parent laminate and adhesive interface for all patch configurations 107

6.9 σ_3 stress at patch laminate and adhesive interface for all patch configurations 108

6.10 τ_{23} stress at patch laminate and adhesive interface for all patch configurations 108

6.11 Comparison of in-plane stresses (bottom 0^0 layer) for TBH pattern with different patch configurations 110

6.12 Stress contour for 0^0 layer with different patch configuration for TBH pattern (a) no patch (b) square (c) hexagonal (d) octagonal (e) circular (f) elliptical 111

6.13 Stress contour for 45^0 layer with different patch configuration for TBH pattern at parent and patch interface (a) no patch (b) square (c) hexagonal (d) octagonal (e) circular (f) elliptical 112

6.14 Comparison of in-plane stresses (bottom 45^0 layer) for TBH pattern with different patch configurations 114

6.15 Comparison of in-plane stresses (bottom -45^0 layer) for TBH pattern with different patch configurations 114

6.16 Location of stress plot along width of the laminate 115

6.17 σ_3 stress at parent laminate and adhesive interface for all patch configurations 116

6.18 τ_{23} stress at parent laminate and adhesive interface for all patch configurations 116

6.19 σ_3 stress at patch laminate and adhesive interface for all patch configurations 117

6.20 τ_{23} stress at patch laminate and adhesive interface for all patch configurations 117

6.21 Comparison of in-plane stresses (bottom 0^0 layer) for SSH pattern with different patch configurations 119

6.22 Stress contour for 0^0 layer with different patch configuration for SSH pattern (a) no patch (b) square (c) hexagonal (d) octagonal (e) circular (f) elliptical 120

6.23 Stress contour for 45^0 layer with different patch configuration for SSH pattern at parent and patch interface (a) no patch (b) square (c) hexagonal (d) octagonal (e) circular (f) elliptical 121

6.24 Comparison of in-plane stresses (bottom 45^0 layer) for SSH pattern with different patch configurations 123

6.25 Comparison of in-plane stresses (bottom -45^0 layer) for SSH pattern with different patch configurations 123

6.26 Location of stress plot along width of the laminate 124

6.27 σ_3 stress at parent laminate and adhesive interface for all patch configurations 125

6.28 τ_{23} stress at parent laminate and adhesive interface for all patch configurations 125

6.29 σ_3 stress at patch laminate and adhesive interface for all patch configurations 126

6.30 τ_{23} stress at patch laminate and adhesive interface for all patch configurations 126

6.31 Comparison of in-plane stresses (bottom 0^0 layer) for SA pattern with different patch configurations 128

6.32 Stress contour for 0^0 layer with different patch configuration for SA pattern (a) no patch (b) square (c) hexagonal (d) octagonal (e) circular (f) elliptical 129

6.33 Stress contour for 45^0 layer with different patch configuration for SA pattern at parent and patch interface (a) no patch (b) square (c) hexagonal (d) octagonal (e) circular (f) elliptical 130

6.34 Comparison of in-plane stresses (bottom 45^0 layer) for SA pattern with different patch configurations 132

6.35 Comparison of in-plane stresses (bottom -45^0 layer) for SA pattern with different patch configurations 132

6.36 Location of stress plot along width of the laminate 133

6.37 σ_3 stresses at parent laminate and adhesive interface for all patch configurations 134

6.38 τ_{23} stresses at parent laminate and adhesive interface for all patch configurations 134

6.39 σ_3 stresses at patch laminate and adhesive interface for all patch configurations 135

6.40 τ_{23} stresses at patch laminate and adhesive interface for all patch configurations 135

6.41 Comparison of in-plane stresses (bottom 0^0 layer) for DA pattern with different patch configurations 137

6.42 Stress contour for 0^0 layer with different patch configuration for DA pattern (a) No patch (b) Square (c) Hexagonal (d) Octagonal (e) Circular (f) Elliptical 138

6.43 Stress contour for 45^0 layer with different patch configuration for DA pattern at parent and patch interface (a) No patch (b) Square (c) Hexagonal (d) Octagonal (e) Circular (f) Elliptical 139

6.44 Comparison of in-plane stresses (bottom 45^0 layer) for DA pattern with different patch configurations 141

6.45 Comparison of in-plane stresses (bottom -45^0 layer) for DA pattern with different patch configurations 141

6.46 Location of stress plot along width of the laminate 142

6.47 σ_3 stress at parent laminate and adhesive interface for all patch configurations 143

6.48 τ_{23} stress at parent laminate and adhesive interface for all patch configurations 143

6.49 σ_3 stress at patch laminate and adhesive interface for all patch configurations 144

6.50 τ_{23} stress at patch laminate and adhesive interface for all patch configurations 144

6.51 Comparison of in-plane stresses (bottom 0^0 layer) for FH pattern with different patch configurations 146

6.52 Stress contour for 0^0 layer with different patch configuration for FH pattern (a) No patch (b) Square (c) Hexagonal (d) Octagonal (e) Circular (f) Elliptical 147

6.53 Stress contour for 45^0 layer with different patch configuration for DA pattern at parent and patch interface (a) No patch (b) Square (c) Hexagonal (d) Octagonal (e) Circular (f) Elliptical 148

6.54 Comparison of in-plane stresses (bottom 45^0 layer) for FH pattern with different patch configurations 150

6.55 Comparison of in-plane stresses (bottom -45^0 layer) for FH pattern with different patch configurations 150

6.56 Location of stress plot along width of the laminate 151

6.57 σ_3 stress at parent laminate and adhesive interface for all patch configurations 152

6.58 τ_{23} stress at parent laminate and adhesive interface for all patch configurations 152

6.59 σ_3 stress at patch laminate and adhesive interface for all patch configurations 153

6.60 τ_{23} stress at patch laminate and adhesive interface for all patch configurations 153

6.61 Comparison of peak stress for various configurations with different hole patterns 154

6.62 Comparison of peak stress for various configurations between single and double patch 155

LIST OF TABLES

Table Page

2.1 Location of holes 6

2.2 List of local coordinates in parent and patch laminates. 10

2.3 Total number of nodes and elements for different cases 12

2.4 Illustration of laminas lumped in finite element model. 13

2.5 Number of elements in FE model for all patch configurations with different hole patterns 14

3.1 Normalized maximum In-plane stresses for 0^0 ply 18

3.2 Normalized maximum interlaminar stresses for 0^0 ply 24

3.3 Normalized Maximum stress for 45^0 ply 26

3.5 Inter-laminar stresses in $+45^0$ for ply different hole pattern 32

3.6 Inter-laminar stresses in -45^0 for plies different hole patterns 33

4.1 Strength of different hole patterns 37

5.1 Normalized maximum stress for SH (0^0 ply -bottom) with different patch configuration 45

5.2 Normalized maximum in-plane stress for SH (45^0 ply -bottom) with different patch configurations 49

5.3 Normalized maximum in-plane stress for SH (-45^0 ply -bottom) with different patch configurations 49

5.4 Normalized maximum stress for TBH (0^0 ply -bottom) with different patch configuration 54

5.5 Normalized maximum in-plane stress for TBH (45^0 ply -bottom) with different patch configurations 58

5.6 Normalized maximum in-plane stress for TBH (-45^0 ply -bottom) with different patch configurations 58

5.7 Normalized maximum stress for SSH (0^0 ply -bottom) with different patch configuration 63

5.9 Normalized maximum in-plane stress for SSH (-45^0 ply -bottom) with different patch configurations 67

5.10 Normalized maximum stress for SA (0^0 ply -bottom) with different patch configuration 72

5.11 Normalized maximum in-plane stress for SA (45^0 ply -bottom) with different patch configurations 76

5.12 Normalized maximum in-plane stress for SA (-45^0 ply -bottom) with different patch configurations 76

5.13 Normalized maximum stress for DA (0^0 ply -bottom) with different patch configuration 81

5.14 Normalized maximum in-plane stress for DA (45^0 ply -bottom) with different patch configurations 85

5.15 Normalized maximum in-plane stress for DA (-45^0 ply -bottom) with different patch configurations 85

5.16 Normalized maximum stress for FH (0^0 ply -bottom) with different patch configuration 90

5.17 Normalized maximum in-plane stress for FH (45^0 ply -bottom) with different patch configurations 94

5.18 Normalized maximum in-plane stress for FH (-45^0 ply -bottom) with different patch configurations 94

6.1 Normalized maximum stress for SH (0^0 ply -bottom) with different patch configuration 101

6.2 Normalized maximum in-plane stress for SH (45^0 ply -bottom) with different patch configurations 104

6.3 Normalized maximum in-plane stress for SH (-45^0 ply -bottom) with different patch configurations 104

6.4 Normalized maximum stress for TBH (0^0 ply -bottom) with different patch configuration 109

6.5 Normalized maximum in-plane stress for TBH (45^0 ply -bottom) with different patch configurations 113

6.6 Normalized maximum in-plane stress for TBH (-45^0 ply -bottom) with different patch configurations 113

6.7 Normalized maximum stress for SSH (0^0 ply -bottom) with different patch configuration 118

6.8 Normalized maximum in-plane stress for SSH (45^0 ply -bottom) with different patch configurations 122

6.9 Normalized maximum in-plane stress for SSH (-45^0 ply -bottom) with different patch configurations 122

6.10 Normalized maximum stress for SA (0^0 ply -bottom) with different patch configuration 127

6.11 Normalized maximum in-plane stress for SA (45^0 ply -bottom) with different patch configurations 131

6.12 Normalized maximum in-plane stress for SA (-45^0 ply -bottom) with different patch configurations 131

6.13 Normalized maximum stress for DA (0^0 ply -bottom) with different patch configuration..... 136

6.14 Normalized maximum in-plane stress for DA (45^0 ply -bottom)
with different patch configurations 140

6.15 Normalized maximum in-plane stress for DA (-45^0 ply -bottom)
with different patch configurations 140

6.16 Normalized maximum stress for FH (0^0 ply -bottom) with different patch configuration..... 145

6.17 Normalized maximum in-plane stress for FH (45^0 ply -bottom)
with different patch configurations 149

6.18 Normalized maximum in-plane stress for FH (-45^0 ply -bottom)
with different patch configurations 149

CHAPTER 1

INTRODUCTION

1.1 Background

In recent decades the uses of composite materials in various industries like aerospace, automotive, marine, sports, railways has increased tremendously. Composite materials has numerous advantages over metals like high stiffness to weight ratio, corrosion resistance, good fatigue resistance and can be tailored to meet any property requirement. As damage is inevitable for any structure, composite structures are prone to damages like delamination, debonding, impact damage and internal crushing etc. Therefore it is important to improve the performance of the structure by making it maintainable, repairable and thereby increasing the life of the structure.

The damages in the composite materials are caused by abrasion, scratches, gouges, dents, lightening strike, water absorption, debris, manufacturing defect etc. The extent of damage decides whether the composite part can be repaired or has to be replaced. It is not always feasible to replace the complete part because of constraints like time, cost, availability of raw materials to manufacture the part etc. Hence, repairing the composite part is the most feasible solution.

The composite repair should be performed to ensure the structural integrity and repair effectiveness. There are various repair options available like cosmetic repairs, interim repairs and structural repairs. Cosmetic repairs are mainly protecting or decorative repairs when the damage does not affect the structural integrity. Interim repairs are done for small damages that threaten to grow big if unrepaired. Structural repairs are those which affect the structural integrity. Structural repairs are classified as patch repair, scarf repair and step sanded repair.

In patch repair the damage in the laminate is removed in the form of circular cutouts and patch

laminate is adhesively bonded to the damaged structure. The advantage of this repair is, its quick and simple to do and minimum preparation. The disadvantages are thickness of the structure increases and careful preparation of the surface is required for good adhesion. The patch repair is shown in Figure 1.1

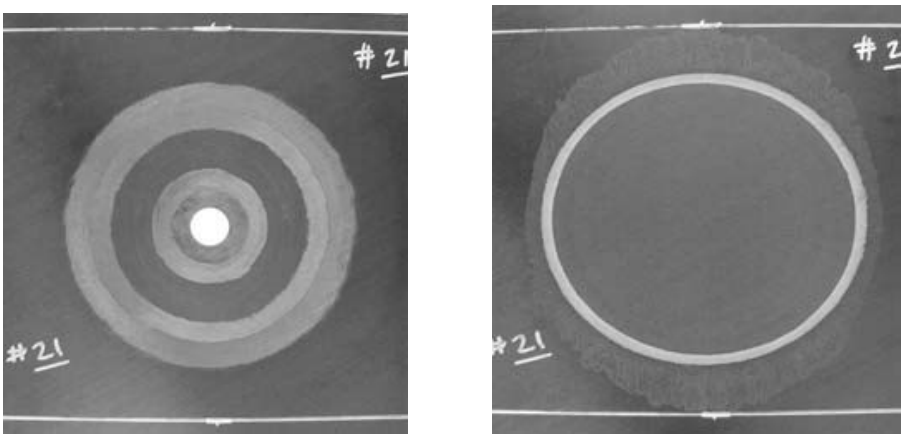

(a) (b)

Figure 1.1 Patch repair (a) Damaged structure (b) Repair patch applied on the damaged structure

The repair may increase the stiffness of the structure there by drawing much load on to the damaged area or can decrease the stiffness of the structure increasing the load on to the structure. Therefore it is important to study the strength of the repaired structure which gives a good guideline to composite repair design.

The circular cutouts created due to removal of damaged material on the composite structure causes stress concentrations at the edge of the hole which is the initiation for structure failure. Stress concentration is a major factor considered in any structural design. The analytical expression for stress concentrations on isotropic materials is well defined but not for composite laminates. Usually multiple holes are created during repair process. The strength determination for laminates with multiple holes has not been studied extremely before. The shape of the patch can also affect the stress distribution on the damaged laminate which is also an important study to be made in larger perspective. As no analytical solutions are available for this problem, finite element serves as an excellent tool in determining the stress concentrations of the composite laminates and understand the effect of patches on the damaged composite laminate. Additionally, 3D modeling in composite provides interlaminar stress distribution which

helps us determine the effectiveness of the bonding between patch and parent laminates.

Tomblin, et.al [1] published a report on the 'Bonded repair of aircraft composite sandwich structures' which gives us a basic understanding on the composite repair procedure. A detailed repair procedure of composite laminates is discussed by Reis [2] .The various types of repair process and their procedures are given by Hexcel Composites, Duxford [3].

In study of stress concentration, Lekhniskii [4] in 1968 used anisotropic elasticity with complex variable method to give close from solution to compute stress distributions around a circular hole in an infinite anisotropic plate. Fan and Wu [5] employed the faber series expansion to obtain the stress concentration factor for an infinite sized laminate with multiple holes.

Ochoa and Reddy [6] used finite element method to determine the stress concentration factor in composite laminates having three holes placed in-line with a tensile load. Xu et.al [7] studied the strength prediction of composite laminate with multiple elliptical holes. Neelkantan et.al [8] obtained the stress distribution around multiple circular loaded holes in a stiffener reinforced laminate. Later, Vendhagiri and Chan [9] investigated the stress distribution around the hole in composite bonded and bolted joints. Recently, Kheradiya [10] studied the effect of the edge distance, hole size and hole spacing on stress concentrations of composite laminate with multiple holes.

1.2 Objectives of this study

The primary objective of the study is to investigate the maximum stress of the composite laminate with multiple hole patterns and effect of different patch configurations on these hole patterns. There are six different hole patterns and five different patch configurations are considered for the study. Also the effect of having single and double patch on the parent laminate is studied. Specifically, stress concentrations for all the cases i.e. no patch, single patch and double patch are recorded and compared. The interlaminar stress distribution between patch and the parent laminates. It is the intent of this study to provide a good guideline for composite patch repair.

1.3 General Outline

Chapter 2 describes the geometry of the different hole patterns on the parent laminate and different configurations of the patch. The finite element modeling of the parent laminate and creating single and double patch, respectively on the parent laminate with different hole patterns and different patch configurations are discussed.

Chapter 3 gives the stress distribution of the parent laminate with multiple hole patterns. The stress concentrations for different hole patterns for 0^0,45^0, -45^0 are tabulated and compared. The interlaminar stresses are also shown.

An experimental study of the repaired laminates with no patch is attempted in this study. The experimental procedure, test results and inferences of the test are discussed in Chapter 4.

Chapter 5 & Chapter 6 tabulate and describe the results of maximum stress that are obtained for single and double patch on the parent laminate with different hole patterns and different patch configurations.

Conclusion of the study is drawn in Chapter 7.

CHAPTER 2

FINITE ELEMENT MODEL

The finite element model was developed to study the effect of different patch configurations on single and multiple hole patterns. The 3D Finite element laminated composite model is developed using ANSYS 11.0. This chapter describes about the details of finite element modeling. This includes, the geometry description, element type used, material used, modeling and meshing, load application and boundary conditions.

2.1 Geometric Description

The dimensions of the parent laminate are 2” width and 5” length. All the holes have identical size with a diameter of 0.25 in. The location of the hole center is listed in Table 2.1

The parent laminate has the following hole patterns shown in Figure 2.1 as follows,

1. Single Hole (SH).

2. Two holes - in line with the load (TBH).

3. Two holes - transverse to the load (SSH).

4. Four holes-square pattern (SA).

5. Four holes- diamond pattern (DA).

6. Five hole pattern (FH).

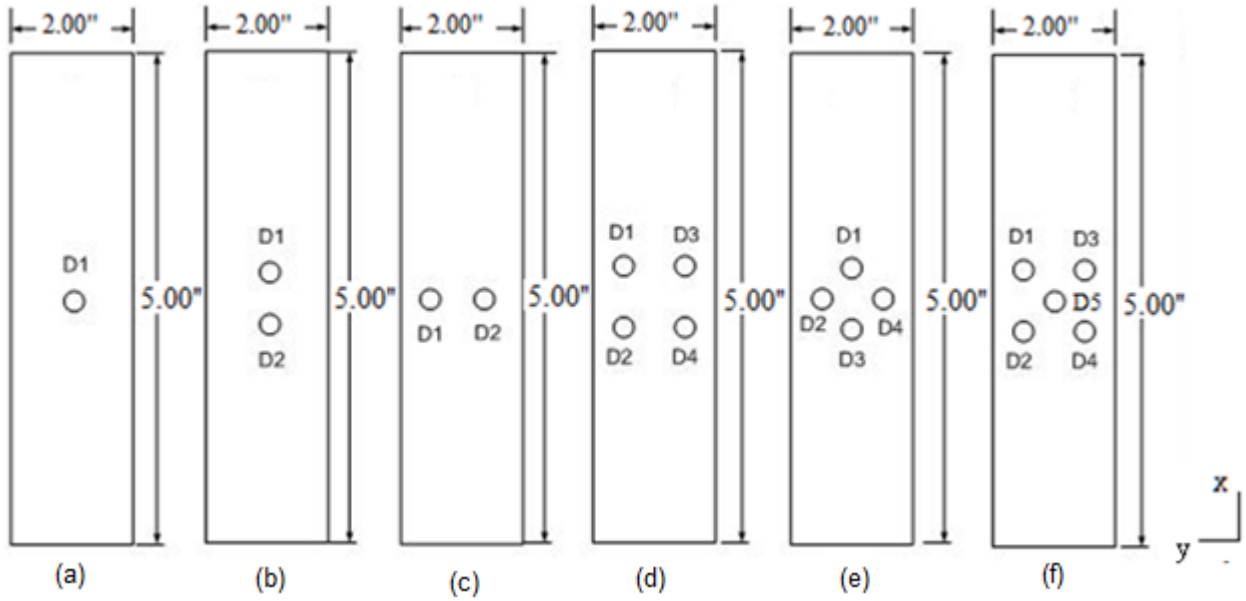

Figure 2.1 Hole pattern in parent laminates (a) Single hole (SH) (b) Top & Bottom hole (TBH) (c) Side-by-side hole (SSH) (d) Square array (SA) (e) Diamond array (DA) (f) Five Hole (FH)

Table 2.1 Location of holes

Hole Pattern	Hole location from center of the parent laminate (inches)									
	D1		D2		D3		D4		D5	
	x	y	x	y	x	y	x	y	x	y
SH	0	0	-	-	-	-	-	-	-	-
TBH	0.375	0	-0.375	0	-	-	-	-	-	-
SSH	0	-0.375	0	0.375	-	-	-	-	-	-
SA	0.375	-0.375	-0.375	-0.375	0.375	0.375	-0.375	0.375	-	-
DA	0.375	0	0	-0.375	-0.375	0	0	0.375	-	-
FH	0.375	-0.375	-0.375	-0.375	0.375	0.375	-0.375	0.375	0	0

The patch configurations are shown in Figure 2.2 as follows,

1. Square patch.

2. Hexagonal patch.

3. Octagonal patch.

4. Circular patch.

5. Elliptical patch.

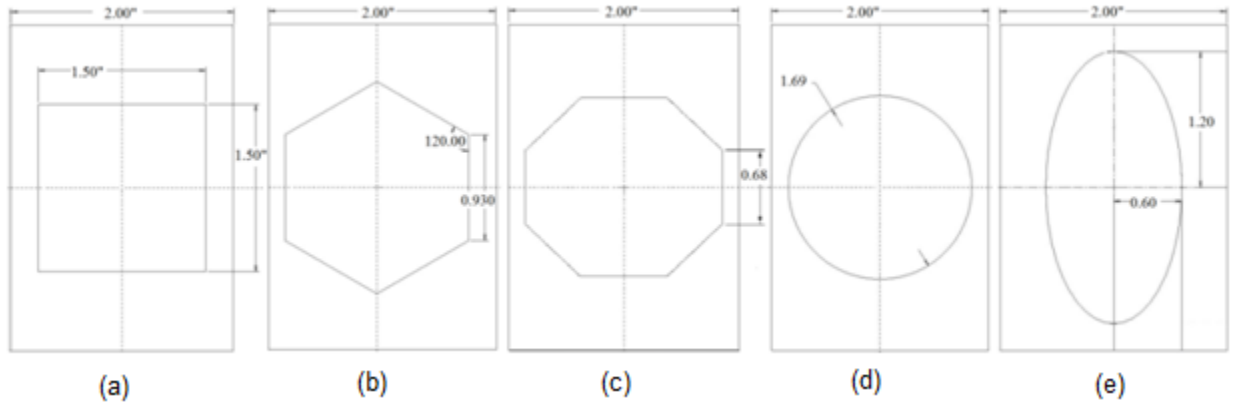

Figure 2.2 Dimension of the Patch configurations (a) Square patch (b) Hexagonal Patch (c) Octagonal Patch (d) Circular patch (e) Elliptical Patch

Each patch has the identical area of 2.25 in^2. The patch laminate is adhesively bonded to the parent laminate.

2.2 Material used

The composite laminate is made of graphite/epoxy lamina with intermediate modulus of the fiber and toughened epoxy matrix. The stacking sequence of the parent laminate is $[\pm 45/0_3/90]_S$ and patch laminate is $[\pm 45/0/90]_S$. Each layer of the parent and patch laminate has the thickness of 0.0074".

The orthotropic material properties of the lamina are,

$E_{11}=20.6 \times 10^6$ psi, $E_{22}=1.13 \times 10^6$ psi, $E_{33}=1.13 \times 10^6$ psi,

$v_{12}=0.34$, $v_{23}=0.53$, $v_{13}=0.34$,

G_{12}=0.58 x10^6 psi, G_{23}=0.37 x 10^6 psi, G_{13}=0.58 x 10^6 psi

The epoxy glue used to bond the parent and patch laminate has the isotropic properties of

E= 0.6 x 10^6 psi.

v =0.3.

where the subscripts 1 refers to fiber direction 2 is transverse to fiber direction and 3 is perpendicular to the 1-2 plane. $E_{11,\ E22}$ and E_{33} are the Young's moduli in 1-2-3 coordinate. $G_{12,}$ G_{23} and G_{13} are the shear moduli along the 1-2, 2-3, 3-1 planes respectively. v_{12} , v_{23} and v_{13} are the Poisson's ratio.

2.3 Element Type used

ANSYS 11.0 has various solid elements like SOLID 182, SOLID 82, SOLID186, SOLID 45 etc. It is very important to choose proper element type for accurate results. SOLID 186 is a 20-node element with three degrees of freedom in each node. It is a higher order 3D element with quadratic displacement behavior. Since the stress field near the hole exhibits a high stress gradient, the higher order 3D element is a better candidate for analysis. Hence, SOLID 186 is chosen for our finite element modeling.

2.4 Modeling and Meshing in ANSYS 11.0

The modeling and meshing is done using ANSYS 11.0 preprocessor tool. The procedure used to develop a square patch model is described below.

1. Define PLANE183 as element type1 and SOLID 186 as element type 2.

2. Create the material model 1 with unidirectional orthotropic properties and the material model 2 with isotropic properties of the epoxy.

3. Create a 3D model by extruding the meshed 2D areas. Then, create the areas at Z=0 as shown in Figure 2.3 for different hole patterns. As mapped meshing gives better accuracy over free mesh it is important to divide the areas properly for a good mapped mesh. It can be done using the ANSYS 11.0 modeling tool box. A square area is generated around the hole to get finer mapped mesh. The areas are

grouped as parent laminate and patch laminate areas which make easier for extrusion.

4. Create a 2D mesh using the ANSYS11.0 mesh tool box. Select PLANE183 as element type It is recommended to start the meshing around the hole and move away from it. This helps to get a gradation in the mesh with finer mesh around the hole and coarse mesh far away from hole. The finer mesh of 70 elements per quarter hole is used to capture the stress gradient around the hole as shown in Figure 2.4.

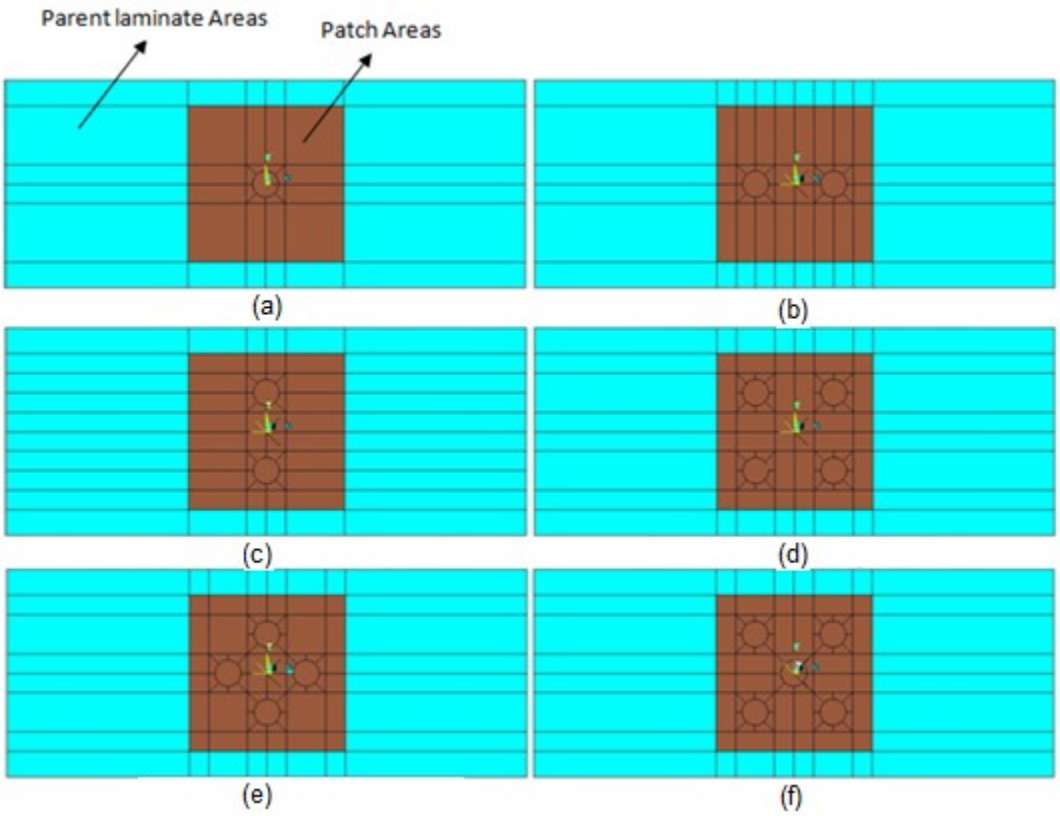

Figure 2.3 Areas for different hole patterns grouped as parent and patch laminate areas for 2D meshing (a) SH (b) TBH (c) SSH (d) SA (e) DA (f) FH

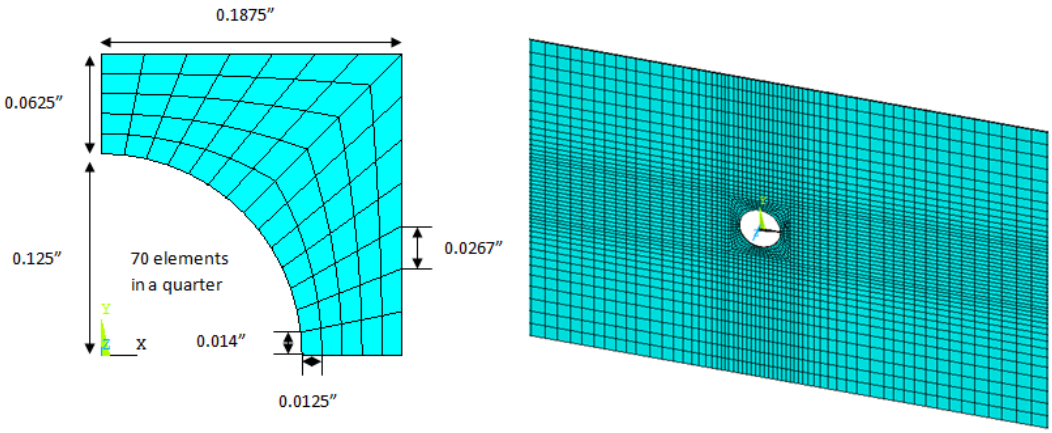

Figure 2.4 Finer mesh in the hole and gradation of finer mesh near the hole to coarse mesh away from it.

5. The local coordinates 11-24 are tabulated in Table 2.2 which is created to define the stacking sequence for parent and patch laminates. The stacking sequence of the parent and patch laminate is shown in Figure 2.5 and Figure 2.6, respectively.

Table 2.2 List of local coordinates in parent and patch laminates.

Local coordinate number	Angle	Local coordinate number	Angle
Parent laminate		Patch laminate	
11	45	18	45
12	-45	19	-45
13	0	20	0
14	90	21	90
15	0	22	0
16	-45	23	-45
17	45	24	45

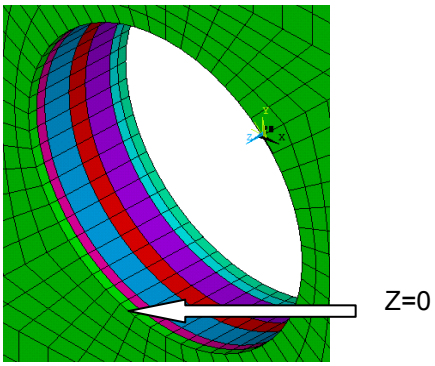

Figure 2.5 stacking sequence of parent laminate shown in different colors

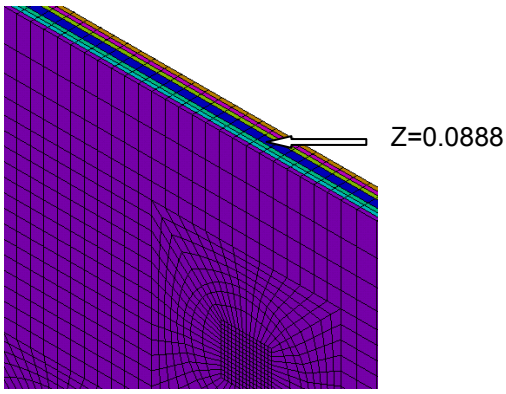

Figure 2.6 stacking sequence of patch laminate shown in different colors

6. The 2D mesh is extruded to create a 3D mesh as shown in Figure 2.7. This is done using the extrusion option in ANSYS 11.0 Modeling tool box. Set element type to SOLID186, material number to 1, element coordinate system to 11(which refer to 45 deg layer of parent laminate) and no of division to 1. Now extrude the areas with 0.0074 as the extrusion length. The volume mesh is created with one element division along the thickness. Select the top surface of the volume (done by select entries by location option in ANSYS 11.0) and repeat the same, changing the extrusion option appropriately. Thus, the finite element model for the parent laminate with different hole pattern is created. The number elements for different hole patterns is tabulated in Table 2.3.

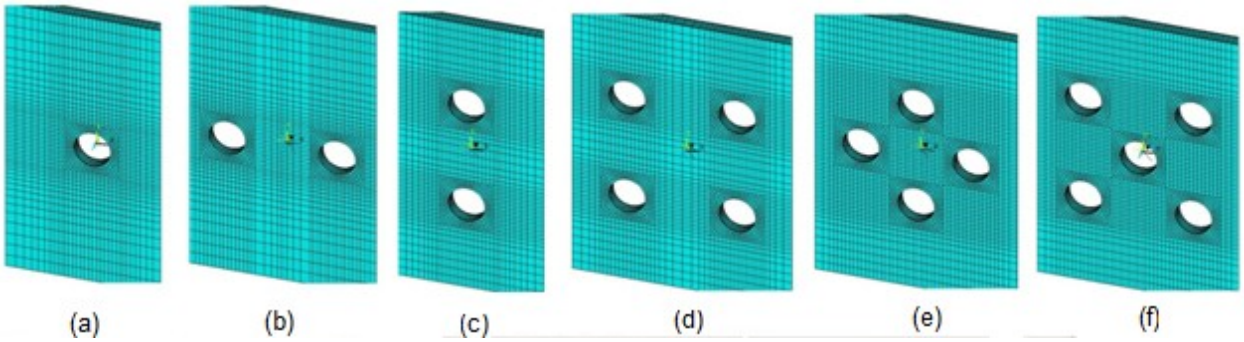

Figure 2.7 Close view of the parent laminate with different hole patterns (a) SH (b) TBH (c) SSH (d) SA (e) DA (f) FH

Table 2.3 Total number of nodes and elements for different cases

Cases	No. of nodes	No. of elements
Single hole	112446	24612
Top and bottom hole	137871	30128
Side by side hole	151557	33208
Square array	167833	36568
Diamond array	196381	42952
five hole	203256	44352

7. After creating parent laminate, create the patch area on the extreme top surface of the parent laminate. Again repeat the extrusion procedure by selecting only the patch areas. Select appropriate extrusion options for creating glue layer (e.g. material number 2 and element coordinate system 0 for glue layer) and patch laminates. The element division is maintained one per layer throughout. The mesh for square patch with different hole patterns is shown in Figure 2.8

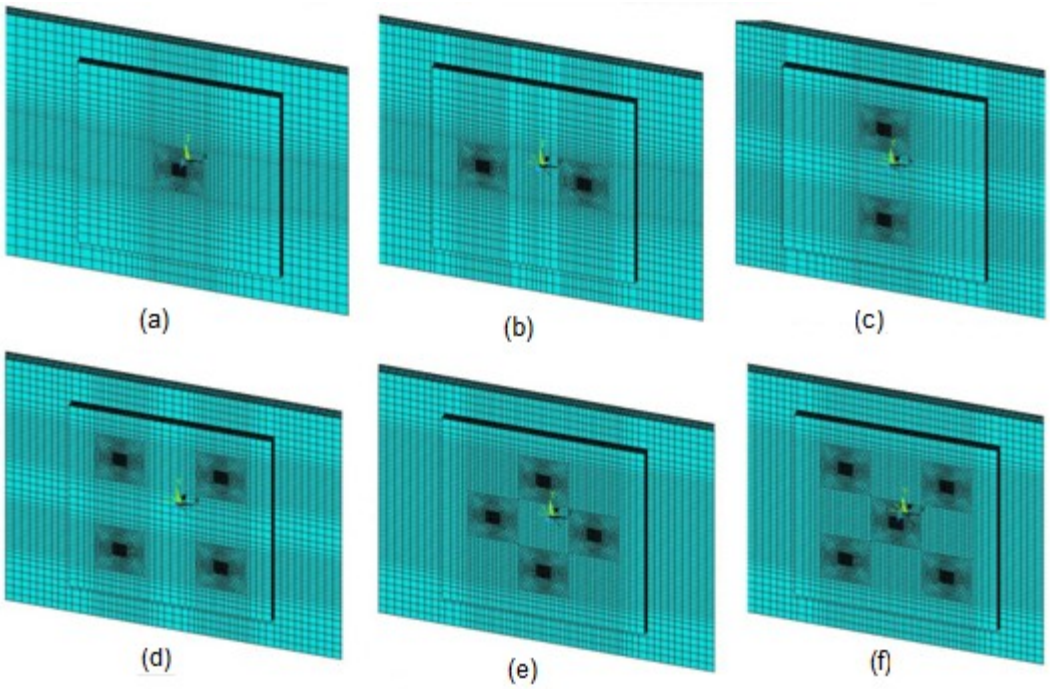

Figure 2.8 Mapped mesh of different hole patterns with square patch (a) SH (b) TBH (c) SSH (d) SA (e) DA (f) FH

The 0_3 and 90 layers are merged as one to reduce the number of elements which in turn reduces computation effort. The merging of the layers is tabulated in Table 2.4.

Table 2.4 Illustration of laminas lumped in finite element model.

parent laminate	
stacking sequence	thickness(inches)
45	0.0074
-45	0.0074
0	0.0074
0	0.0074
0	0.0074
90	0.0074
90	0.0074
0	0.0074
0	0.0074
0	0.0074
-45	0.0074
45	0.0074

0 deg layers merged
Thk=3*0.0074=0.0222 in

90 deg layers merged
Thk=2*0.0074=0.0148 in

0 deg layers merged
Thk=3*0.0074=0.0222 in

patch laminate	
stacking sequence	thickness(inches)
45	0.0074
-45	0.0074
0	0.0074
90	0.0074
90	0.0074
0	0.0074
-45	0.0074
45	0.0074

90 deg layers merged
Thk=2*0.0074=0.0148 in

8. Following the above procedure all the finite element models with different hole patterns and different patches are created. Figure 2.9 shows the different patch configurations for single hole pattern. The

number elements for all patch configurations with different hole patterns is tabulated in Table 2.5.

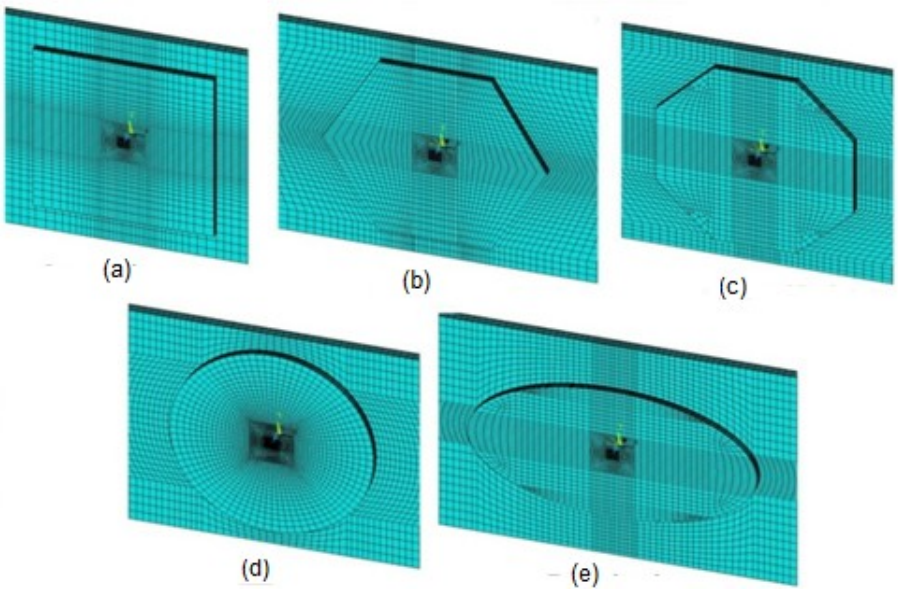

Figure 2.9 Mapped mesh of different patches for single hole pattern (a) Square patch (b) Hexagonal Patch (c) Octagonal Patch (d) Circular patch (e) Elliptical Patch

Table 2.5 Number of elements in FE model for all patch configurations with different hole patterns

Number of elements in entire FE model						
Patch Configuration	Hole patterns					
	SH	TBH	SSH	SA	DA	FH
Square Patch	29448	38040	35280	57480	67248	70160
Hexagonal patch	38680	45740	42496	60868	66660	73776
Octagonal patch	37788	52548	45056	59404	61548	70316
Circular patch	20524	50216	52420	72200	71656	82480
Elliptical patch	39608	48796	51032	60636	66064	67376

2.5 Boundary Conditions

The boundary conditions enforced in the finite element model are described below,

1. All the nodes at edge x=0 are constrained along the x-axis (loading axis) ie U_x=0.

2. The nodes along the edges at x=0,y=0 are constrained along x-axis (loading axis) and y-axis (transverse to loading axis) ie $U_x=U_y=0$.

3. The middle node at x=0, y=0 and z=1/2*total laminate thickness is constrained for all degrees of freedom ie $U_z=U_y=U_z=0$

The same boundary conditions are used for all models. This is done by using the Loads tool box in ANSYS 11.0. The exploded view of the boundary conditions on finite element model is shown in the Figure 2.10.

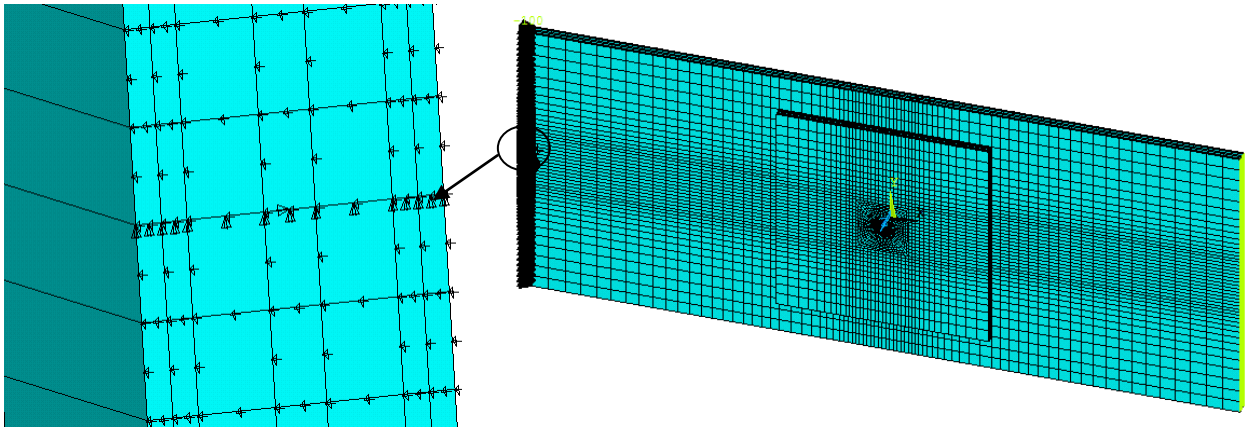

Figure 2.10 Exploded view of the boundary conditions

2.6 Loading condition

An in-plane tensile stress of 100 psi is applied at x=5 in. This is done by using the ANSYS 11.0 Loads tool box. The same loads were used for all the finite element models developed. Only tensile stress is considered for the study.

CHAPTER 3

PEAK STRESS OF COMPOSITE LAMINATE WITH MULTIPLE HOLES

The peak stress of the composite laminate due to different hole patterns is discussed in this chapter. A significant variation in the stress concentration is found with different hole pattern. This study gives us various information about effect of multiple hole arrangement of holes in composite laminate. The material property, laminate stacking sequence and hole radius is considered same for all cases. The analysis is done using ANSYS 11.0 and results are discussed. The different hole patterns discussed in Chapter II is considered for the study. The geometric description, material and stacking sequence are given in sections 2.1 and 2.2, respectively.

3.1 General discussion on stress profiles

The composite laminate subjected to tension has constant force flux lines runs along the length of the specimen in the loading direction for a 0^0 ply as shown in Figure 3.1. A constant σ_x exists for each angle ply of the laminate.

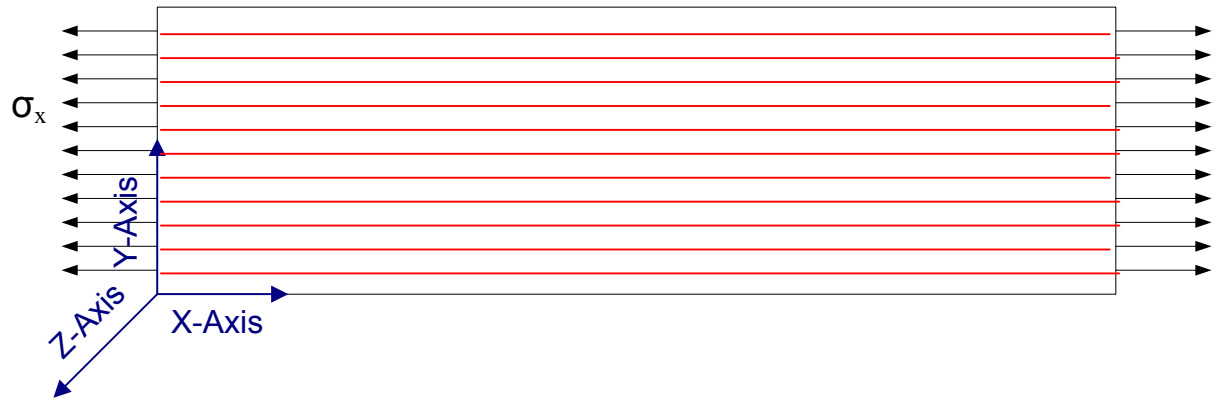

Figure 3.1 Force flux lines for a 0^0 ply composite laminate

In the presence of hole the force flux lines are concentrated closely near the hole inducing high stress concentrations at point A and B as shown in Figure 3.2.

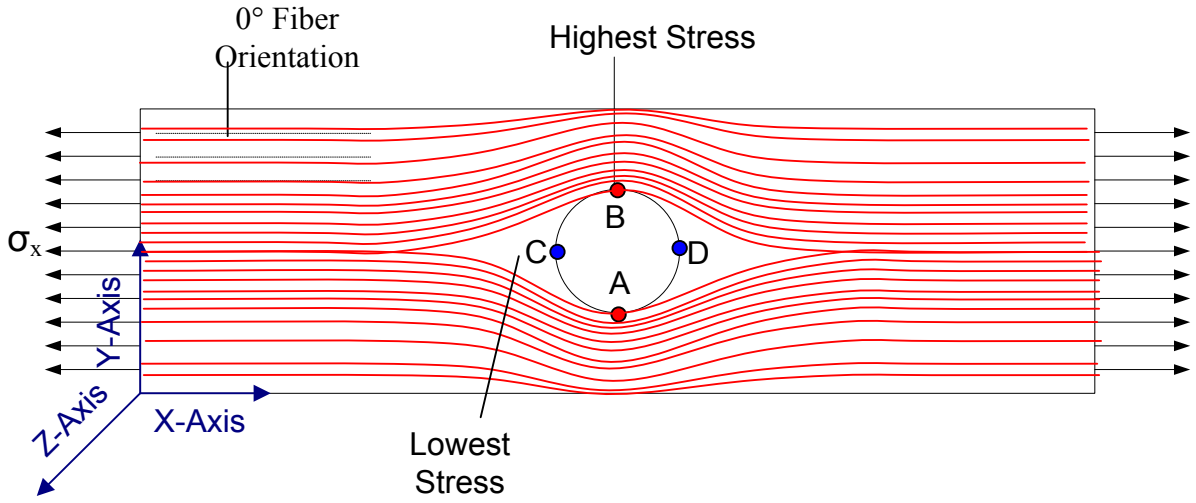

Figure 3.2 Force flux lines for a 0^0 ply composite laminate with single hole

The force flux lines turns according to the net section area at the hole region becoming denser near point A and B. As a result the stress levels on the periphery of the holes increases. The point A & B are the locations of high stress concentrations. At locations of C and D points there is no force flux passing through, hence no axial force at these points. Figure 3.1 shows the stress distribution on 0^0 ply of the composite laminate with single hole.

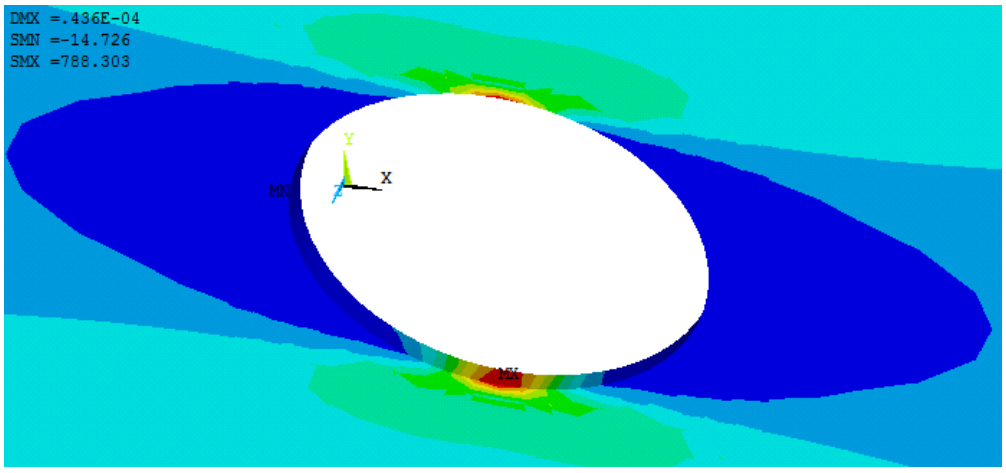

Figure 3.3 Closer view of the stress contour on the periphery of the hole for 0^0 ply

As explained, the maximum stress concentration occurs at point A & B and zero or near zero stress concentration at neighborhood of points C & D was observed. The magnitude of σ_x is the same at points A & B. The equal magnitude of maximum σ_x occurs at points A & B in 0^0 ply. The close view of the stress concentration at the hole is shown in the figure above.

3.2 Results of 0^0 ply

3.2.1 In-Plane stresses σ1. σ2, τ12 for 0^0 ply

The in-plane stress is maximum at 0^0 ply in all configurations. The maximum in-plane stresses for different hole patterns are normalized by the applied stress, σ_0 are tabulated in Table 3.1 and shown in Figure 3.4.

Table 3.1 Normalized maximum In-plane stresses for 0^0 ply

Normalized Maximum stress for 0^0 ply (psi)	Hole patterns					
	SH	TBH	SSH	SA	DA	FH
σ_1 / σ_0	7.88	7.19	8.16	7.62	10.25	11.20
σ_2 / σ_0	0.36	0.34	0.37	0.36	0.47	0.51
τ_{12} / σ_0	0.57	0.53	0.59	0.56	0.74	0.81

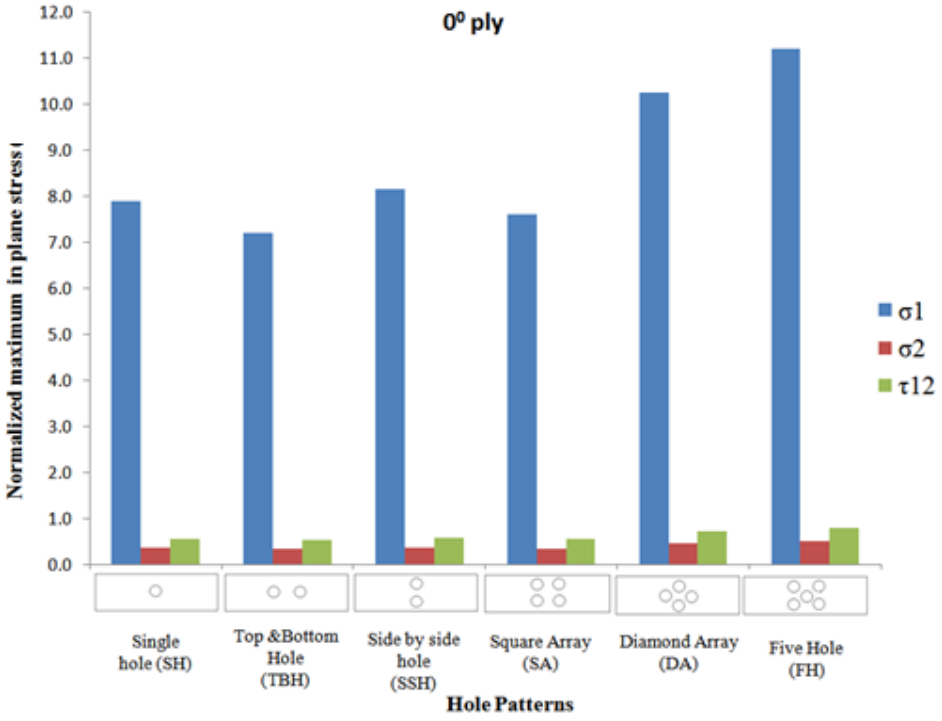

Figure 3.4 Comparison of Normalized maximum In-plane stress for different hole patterns

From the stress values we can infer that,

1) The peak value of stress for all the hole patterns occur in the periphery of the hole at the point A & B as shown in Figure 3.5

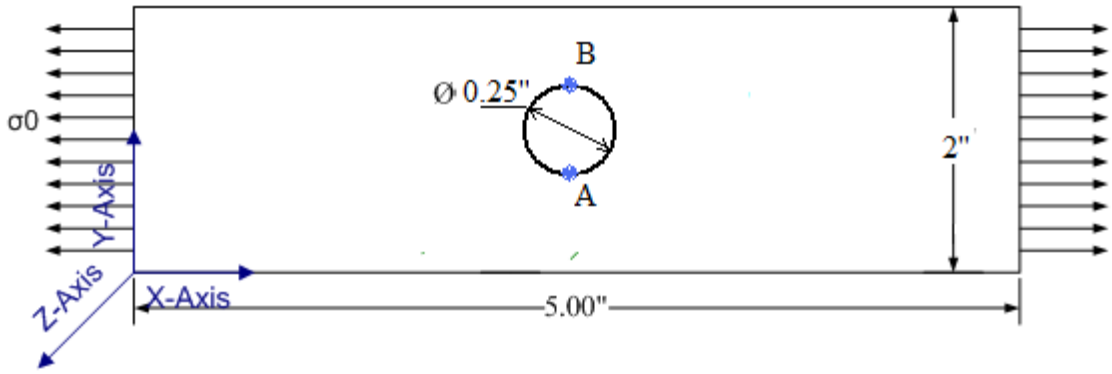

Figure 3.5 Peak stress at Points A&B

2) After Five Hole pattern (FH), Diamond Array (DA) and Side by Side Hole (SSH) has the highest stress followed by Square Array(SA), Single Hole(SH) and Top & Bottom Hole (TBH), respectively. The peak stress occurs in the sequence, FH, DA, SSH, SA, SH and TBH.

3) SH has higher stress compared to TBH (two holes). This indicates that another hole in loading direction reduces the stress concentration at the holes in TBH. It can be explained that the force flux lines are redistributed uniformly when the another hole in the loading direction is present.

4) SA (four holes) has lower stress than SSH (two holes).The increase in stress for SSH compared with SH is because of the reduction in the net section area. The same explanation holds good for higher stress in DA as it embeds SSH in it and a reduced stress of SA is due to extra holes in the loading direction which decrease stress concentration at holes effectively.

It is interesting to examine the occurrence of maximum stress concentration in the holes for a multi hole patterns.

a) For TBH, SSH and SA all the holes within the pattern have same stress concentration as shown in the Figure 3.6. This is because of no interaction between the holes.

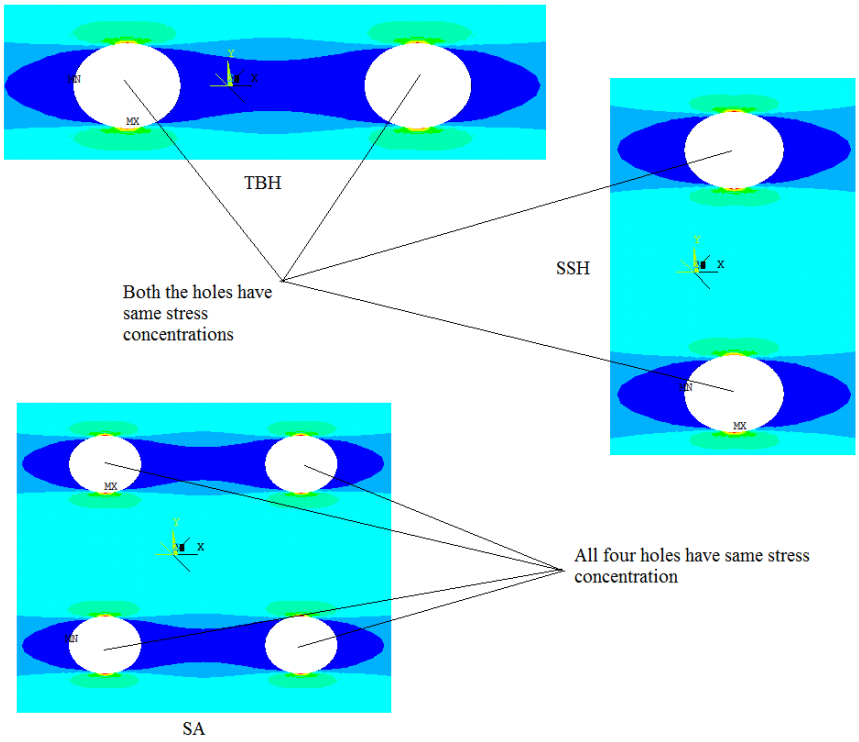

Figure 3.6 Holes in TBH, SSH & SA has same stress concentrations

5) In DA pattern the holes transverse to the loading direction has higher stress concentration than the holes along the loading direction. In FH configuration the center hole has higher stress concentration compared to other four holes which have same magnitude of stress concentrations. The reason is because of the interaction of the holes within DA and FH hole pattern. The close view of DA and FH is shown in Figure 3.7

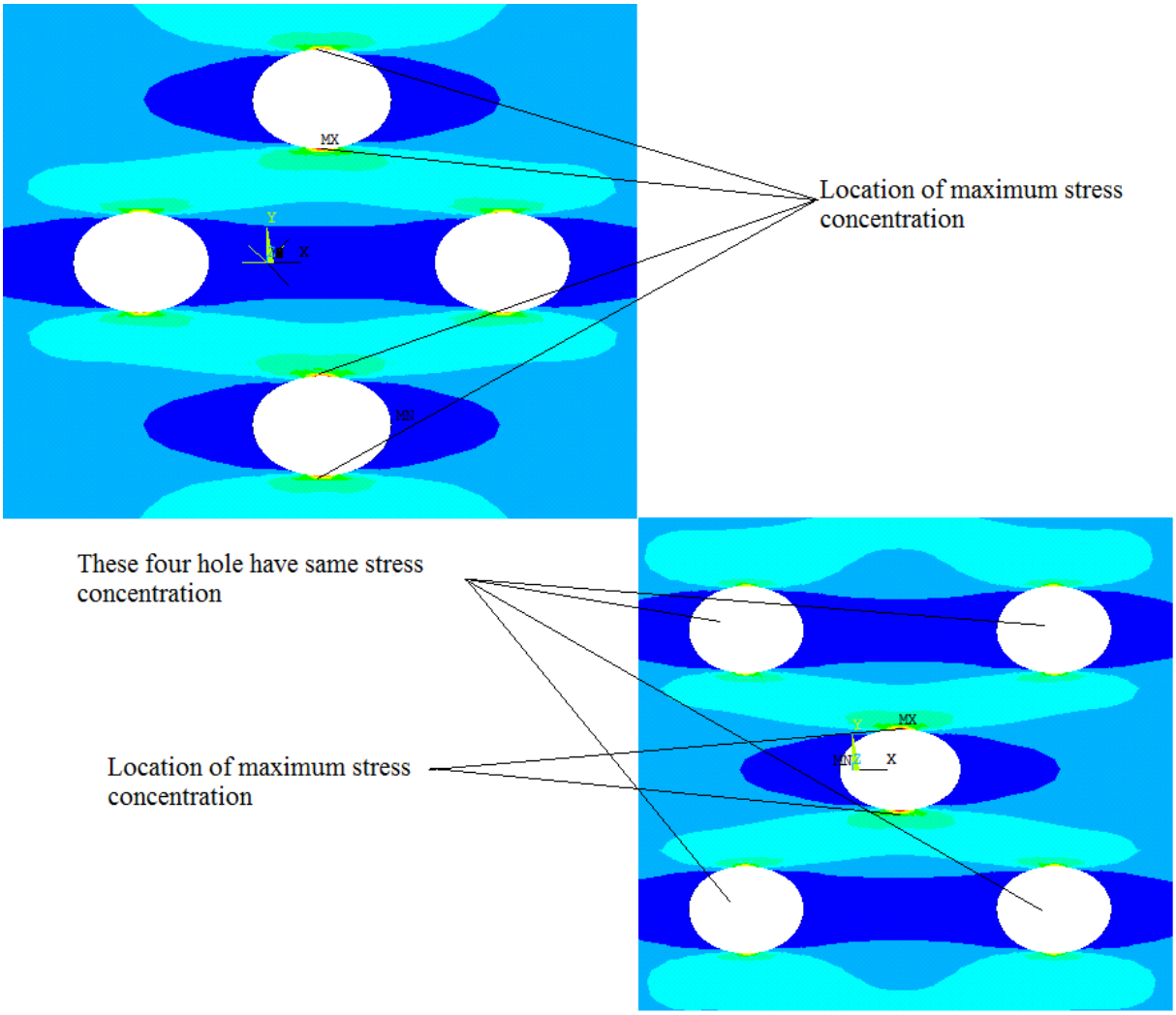

Figure 3.7 Different stress concentrations in holes within DA & FH pattern

6) The comparison of stress contours for 0^0 ply in different configurations is shown in Figure 3.8. As shown, all the stress contours indicate the non zero or negative stress along the loading direction.

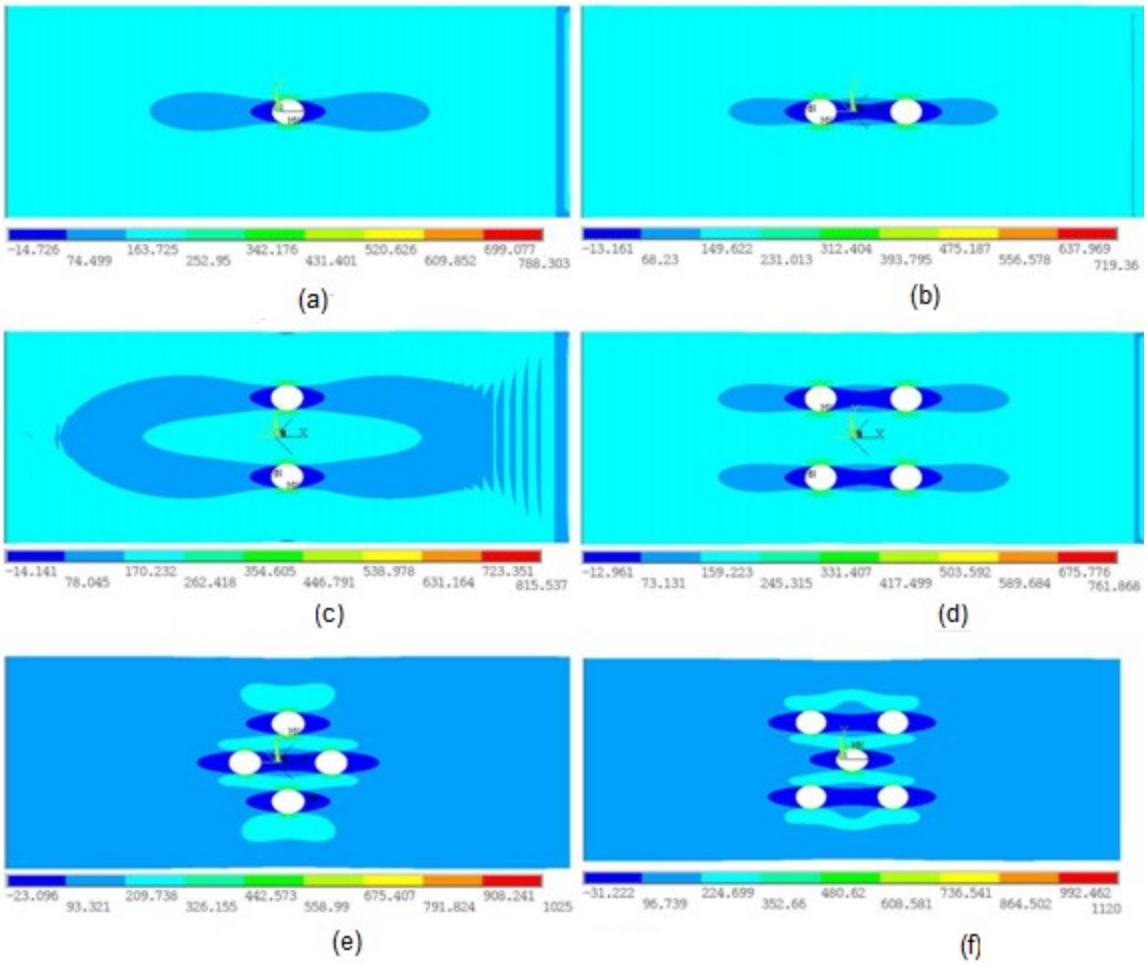

Figure 3.8 Comparison of Stress contours for 0^0 ply in different configurations (a) SH (b) TBH (c) SSH (d) SA (e) DA (f) FH

3.2.2 Inter-laminar stresses σ_1, τ_{13}, τ_{23} for 0^0 ply

The interlaminar stresses are tabulated in Table 3.2 and a comparison of normalized maximum interlaminar stresses for 0^0 ply for different hole pattern is shown in Figure 3.9.

Table 3.2 Normalized maximum interlaminar stresses for 0^0 ply

Normalized Maximum stress for 0^0 ply	Hole patterns					
	SH	TBH	SSH	SA	DA	FH
σ_3 / σ_0	0.23	0.24	0.24	0.29	0.29	0.26
τ_{13} / σ_0	0.41	0.40	0.43	0.42	0.52	0.57
τ_{23} / σ_0	0.17	0.17	0.18	0.18	0.22	0.24

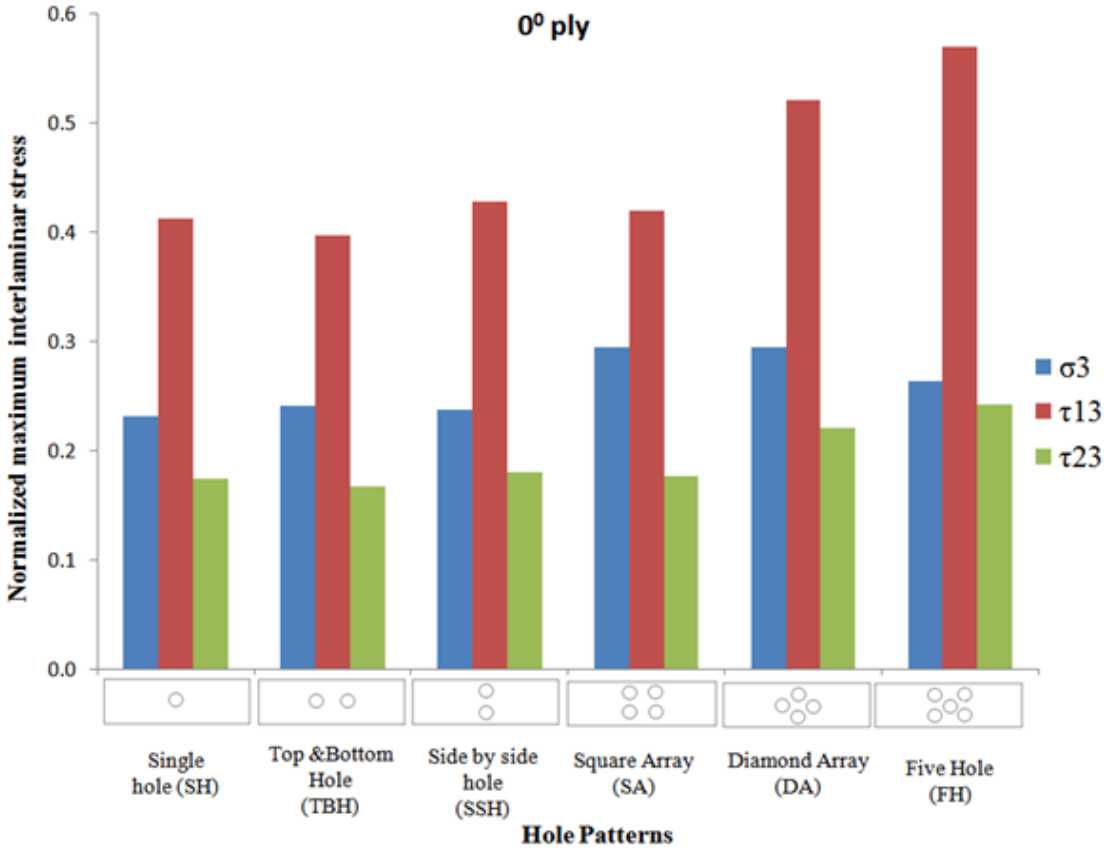

Figure 3.9 Comparison of Interlaminar stresses for different hole patterns for 0^0 ply

From the interlaminar stress values we can infer that,

1) The maximum value of σ_3 occurs at point A & B for all the hole patterns However, τ_{13}, τ_{23} occurs at an angle to point A & B as shown in Figure 3.10. All configurations follow the same pattern of stress occurrence at all holes.

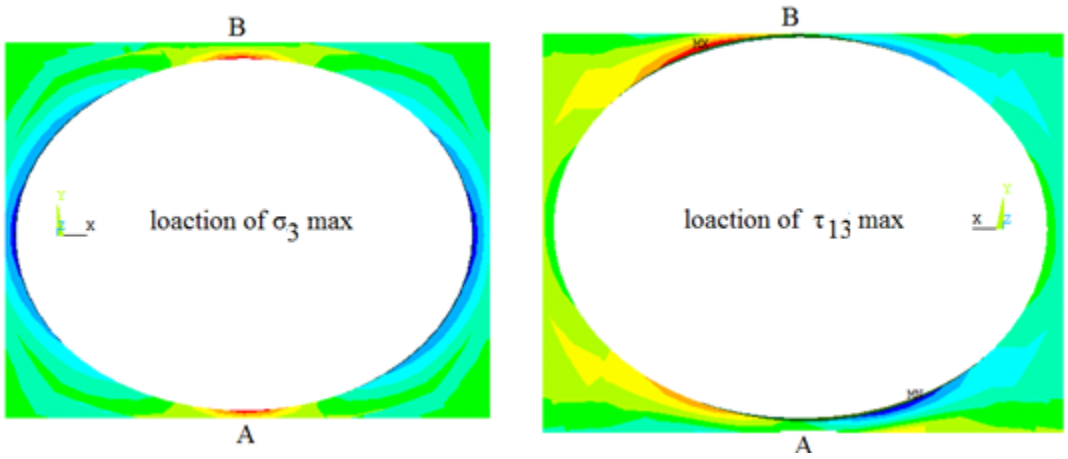

Figure 3.10 peak values of σ_3, τ_{13} and τ_{23} at point A&B

2) Among all configurations FH has maximum inter-laminar stress followed by DA, SSH, SA, SH and TBH respectively.

3) For all the interlaminar stresses, τ_{13} is the maximum out of inter laminar stresses for all hole patterns.

3.6 Results of $\pm 45^0$ plies

3.3.1 In-plane stresses σ_1. σ_2, τ_{12} for $\pm 45^0$ ply

The normalized maximum in-plane stresses for $+45^0$ & -45^0 plies are tabulated in Table 3.3 & 3.4, respectively and comparison of normalized maximum In-plane stresses for $+45^0$ & -45^0 plies for different hole pattern is shown in Figures 3.11 & 3.12, respectively

Table 3.3 Normalized Maximum stress for 45^0 ply

Normalized Maximum stress for 45^0 ply	Hole patterns					
	SH	TBH	SSH	SA	DA	FH
σ_1 / σ_0	1.82	1.78	1.96	1.93	2.24	2.29
σ_2 / σ_0	1.41	1.39	1.56	1.53	1.74	1.70
τ_{12} / σ_0	1.51	1.49	1.66	1.64	1.87	1.90

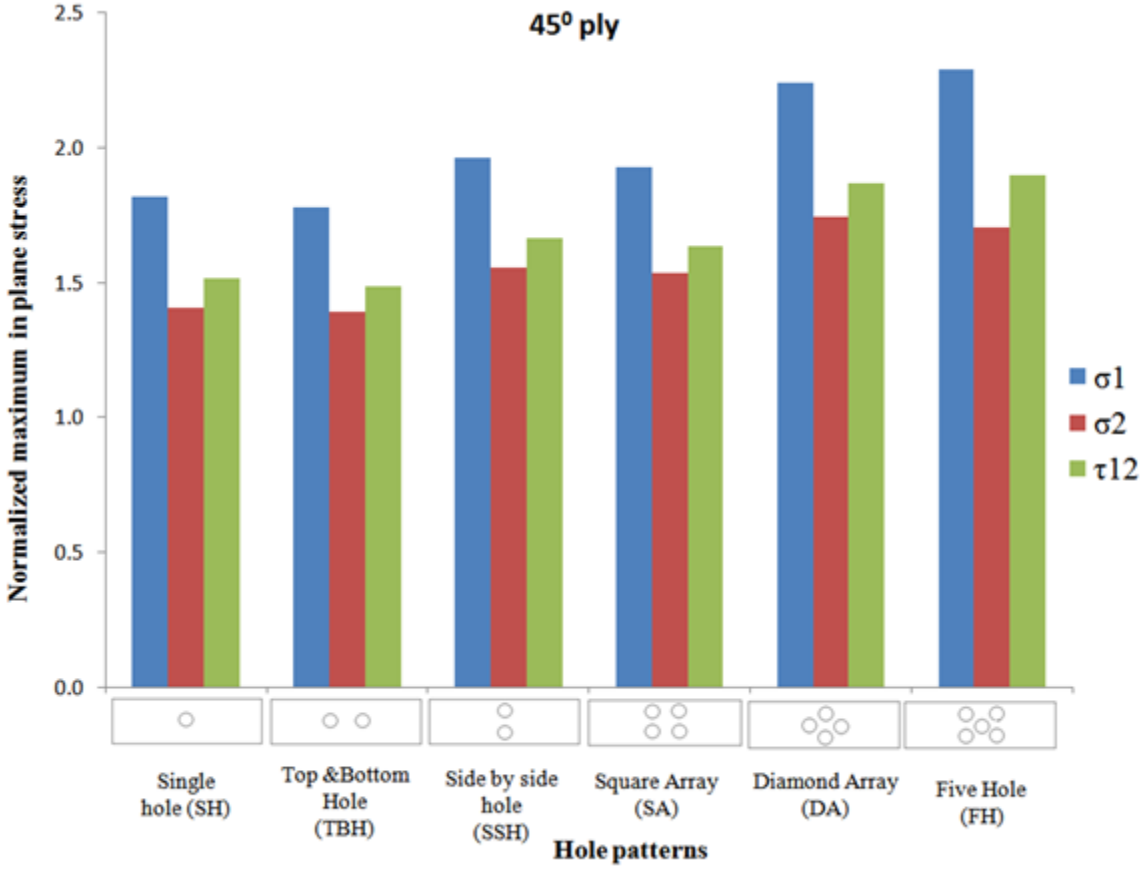

Figure 3.11 Comparison of in-plane stresses for different configuration for 45^0 ply

Table 3.4 Normalized Maximum stress for -45^0 ply

Normalized Maximum stress for -45^0 ply	Hole patterns					
	SH	TBH	SSH	SA	DA	FH
σ_1 / σ_0	2.49	2.40	2.63	2.56	3.17	3.48
σ_2 / σ_0	2.07	2.00	2.18	2.13	2.58	2.82
τ_{12} / σ_0	1.45	1.35	1.50	1.42	1.86	2.04

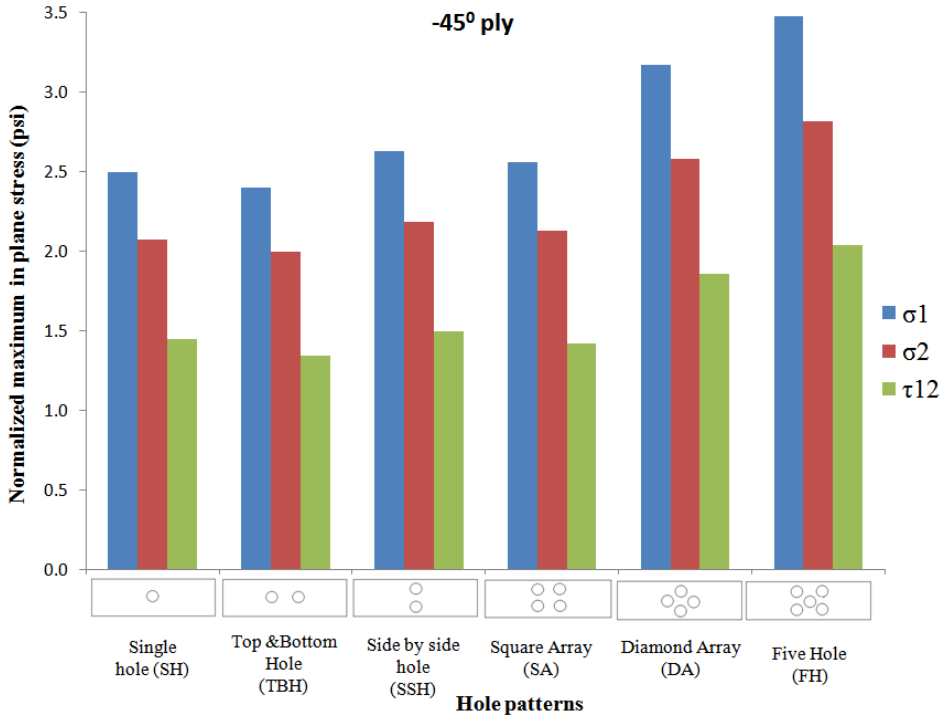

Figure 3.12 Comparison of in-plane stresses for different configuration for -45^0 ply

From the stress values it can be inferred that,

1) The maximum in-plane stress σ_1, σ_2, and τ_{12} occurs at point A and B on the periphery of the hole as shown in Figure 3.13 which is at $\theta = -67.5^0$ and $\theta = 112.5^0$, respectively measured from the loading direction. This is due to the shearing rotation of 45^0 ply. The same occurs in -45^0 ply.

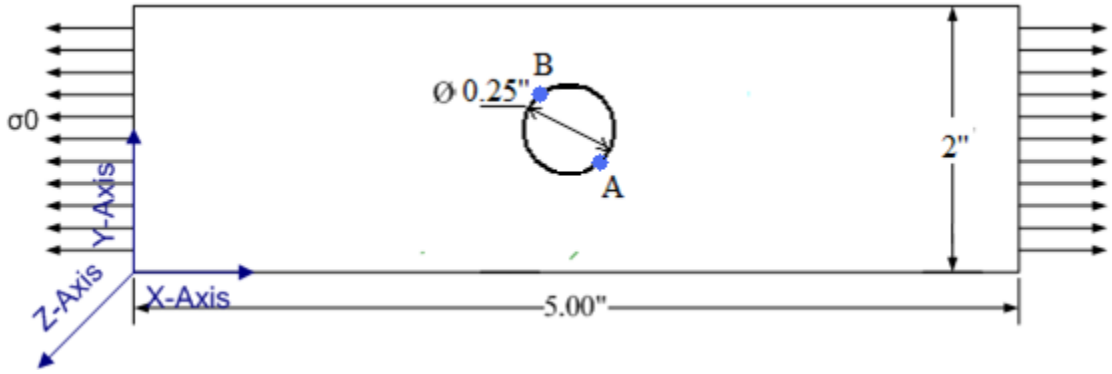

Figure 3.13 Location of maximum stress for 45^0 ply

2) Among the configurations FH has the maximum in-plane stress followed by DA& SSH. This is due to reduction in the net section area for these hole patterns. The SA, TBH patterns has holes along the loading direction which reduces the stress.

3) Both holes in the TBH & SSH and all four holes in SA have same stress concentrations where as for DA the holes transverse to loading direction has the maximum stress concentration and in FH, the center hole has the maximum stress concentration compared to other four holes. The detailed view is shown in Figure 3.14.

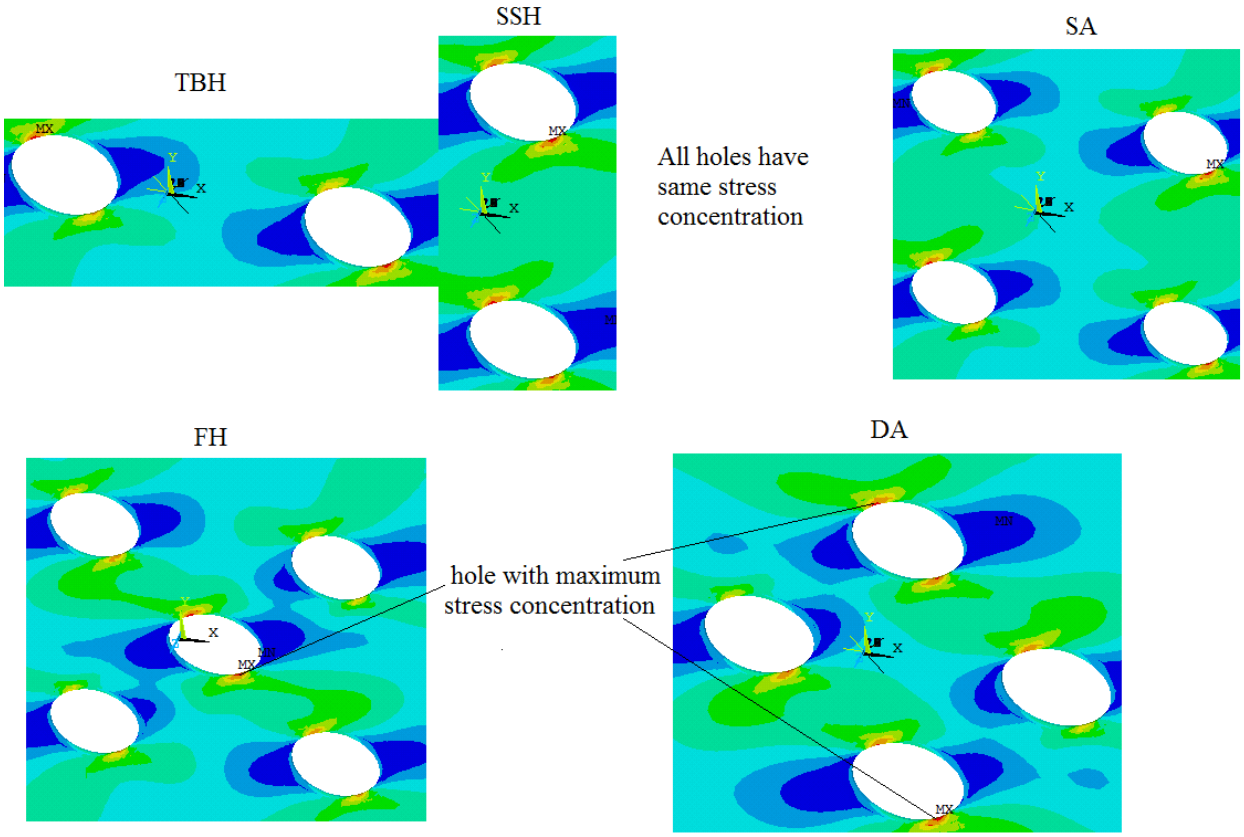

Figure 3.14 Close view for different hole patterns showing peak stress locations for 45^0 ply.

4) The stress contours for the $+45^0$ and -45^0 plies are shown in the Figure 3.15 and 3.16, respectively. As indicated, the contours illustrate the load path along the fiber direction in the neighborhood of the hole in each configuration.

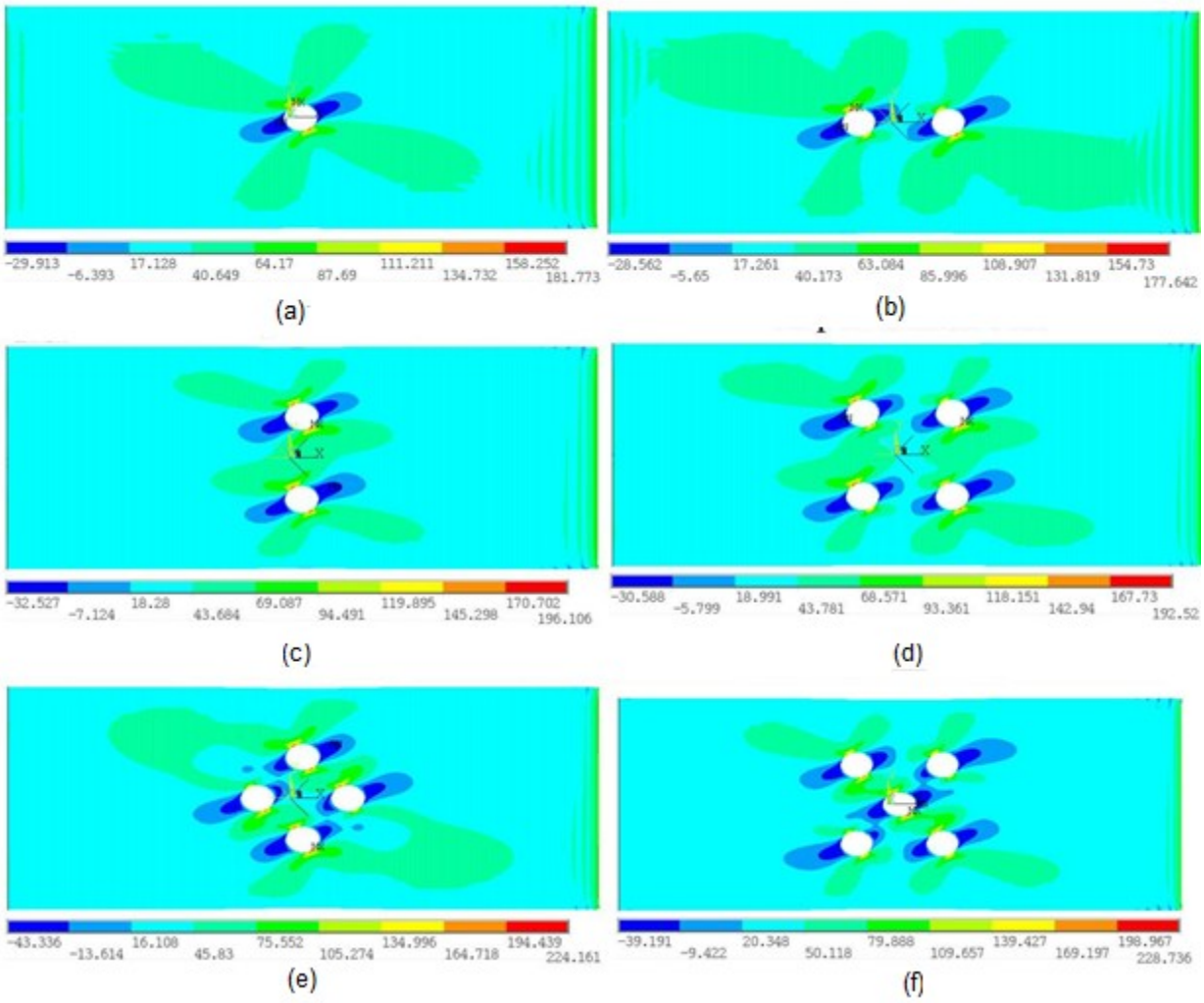

Figure 3.15 Stress contour comparison of different configuration for 45^0 ply (a) SH (b) TBH (c) SSH (d) SA (e) DA (f) FH

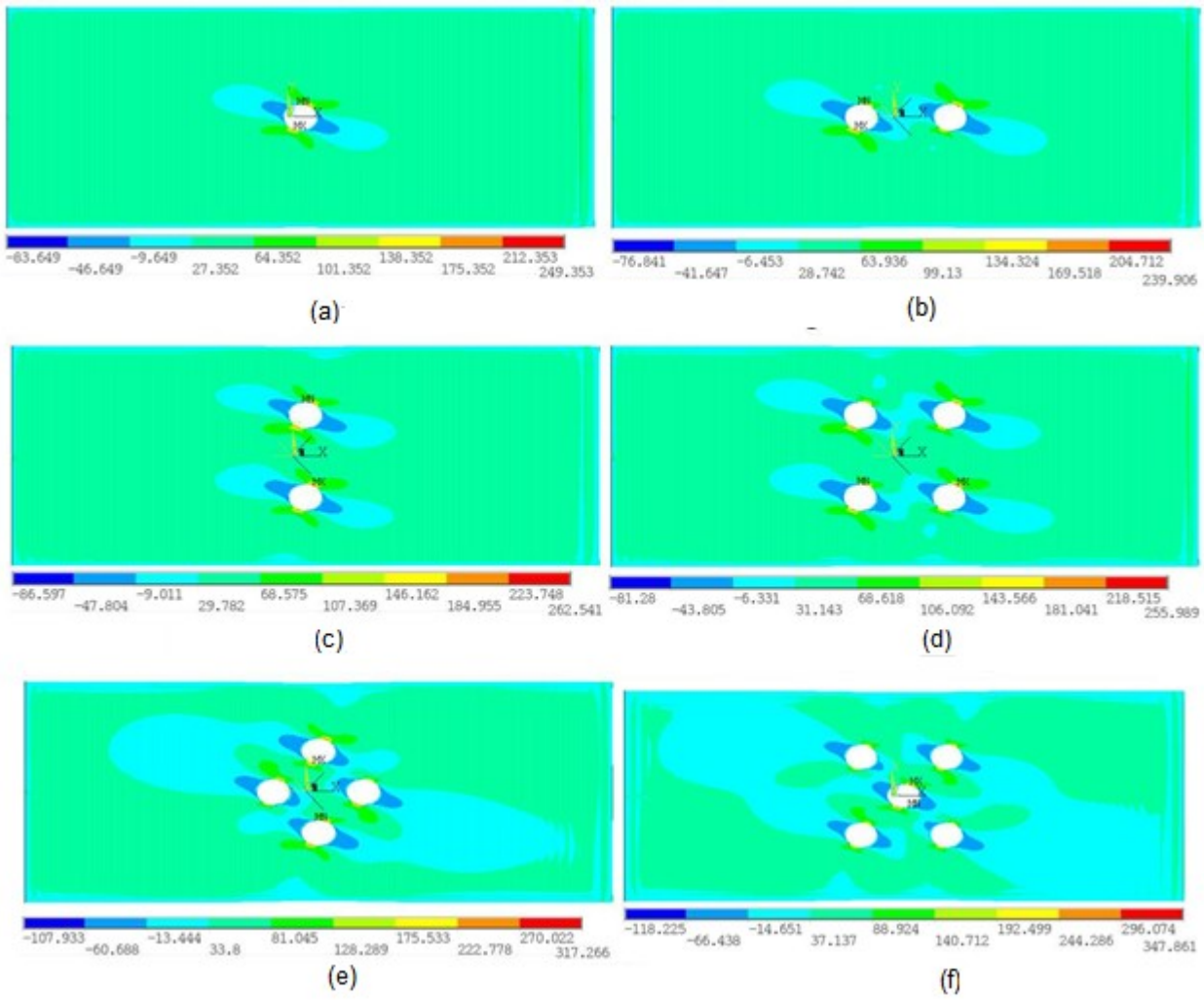

Figure 3.16 Stress contour comparison of different configuration for -45^0 ply (a) SH (b) TBH (c) SSH (d) SA (e) DA (f) FH

3.3.2 Inter-laminar stresses σ_1, τ_{13}, τ_{23} for $\pm 45^0$ plies

The interlaminar stresses for $\pm 45^0$ plies are tabulated in Tables 3.5 & 3.6 and comparison of Normalized maximum interlaminar stresses for $\pm 45^0$ plies for different hole pattern is shown in Figures 3.17 & 3.18.

Table 3.5 Inter-laminar stresses in $+45^0$ for ply different hole pattern

Normalized Maximum stress for 45^0 ply (psi)	Hole Patterns					
	SH	TBH	SSH	SA	DA	FH
σ_3 / σ_0	0.07	0.07	0.08	0.07	0.09	0.10
τ_{13} / σ_0	0.24	0.24	0.25	0.25	0.30	0.32
τ_{23} / σ_0	0.17	0.18	0.17	0.22	0.22	0.20

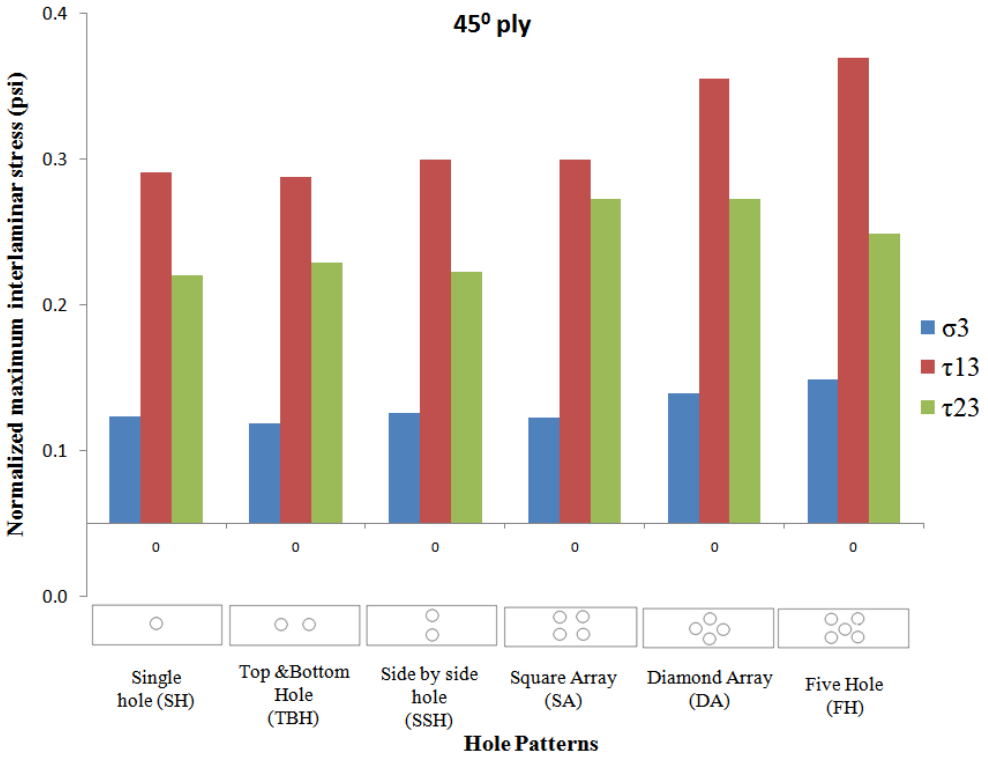

Figure 3.17 Comparison of Inter-laminar stresses for different hole patterns for 45^0 ply

Table 3.6 Inter-laminar stresses in -45^0 for plies different hole patterns

Normalized Maximum stress for -45^0 ply	Configurations					
	SH	TBH	SSH	SA	DA	FH
σ_3 / σ_0	0.14	0.15	0.15	0.18	0.18	0.18
τ_{13} / σ_0	0.46	0.45	0.48	0.48	0.58	0.63
τ_{23} / σ_0	0.21	0.20	0.22	0.22	0.26	0.28

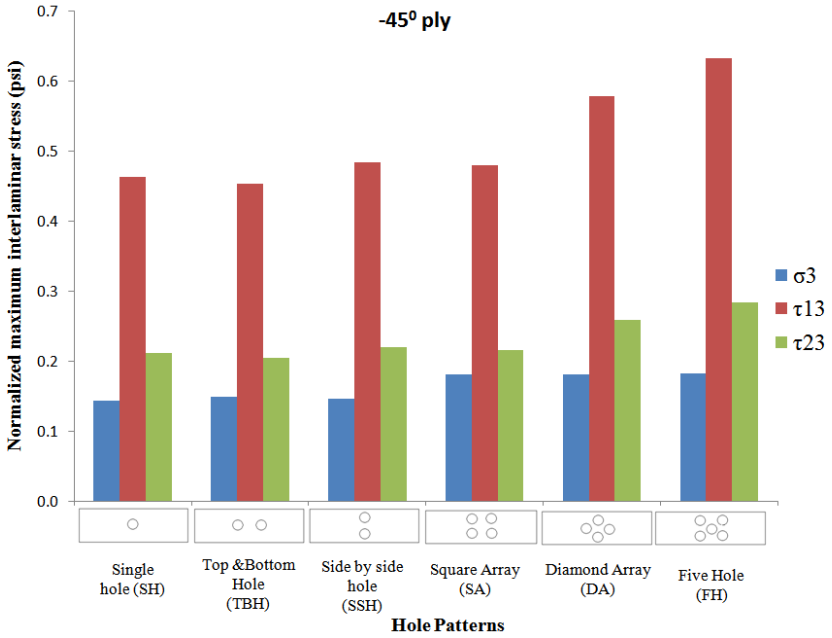

Figure 3.18 Comparison of Inter-laminar stresses for different hole patterns for -45^0 ply

From the stress values we can infer that,

1) The location of maximum interlaminar stress is the same as 0^0 ply. The maximum σ_3 occurs at points A and B and τ_{13}, τ_{23} at an angle to point A and B.

2) FH has maximum inter-laminar stress followed by DA, SSH, SA, SH and TBH, respectively for $\pm 45^0$plies.

CHAPTER 4

EXPERIMENTAL STUDY ON STRENGTH OF COMPOSITE LAMINATE WITH MULTIPLE HOLES

An experimental study is conducted to determine the effects of multiple hole patterns on composite laminate. Five different hole patterns are studied. All the test coupons are of the same material and dimensions. The high stress gradient occurs at the vicinity of the hole edges. This data helps us in understanding different kinds of damages and also provides good idea on the repair design.

4.1 Description of Test coupon

Five configurations of hole orientation patterns, Figure 4.1, in a graphite/epoxy laminate with a layup of $[\pm 45/0_3/90]s$ were studied. Configuration A contains a single hole, designated as SH. Configurations B and C have two holes, with one having in-line holes (top and bottom), designated TBH, and one having side-by-side holes, designated SSH. Four holes placed in a square (SA) and diamond (DA) arrays are configurations D and E, respectively. The coupons were supplied by The Boeing Company.

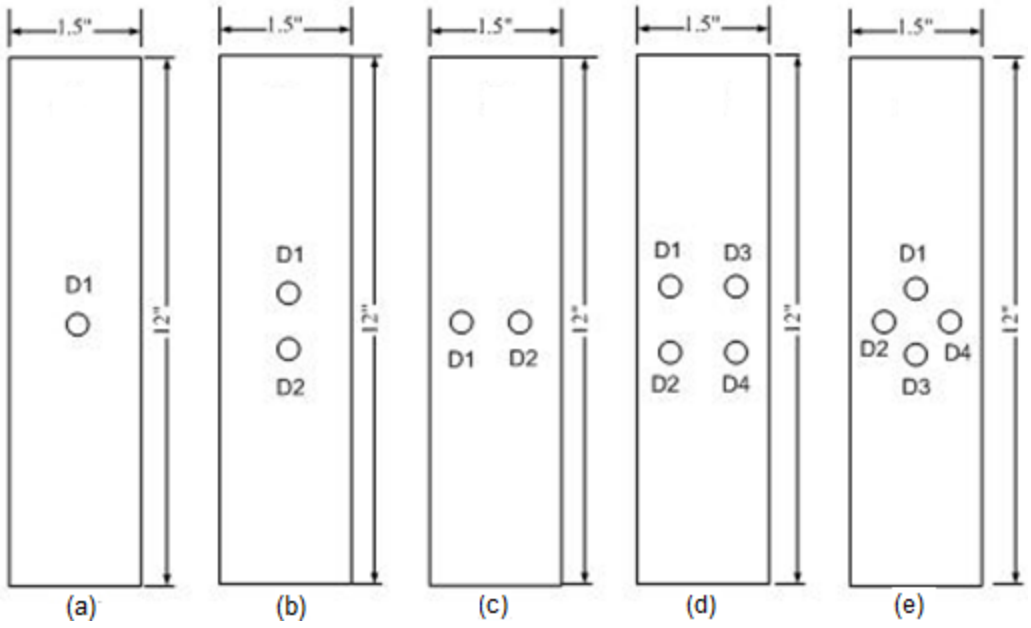

Figure 4.1 Test coupons with different hole patterns (a) SH (b) TBH (c) SSH (d) SA (e) DA

The holes are all ¼-inch in diameter and the distance between holes in both the side-by-side and top- and -bottom hole configurations is 0.75 inches. Aluminum end tabs, 2-inches long, were attached with film adhesive and an axial strain gage was bonded to the specimen at the location away from the hole. The coupons were inspected to see if any damage occurred around the hole during fabrication. The material constants are given as

E_1=20.6 x10^6 psi, E_2=E_3=1.13 x10^6 psi, G_{12}=G_{13}=0.58 x10^6 psi,

G_{23}=0.37 x10^6 psi, ν_{12}=ν_{13}=0.34; ν_{23}=0.53 ply thickness=0.0074 in

where the subscripts 1, 2 and 3 refer to “along the fiber direction,” “transverse to the fiber direction” and “perpendicular to the plane” respectively.

4.2 Experimental setup

The MTS testing machine QTest/150 shown in Figure 4.2 used for the test. The machine can loaded to maximum load of 33000 lbf.

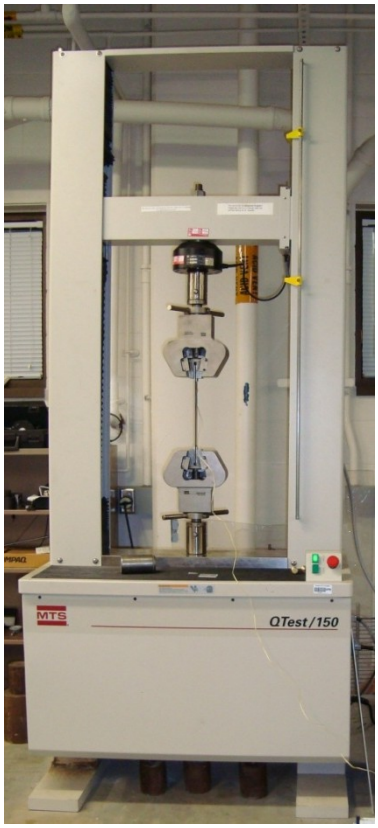

Figure 4.2 MTS machine used for the test

4.3 Test procedure

1. Prepare the coupons for the test by attaching aluminum end tabs using epoxy glue.
2. The specimens are dried at room temperature till the aluminum end tabs are firmly bonded to the test coupons.
3. Make white markings using liquid paper at the edges and around the holes to enhance the visibility during failure progression.
4. Load the test specimen into MTS machine.
5. Connect the strain gauge wires to the strain gauge recording system.
6. The data acquisition system used was QT test works to record load vs. deflection data and a LABVIEW program is used to record strain.

7. The specimens were loaded to failure at a rate of 0.02 inch per minute using an MTS test frame.

8. The load vs. deflection data and strains are automatically recorded by QT test works and labview program simultaneously.

9. The test is interrupted to take pictures of failure.

4.4 Test Results

A set of three to five samples is tested and the resulting strength of the each hole pattern is tabulated in Table 4.1 and also plotted in Figure 4.3. The test scatter data of the test results are also shown in Figure 4.3. The average strength of all the test configurations from high to low is in the following sequence; TBH, SH, SA, SSH and DA. The trend is in consistent with the peak stress of finite element results shown in Figure 3.9.

Table 4.1 Strength of different hole patterns

Configuration	Maximum Stress (ksi)			
	Set 1	Set 2	Set 3	Average
SH	166.23	128.68	172.368	155.760
TBH	161.98	179.02	156.963	165.987
SSH	137.91	132.90	133.114	134.640
SA	146.99	141.05	142.531	143.524
DA	88.75	91.52	91.034	90.435

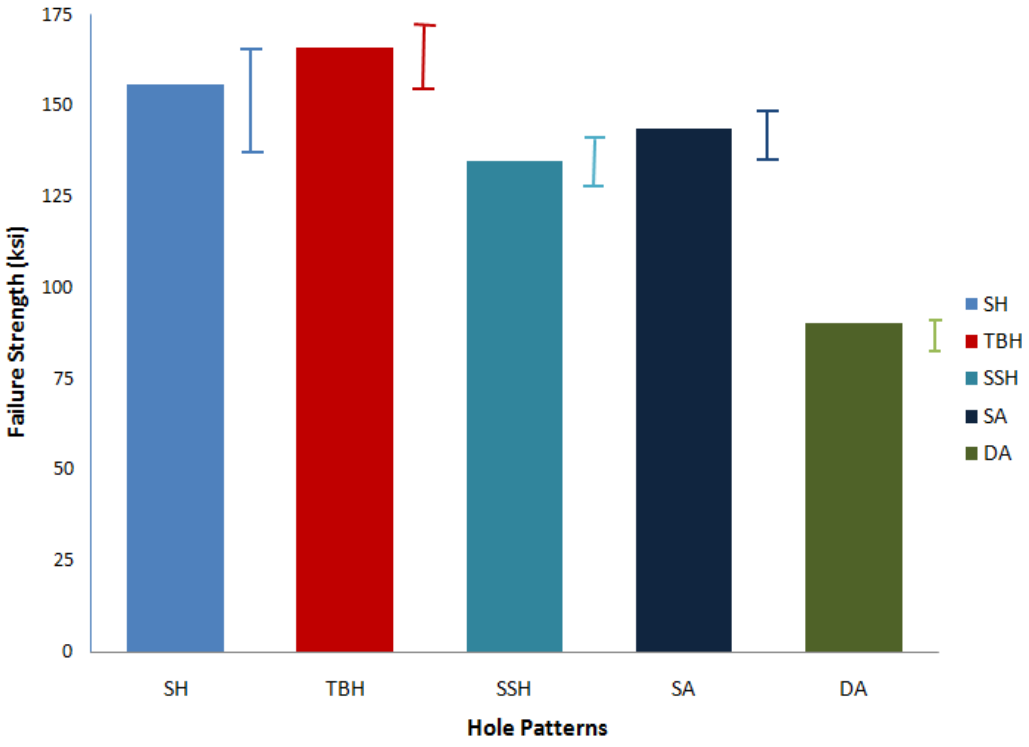

Figure 4.3 Strength of different hole pattern

The linear stress strain diagram is plotted and compared between different hole patterns. The are three sets of specimen tested and stress diagram for each set. The stress strain diagram for set 1, set 2 and set 3 specimens are shown in Figures 4.4, 4.5 and 4.6, respectively.

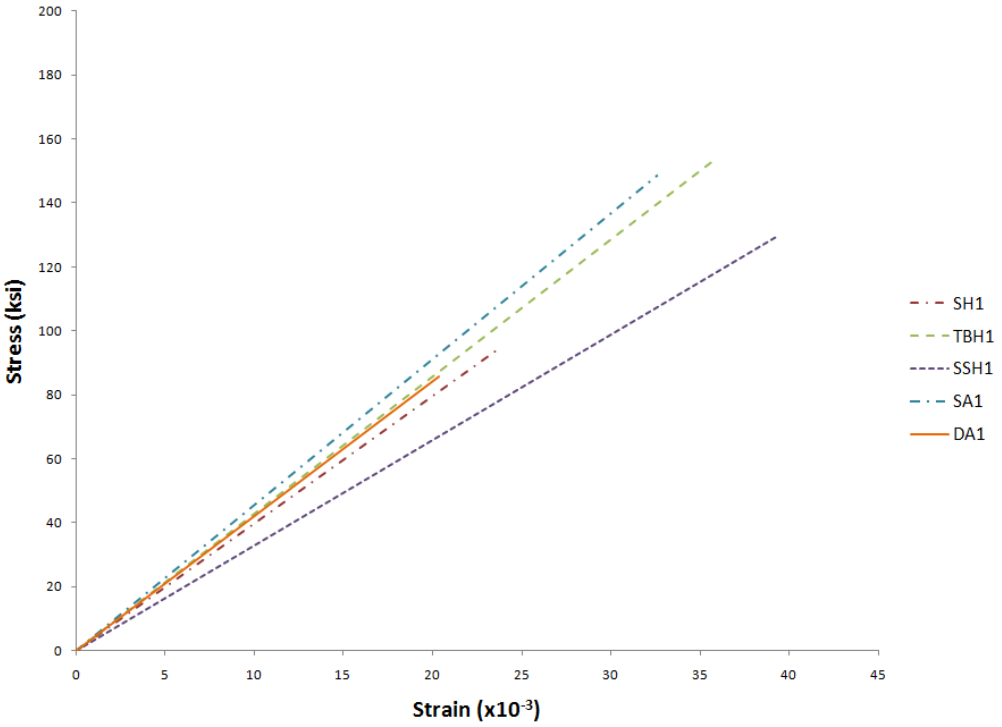

Figure 4.4 Linear stress-strain diagrams for set1 samples

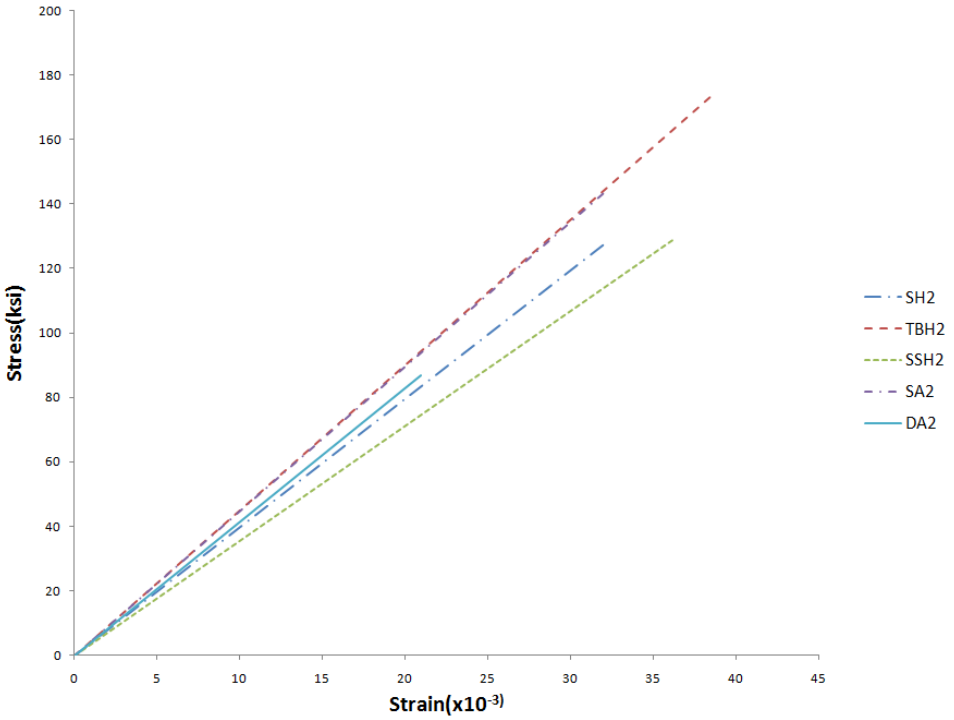

Figure 4.5 Linear stress-strain diagrams for set2 samples

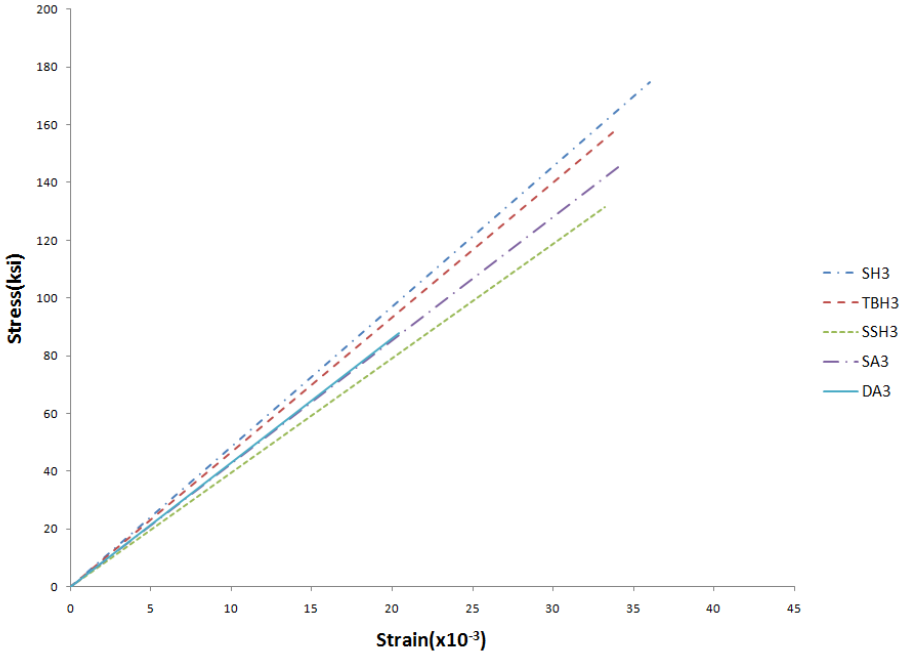

Figure 4.6 Linear stress-strain diagrams for set 3 samples

4.5 Damage observation

All the test specimens exhibited edge delamination before the presence of visible damage around the hole. Figure 4.7 shows the edge delamination of a specimen. The final failure occurs near the hole for all specimens except the SH specimen. The failure in the SH specimen occur not only near the hole but also at location away from the hole as shown in Figure 4.7. The final failure of SH specimen reveal a significant delamination at the neighborhood of the hole and free edge. This may result higher strength of the specimen.

Figure 4.7 Edge delamination

4.5.1 Comparison of failures for SH & TBH hole laminates.

The failure pattern between SH & TBH is shown Figure 4.8. For SH & TBH the failure is significantly due to longitudinal direction. This indicates the splitting failure of 0^0 plies. The failure at the hole is not prominent for these patterns. The TBH has more strength because of an additional hole in-line with the load, resulting in the reduction of peak stress at the hole.

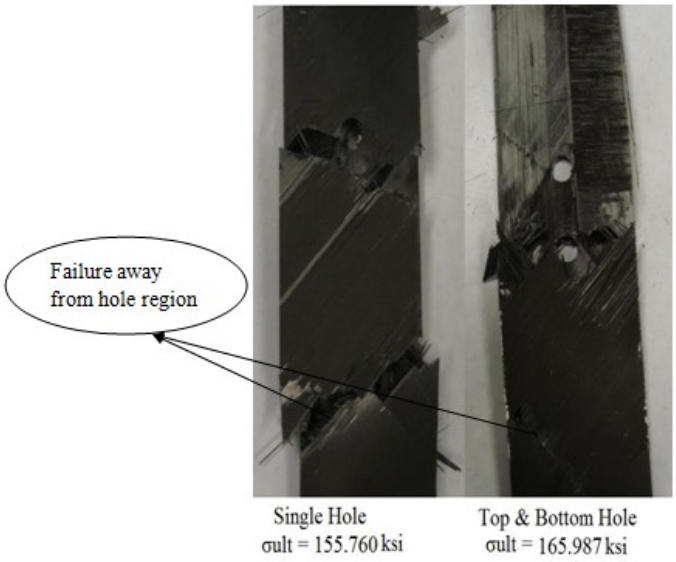

Figure 4.8 Failure comparisons of laminates with SH & TBH pattern

4.5.2 Comparison of failures for SSH & SA hole laminates.

The failure comparison between SSH & SA laminate is shown in Figure 4.9. For SSH laminate the fiber breakage occurs between the holes. The primary failure location is between the hole region. The SA pattern exhibits similar failure pattern as TBH more inclined towards longitudinal direction. Although SA laminate has four hole the laminate strength is higher than the SSH pattern because of the fiber breakage between the holes.

4.5.3 Comparison of failures for SA & DA hole laminates.

The failure comparison between SA & DA pattern is shown in Figure 4.10. Among the both four hole patterns DA has the extensive fiber breakage and the breakage occurs at angle close to the holes. The most prominent failure occurs around the hole region. The interaction between the holes reduces the strength of the laminate. As a four hole pattern SA exhibits highest strength than DA.

Side by Side hole
σult = 134.650 ksi

Square array
σult = 143.524 ksi

Figure 4.9 Failure comparisons of laminates with SSH & SA pattern

Diamond Array
σult = 90.435 ksi

Square Array
σult = 143.524 ksi

Figure 4.10 Failure comparisons of laminates with SA & DA pattern

CHAPTER 5

EFFECTS OF SINGLE PATCH CONFIGURATIONS IN COMPOSITE BONDED REPAIR

The damage in the composite laminate is usually repaired by making circular cutouts at the damaged region. The effect of these circular cutouts on the damaged laminate is studied in the previous chapter. A patch is adhesively bonded to cutout region which changes the load path affecting the stress distribution of the laminate with circular cutouts. In this chapter, the damaged laminate with circular cutouts are designated as parent laminate and laminate which is glued on the parent laminate at the cutout region is designated as patch laminate. Different configurations of patch laminate with multiple hole patterns on the parent laminate are studied which will provide a guideline for structural repair design. The material property, laminate stacking sequence and hole radius is considered the same for all cases.

5.1 Cases investigated

The different hole patterns of parent laminate and patch configurations discussed in Chapter II is considered for the study. The geometric description, material and stacking sequence is given in Chapter 2.1 and Chapter 2.2, respectively.

5.2 General discussion on stress increase due to patch

When the patch is adhesively bonded to parent laminate, the eccentricity of the patch creates moment in addition to the applied load as shown in Figure 5.1. The additional moment greatly influence the increase in the peak stresses on the parent laminate. The deformation plot for an elliptical patch with single hole in parent laminate is shown in Figure 5.2.

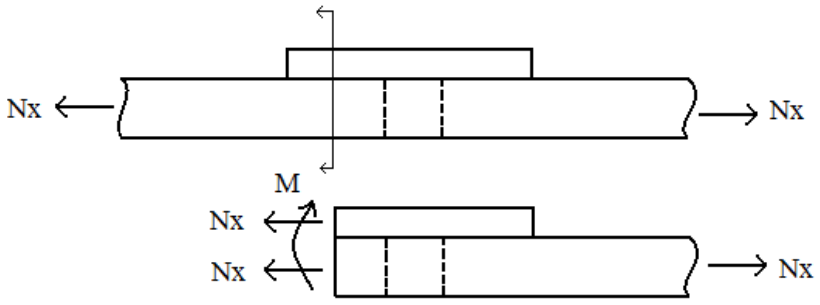

Figure 5.1 Eccentricity of the Patch laminate.

Figure 5.2 Bending due to additional moment

5.4 Effect of patch configurations with SH pattern on parent laminate

5.4.1 In-plane stresses σ_1. σ_2, τ_{12} for bottom 0^0 ply

The in-plane stress is maximum at bottom 0^0 ply in all configurations. The in-plane stresses are tabulated in Table 5.1 and comparison of normalized maximum in-plane stresses for bottom 0^0 ply for SH pattern with different patch configurations is shown in Figure 5.3.

Table 5.1 Normalized maximum stress for SH (0^0 ply -bottom) with different patch configuration

SH - 0^0 ply(bottom)-Normalized maximum in-plane stress			
Configuration	σ_1 / σ_0	σ_2 / σ_0	τ_{12} / σ_0
Without Patch	7.88	0.36	0.57
Square Patch	7.95	0.37	0.55
Hexagonal patch	7.96	0.37	0.55
Octagonal patch	7.97	0.37	0.55
Circular patch	7.97	0.37	0.55
Elliptical patch	7.89	0.37	0.55

The peak stress (σ_1) increases with all patch configurations when compared to No patch in the SH pattern. Among the patch configurations the peak stress (σ_1) is least for elliptical patch configuration but not too significant. σ_2 and τ_{12} show insignificant change with patch attached to the parent laminate.

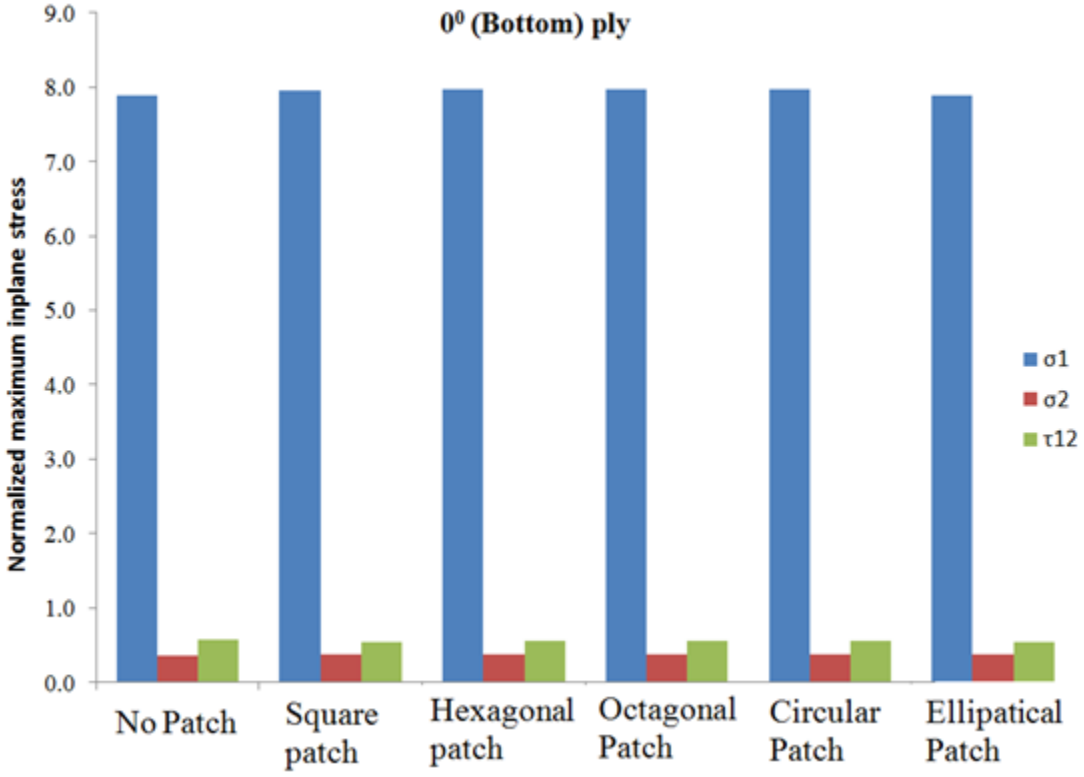

Figure 5.3 Comparison of in-plane stresses (bottom 0^0 layer) for SH pattern with different patch configurations

The stress contour for 0^0 layer in the parent laminate with different patch configuration for SH pattern is shown in figure 5.4,

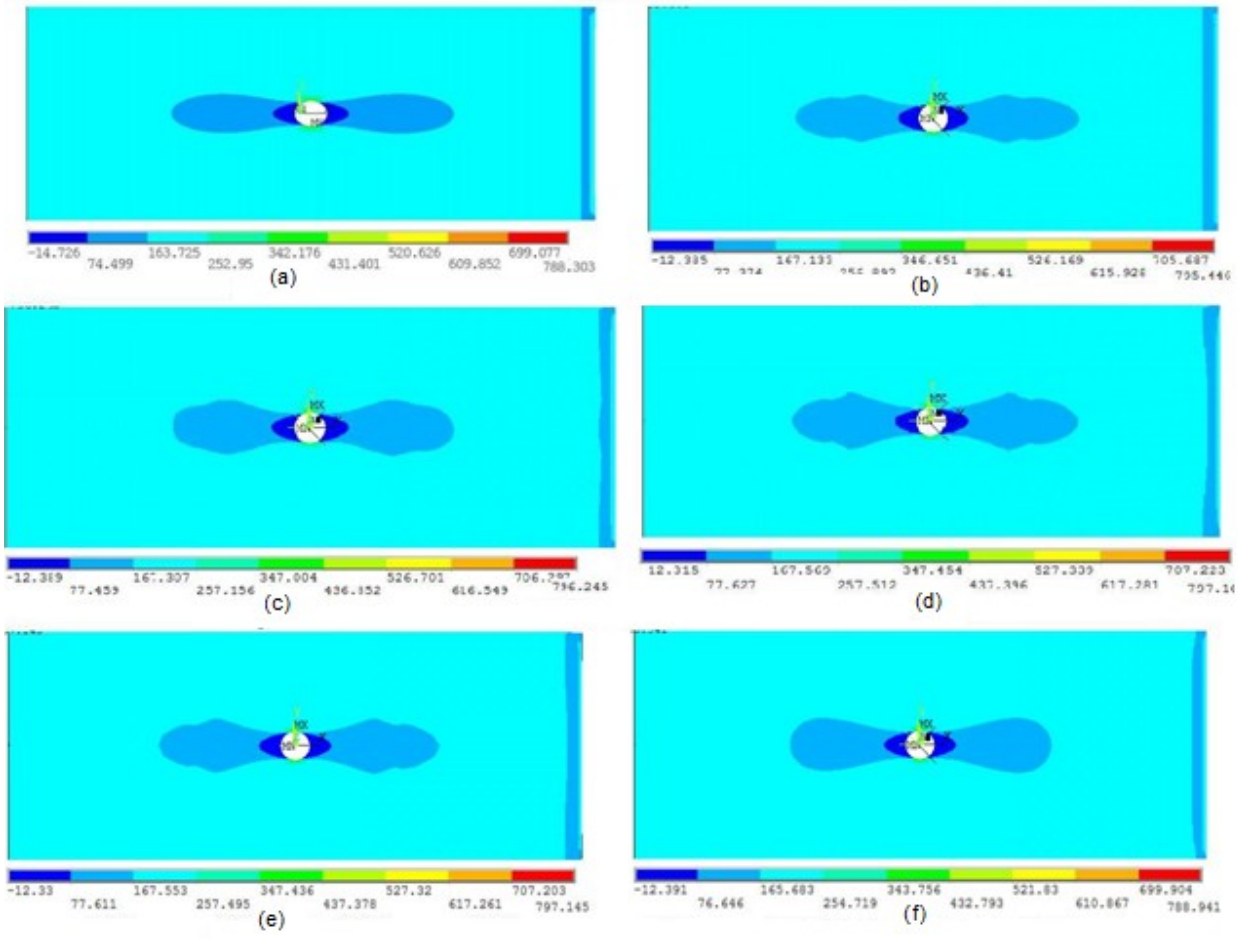

Figure 5.4 Stress contour for 0^0 layer with different patch configuration for SH pattern (a) no patch (b) square (c) hexagonal (d) octagonal (e) circular (f) elliptical

Comparison of the stress contours of the parent laminate (45^0 layer) at the interface between parent and patch laminate for different patch configuration in SH pattern is shown in Figure 5.5,

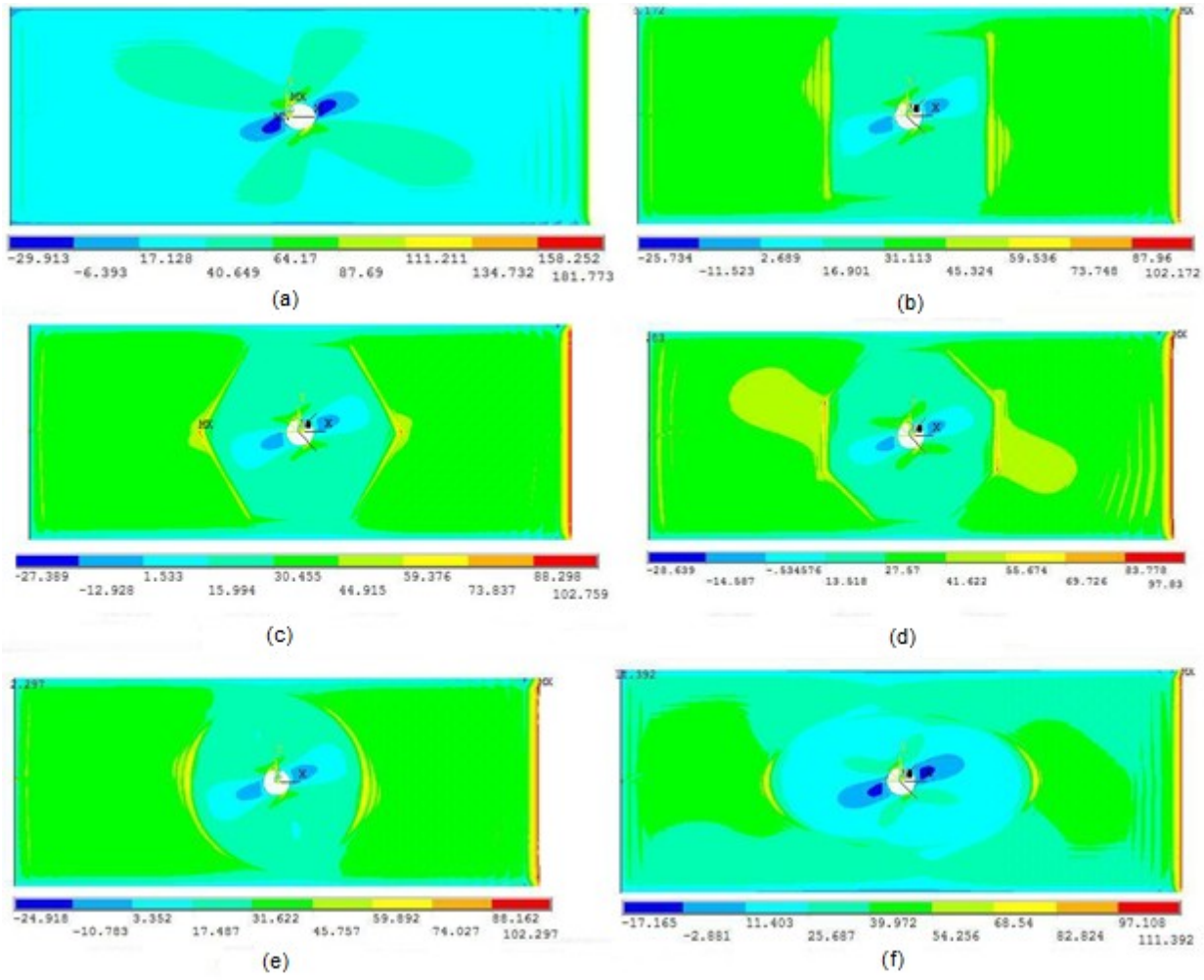

Figure 5.5 Stress contour for 45^0 layer with different patch configuration for SH pattern at parent and patch interface (a) no patch (b) square (c) hexagonal (d) octagonal (e) circular (f) elliptical

5.4.2 In-plane stresses σ_1, σ_2, τ_{12} for bottom $+45^0$ & -45^0 ply

The normalized maximum in-plane stresses for $+45^0$ & -45^0 plies are tabulated in Tables 5.2 & 5.3, respectively and comparison of normalized maximum in-plane stresses for $+45^0$ & -45^0 plies for SH pattern with different patch configurations is shown in Figure 5.6 & 5.7, respectively. Like 0^0 ply, σ_2 and τ_{12} of $+45^0$ & -45^0 plies remain insignificant change for the laminate with a patch.

Table 5.2 Normalized maximum in-plane stress for SH (45^0 ply -bottom) with different patch configurations

SH 45^0 ply(bottom)-Normalized in-plane stress			
Configuration	σ_1 / σ_0	σ_2 / σ_0	τ_{12} / σ_0
Without Patch	1.82	1.41	1.51
Square Patch	2.10	1.69	1.80
Hexagonal patch	2.10	1.69	1.80
Octagonal patch	2.10	1.68	1.80
Circular patch	2.10	1.68	1.80
Elliptical patch	2.08	1.67	1.78

Table 5.3 Normalized maximum in-plane stress for SH (-45^0 ply -bottom) with different patch configurations

SH -45^0ply(bottom)-Normalized in-plane stress			
Configuration	σ_1 / σ_0	σ_2 / σ_0	τ_{12} / σ_0
Without Patch	2.49	2.07	1.45
Square Patch	2.70	2.23	1.50
Hexagonal patch	2.70	2.23	1.50
Octagonal patch	2.70	2.23	1.50
Circular patch	2.70	2.23	1.50
Elliptical patch	2.68	2.22	1.49

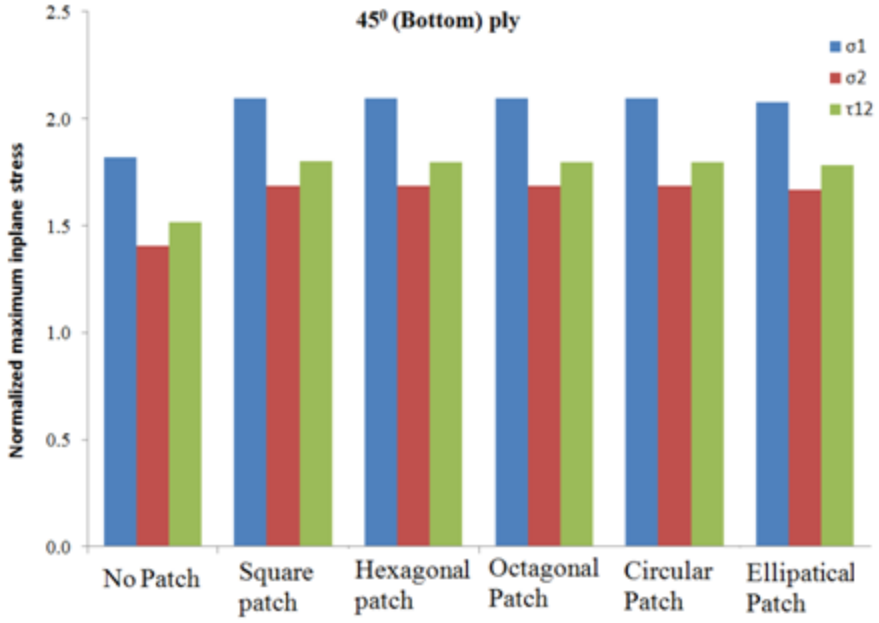

Figure 5.6 Comparison of in-plane stresses (bottom 45^0 layer) for SH pattern with different patch configurations

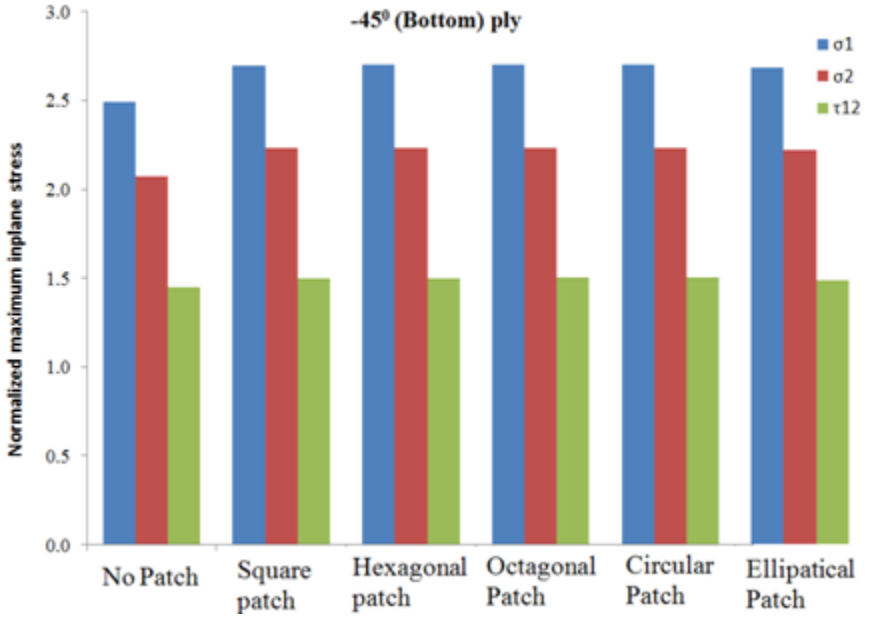

Figure 5.7 Comparison of in-plane stresses (bottom -45^0 layer) for SH pattern with different patch configurations

5.5.3 Interlaminar stresses σ_3, τ_{23} at the interfaces

There are two interfaces where the interlaminar stresses are critical.

1. Interface between parent laminate and adhesive.

2. Interface between patch laminate and adhesive.

The interlaminar stresses are plotted across the width of the laminate at the center as shown in Figure 5.8. The interlaminar stresses are maximum at the edge of the patch and holes.

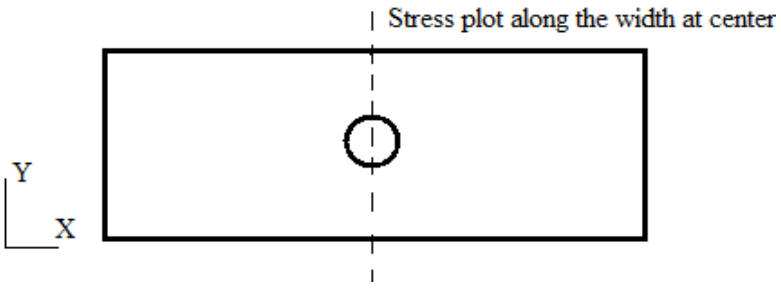

Figure 5.8 Location of stress plot along width of the laminate

The σ_3, τ_{23} distribution is along the width of the laminate at parent and adhesive interface is shown in Figures 5.9 & 5.10.

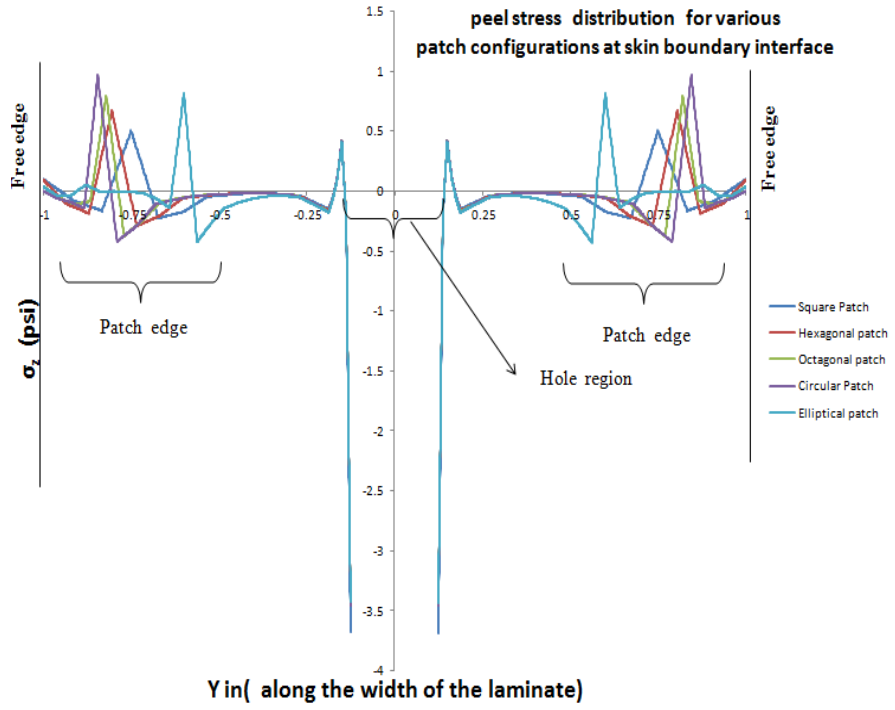

Figure 5.9 σ_3 stress at parent laminate and adhesive interface for all patch configurations

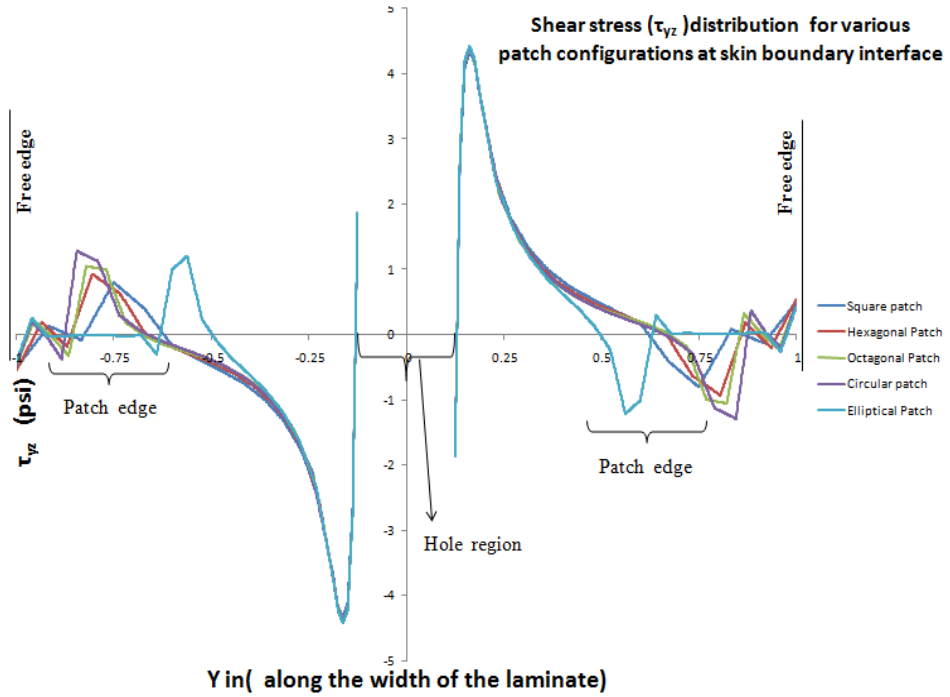

Figure 5.10 τ_{23} stress at parent laminate and adhesive interface for all patch configurations

The σ_3, τ_{23} distribution is along the width of the laminate at patch and adhesive interface is shown in the figures 5.11 and 5.12.

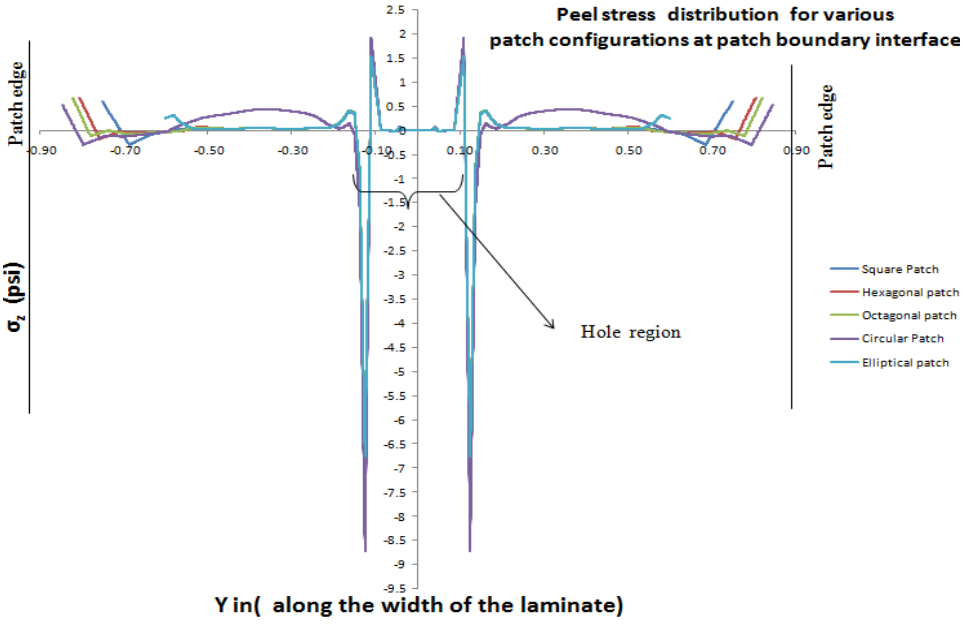

Figure 5.11 σ_3 stress at patch laminate and adhesive interface for all patch configurations

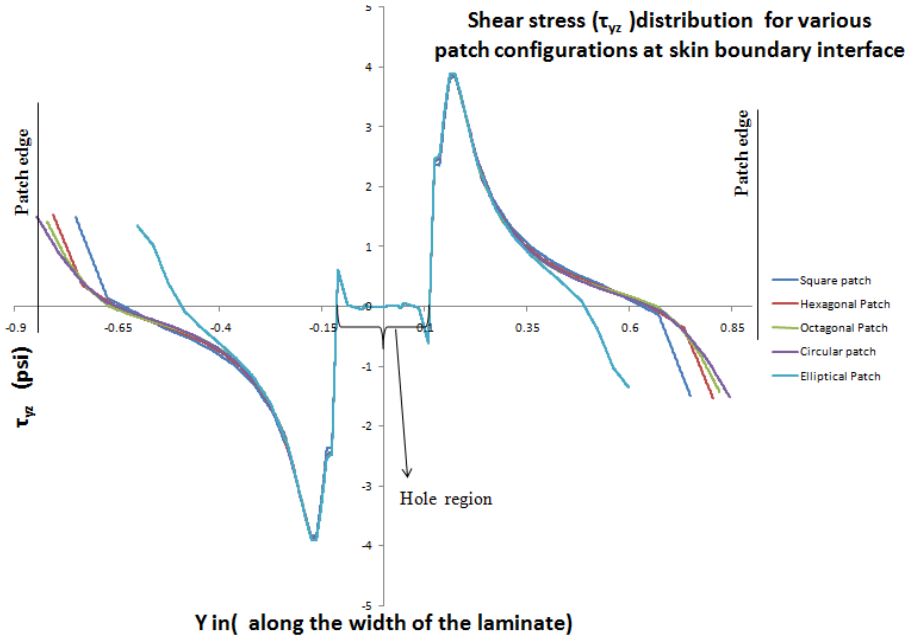

Figure 5.12 τ_{23} stress at patch laminate and adhesive interface for all patch configurations

5.5 Effect of patch configurations with TBH pattern on parent laminate

5.5.1 In-plane stresses σ_1. σ_2, τ_{12} for bottom 0^0 ply

The in-plane stress is maximum at bottom 0^0 ply in all configurations. The in-plane stresses are tabulated in Table 5.4 and comparison of normalized maximum in-plane stresses for bottom 0^0 ply for TBH pattern with different patch configurations is shown in Figure 5.13.

Table 5.4 Normalized maximum stress for TBH (0^0 ply -bottom) with different patch configuration

TBH -0^0 ply(bottom)-Normalized in-plane stress			
Configuration	σ_1 / σ_0	σ_2 / σ_0	τ_{12} / σ_0
Without Patch	7.19	0.34	0.53
Square Patch	7.47	0.36	0.52
Hexagonal patch	7.42	0.35	0.52
Octagonal patch	7.64	0.35	0.54
Circular patch	7.43	0.35	0.52
Elliptical patch	7.37	0.35	0.51

The peak stress (σ_1) increases with all patch configurations when compared to No patch in the TBH pattern. Among the patch configurations the peak stress (σ_1) is least for elliptical patch configuration but not too significant.

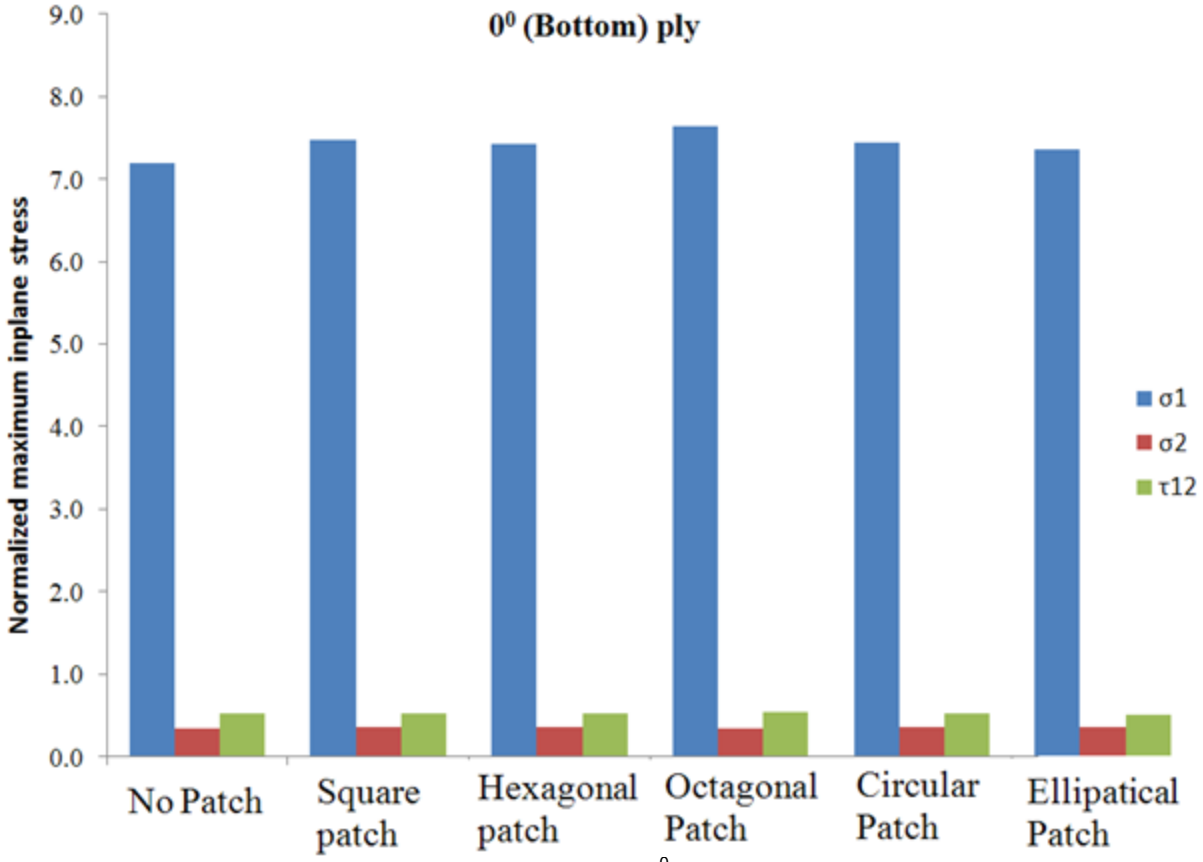

Figure 5.13 Comparison of in-plane stresses (bottom 0^0 layer) for TBH pattern with different patch configurations

The stress contour for 0^0 layer with different patch configuration for TBH pattern is shown in Figure 5.14,

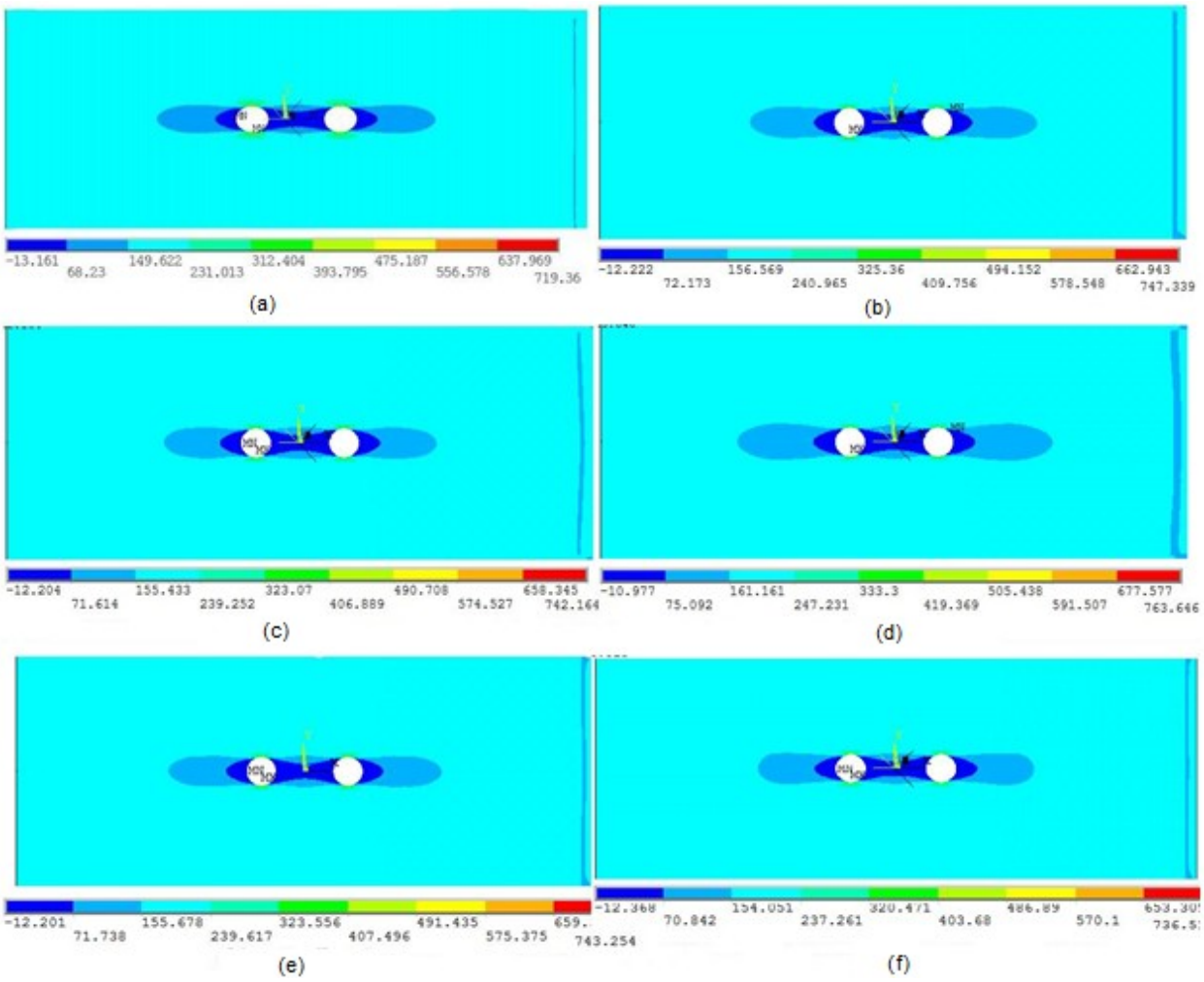

Figure 5.14 Stress contour for 0^0 layer with different patch configuration for TBH pattern (a) no patch (b) square (c) hexagonal (d) octagonal (e) circular (f) elliptical

Comparison of the stress contours of the parent laminate (45^0 layer) at the interface between parent and patch laminate for different patch configuration in TBH pattern is shown in Figure 5.15,

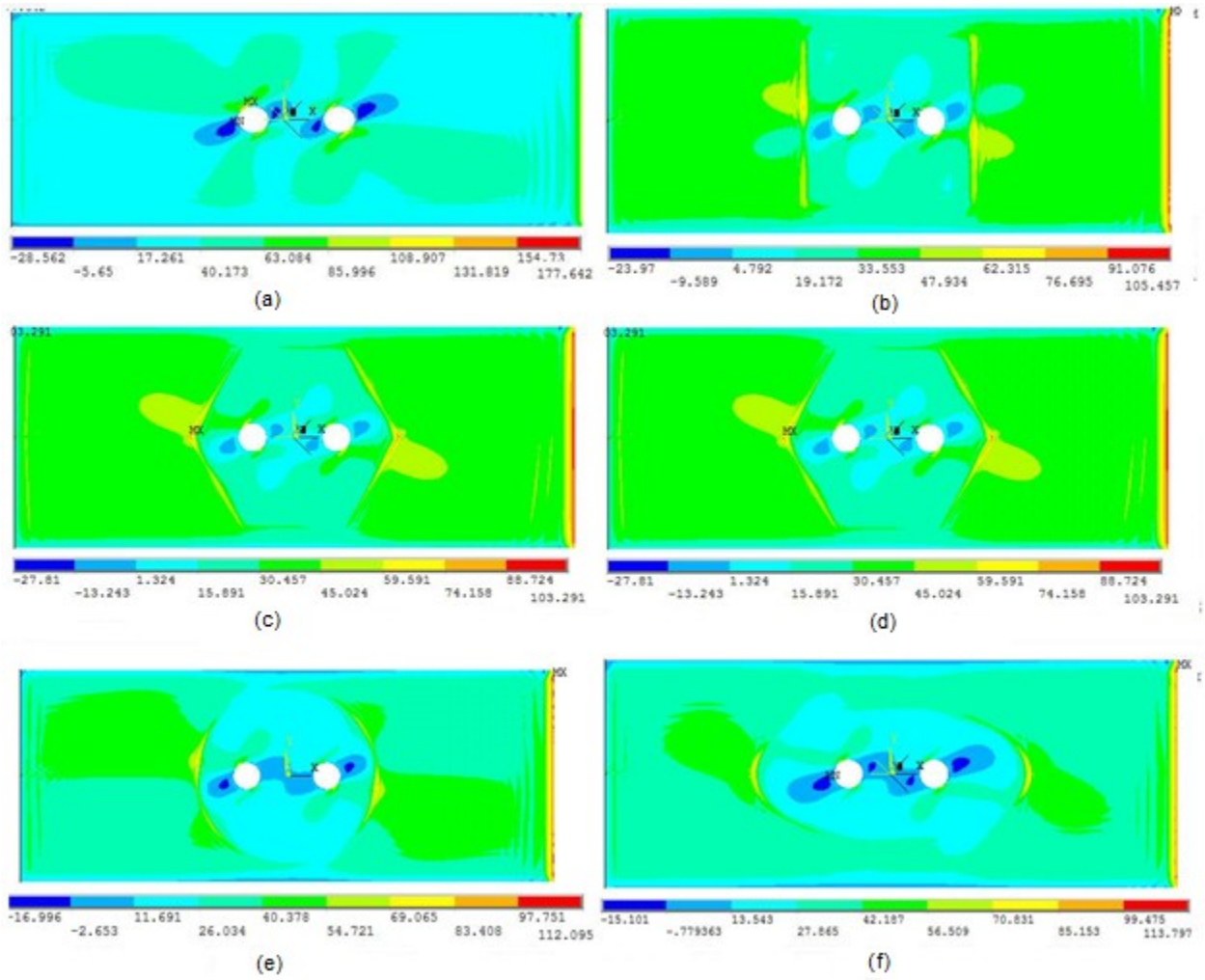

Figure 5.15 Stress contour for 45^0 layer with different patch configuration for TBH pattern at parent and patch interface (a) no patch (b) square (c) hexagonal (d) octagonal (e) circular (f) elliptical

5.5.2 In-plane stresses σ_1. σ_2, τ_{12} for bottom $+45^0$& -45^0ply

The normalized maximum in-plane stresses for $+45^0$ & -45^0 plies are tabulated in Tables 5.5 & 5.6 respectively and comparison of normalized maximum in-plane stresses for $+45^0$ & -45^0 plies for TBH pattern with different patch configurations is shown in Figures 5.16 & 5.17, respectively.

Table 5.5 Normalized maximum in-plane stress for TBH (45^0 ply -bottom) with different patch configurations

TBH 45^0 ply(bottom)-Normalized in-plane stress			
Configuration	σ_1 / σ_0	σ_2 / σ_0	τ_{12} / σ_0
Without Patch	1.78	1.39	1.49
Square Patch	2.05	1.65	1.76
Hexagonal patch	2.02	1.63	1.73
Octagonal patch	2.06	1.66	1.80
Circular patch	2.03	1.63	1.74
Elliptical patch	2.02	1.63	1.74

Table 5.6 Normalized maximum in-plane stress for TBH (-45^0 ply -bottom) with different patch configurations

TBH -45^0 ply(bottom)-Normalized in-plane stress			
Configuration	σ_1 / σ_0	σ_2 / σ_0	τ_{12} / σ_0
Without Patch	2.40	2.00	1.35
Square Patch	2.63	2.18	1.43
Hexagonal patch	2.59	2.15	1.41
Octagonal patch	2.56	2.17	1.40
Circular patch	2.60	2.16	1.42
Elliptical patch	2.59	2.15	1.40

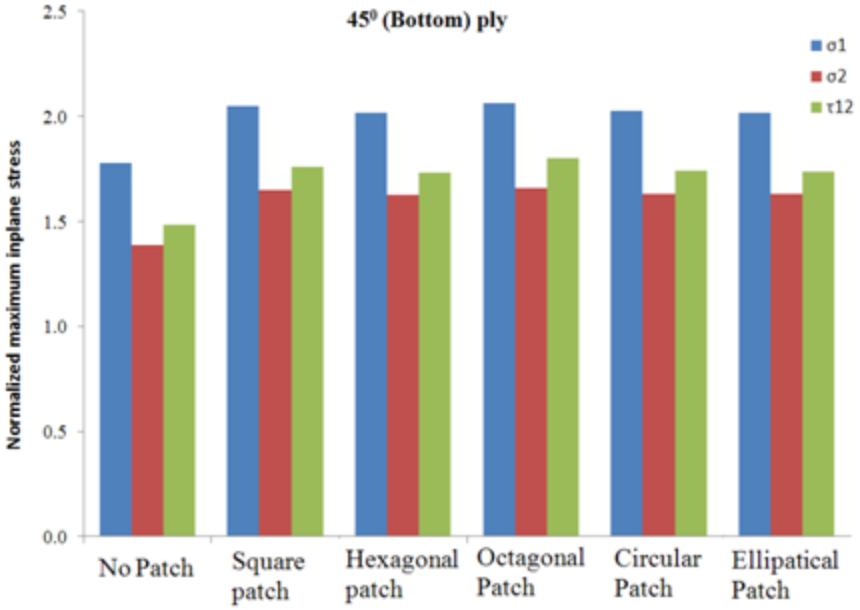

Figure 5.16 Comparison of in-plane stresses (bottom 45^0 layer) for TBH pattern with different patch configurations

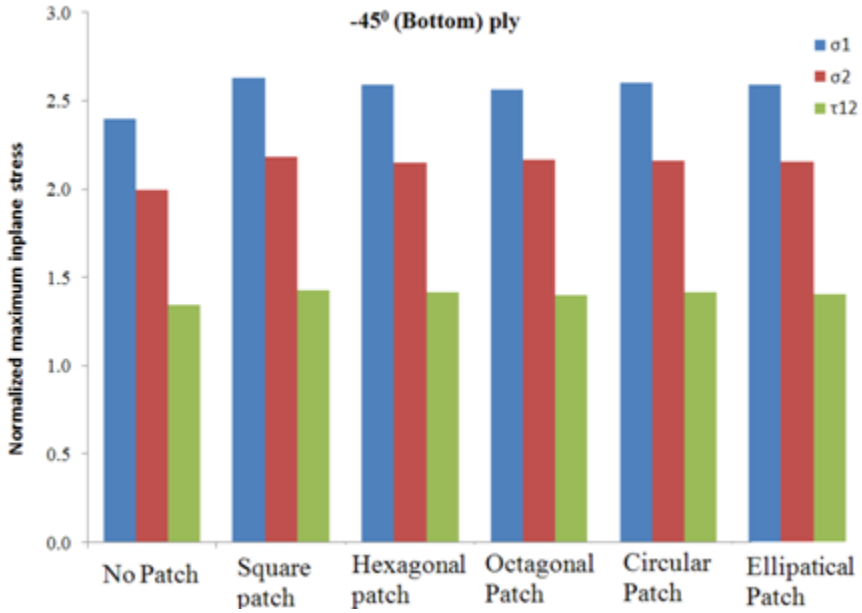

Figure 5.17 Comparison of in-plane stresses (bottom -45^0 layer) for TBH pattern with different patch configurations

5.5.3 Interlaminar stresses σ_3, τ_{23} at the interfaces

There are two interfaces where the interlaminar stresses are critical.

1. Interface between parent laminate and adhesive.

2. Interface between patch laminate and adhesive.

The interlaminar stresses are plotted across the width of the laminate at the center as shown in Figure 5.18. The interlaminar stresses are maximum at the edge of the patch and holes.

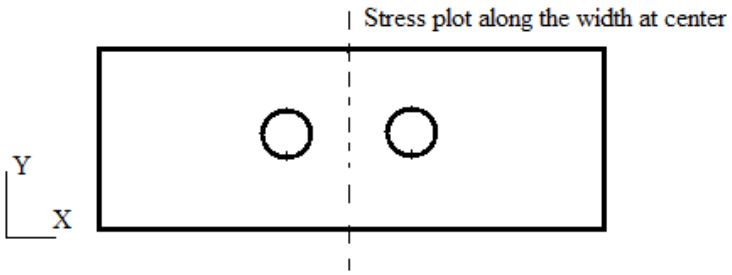

Figure 5.18 Location of stress plot along width of the laminate

The σ_3, τ_{23} distribution is along the width of the laminate at parent and adhesive interface is shown in Figures 5.19 & 5.20.

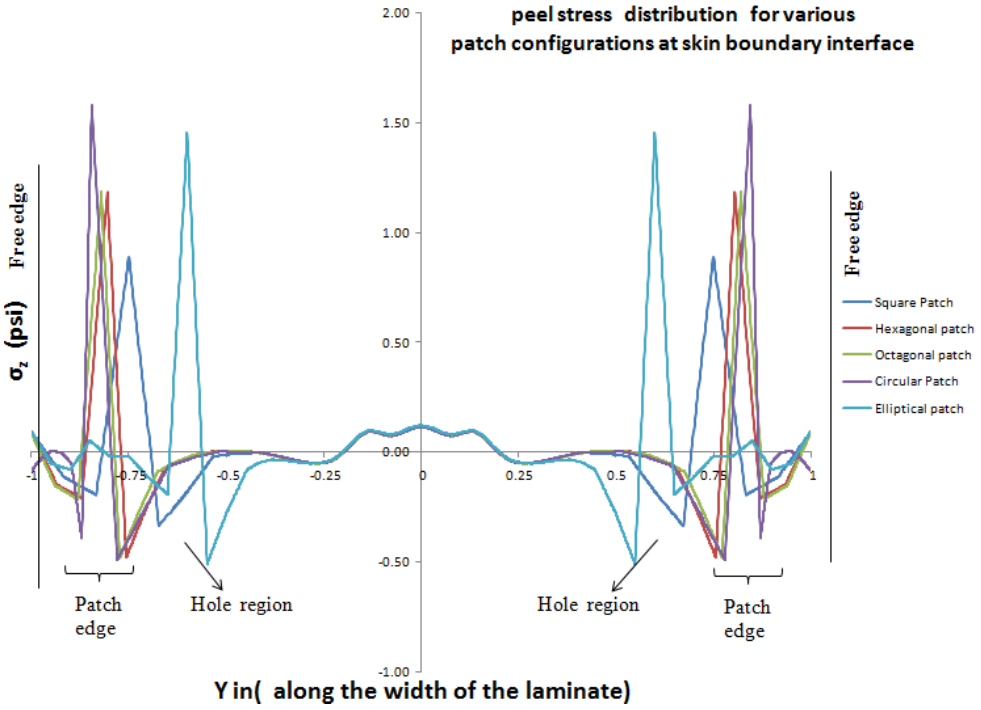

Figure 5.19 σ_3 stress at parent laminate and adhesive interface for all patch configurations

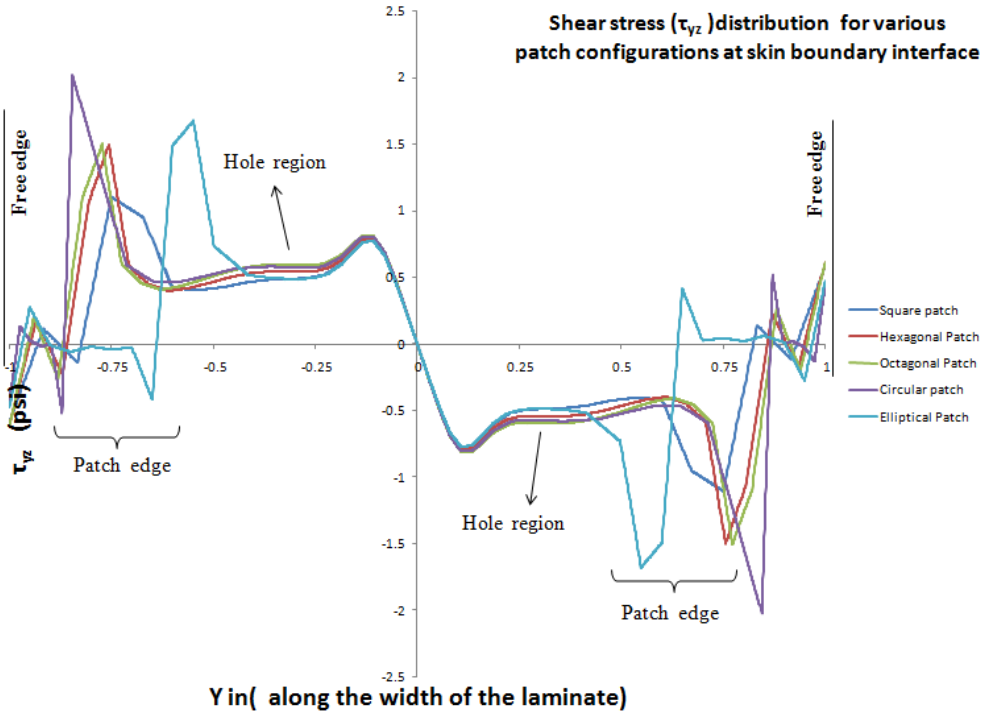

Figure 5.20 τ_{23} stress at parent laminate and adhesive interface for all patch configurations

The σ_3, τ_{23} distribution is along the width of the laminate at patch and adhesive interface is shown in Figures 5.21 & 5.22.

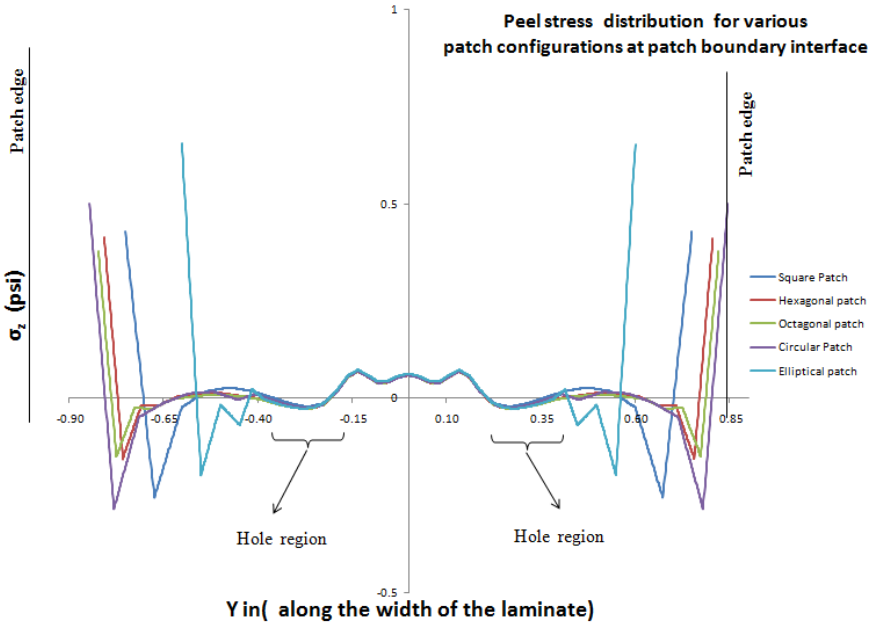

Figure 5.21 σ_3 stress at patch laminate and adhesive interface for all patch configurations

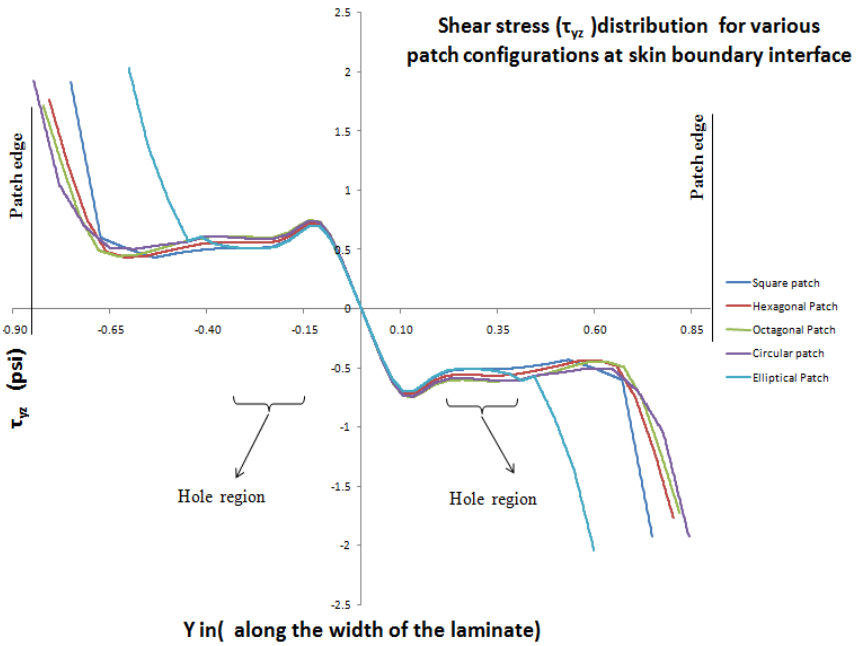

Figure 5.22 τ_{23} stress at patch laminate and adhesive interface for all patch configurations

5.6 Effect of patch configurations with SSH pattern on parent laminate

5.6.1 In-plane stresses σ_1, σ_2, τ_{12} for bottom 0^0 ply

The in-plane stress is maximum at bottom 0^0 ply in all configurations. The in-plane stresses are tabulated in Table 5.7 and comparison of normalized maximum in-plane stresses for bottom 0^0 ply for SSH pattern with different patch configurations is shown in Figure 5.23.

Table 5.7 Normalized maximum stress for SSH (0^0 ply -bottom) with different patch configuration

SSH -0^0 ply(bottom)-Normalized in-plane stress			
Configuration	σ_1 / σ_0	σ_2 / σ_0	τ_{12} / σ_0
Without Patch	8.16	0.37	0.59
Square Patch	8.44	0.40	0.58
Hexagonal patch	8.45	0.40	0.58
Octagonal patch	8.45	0.40	0.58
Circular patch	8.45	0.40	0.58
Elliptical patch	8.49	0.40	0.58

The peak stress (σ_1) increases with all patch configurations when compared to No patch in the SSH pattern. Among the patch configurations the peak stress (σ_1) is least for square patch configuration but not too significant.

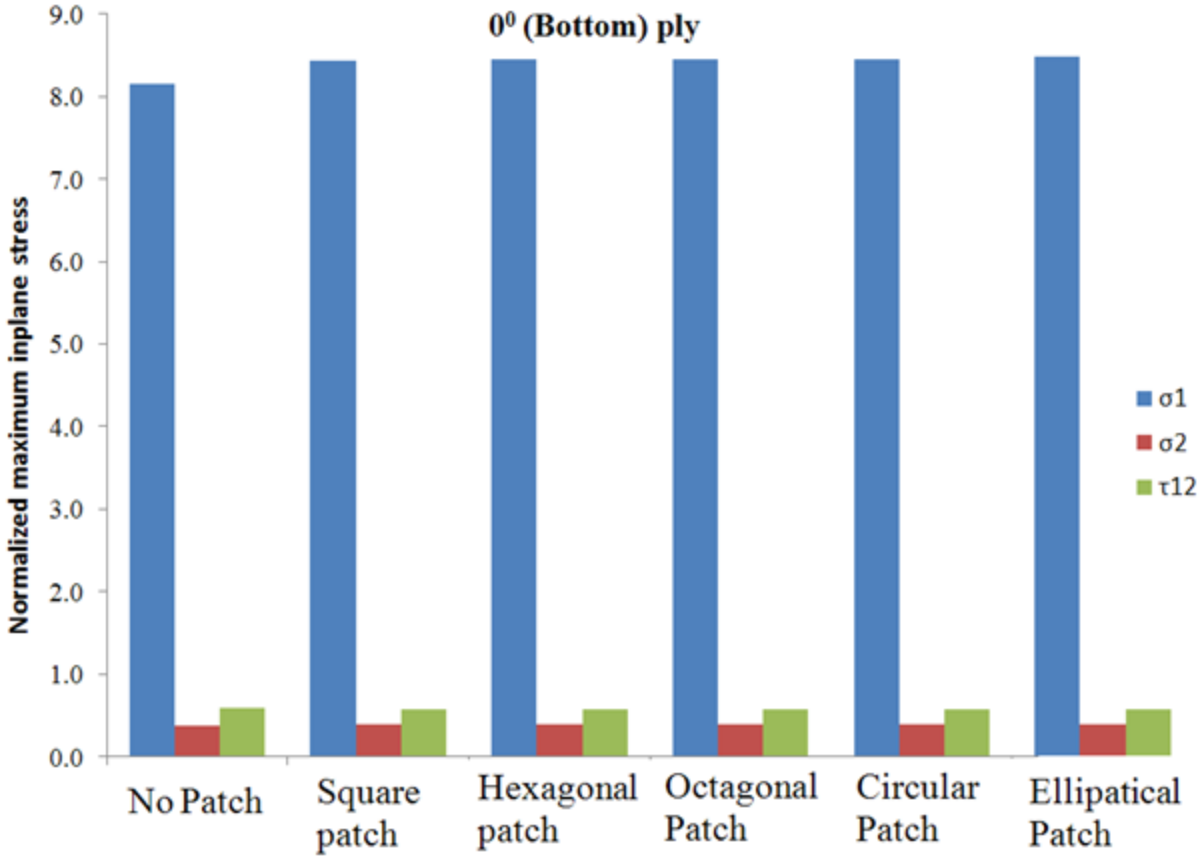

Figure 5.23 Comparison of in-plane stresses (bottom 0^0 layer) for SSH pattern with different patch configurations

The stress contour for 0^0 layer with different patch configuration for SSH pattern is shown in Figure 5.24. The contours of the parent laminate with a patch depict insignificant among all the different patch configurations. This results in no difference of the peak stress in those laminates.

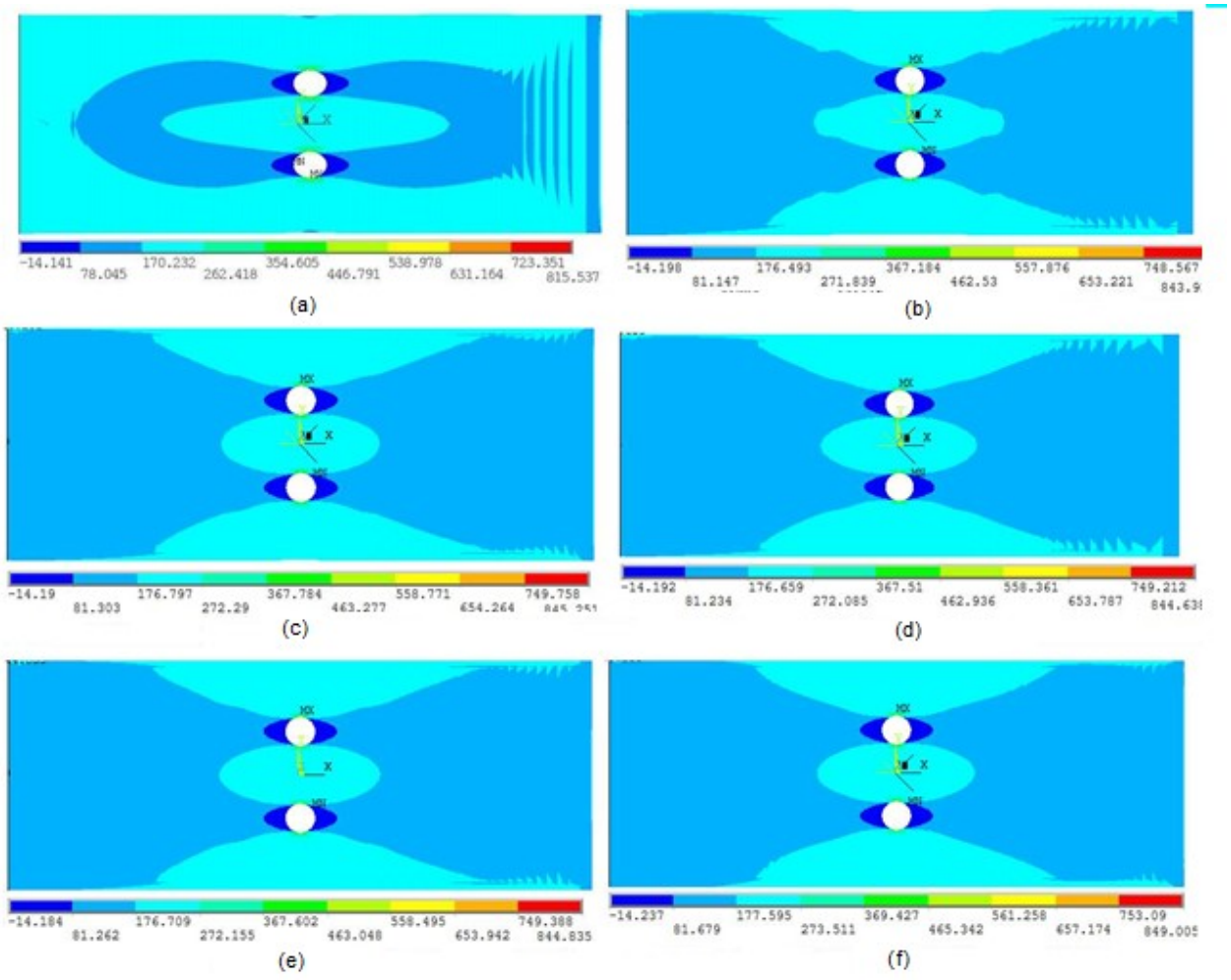

Figure 5.24 Stress contour for 0^0 layer with different patch configuration for SSH pattern (a) no patch (b) square (c) hexagonal (d) octagonal (e) circular (f) elliptical

Comparison of the stress contours of the parent laminate (45^0 layer) at the interface between parent and patch laminate for different patch configuration in SSH pattern is shown in Figure 5.25,

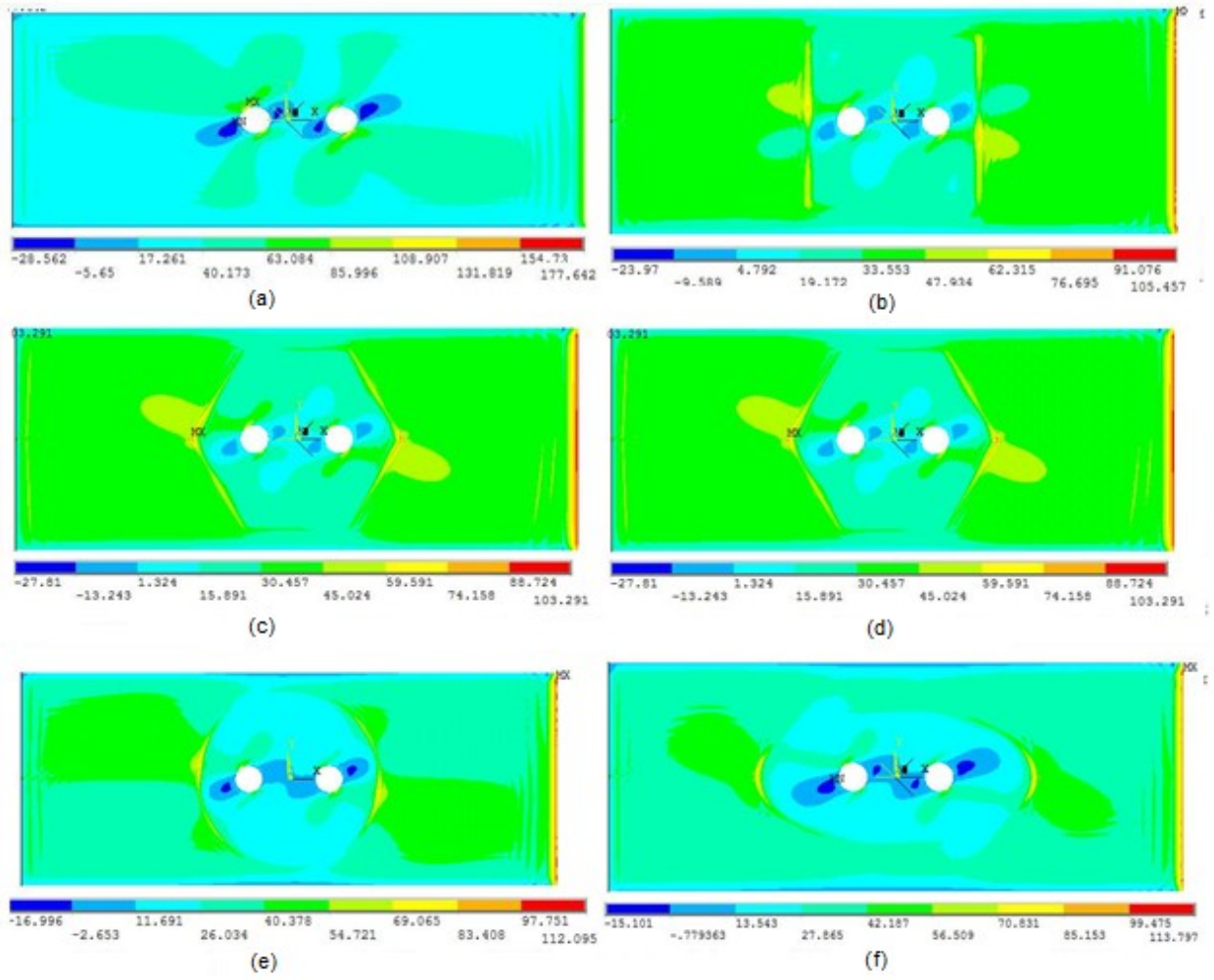

Figure 5.25 Stress contour for 45^0 layer with different patch configuration for SSH pattern at parent and patch interface (a) no patch (b) square (c) hexagonal (d) octagonal (e) circular (f) elliptical

5.6.2 In-plane stresses σ_1. σ_2, τ_{12} for bottom $+45^0$& -45^0ply

The normalized maximum in-plane stresses for $+45^0$ & -45^0 plies are tabulated in Tables 5.8 & 5.9 respectively and comparison of normalized maximum in-plane stresses for $+45^0$ & -45^0 plies for SSH pattern with different patch configurations is shown in Figures 5.26 & 5.27, respectively.

Table 5.8 Normalized maximum in-plane stress for SSH (45^0 ply -bottom) with different patch configurations

SSH 45^0 ply(bottom)-Normalized in-plane stress			
Configuration	σ_1 / σ_0	σ_2 / σ_0	τ_{12} / σ_0
Without Patch	1.96	1.56	1.66
Square Patch	2.27	1.85	1.97
Hexagonal patch	2.27	1.85	1.97
Octagonal patch	2.27	1.84	1.96
Circular patch	2.27	1.84	1.96
Elliptical patch	2.26	1.84	1.96

Table 5.9 Normalized maximum in-plane stress for SSH (-45^0 ply -bottom) with different patch configurations

SSH -45^0 ply(bottom)-Normalized in-plane stress			
Configuration	σ_1 / σ_0	σ_2 / σ_0	τ_{12} / σ_0
Without Patch	2.63	2.18	1.50
Square Patch	2.88	2.40	1.59
Hexagonal patch	2.88	2.40	1.59
Octagonal patch	2.88	2.40	1.59
Circular patch	2.88	2.40	1.59
Elliptical patch	2.88	2.40	1.59

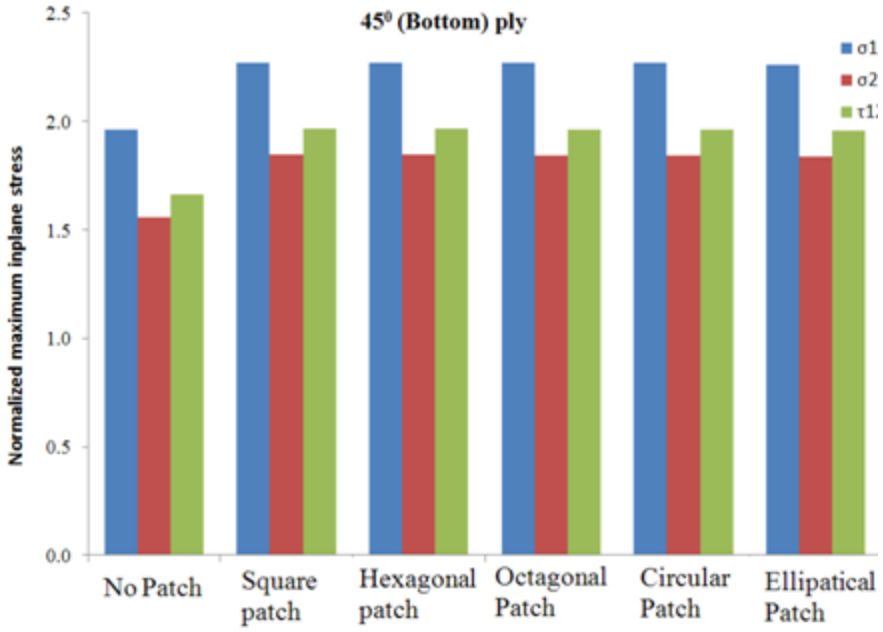

Figure 5.26 Comparison of in-plane stresses (bottom 45^0 layer) for SSH pattern with different patch configurations

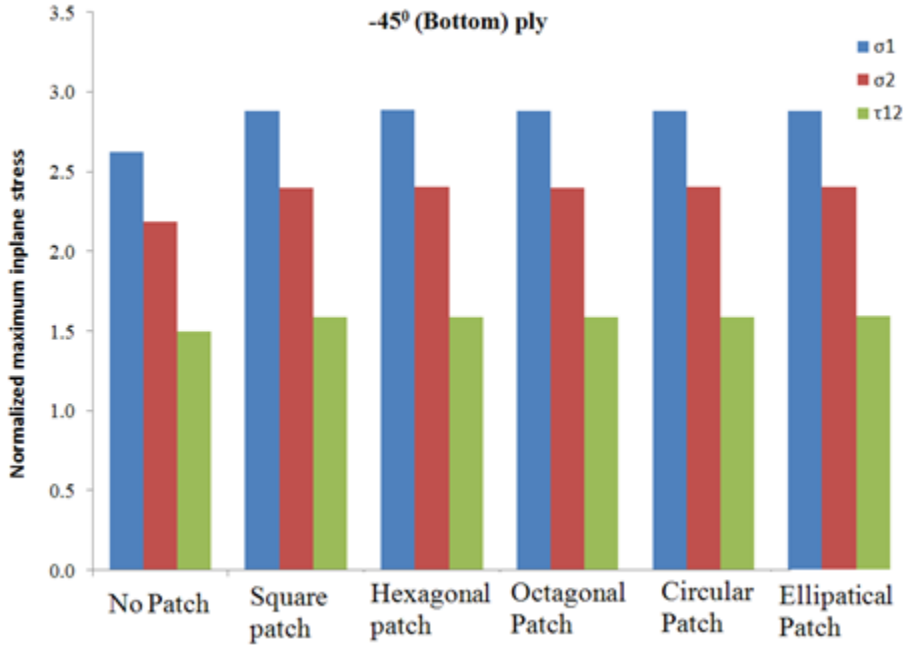

Figure 5.27 Comparison of in-plane stresses (bottom -45^0 layer) for SSH pattern with different patch configurations

5.6.3 Interlaminar stresses σ_3, τ_{23} at the interfaces

There are two interfaces where the interlaminar stresses are critical.

1. Interface between parent laminate and adhesive.

2. Interface between patch laminate and adhesive.

The interlaminar stresses are plotted across the width of the laminate at the center as shown in Figure 5.28. The interlaminar stresses are maximum at the edge of the patch and holes.

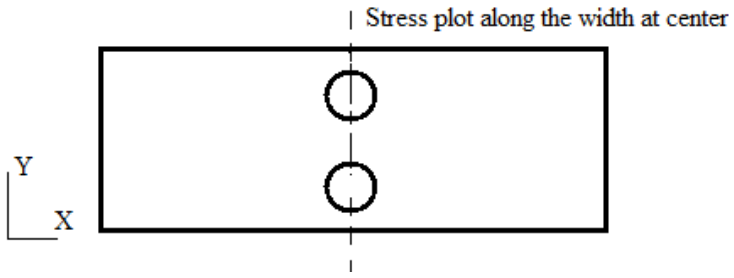

Figure 5.28 Location of stress plot along width of the laminate

The σ_3, τ_{23} distribution is along the width of the laminate at parent and adhesive interface is shown in Figures 5.29 & 5.30.

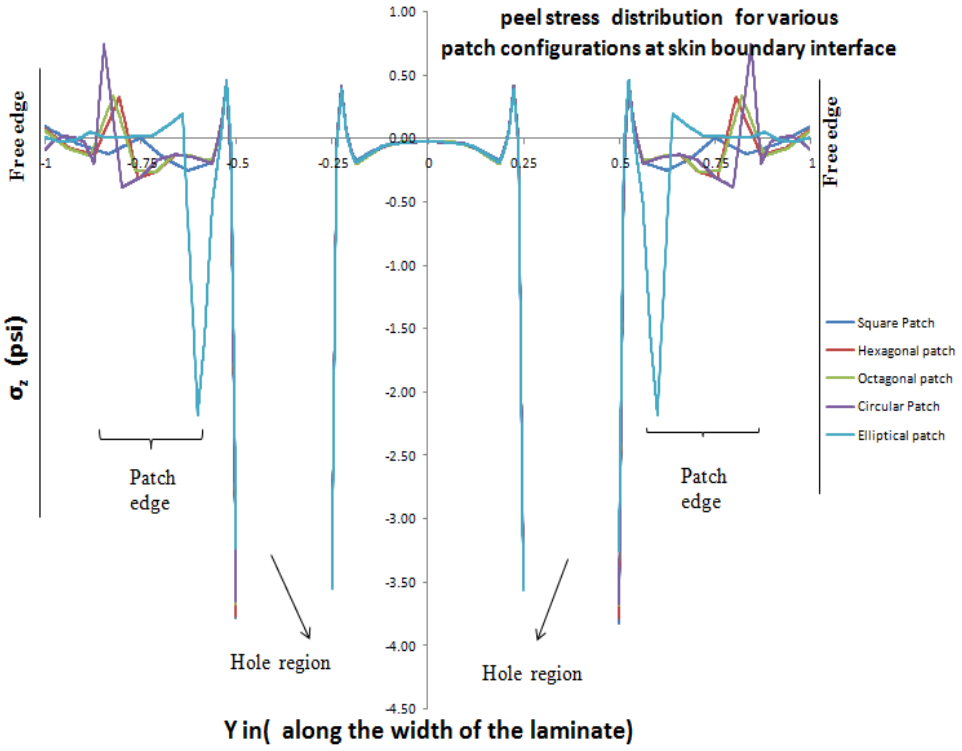

Figure 5.29 σ_3 stress at parent laminate and adhesive interface for all patch configurations

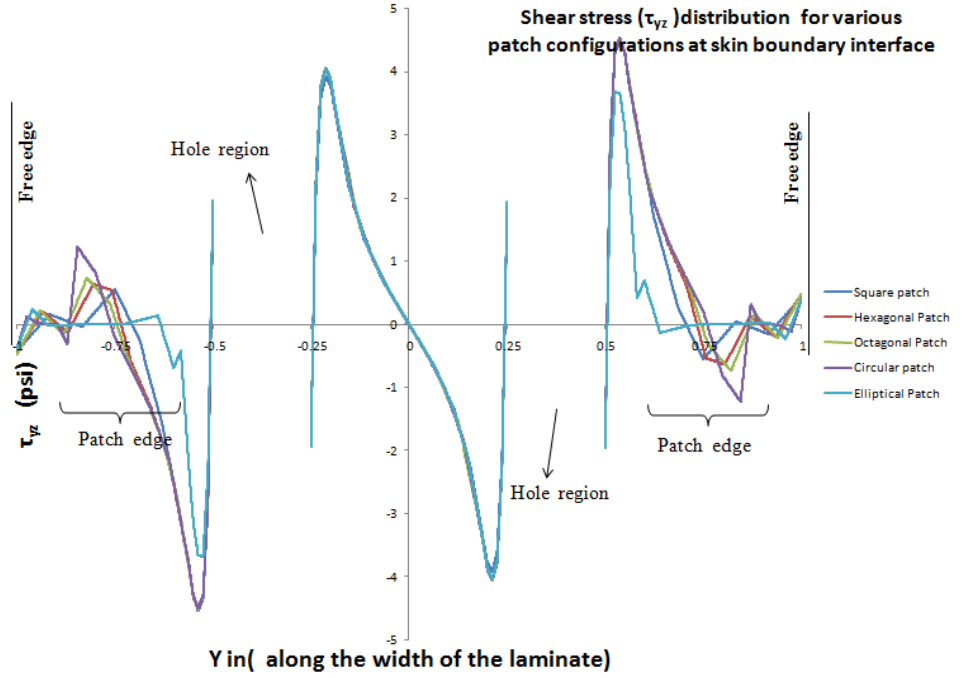

Figure 5.30 τ_{23} stress at parent laminate and adhesive interface for all patch configurations

The σ_3, τ_{23} distribution is along the width of the laminate at patch and adhesive interface is shown in Figures 5.31 & 5.32.

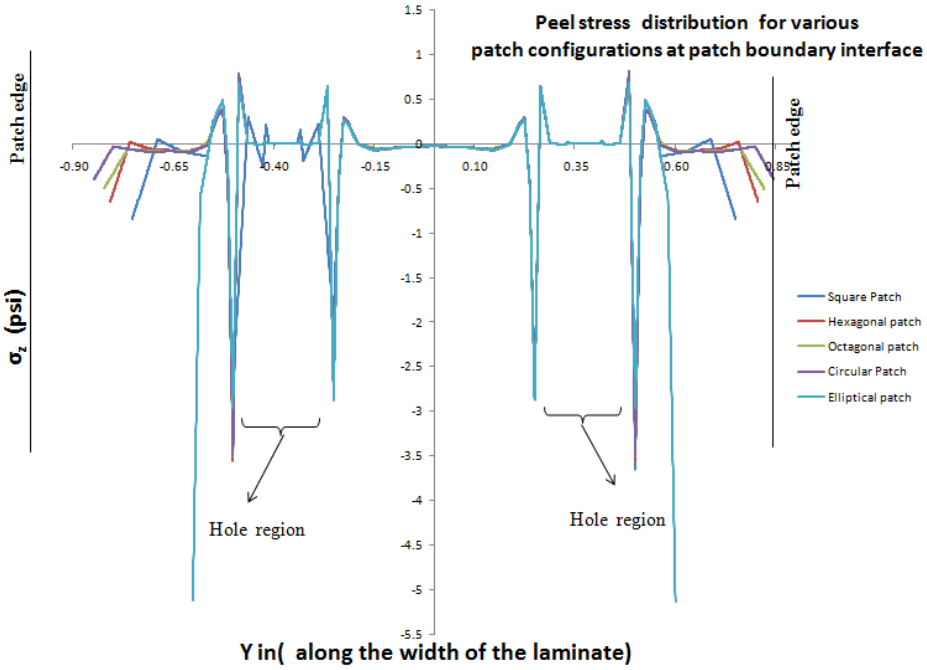

Figure 5.31 σ_3 stress at patch laminate and adhesive interface for all patch configurations

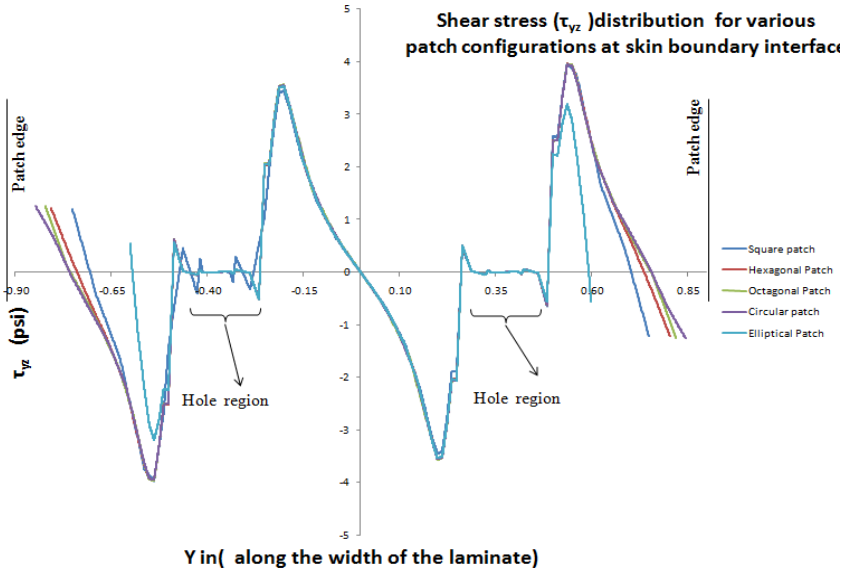

Figure 5.32 τ_{23} stress at patch laminate and adhesive interface for all patch configurations

5.7 Effect of patch configurations with SA pattern on parent laminate

5.7.1 In-plane stresses σ_1. σ_2, τ_{12} for bottom 0^0 ply

The in-plane stress is maximum at bottom 0^0 ply in all configurations. The in-plane stresses are tabulated in Table 5.10 and comparison of normalized maximum in-plane stresses for bottom 0^0 ply for SA pattern with different patch configurations is shown in Figure 5.33.

Table 5.10 Normalized maximum stress for SA (0^0 ply -bottom) with different patch configuration

SA -0^0 ply(bottom)-Normalized in-plane stress			
Configuration	σ_1 / σ_0	σ_2 / σ_0	τ_{12} / σ_0
Without Patch	7.62	0.36	0.56
Square Patch	8.07	0.39	0.56
Hexagonal patch	8.28	0.38	0.58
Octagonal patch	8.23	0.38	0.58
Circular patch	8.50	0.38	0.61
Elliptical patch	8.21	0.39	0.59

The peak stress (σ_1) increases with all patch configurations when compared to No patch in the SA pattern. Among the patch configurations the peak stress (σ_1) is least for square patch configuration but not too significant.

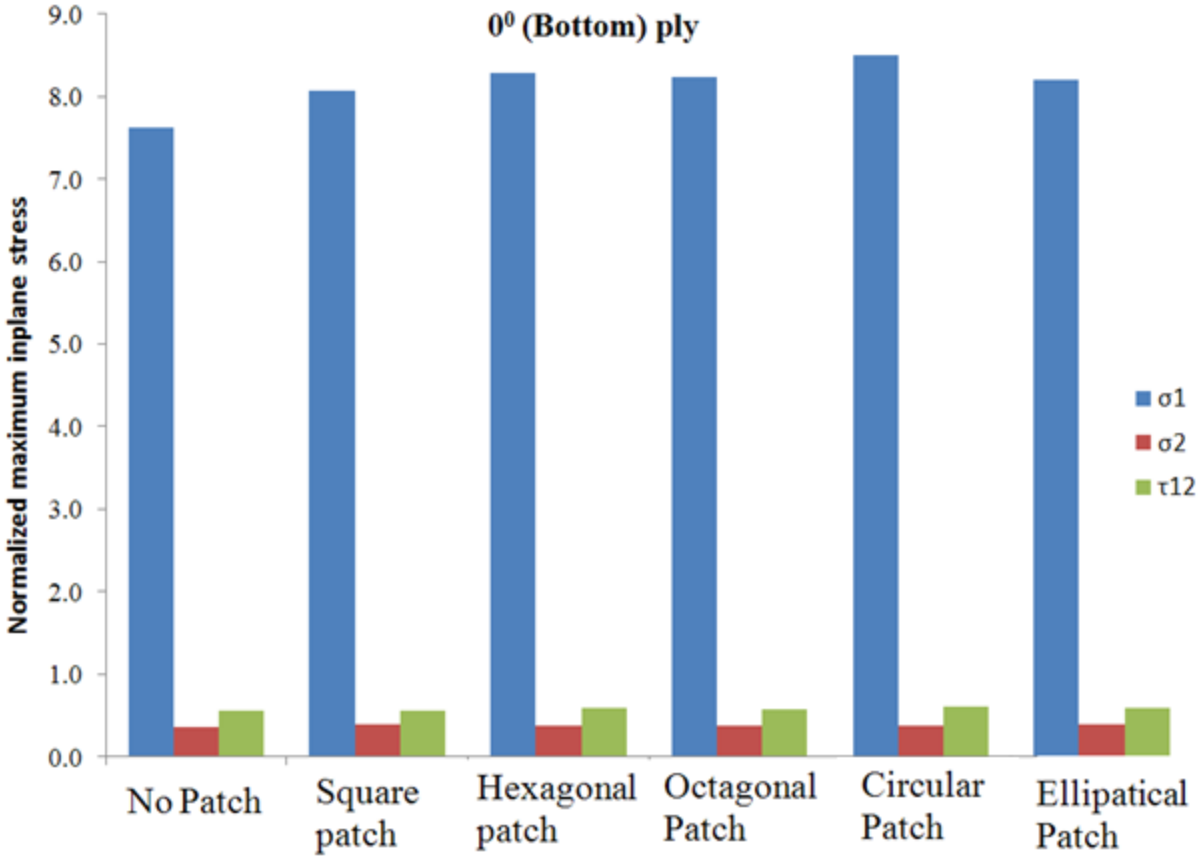

Figure 5.33 Comparison of in-plane stresses (bottom 0^0 layer) for SA pattern with different patch configurations

The stress contour for 0^0 layer with different patch configuration for SA pattern is shown in figure 5.34,

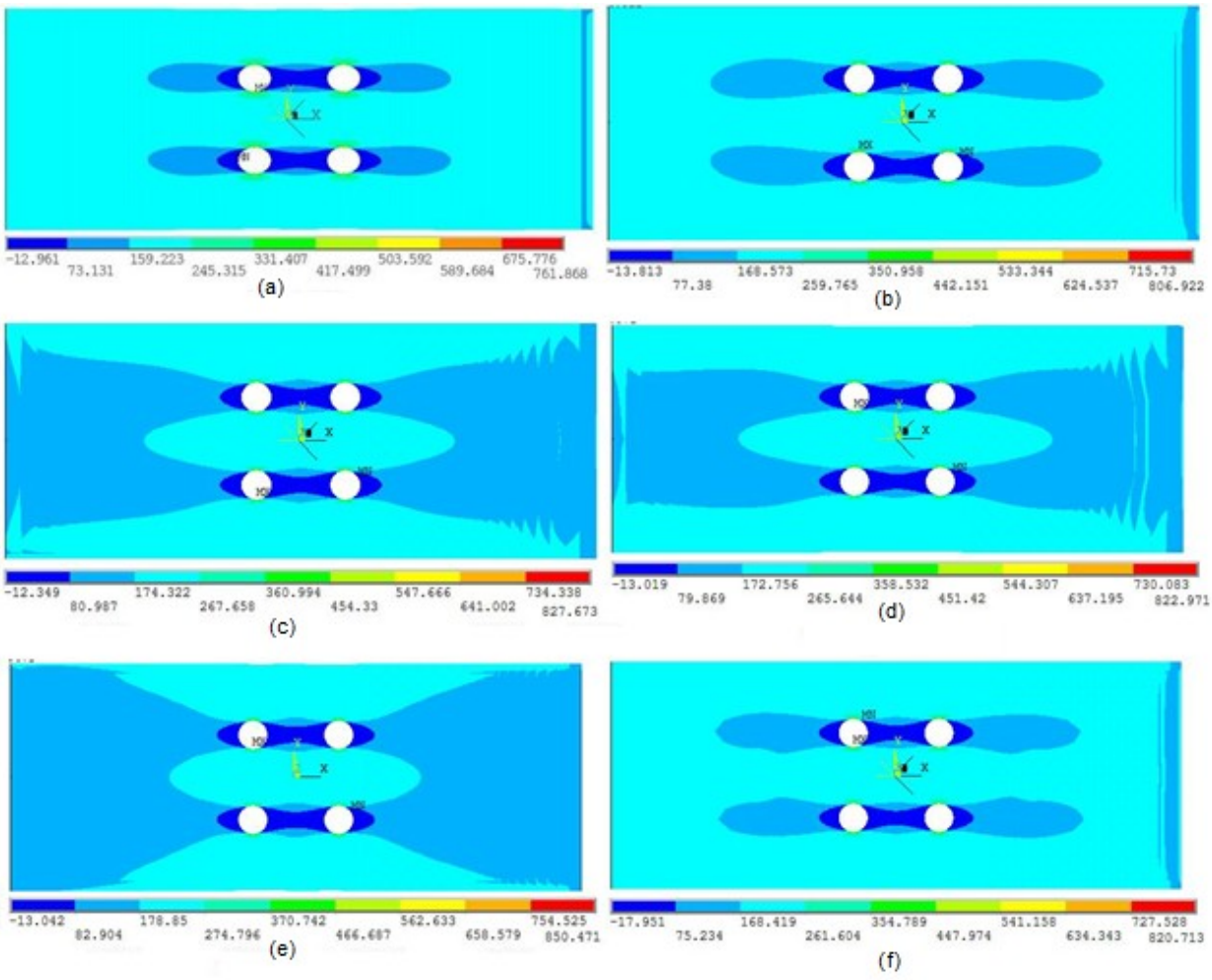

Figure 5.34 Stress contour for 0^0 layer with different patch configuration for SA pattern (a) no patch (b) square (c) hexagonal (d) octagonal (e) circular (f) elliptical

Comparison of the stress contours of the parent laminate (45^0 layer) at the interface between parent and patch laminate for different patch configuration in SA pattern is shown in Figure 5.35,

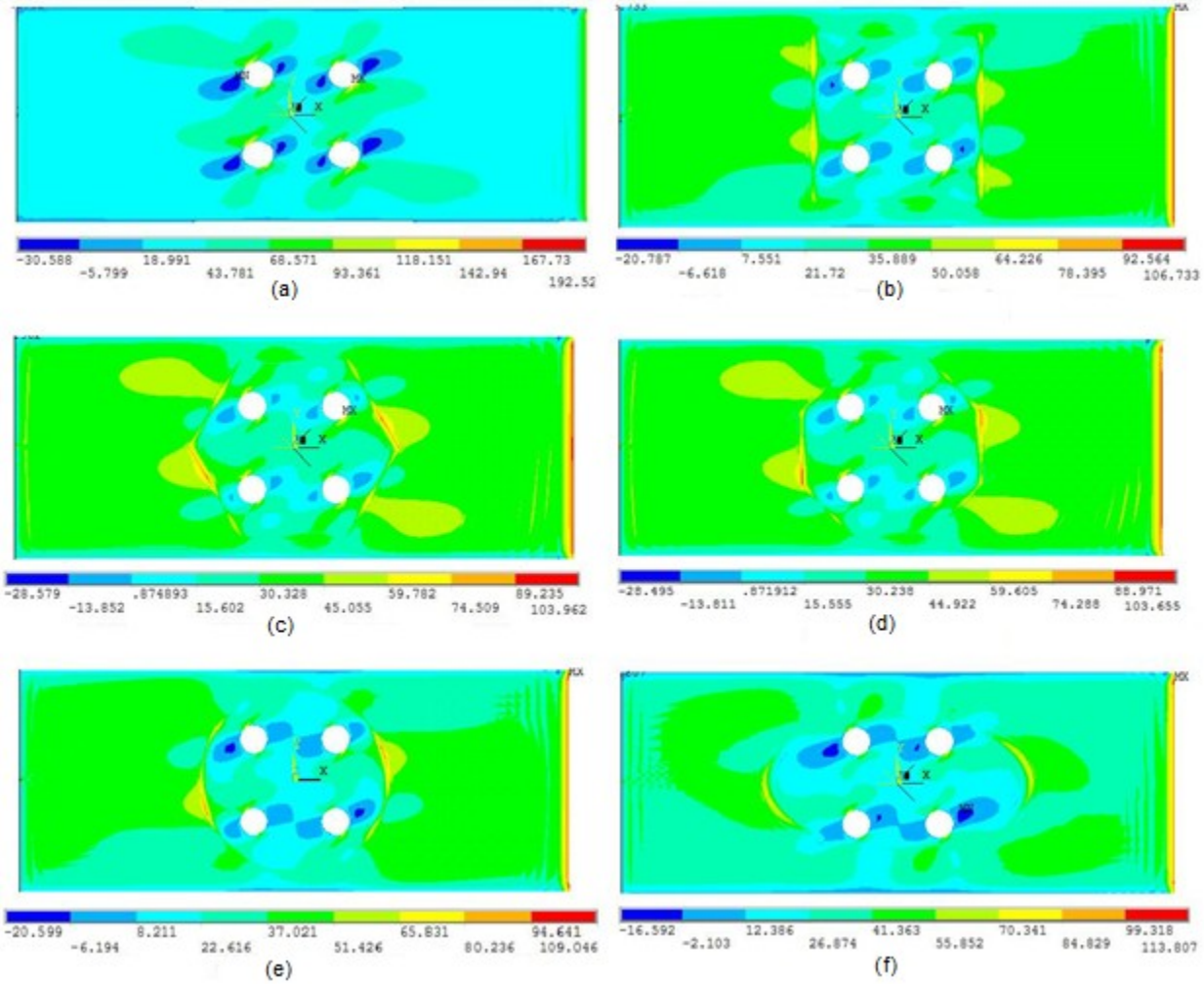

Figure 5.35 Stress contour for 45^0 layer with different patch configuration for SSH pattern at parent and patch interface (a) no patch (b) square (c) hexagonal (d) octagonal (e) circular (f) elliptical

5.7.2 In-plane stresses σ_1. σ_2, τ_{12} for bottom $+45^0$& -45^0ply

The normalized maximum in-plane stresses for $+45^0$ & -45^0 plies are tabulated in Tables 5.11 & 5.12 respectively and comparison of normalized maximum in-plane stresses for $+45^0$ & -45^0 plies for SA pattern with different patch configurations is shown in Figures 5.36 & 5.37, respectively.

Table 5.11 Normalized maximum in-plane stress for SA (45^0 ply -bottom) with different patch configurations

SA 45^0 ply(bottom)-Normalized in-plane stress			
Configuration	σ_1 / σ_0	σ_2 / σ_0	τ_{12} / σ_0
Without Patch	1.93	1.53	1.64
Square Patch	2.23	1.81	1.92
Hexagonal patch	2.26	1.87	2.00
Octagonal patch	2.28	1.84	2.00
Circular patch	2.37	1.92	2.08
Elliptical patch	2.27	1.86	1.99

Table 5.12 Normalized maximum in-plane stress for SA (-45^0 ply -bottom) with different patch configurations

SA -45^0 ply(bottom)-Normalized in-plane stress			
Configuration	σ_1 / σ_0	σ_2 / σ_0	τ_{12} / σ_0
Without Patch	2.56	2.13	1.42
Square Patch	2.83	2.36	1.54
Hexagonal patch	2.80	2.38	1.50
Octagonal patch	2.78	2.36	1.51
Circular patch	2.79	2.36	1.51
Elliptical patch	2.77	2.35	1.50

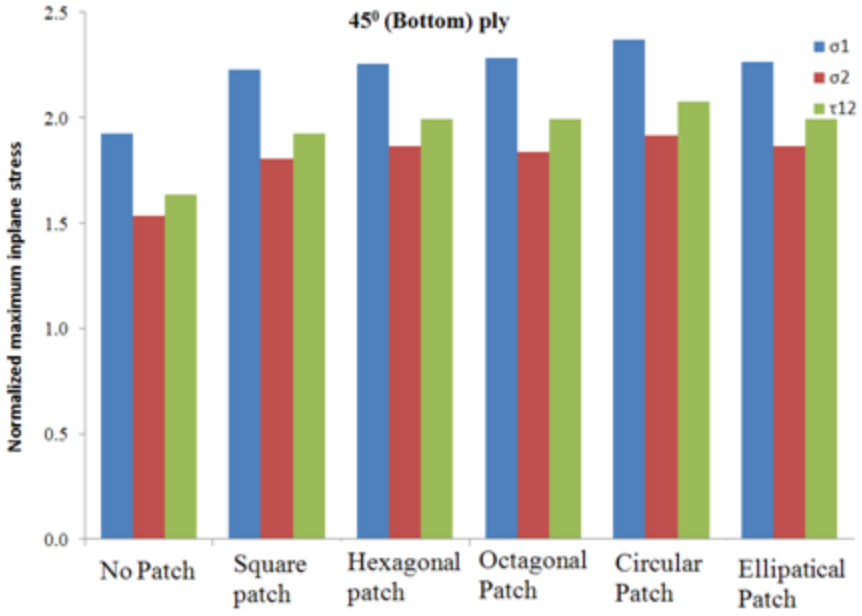

Figure 5.36 Comparison of in-plane stresses (bottom 45^0 layer) for SA pattern with different patch configurations

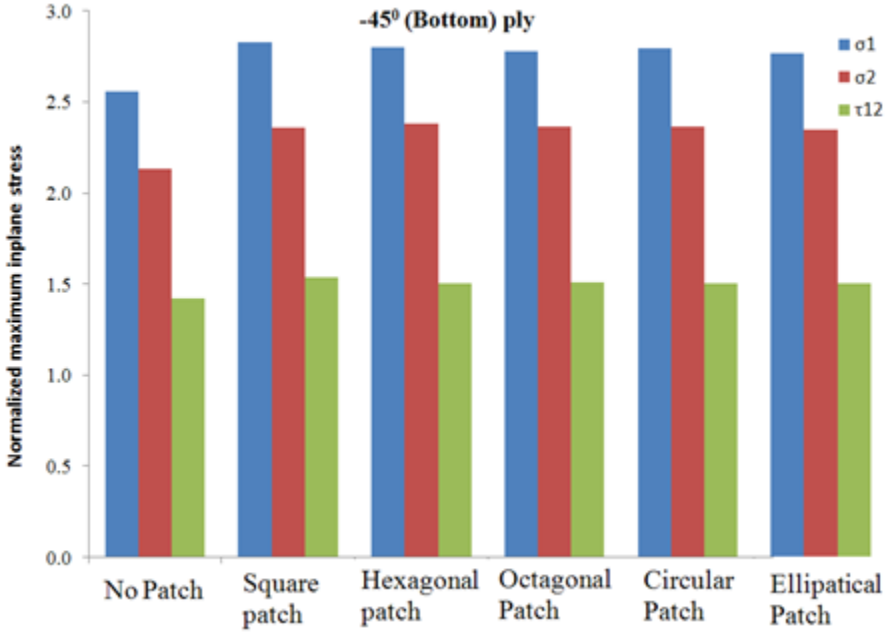

Figure 5.37 Comparison of in-plane stresses (bottom -45^0 layer) for SA pattern with different patch configurations

5.7.3 Interlaminar stresses σ_3, τ_{23} at the interfaces

There are two interfaces where the interlaminar stresses are critical.

1. Interface between parent laminate and adhesive.

2. Interface between patch laminate and adhesive.

The interlaminar stresses are plotted across the width of the laminate at the center as shown in Figure 5.38. The interlaminar stresses are maximum at the edge of the patch and holes.

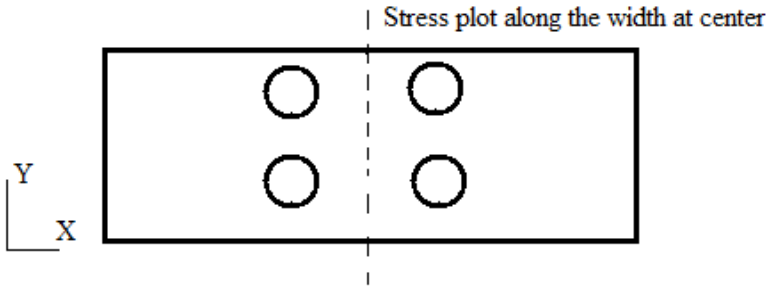

Figure 5.38 Location of stress plot along width of the laminate

The σ_3, τ_{23} distribution is along the width of the laminate at parent and adhesive interface is shown in Figures 5.39 & 5.40.

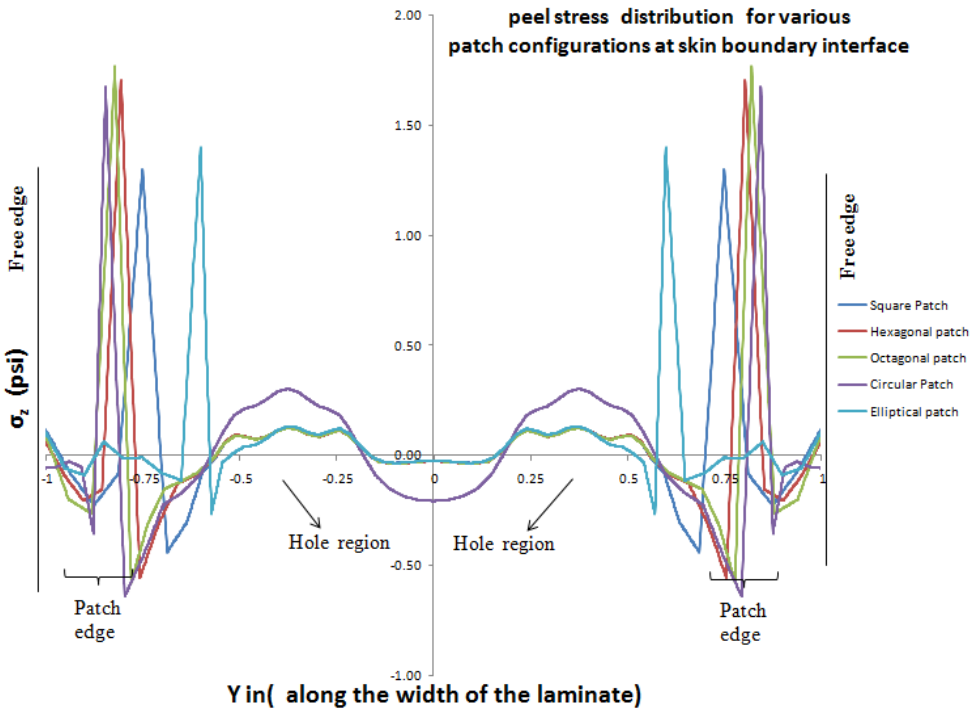

Figure 5.39 σ_3 stress at parent laminate and adhesive interface for all patch configurations

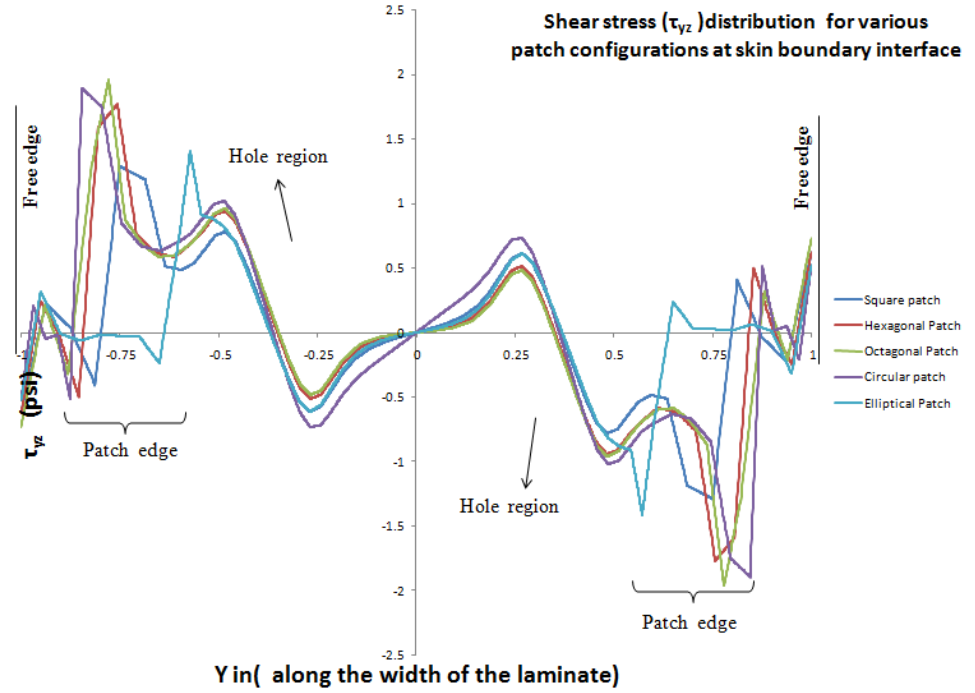

Figure 5.40 τ_{23} stress at parent laminate and adhesive interface for all patch configurations

The σ_3, τ_{23} distribution is along the width of the laminate at patch and adhesive interface is shown in Figures 5.41 & 5.42.

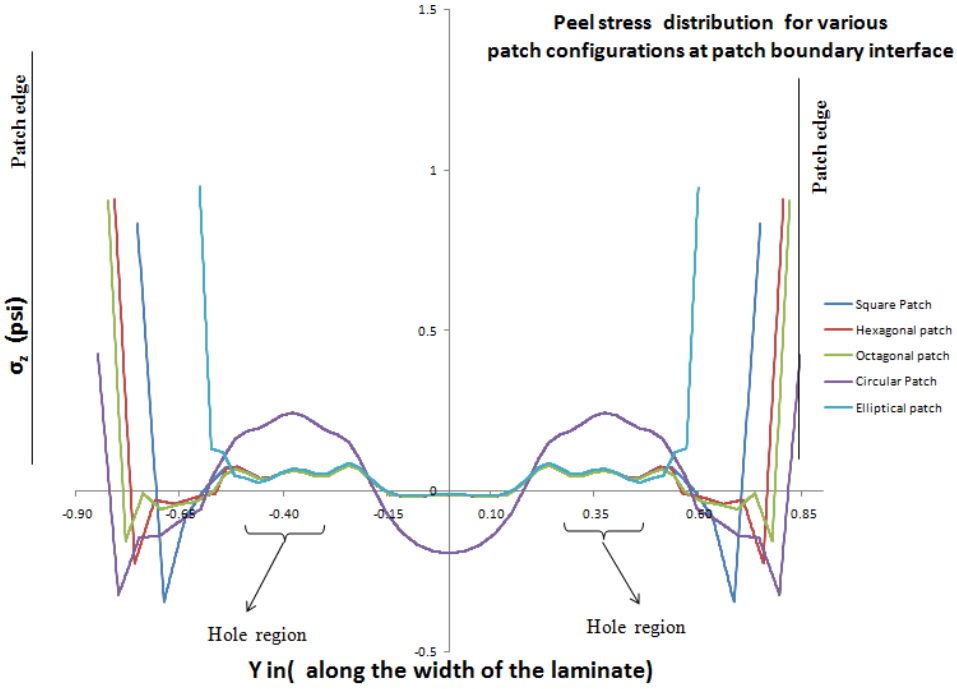

Figure 5.41 σ_3 stress at patch laminate and adhesive interface for all patch configurations

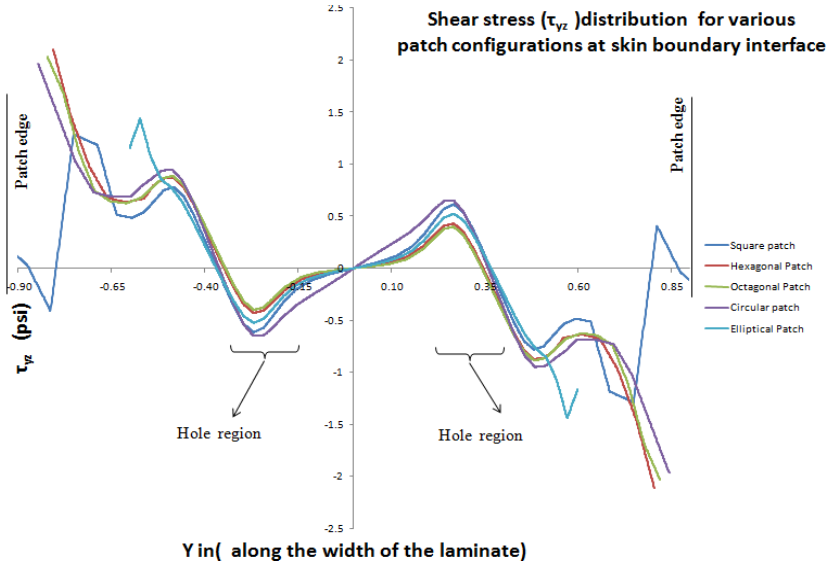

Figure 5.42 τ_{23} stress at patch laminate and adhesive interface for all patch configurations

5.8 Effect of patch configurations with DA pattern on parent laminate

5.8.1 In-plane stresses σ_1. σ_2, τ_{12} for bottom 0^0 ply

The in-plane stress is maximum at bottom 0^0 ply in all configurations. The in-plane stresses are tabulated in Table 5.13 and comparison of normalized maximum in-plane stresses for bottom 0^0 ply for SA pattern with different patch configurations is shown in Figure 5.43.

Table 5.13 Normalized maximum stress for DA (0^0 ply -bottom) with different patch configuration

DA-0^0 ply(bottom)-Normalized in-plane stress			
Configuration	σ_1 / σ_0	σ_2 / σ_0	τ_{12} / σ_0
Without Patch	10.25	0.47	0.74
Square Patch	9.80	0.47	0.69
Hexagonal patch	9.79	0.47	0.69
Octagonal patch	9.79	0.47	0.69
Circular patch	9.84	0.47	0.69
Elliptical patch	9.79	0.47	0.69

The peak stress (σ_1) decreases with all patch configurations when compared to No patch in the DA pattern. Among the Patch configurations the peak stress (σ_1) is least for octagonal patch configuration but not too significant.

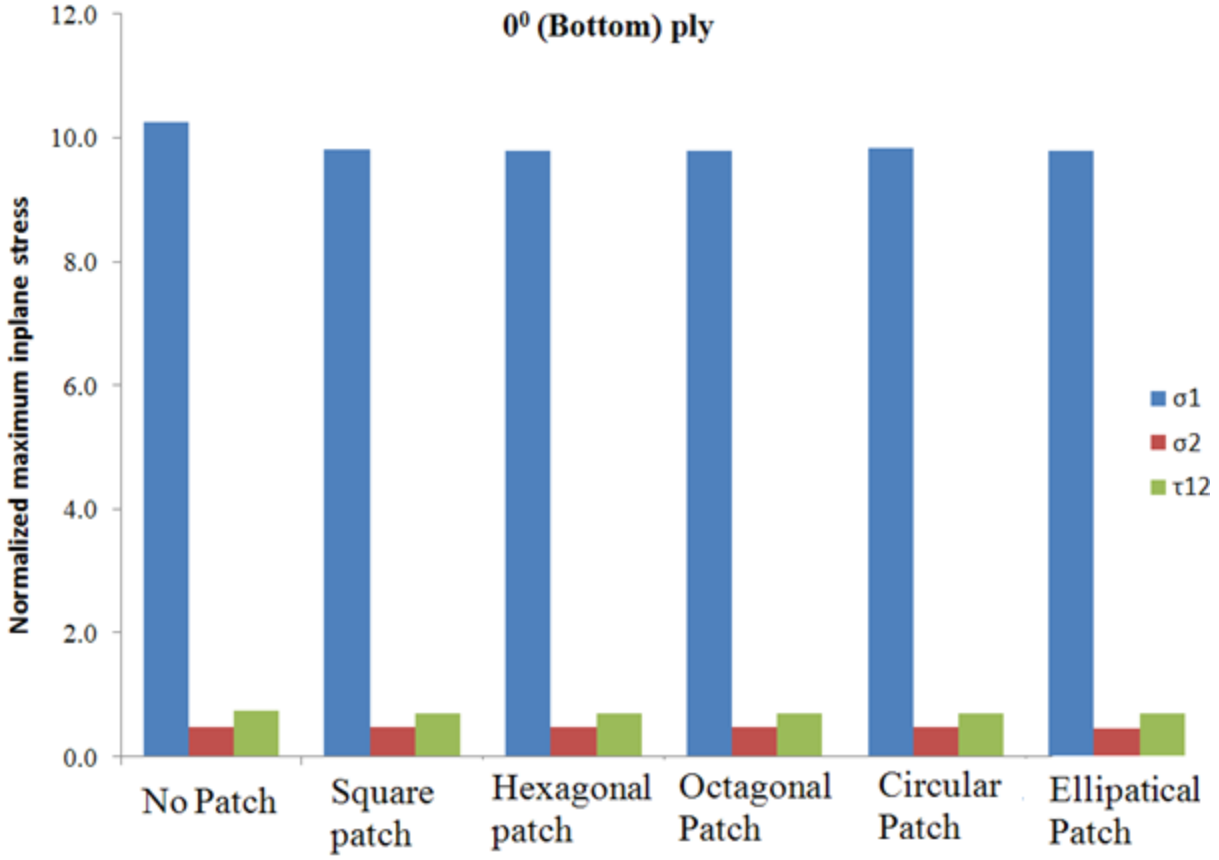

Figure 5.43 Comparison of in-plane stresses (bottom 0^0 layer) for DA pattern with different patch configurations

The stress contour for 0^0 layer with different patch configuration for DA pattern is shown in Figure 5.44,

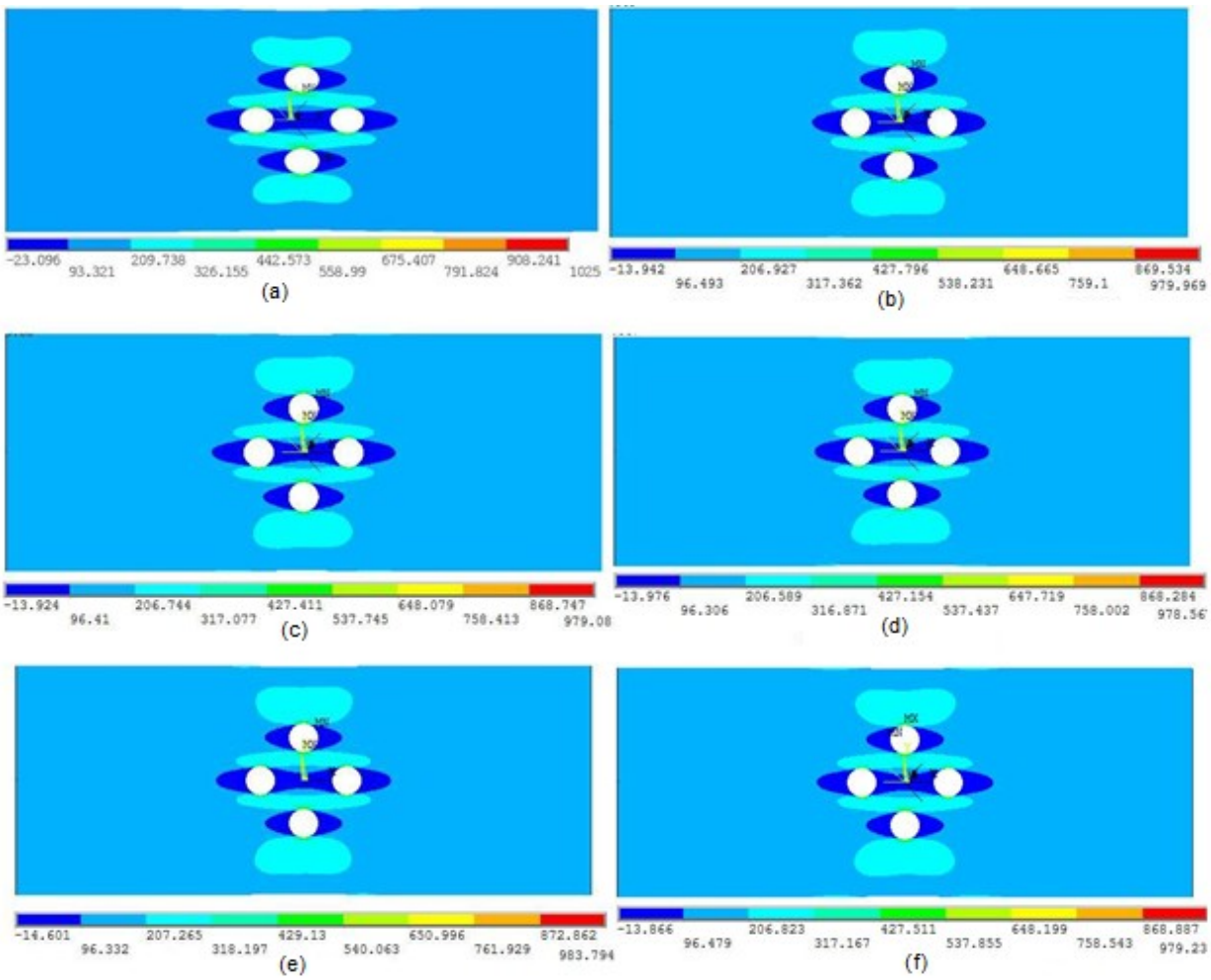

Figure 5.44 Stress contour for 0^0 layer with different patch configuration for DA pattern (a) no patch (b) square (c) hexagonal (d) octagonal (e) circular (f) elliptical

Comparison of the stress contours of the parent laminate (45^0 layer) at the interface between parent and patch laminate for different patch configuration in DA pattern is shown in Figure 5.45,

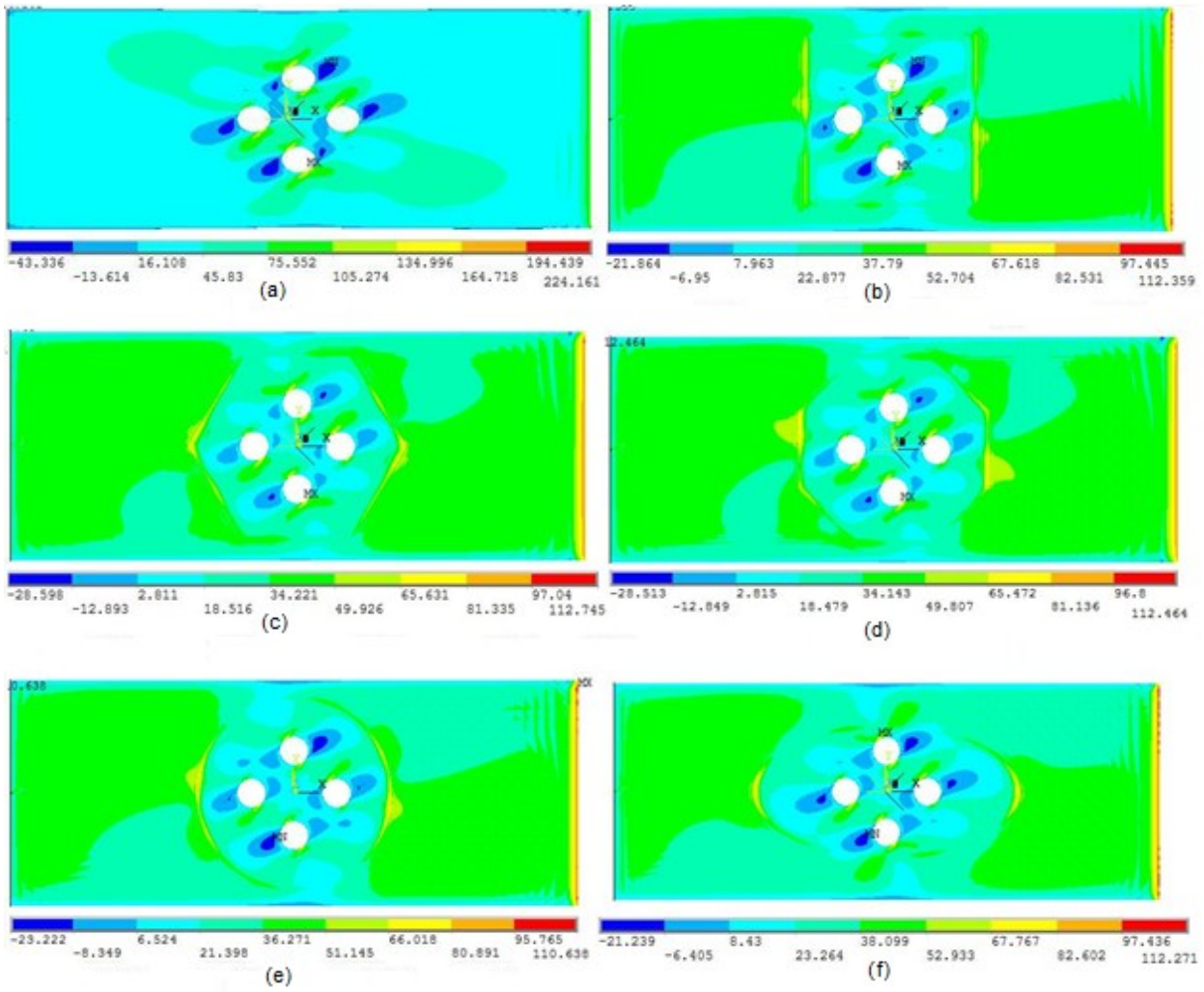

Figure 5.45 Stress contour for 45^0 layer with different patch configuration for SSH pattern at parent and patch interface (a) no patch (b) square (c) hexagonal (d) octagonal (e) circular (f) elliptical

5.8.2 In-plane stresses σ_1. σ_2, τ_{12} for bottom $+45^0$& -45^0ply

The normalized maximum in-plane stresses for $+45^0$ & -45^0 plies are tabulated in Tables 5.14 & 5.15 respectively and comparison of normalized maximum In-plane stresses for $+45^0$ & -45^0 plies for DA pattern with different patch configurations is shown in Figures 5.46 & 5.47, respectively.

Table 5.14 Normalized maximum in-plane stress for DA (45^0 ply -bottom) with different patch configurations

DA 45^0 ply(bottom)-Normalized in-plane stress			
Configuration	σ_1 / σ_0	σ_2 / σ_0	τ_{12} / σ_0
Without Patch	2.24	1.74	1.87
Square Patch	2.54	2.03	2.17
Hexagonal patch	2.54	2.03	2.17
Octagonal patch	2.54	2.03	2.17
Circular patch	2.59	2.08	2.22
Elliptical patch	2.52	2.00	2.14

Table 5.15 Normalized maximum in-plane stress for DA (-45^0 ply -bottom) with different patch configurations

DA -45^0ply(bottom)-Normalized in-plane stress			
Configuration	σ_1 / σ_0	σ_2 / σ_0	τ_{12} / σ_0
Without Patch	3.17	2.58	1.86
Square Patch	3.28	2.71	1.85
Hexagonal patch	3.28	2.71	1.85
Octagonal patch	3.28	2.71	1.85
Circular patch	3.32	2.74	1.86
Elliptical patch	3.28	2.71	1.85

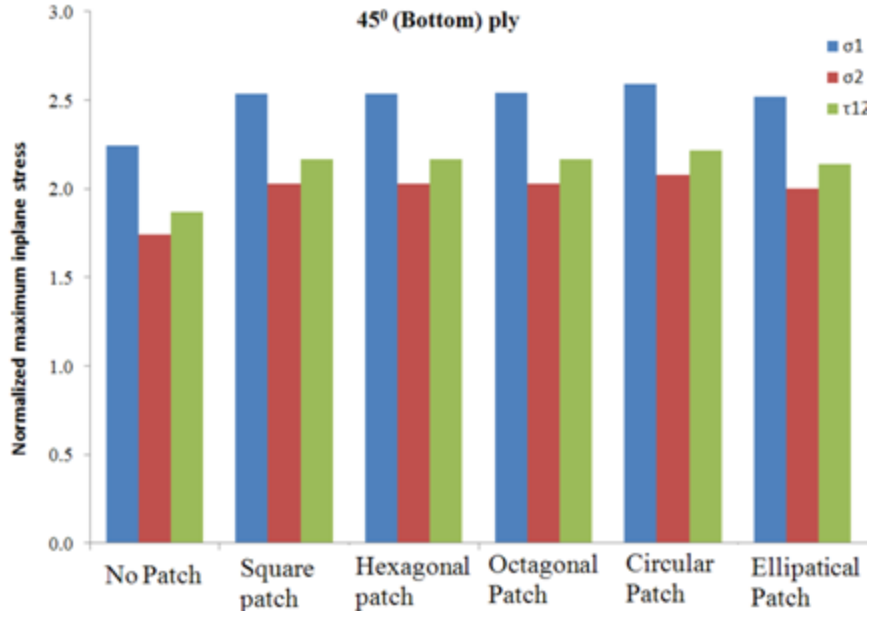

Figure 5.46 Comparison of in-plane stresses (bottom 45^0 layer) for DA pattern with different patch configurations

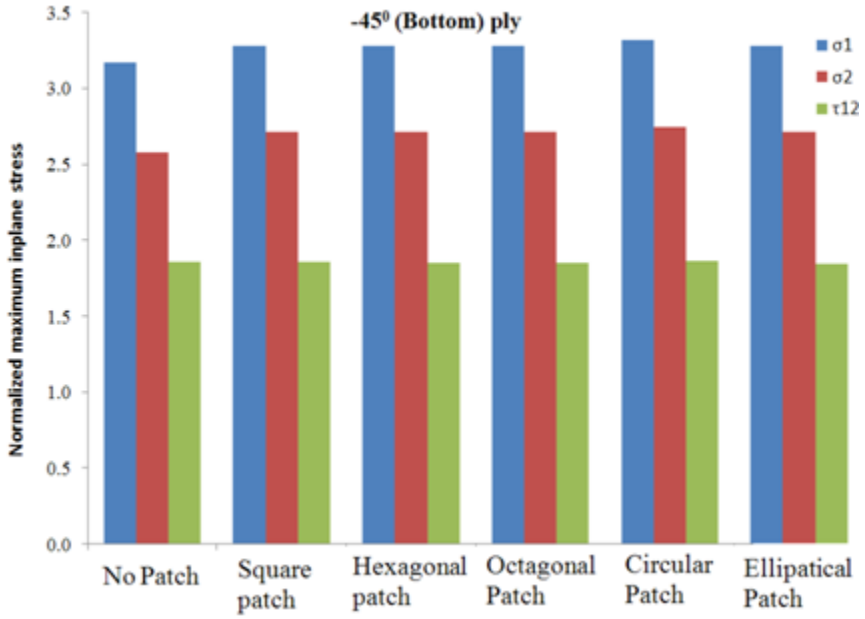

Figure 5.47 Comparison of in-plane stresses (bottom -45^0 layer) for DA pattern with different patch configurations

5.8.3 Interlaminar stresses σ_3, τ_{23} at the interfaces

There are two interfaces where the interlaminar stresses are critical.

1. Interface between parent laminate and adhesive.

2. Interface between patch laminate and adhesive.

The interlaminar stresses are plotted across the width of the laminate at the center as shown in Figure 5.48. The interlaminar stresses are maximum at the edge of the patch and holes.

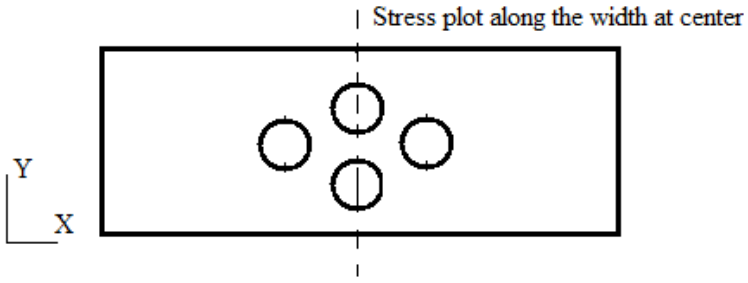

Figure 5.48 Location of stress plot along width of the laminate

The σ_3, τ_{23} distribution is along the width of the laminate at parent and adhesive interface is shown in the Figures 5.49 & 5.50.

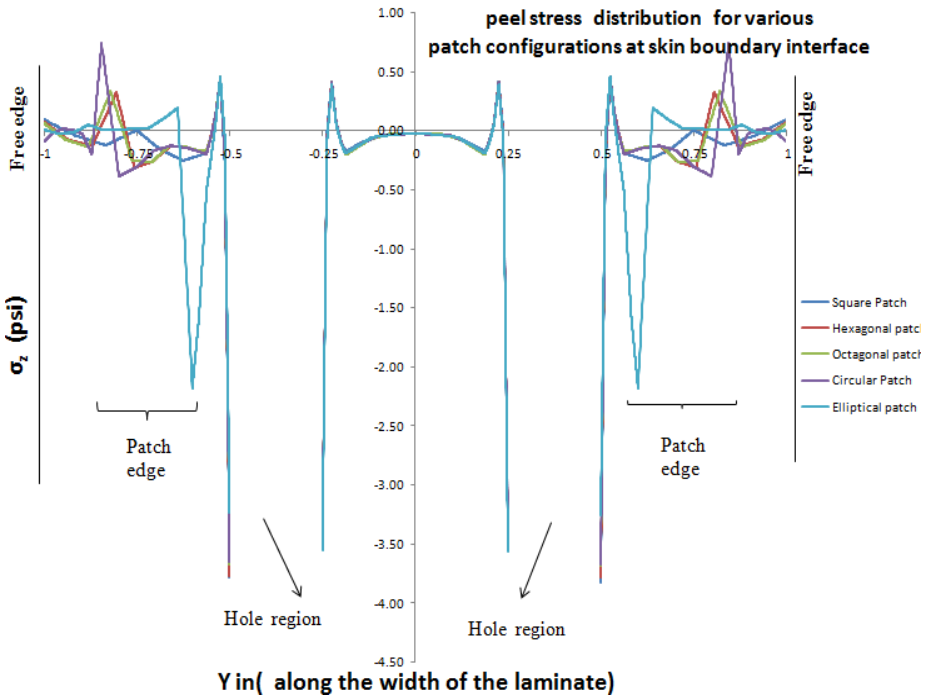

Figure 5.49 σ_3 stress at parent laminate and adhesive interface for all patch configurations

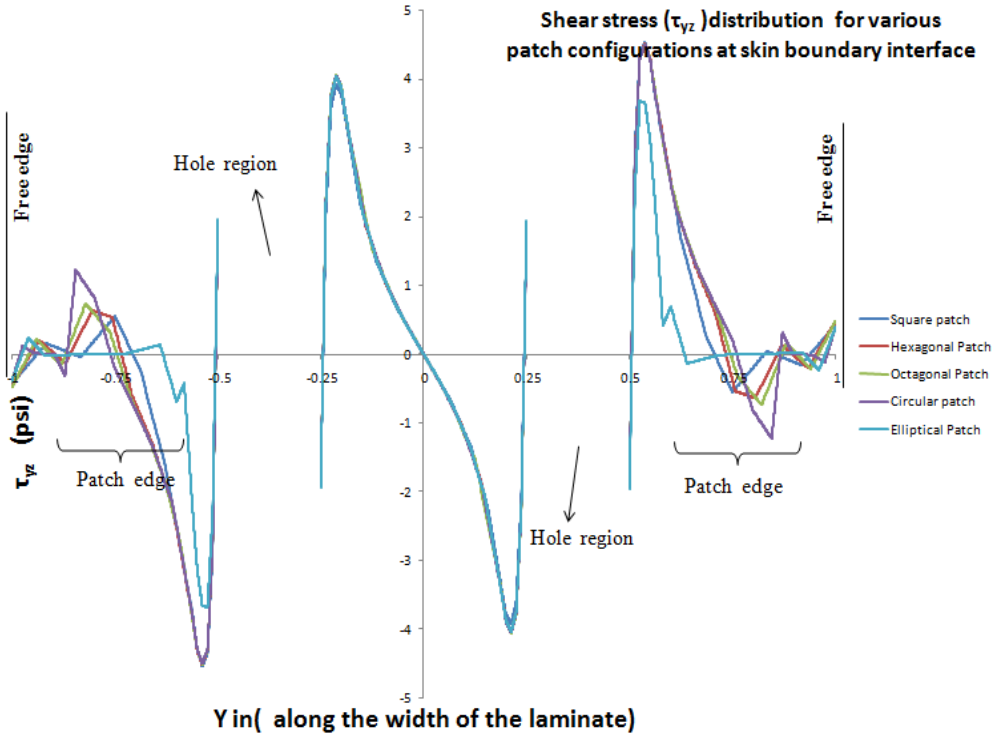

Figure 5.50 τ_{23} stress at parent laminate and adhesive interface for all patch configurations

The σ_3, τ_{23} distribution is along the width of the laminate at patch and adhesive interface is shown in Figures 5.51 & 5.52.

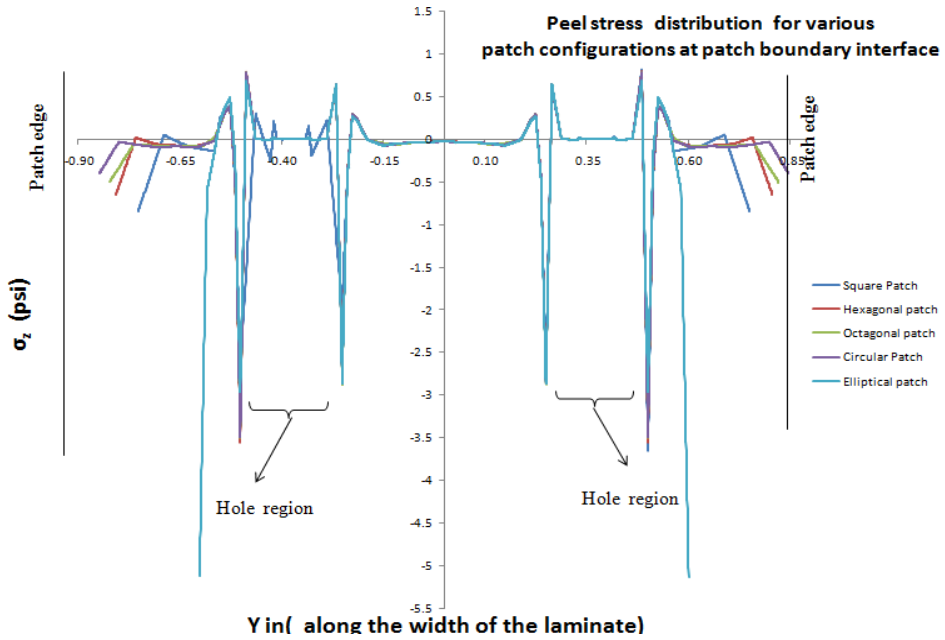

Figure 5.51 σ_3 stress at patch laminate and adhesive interface for all patch configurations

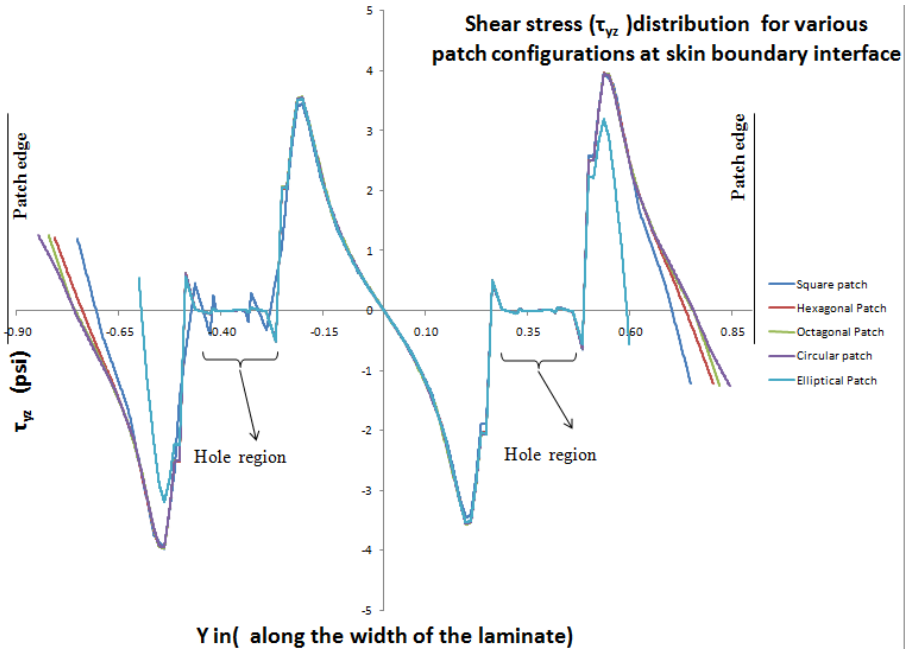

Figure 5.52 τ_{23} stress at patch laminate and adhesive interface for all patch configurations

5.9 Effect of patch configurations with FH pattern on parent laminate

5.9.1 In-plane stresses σ_1. σ_2, τ_{12} for bottom 0^0 ply

The in-plane stress is maximum at bottom 0^0 ply in all configurations. The in-plane stresses are tabulated in Table 5.16 and comparison of normalized maximum in-plane stresses for bottom 0^0 ply for FH pattern with different patch configurations is shown in Figure 5.53.

Table 5.16 Normalized maximum stress for FH (0^0 ply -bottom) with different patch configuration

FH-0^0ply(bottom)-Normalized in-plane stress			
Configuration	σ_1 / σ_0	σ_2 / σ_0	τ_{12} / σ_0
Without Patch	11.20	0.51	0.81
Square Patch	10.43	0.50	0.74
Hexagonal patch	10.45	0.50	0.74
Octagonal patch	10.45	0.50	0.74
Circular patch	10.52	0.50	0.74
Elliptical patch	10.38	0.49	0.73

The peak stress (σ_1) decreases with all patch configurations when compared to No patch in the FH pattern. Among the Patch configurations the peak stress (σ_1) is least for elliptical patch configuration but not too significant.

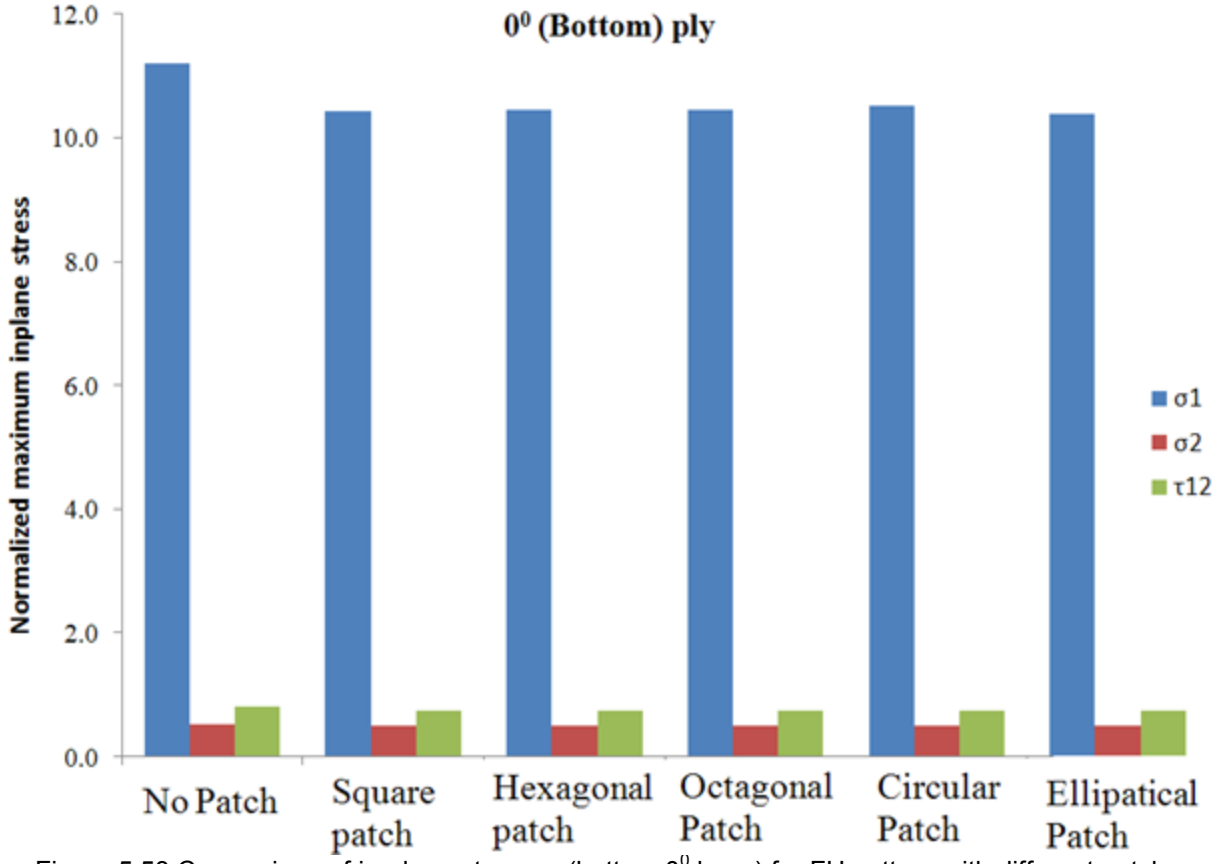

Figure 5.53 Comparison of in-plane stresses (bottom 0^0 layer) for FH pattern with different patch configurations

The stress contour for 0^0 layer with different patch configuration for FH pattern is shown in Figure 5.54. There is little difference in the 0^0 ply stress contour between the No patch and patch laminates.

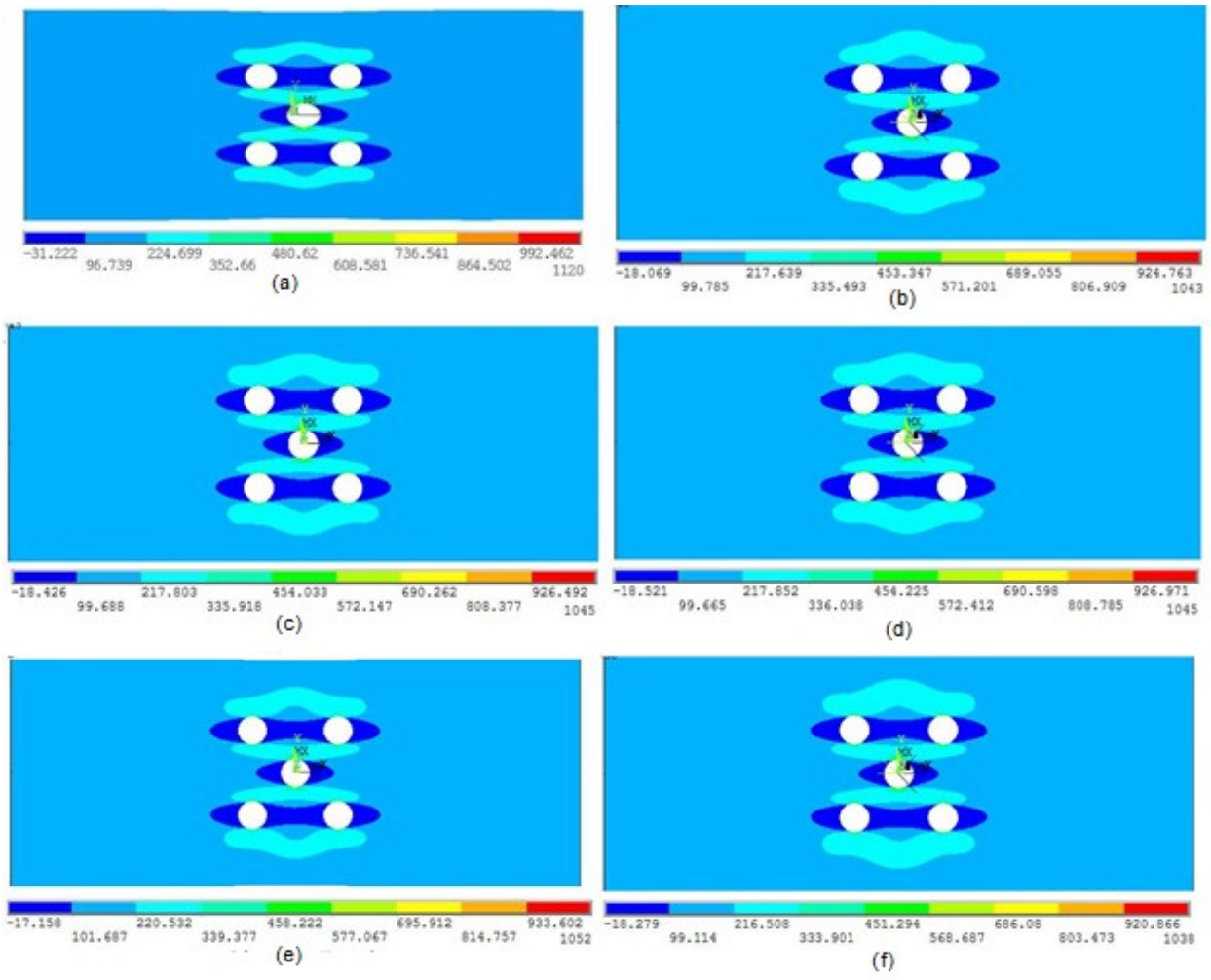

Figure 5.54 Stress contour for 0^0 layer with different patch configuration for FH pattern (a) no patch (b) square (c) hexagonal (d) octagonal (e) circular (f) elliptical

Comparison of the stress contours of the parent laminate (45^0 layer) at the interface between the parent and patch laminate for different patch configuration in FH pattern is shown in Figure 5.55,

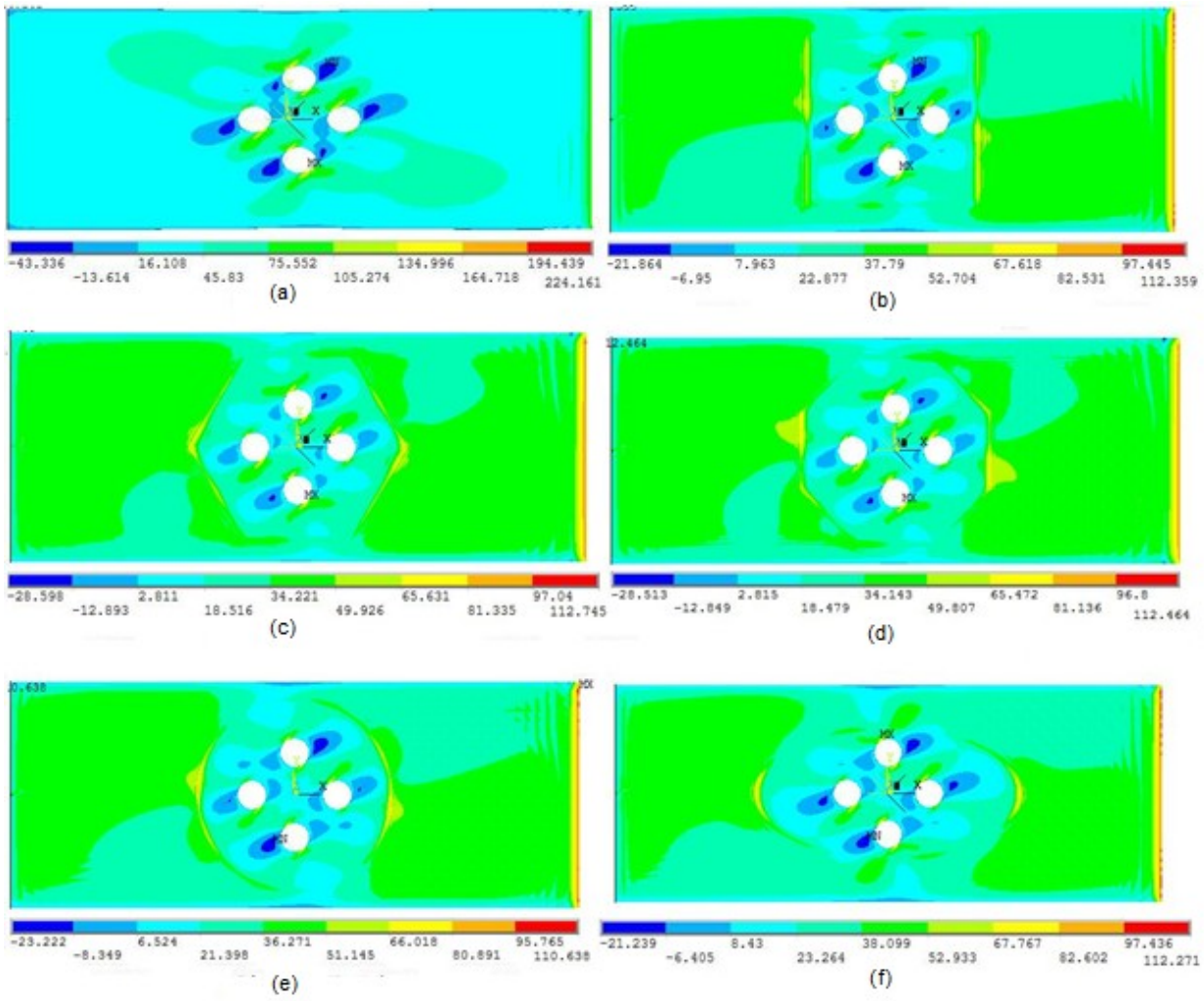

Figure 5.55 Stress contour for 45^0 layer with different patch configuration for SSH pattern at parent and patch interface (a) no patch (b) square (c) hexagonal (d) octagonal (e) circular (f) elliptical

5.9.2 In-plane stresses σ_1. σ_2, τ_{12} for bottom $+45^0$& -45^0ply

The normalized maximum in-plane stresses for $+45^0$ & -45^0 plies are tabulated in Tables 5.17 & 5.18 respectively and comparison of normalized maximum In-plane stresses for $+45^0$ & -45^0 plies for FH pattern with different patch configurations is shown in the Figures 5.56 & 5.57, respectively.

Table 5.17 Normalized maximum in-plane stress for FH (45^0 ply -bottom) with different patch configurations

FH 45^0 ply(bottom)-Normalized in-plane stress			
Configuration	σ_1 / σ_0	σ_2 / σ_0	τ_{12} / σ_0
Without Patch	2.29	1.70	1.90
Square Patch	2.55	1.94	2.12
Hexagonal patch	2.45	1.93	2.11
Octagonal patch	2.54	1.93	2.11
Circular patch	2.63	2.03	2.19
Elliptical patch	2.53	1.92	2.10

Table 5.18 Normalized maximum in-plane stress for FH (-45^0 ply -bottom) with different patch configurations

FH -45^0 ply(bottom)-Normalized in-plane stress			
Configuration	σ_1 / σ_0	σ_2 / σ_0	τ_{12} / σ_0
Without Patch	3.48	2.82	2.04
Square Patch	3.47	2.88	1.97
Hexagonal patch	3.47	2.89	1.98
Octagonal patch	3.47	2.89	1.98
Circular patch	3.50	2.91	1.99
Elliptical patch	3.55	2.88	1.97

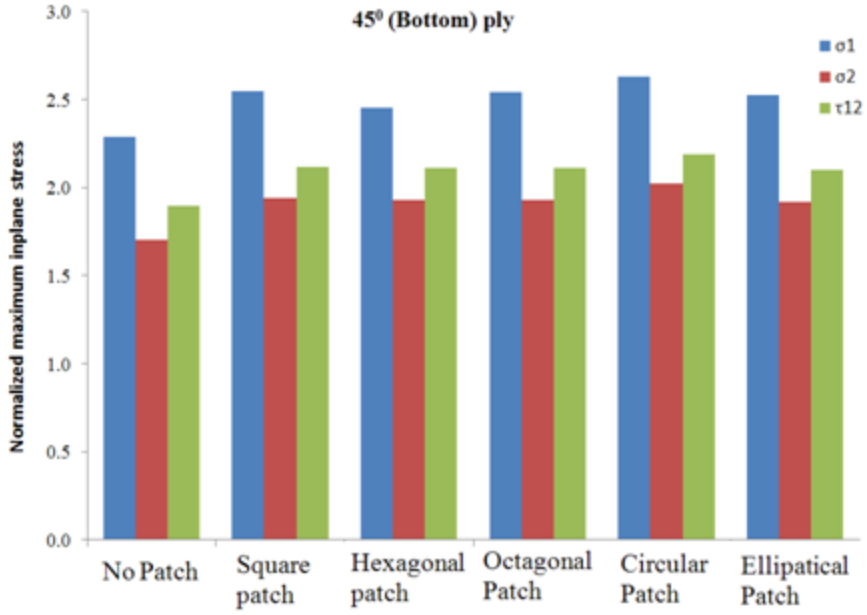

Figure 5.56 Comparison of in-plane stresses (bottom 45^0 layer) for FH pattern with different patch configurations

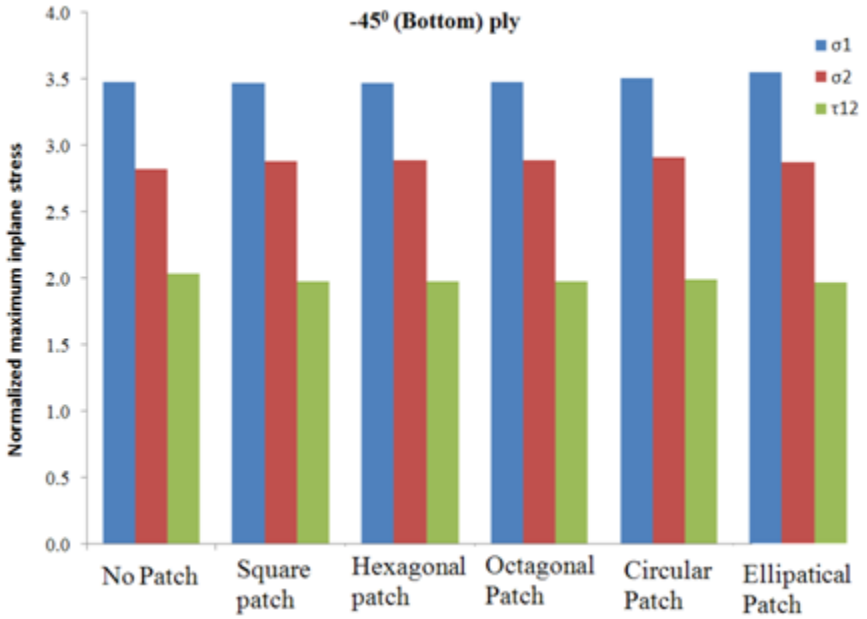

Figure 5.57 Comparison of in-plane stresses (bottom -45^0 layer) for FH pattern with different patch configurations

5.9.3 Interlaminar stresses σ_3, τ_{23} at the interfaces

There are two interfaces where the interlaminar stresses are critical.

1. Interface between parent laminate and adhesive.

2. Interface between patch laminate and adhesive.

The interlaminar stresses are plotted across the width of the laminate at the center as shown in Figure 5.58. The interlaminar stresses are maximum at the edge of the patch and holes.

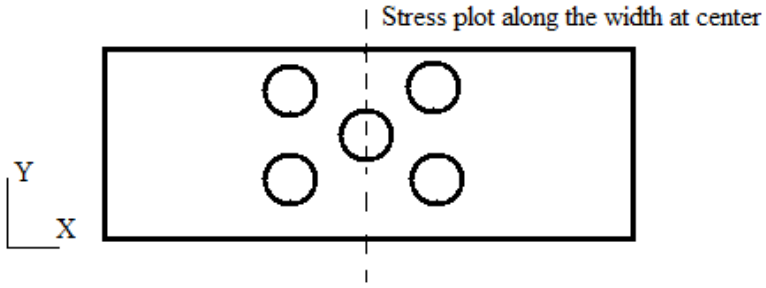

Figure 5.58 Location of stress plot along width of the laminate

The σ_3, τ_{23} distribution is along the width of the laminate at parent and adhesive interface is shown in Figures 5.59 & 5.60.

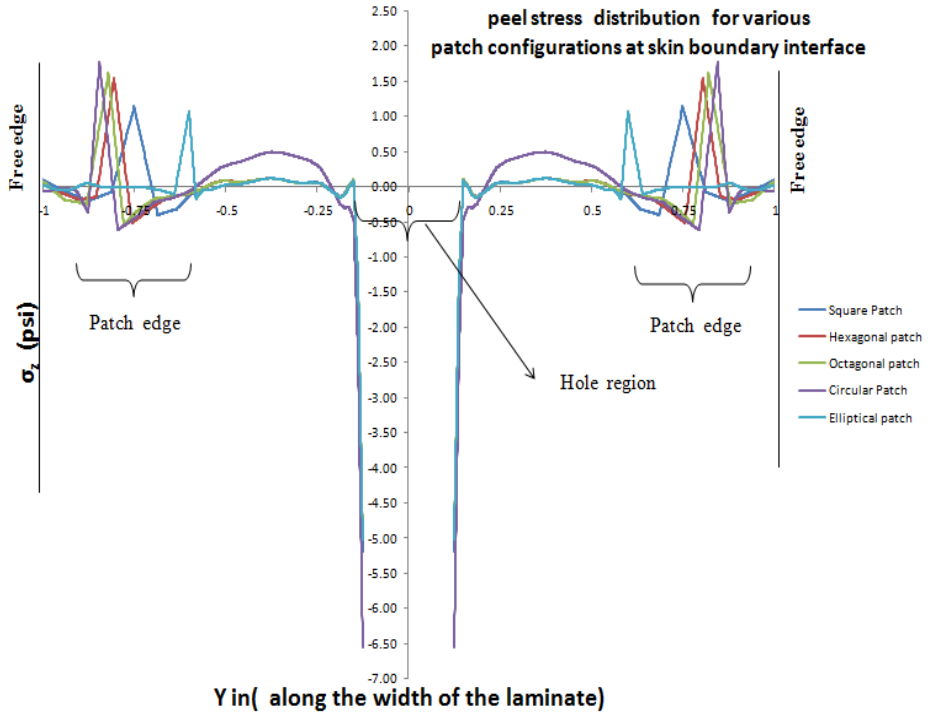

Figure 5.59 σ_3 stress at parent laminate and adhesive interface for all patch configurations

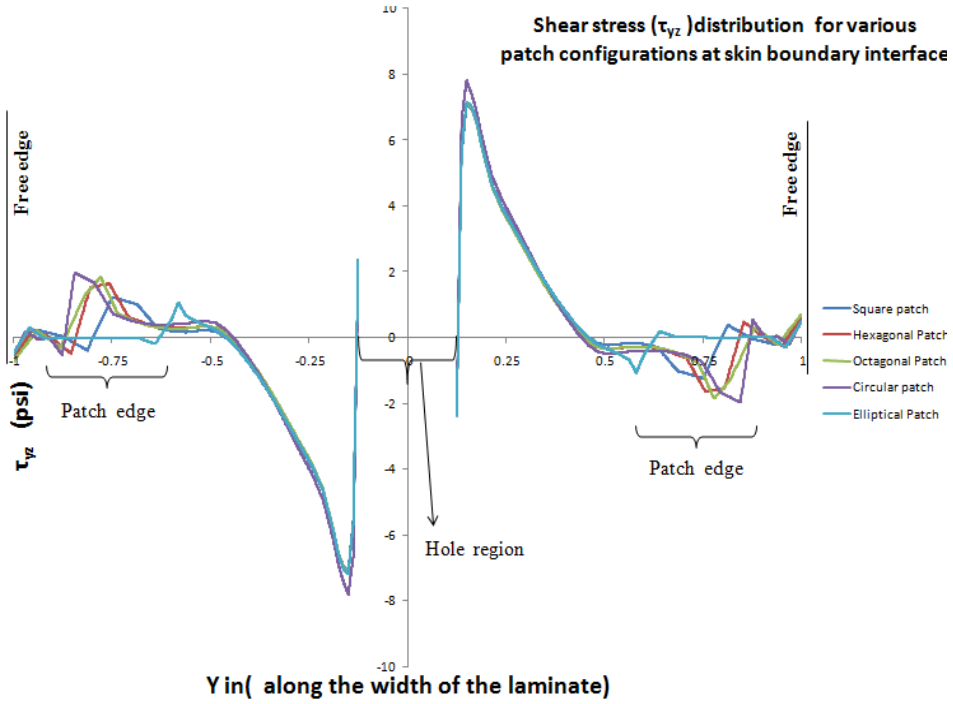

Figure 5.60 τ_{23} stress at parent laminate and adhesive interface for all patch configurations

The σ_3, τ_{23} distribution is along the width of the laminate at patch and adhesive interface is shown in Figures 5.61 & 5.62.

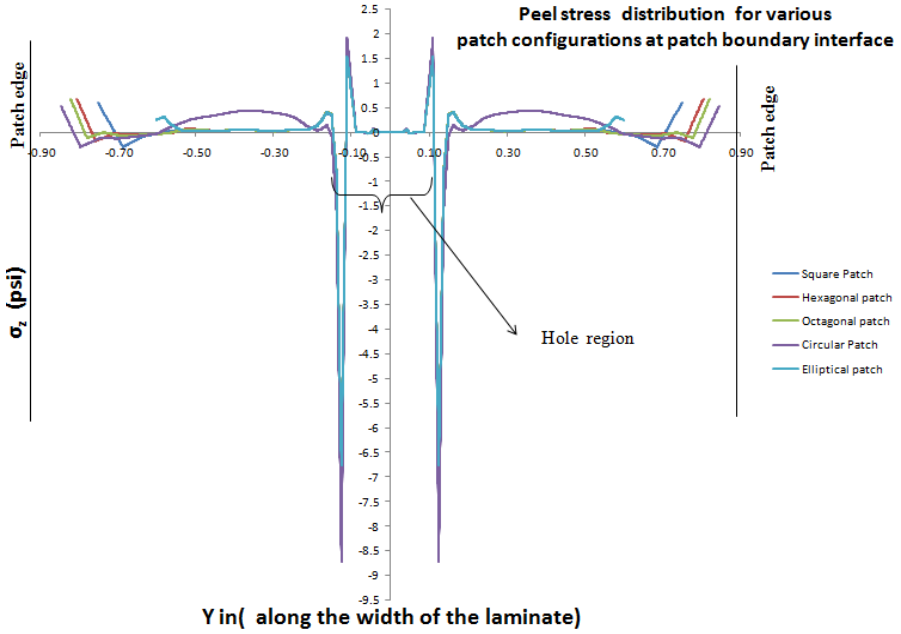

Figure 5.61 σ_3 stress at patch laminate and adhesive interface for all patch configurations

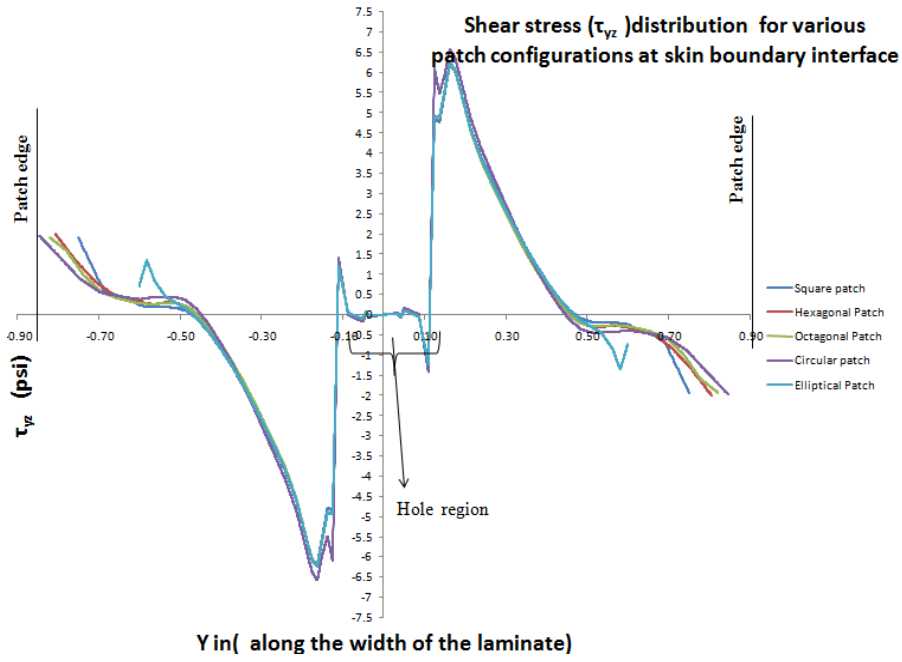

Figure 5.62 τ_{23} stress at patch laminate and adhesive interface for all patch configurations

5.11 Result Summary of Single Patch laminate

1. For a SH, TBH&FH pattern the peak stress is less for elliptical patch configuration.

2. For SSH, SA pattern the peak stress is less for square patch configuration.

3. For DA pattern the peak stress is less for octagonal patch configuration.

4. The peak stress variation for various patch configuration with different hole patterns is shown in Figure 5.63

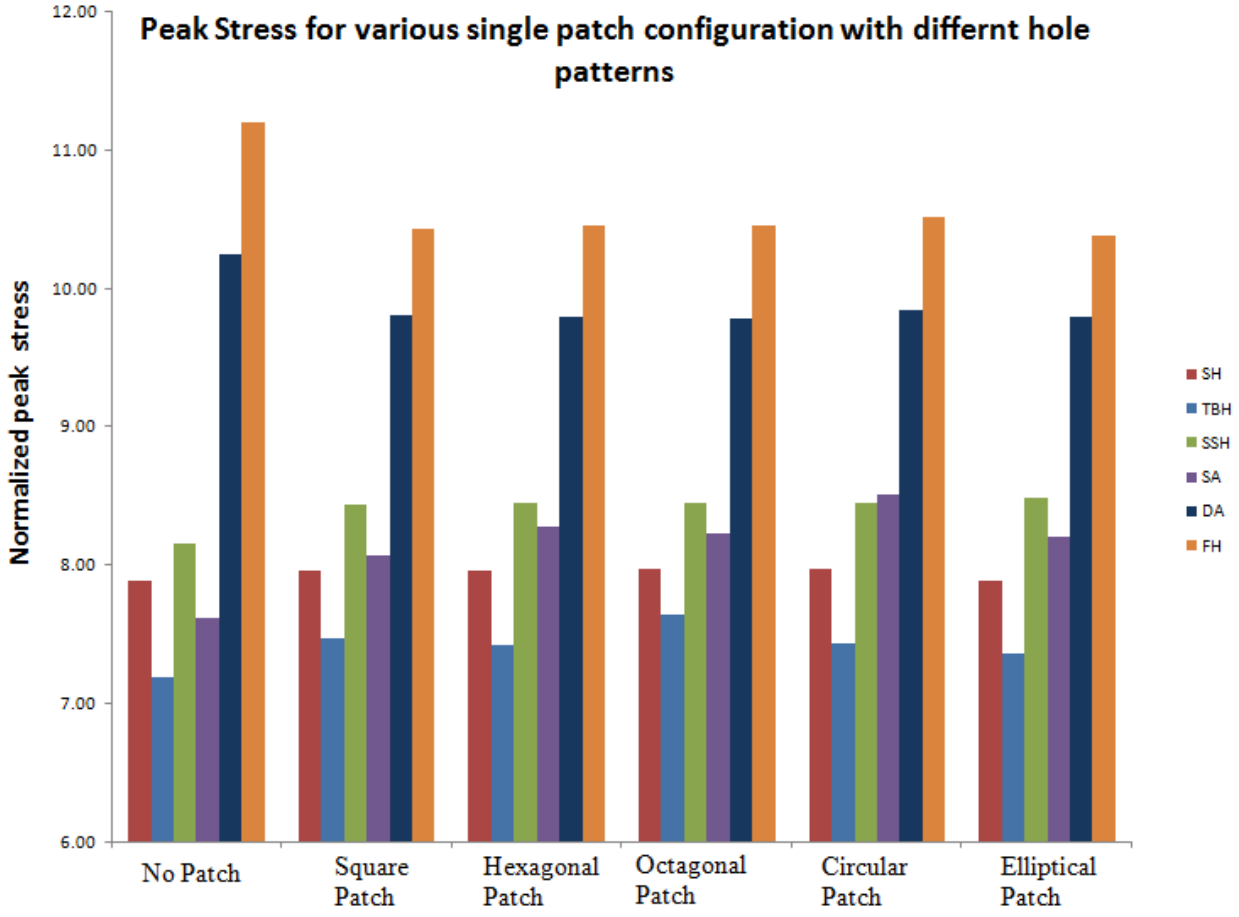

Figure 5.63 Comparison of peak stress for various configurations with different hole patterns

CHAPTER 6

EFFECTS OF DOUBLE PATCH CONFIGURATIONS IN COMPOSITE BONDED REPAIR

The moment induced due to the single patch on the parent laminate increases the stresses on the laminate. Hence the idea for double patch is proposed for eliminating the induced moment. In this chapter the parent laminate is glued with two patches one on the top and bottom surfaces of the laminate. Different configurations of the patch laminate glued both the sides of the parent laminate with multiple hole pattern is studied. The material property, laminate stacking sequence and hole radius are considered the same for all cases.

6.1 Cases investigated

The different hole patterns of parent laminate and patch configurations discussed in Chapter II is considered for the study. The geometric description, material and stacking sequence is given in Sections 2.1 and 2.2, respectively.

6.2 Effect of patch configurations with SH pattern on parent laminate

6.2.1 In-plane stresses σ_1. σ_2, τ_{12} for bottom 0^0 ply

The in-plane stress is maximum at bottom 0^0 ply in all configurations. The in-plane stresses are tabulated in Table 6.1 and comparison of normalized maximum in-plane stresses for bottom 0^0 ply for SH pattern with different patch configurations is shown in Figure 6.1.

Table 6.1 Normalized maximum stress for SH (0^0 ply -bottom) with different patch configuration

Single Hole -0^0 ply(bottom)-Normalized in-plane stress			
Configuration	σ_1 / σ_0	σ_2 / σ_0	τ_{12} / σ_0
Without Patch	7.88	0.36	0.57
Square Patch	5.52	0.24	0.40
Hexagonal patch	5.67	0.25	0.41
Octagonal patch	5.69	0.25	0.41
Circular patch	4.64	0.20	0.34
Elliptical patch	5.95	0.26	0.43

The peak stress (σ_1) significantly decreases with all patch configurations when compared to No patch in the SH laminate. Among the patch configurations the peak stress (σ_1) is the least for circular patch configuration.

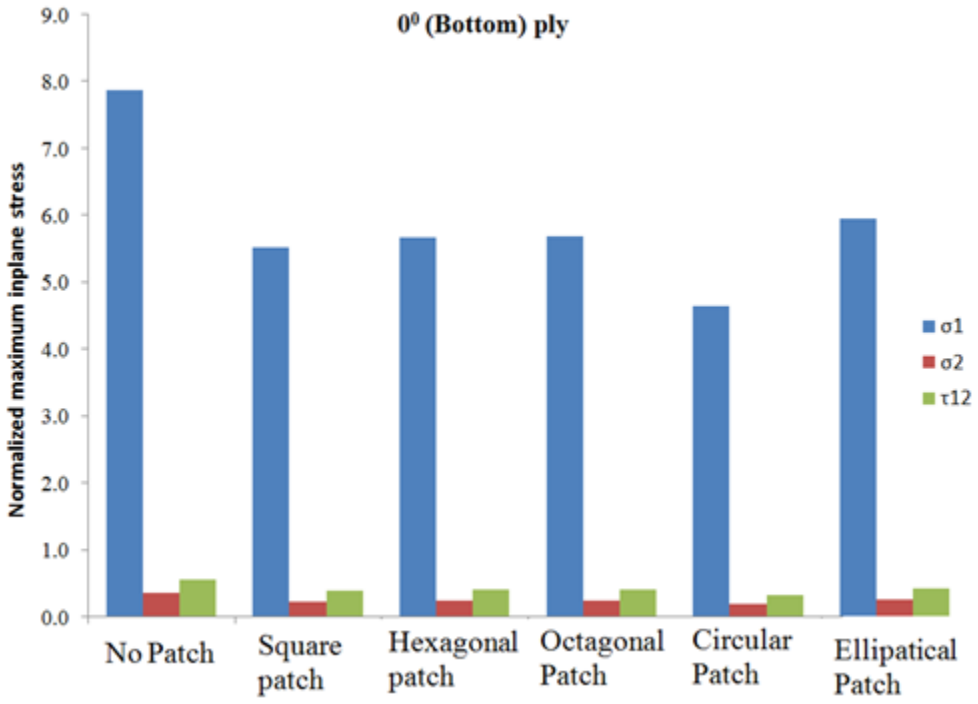

Figure 6.1 Comparison of in-plane stresses (bottom 0^0 layer) for SH pattern with different patch configurations

The stress contour for 0^0 layer with different patch configuration for SH pattern is shown in Figure 6.2,

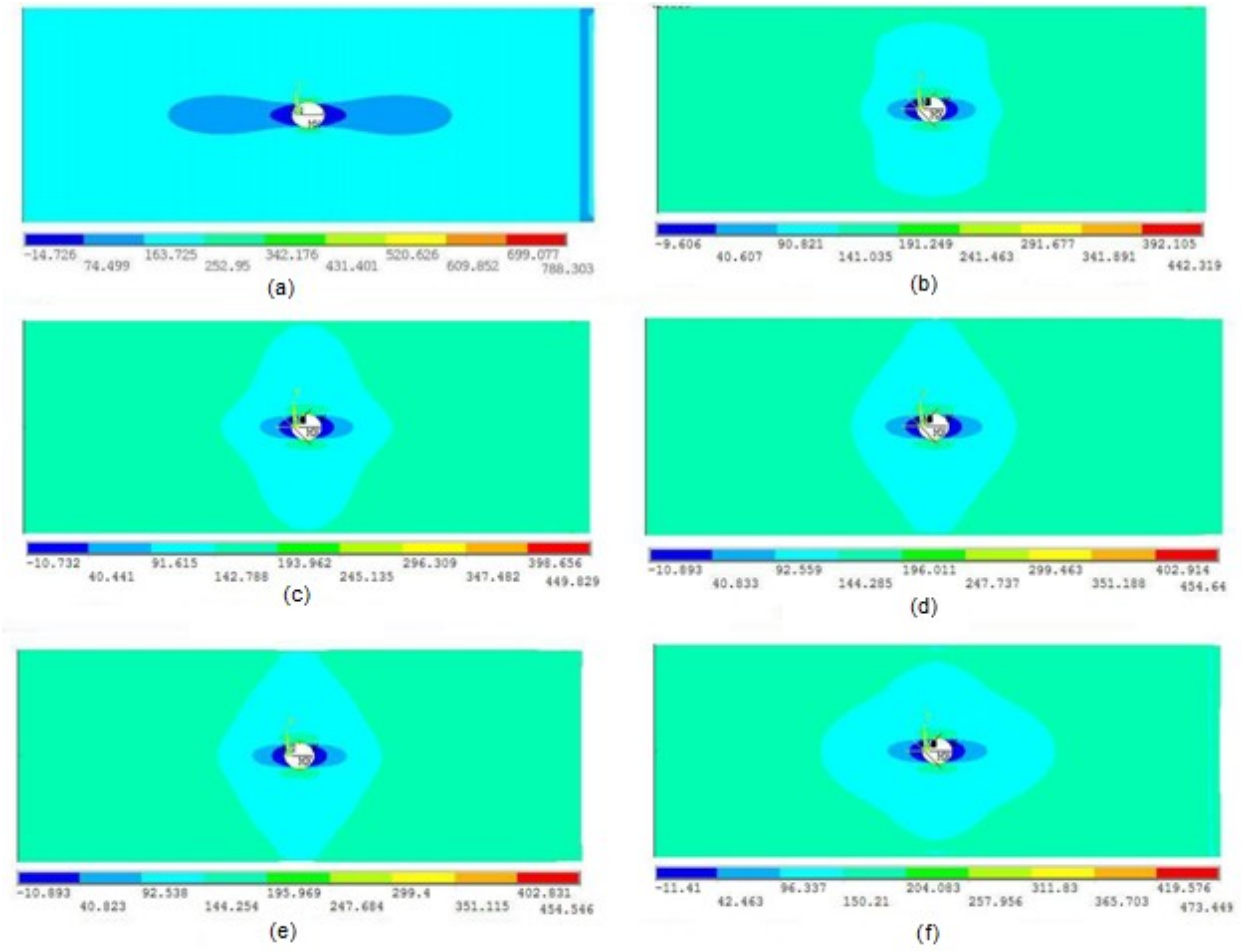

Figure 6.2 Stress contour for 0^0 layer with different patch configuration for SH pattern (a) no patch (b) square (c) hexagonal (d) octagonal (e) circular (f) elliptical

Comparison of the stress contours of the parent laminate (45^0 layer) at the interface between parent and patch laminate for different patch configuration in SH pattern is shown in Figure 6.3,

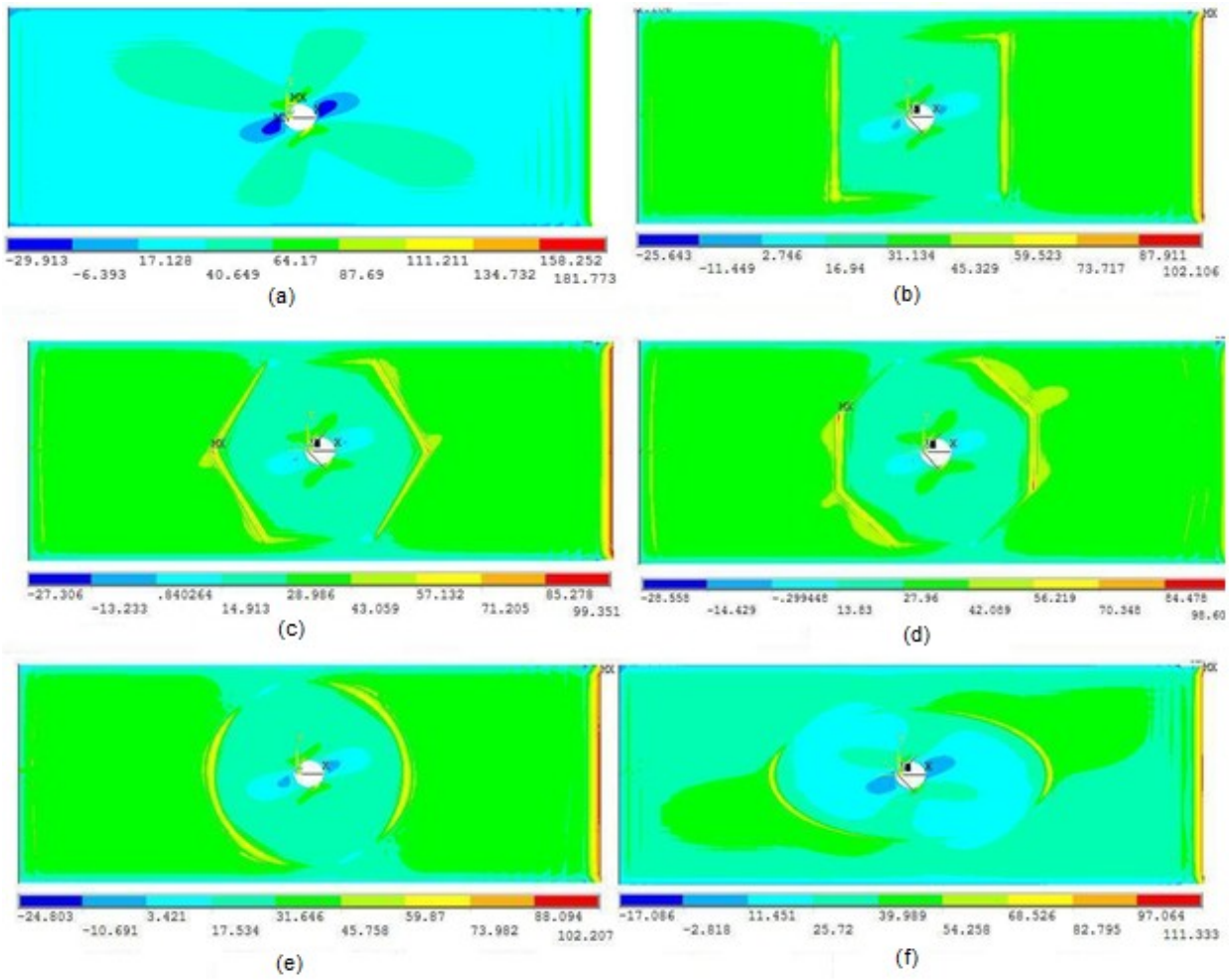

Figure 6.3 Stress contour for 45^0 layer with different patch configuration for SH pattern at parent and patch interface (a) no patch (b) square (c) hexagonal (d) octagonal (e) circular (f) elliptical

6.2.2 In-plane stresses σ_1. σ_2, τ_{12} for bottom $+45^0$& -45^0ply

The normalized maximum in-plane stresses for $+45^0$ & -45^0 plies are tabulated in Tables 6.2 & 6.3, respectively and comparison of normalized maximum In-plane stresses for $+45^0$ & -45^0 plies for SH pattern with different patch configurations is shown in Figure 6.4 & 6.4, respectively.

Table 6.2 Normalized maximum in-plane stress for SH (45^0 ply -bottom) with different patch configurations

Single Hole 45^0 ply(bottom)-Normalized in-plane stress			
Configuration	σ_1 / σ_0	σ_2 / σ_0	τ_{12} / σ_0
Without Patch	1.82	1.41	1.51
Square Patch	1.02	0.66	0.68
Hexagonal patch	0.99	0.68	0.70
Octagonal patch	0.99	0.69	0.68
Circular patch	1.02	0.66	0.68
Elliptical patch	1.11	0.68	0.71

Table 6.3 Normalized maximum in-plane stress for SH (-45^0 ply -bottom) with different patch configurations

Single Hole -45^0 ply(bottom)-Normalized in-plane stress			
Configuration	σ_1 / σ_0	σ_2 / σ_0	τ_{12} / σ_0
Without Patch	2.49	2.07	1.45
Square Patch	1.33	1.10	0.77
Hexagonal patch	1.34	1.10	0.78
Octagonal patch	1.36	1.12	0.79
Circular patch	1.36	1.12	0.79
Elliptical patch	1.11	0.68	0.71

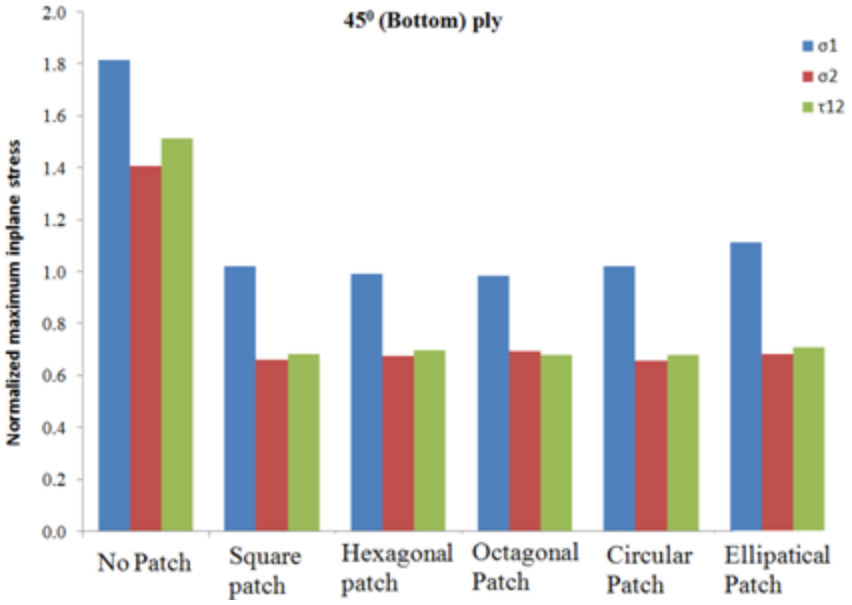

Figure 6.4 Comparison of in-plane stresses (bottom 45^0 layer) for SH pattern with different patch configurations

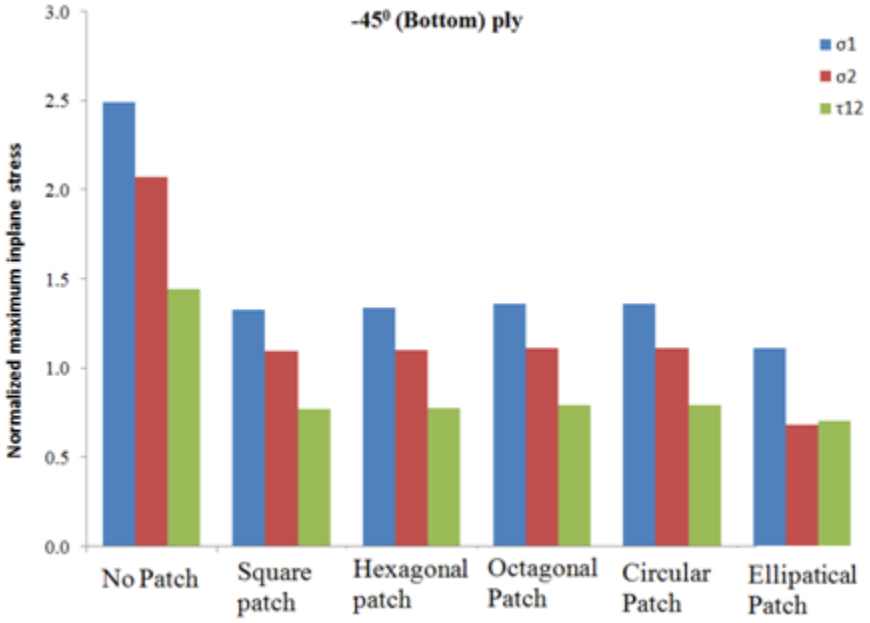

Figure 6.5 Comparison of in-plane stresses (bottom -45^0 layer) for SH pattern with different patch configurations

6.2.3 Interlaminar stresses σ_3, τ_{23} at the interfaces

There are two interfaces where the interlaminar stresses are critical.

1. Interface between parent laminate and adhesive.
2. Interface between patch laminate and adhesive.

The interlaminar stresses are plotted across the width of the laminate at the center as shown in Figure 6.6. The interlaminar stresses are maximum at the edge of the patch and holes.

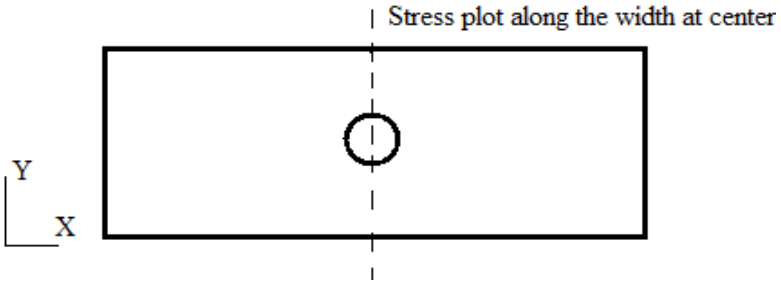

Figure 6.6 Location of stress plot along width of the laminate

The σ_3, τ_{23} distribution is along the width of the laminate at parent and adhesive interface is shown in Figure 6.7 & 6.8.

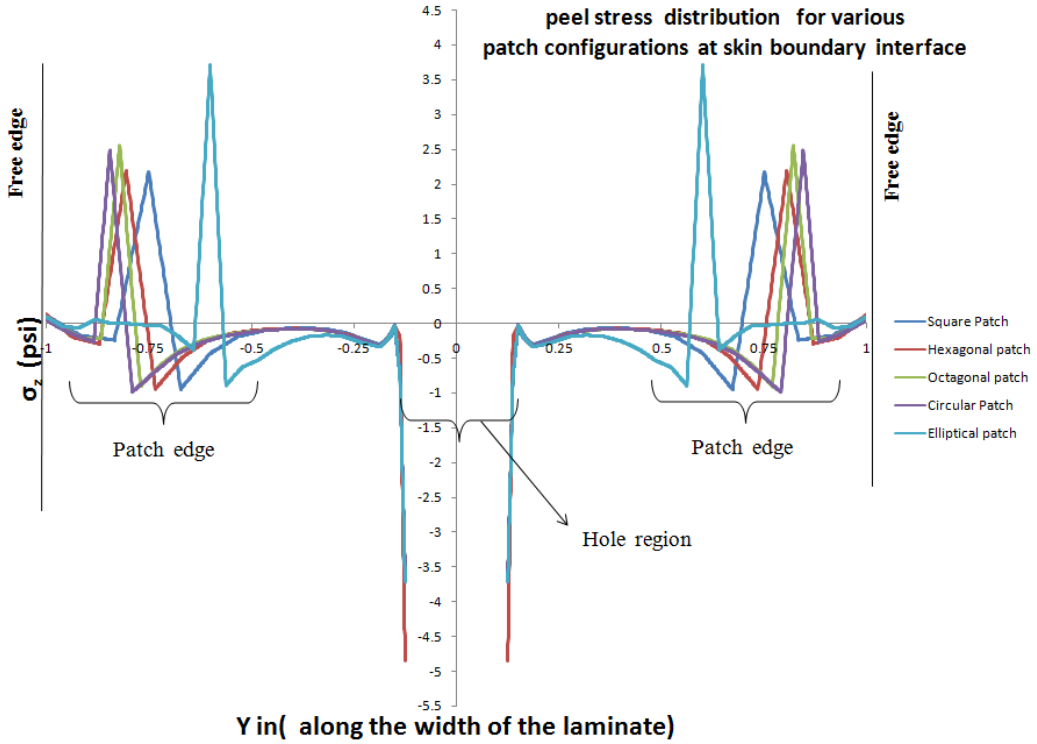

Figure 6.7 σ_3 stress at parent laminate and adhesive interface for all patch configurations

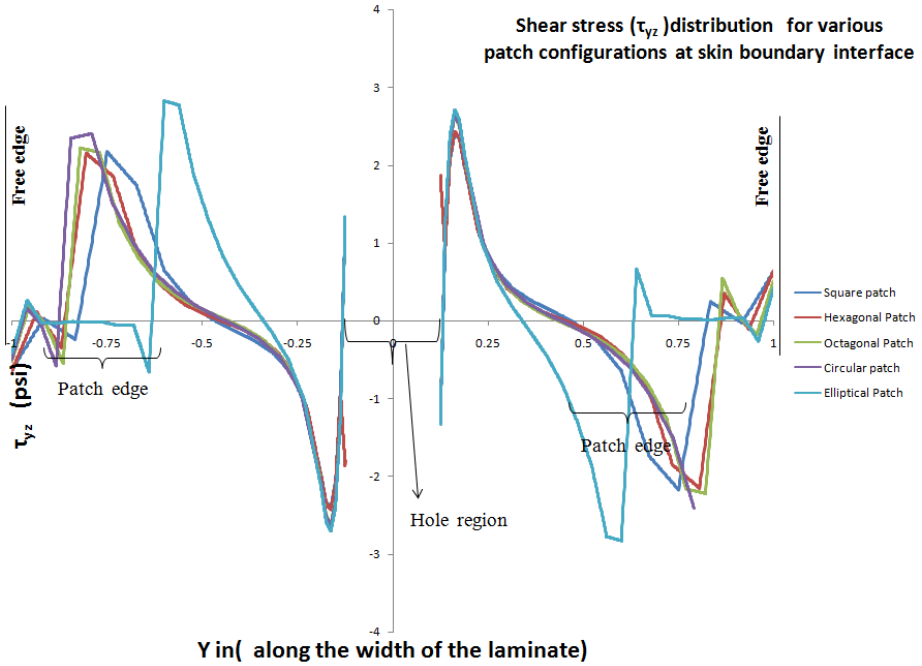

Figure 6.8 τ_{23} stress at parent laminate and adhesive interface for all patch configurations

The σ_3, τ_{23} distribution is along the width of the laminate at patch and adhesive interface is shown in Figures 6.9 & 6.10.

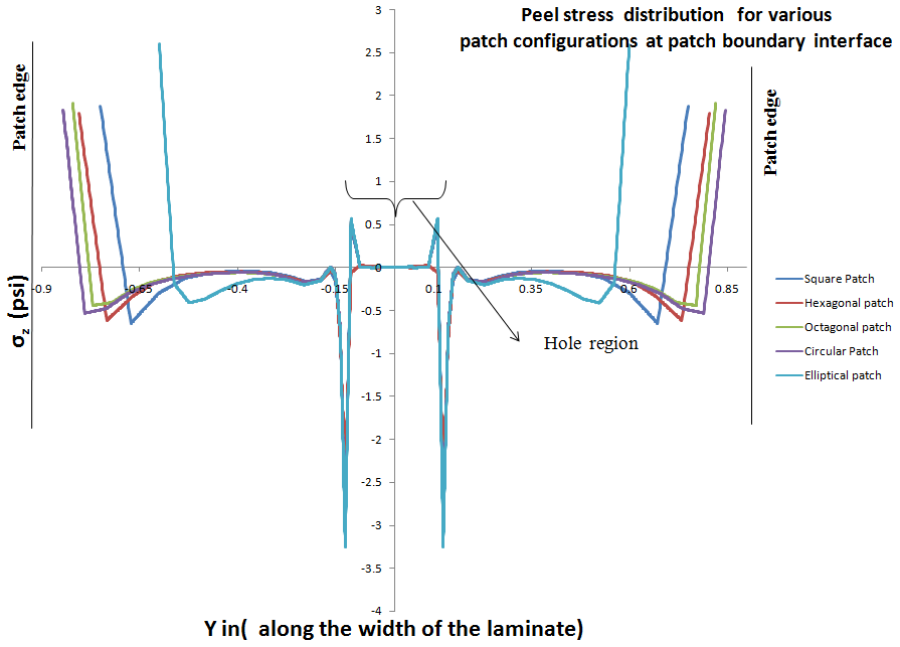

Figure 6.9 σ_3 stress at patch laminate and adhesive interface for all patch configurations

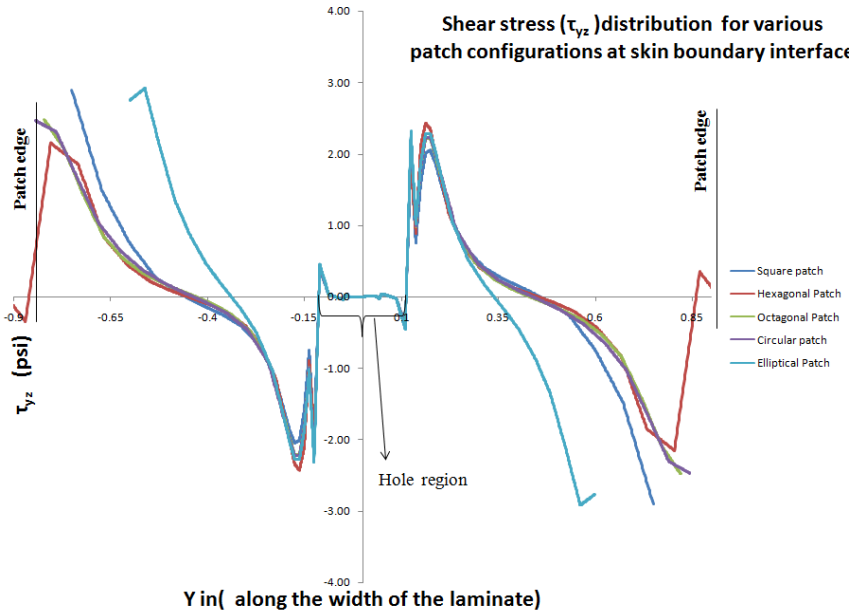

Figure 6.10 τ_{23} stress at patch laminate and adhesive interface for all patch configurations

6.3 Effect of patch configurations with TBH pattern on parent laminate

6.3.1 In-plane stresses σ_1. σ_2, τ_{12} for bottom 0^0 ply

The in-plane stress is maximum at bottom 0^0 ply in all configurations. The in-plane stresses are tabulated in Table 6.4 and comparison of normalized maximum in-plane stresses for bottom 0^0 ply for TBH pattern with different patch configurations is shown in Figure 6.11.

Table 6.4 Normalized maximum stress for TBH (0^0 ply -bottom) with different patch configuration

Top & Bottom hole -0^0 ply(bottom)-Normalized in-plane stress			
Configuration	σ_1 / σ_0	σ_2 / σ_0	τ_{12} / σ_0
Without Patch	7.19	0.34	0.53
Square Patch	4.44	0.19	0.32
Hexagonal patch	4.45	0.19	0.32
Octagonal patch	4.59	0.19	0.34
Circular patch	4.45	0.19	0.32
Elliptical patch	4.54	0.20	0.33

The peak stress (σ_1) significantly decreases with all patch configurations when compared to No patch in the TBH pattern. Among the patch configurations the peak stress (σ_1) is the least for circular and hexagonal patch configurations.

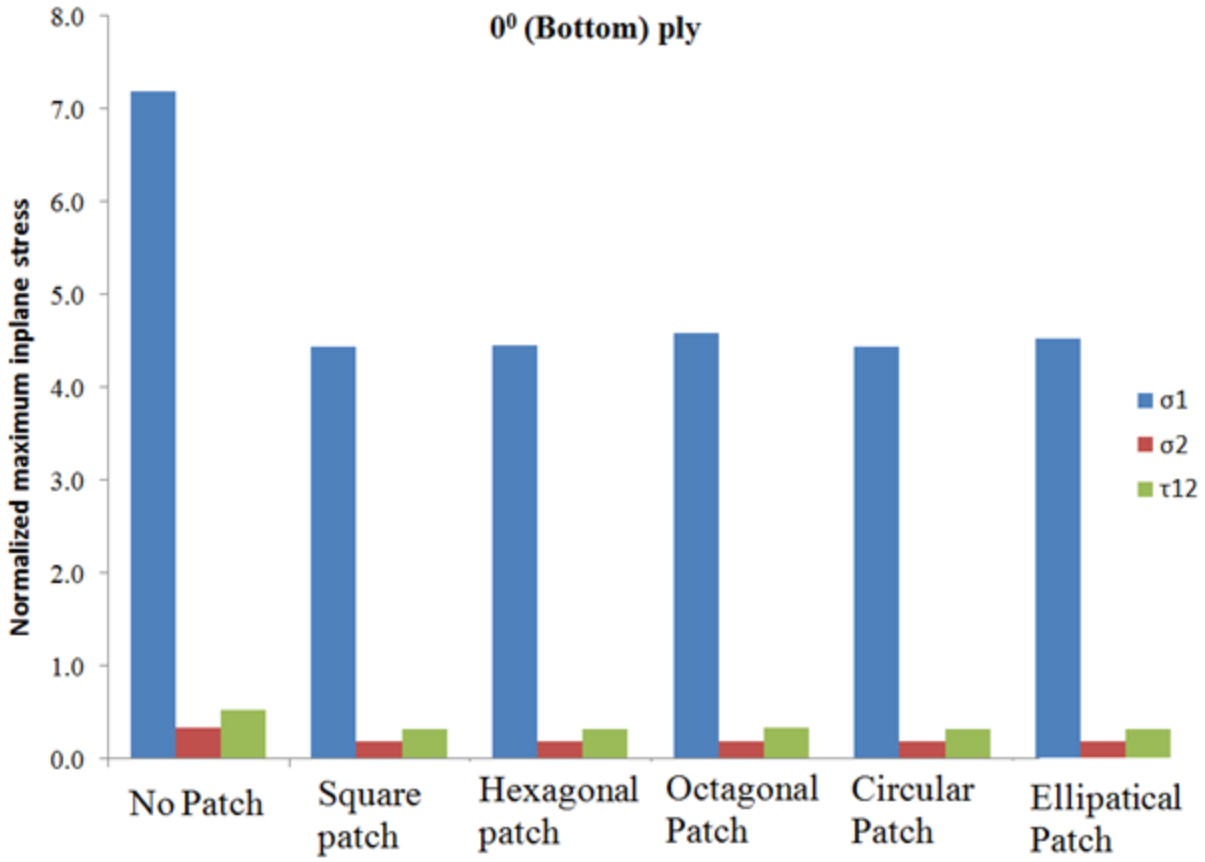

Figure 6.11 Comparison of in-plane stresses (bottom 0^0 layer) for TBH pattern with different patch configurations

The stress contour for 0^0 layer with different patch configuration for TBH pattern is shown in Figure 6.12,

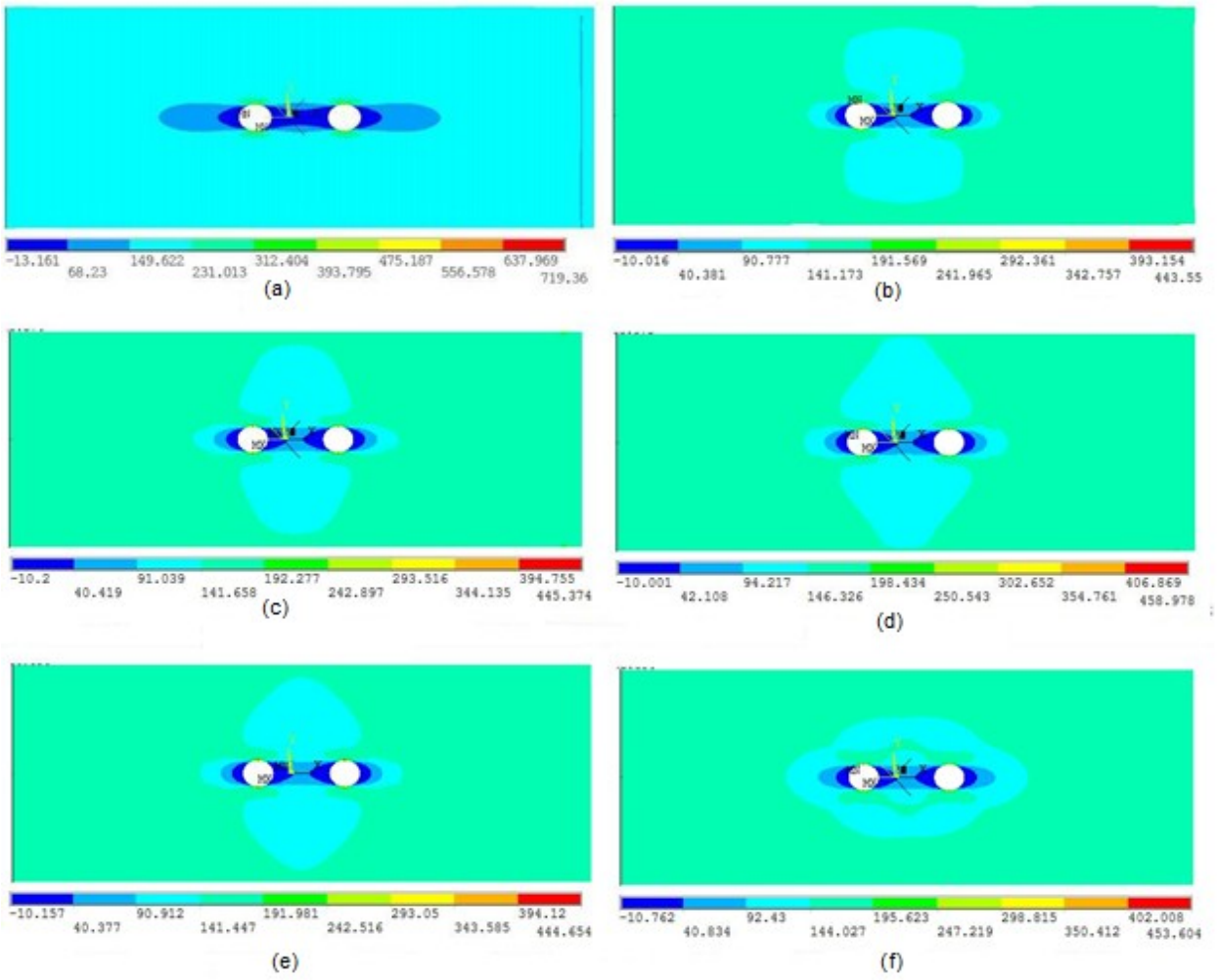

Figure 6.12 Stress contour for 0^0 layer with different patch configuration for TBH pattern (a) no patch (b) square (c) hexagonal (d) octagonal (e) circular (f) elliptical

Comparison of the stress contours of the parent laminate (45^0 layer) at the interface between parent and patch laminate for different patch configuration in TBH pattern is shown in Figure 6.13,

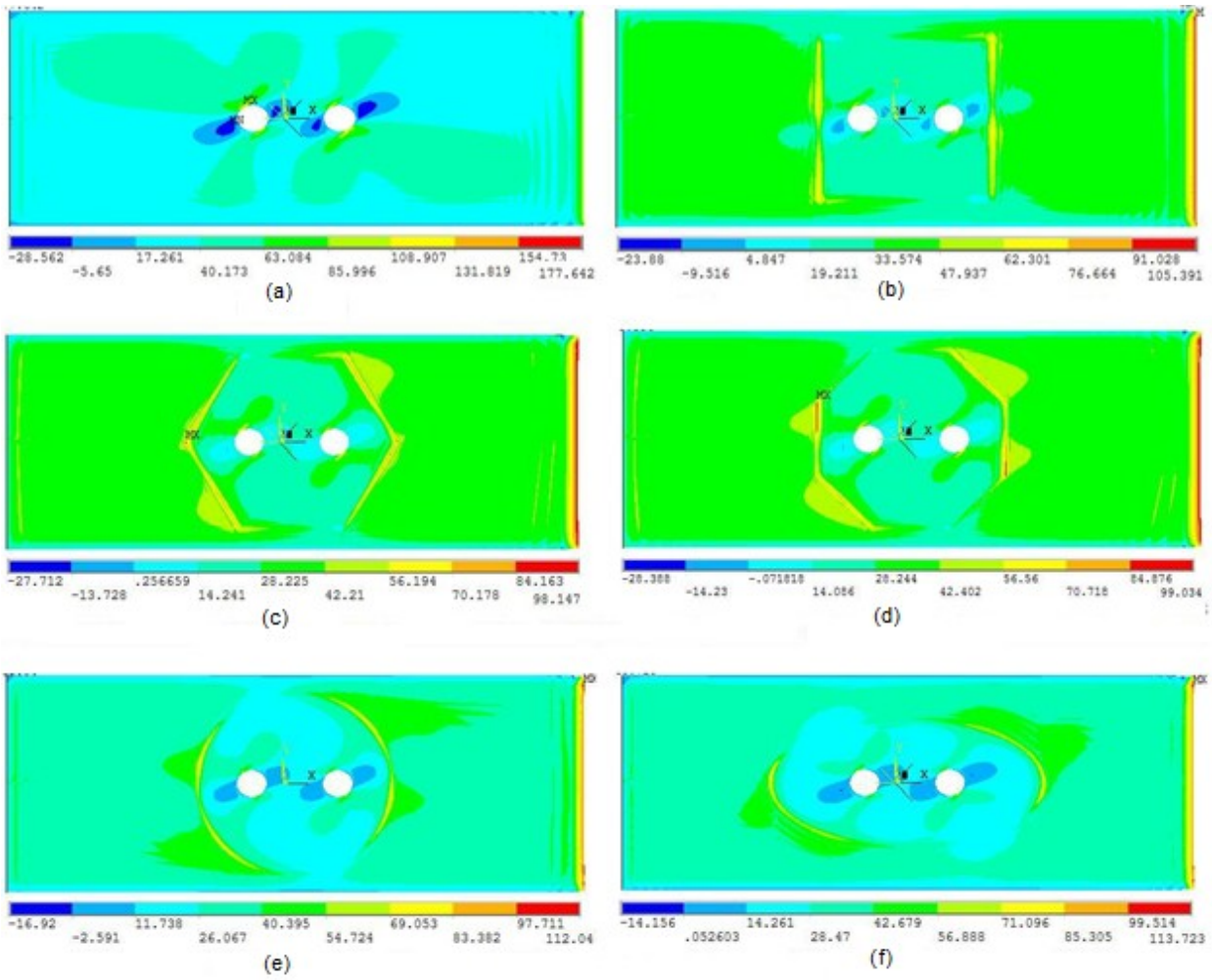

Figure 6.13 Stress contour for 45^0 layer with different patch configuration for TBH pattern at parent and patch interface (a) no patch (b) square (c) hexagonal (d) octagonal (e) circular (f) elliptical

6.3.2 In-plane stresses σ_1. σ_2, τ_{12} for bottom $+45^0$& -45^0ply

The normalized maximum in-plane stresses for $+45^0$ & -45^0 plies are tabulated in Tables 6.5 & 6.6 respectively and comparison of normalized maximum in-plane stresses for $+45^0$ & -45^0 plies for TBH pattern with different patch configurations is shown in the figures 6.14 & 6.15, respectively.

Table 6.5 Normalized maximum in-plane stress for TBH (45^0 ply -bottom) with different patch configurations

Top & Bottom hole 45^0 ply(bottom)-Normalized in-plane stress			
Configuration	σ_1 / σ_0	σ_2 / σ_0	τ_{12} / σ_0
Without Patch	1.78	1.39	1.49
Square Patch	1.05	0.70	0.72
Hexagonal patch	0.98	0.69	0.71
Octagonal patch	0.99	0.72	0.72
Circular patch	1.12	0.69	0.71
Elliptical patch	1.14	0.69	0.71

Table 6.6 Normalized maximum in-plane stress for TBH (-45^0 ply -bottom) with different patch configurations

Top & Bottom hole -45^0 ply(bottom)-Normalized in-plane stress			
Configuration	σ_1 / σ_0	σ_2 / σ_0	τ_{12} / σ_0
Without Patch	2.40	2.00	1.35
Square Patch	1.39	1.17	0.78
Hexagonal patch	1.38	1.15	0.78
Octagonal patch	1.34	1.10	0.77
Circular patch	1.44	1.14	0.78
Elliptical patch	1.46	1.17	0.80

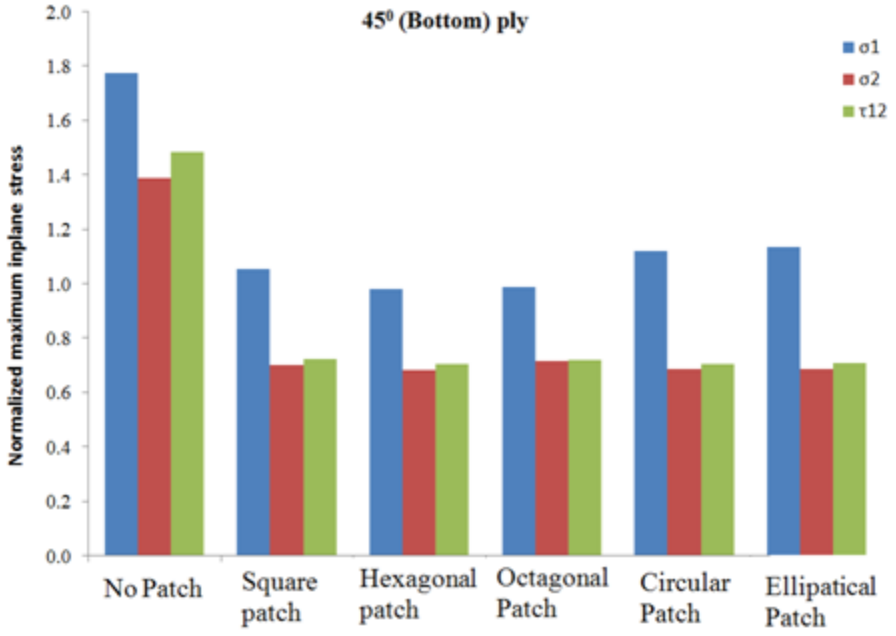

Figure 6.14 Comparison of in-plane stresses (bottom 45^0 layer) for TBH pattern with different patch configurations

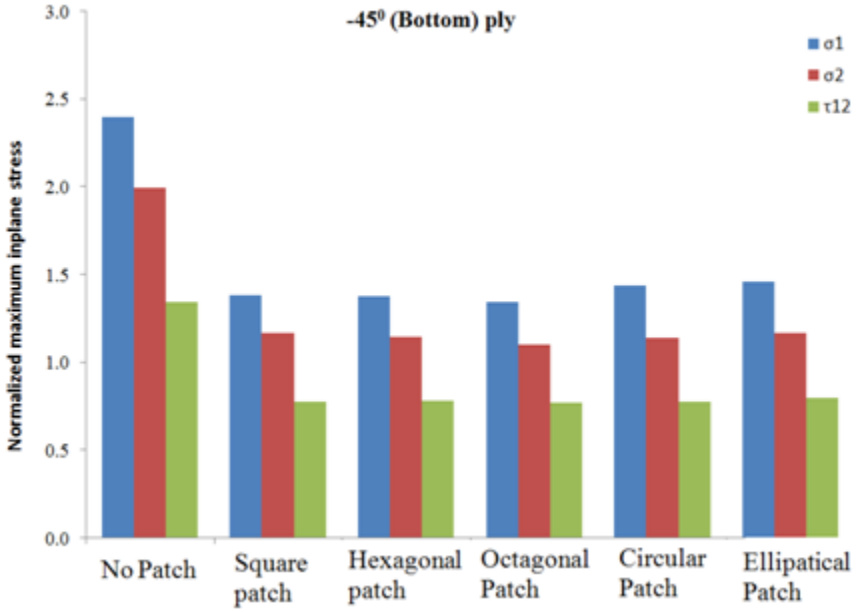

Figure 6.15 Comparison of in-plane stresses (bottom -45^0 layer) for TBH pattern with different patch configurations

6.3.3 Interlaminar stresses σ_3, τ_{23} at the interfaces

There are two interfaces where the interlaminar stresses are critical.

1. Interface between parent laminate and adhesive.
2. Interface between patch laminate and adhesive.

The interlaminar stresses are plotted across the width of the laminate at the center as shown in Figure 6.16. The interlaminar stresses are maximum at the edge of the patch and holes.

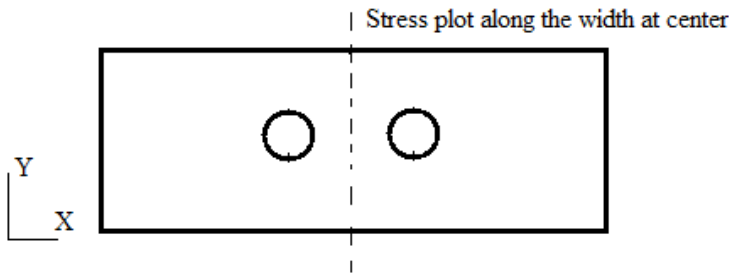

Figure 6.16 Location of stress plot along width of the laminate

The σ_3, τ_{23} distribution is along the width of the laminate at parent and adhesive interface is shown in Figures 6.17 & 6.18.

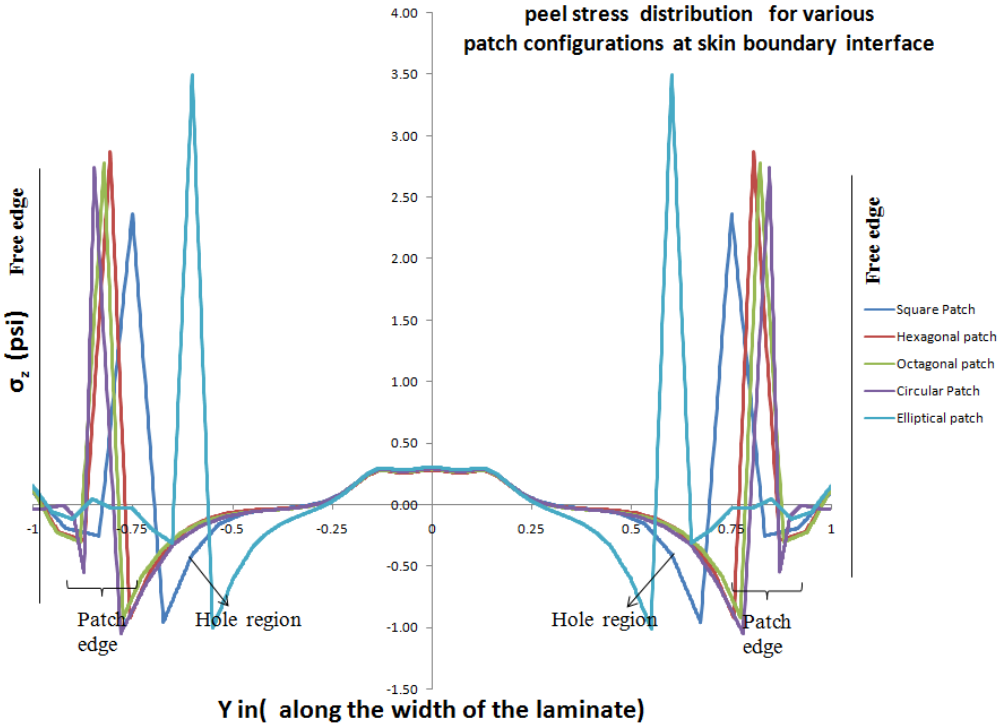

Figure 6.17 σ_3 stress at parent laminate and adhesive interface for all patch configurations

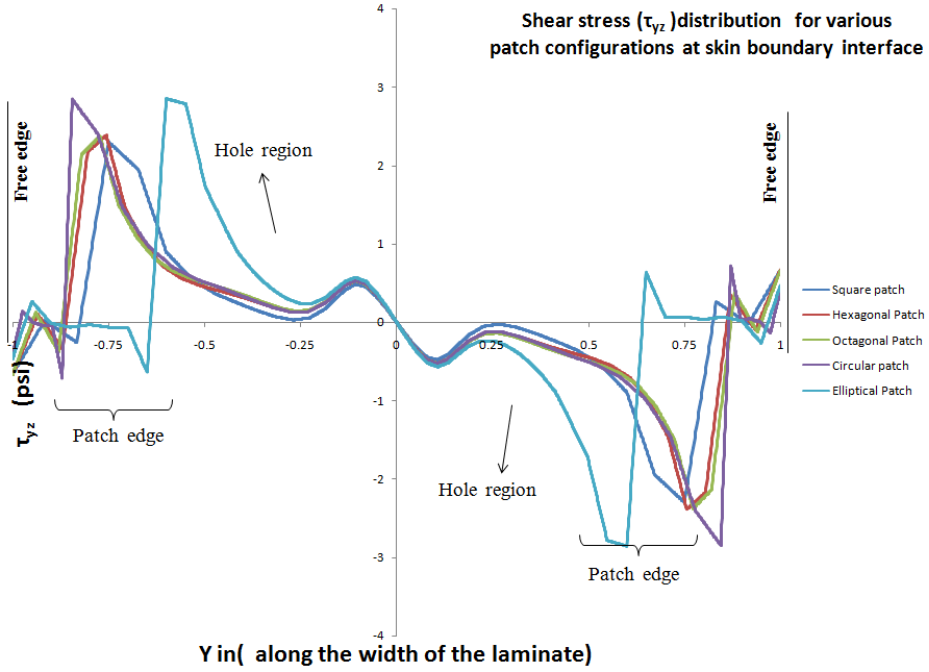

Figure 6.18 τ_{23} stress at parent laminate and adhesive interface for all patch configurations

The σ_3, τ_{23} distribution is along the width of the laminate at patch and adhesive interface is shown in Figures 6.19 & 6.20.

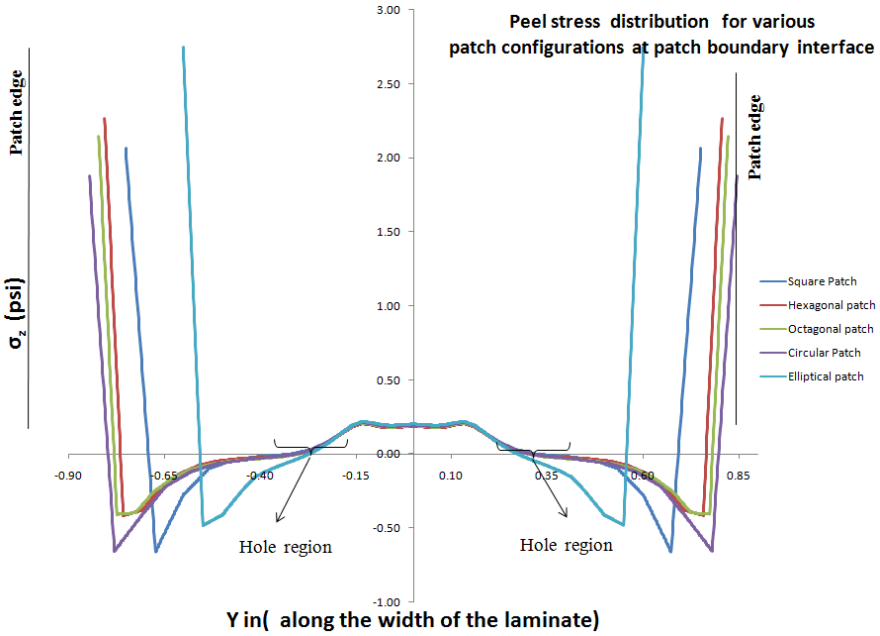

Figure 6.19 σ_3 stress at patch laminate and adhesive interface for all patch configurations

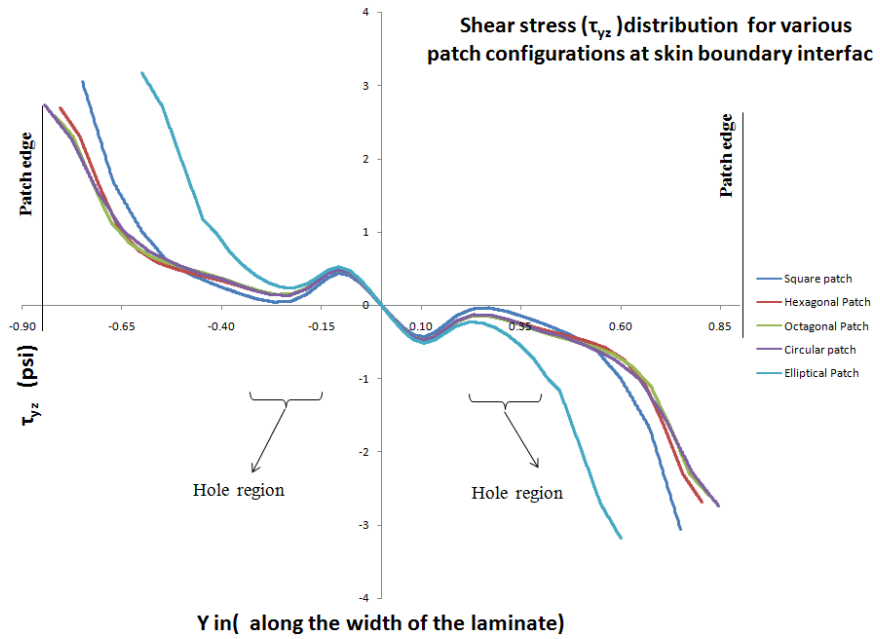

Figure 6.20 τ_{23} stress at patch laminate and adhesive interface for all patch configurations

6.4 Effect of patch configurations with SSH pattern on parent laminate

6.4.1 In-plane stresses σ_1. σ_2, τ_{12} for bottom 0^0 ply

The in-plane stress is maximum at bottom 0^0 ply in all configurations. The in-plane stresses are tabulated in Table 6.7 and comparison of normalized maximum in-plane stresses for bottom 0^0 ply for SSH pattern with different patch configurations is shown in Figure 6.21.

Table 6.7 Normalized maximum stress for SSH (0^0 ply -bottom) with different patch configuration

Side by Side hole -0^0 ply(bottom)-Normalized in-plane stress			
Configuration	σ_1 / σ_0	σ_2 / σ_0	τ_{12} / σ_0
Without Patch	8.16	0.37	0.59
Square Patch	4.67	0.20	0.33
Hexagonal patch	4.58	0.20	0.33
Octagonal patch	4.59	0.20	0.33
Circular patch	4.59	0.20	0.33
Elliptical patch	4.97	0.21	0.35

The peak stress (σ_1) significantly decreases with all patch configurations when compared to No patch in the SSH pattern. Among the patch configurations the peak stress (σ_1) is the least for circular and octagonal patch configurations.

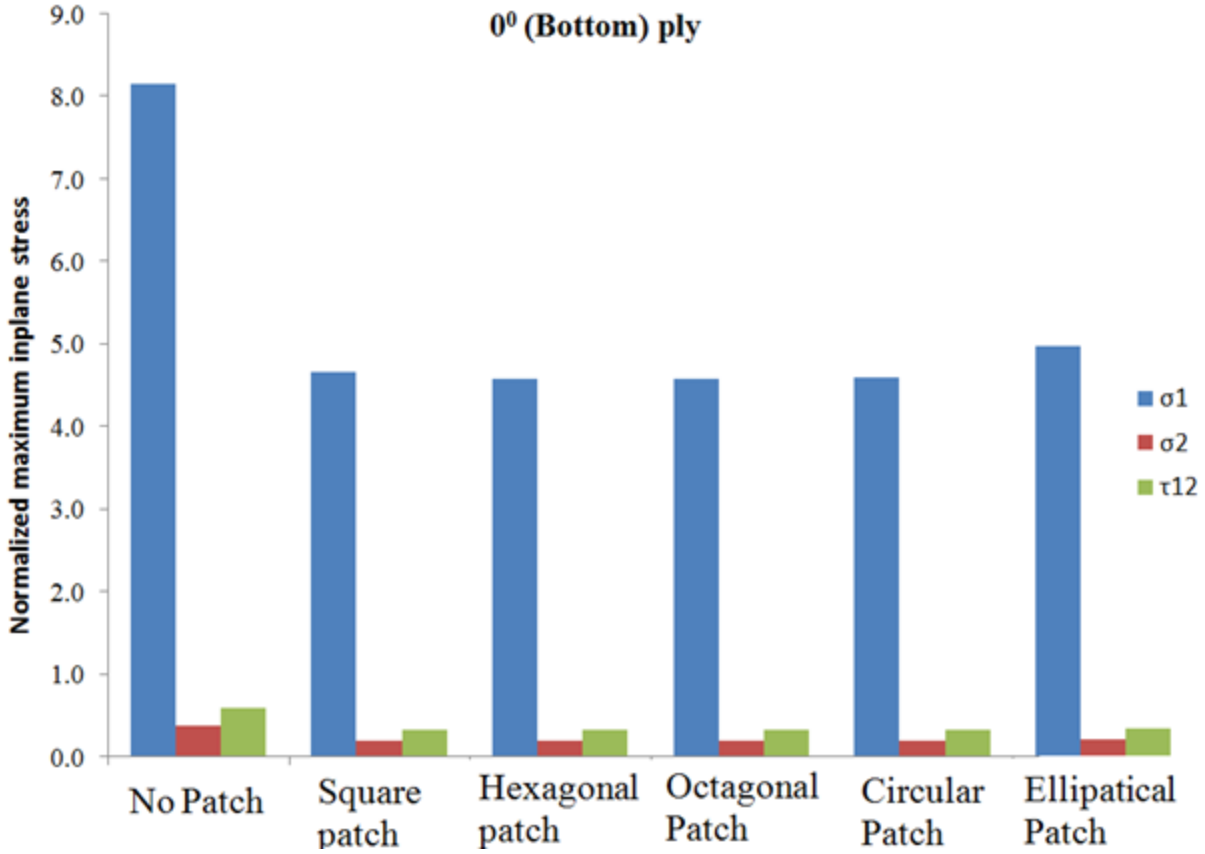

Figure 6.21 Comparison of in-plane stresses (bottom 0^0 layer) for SSH pattern with different patch configurations

The stress contour for 0^0 layer with different patch configuration for SSH pattern is shown in Figure 6.22,

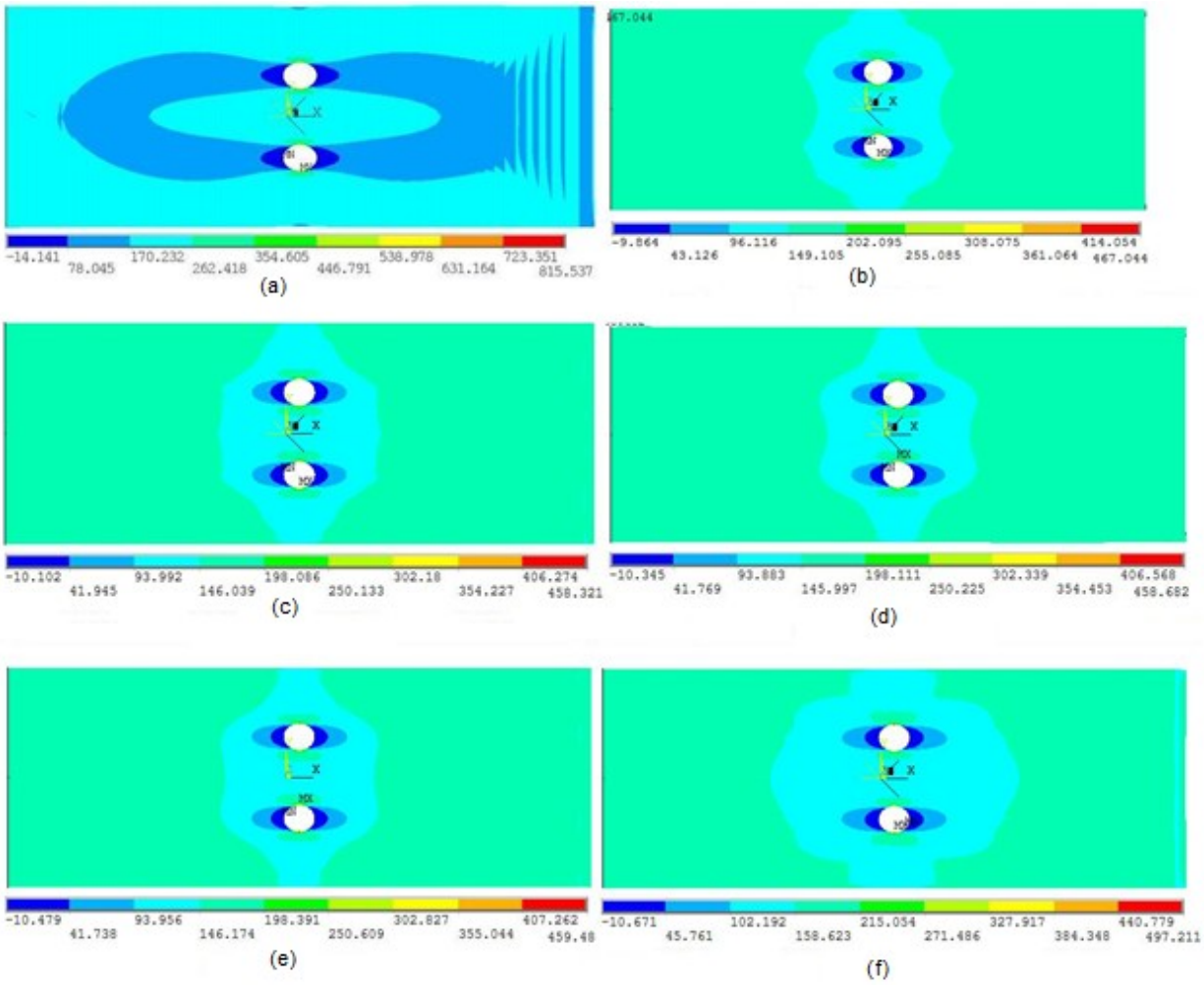

Figure 6.22 Stress contour for 0^0 layer with different patch configuration for SSH pattern (a) no patch (b) square (c) hexagonal (d) octagonal (e) circular (f) elliptical

Comparison of the stress contours of the parent laminate (45^0 layer) at the interface between parent and patch laminate for different patch configuration in SSH pattern is shown in Figure 6.23,

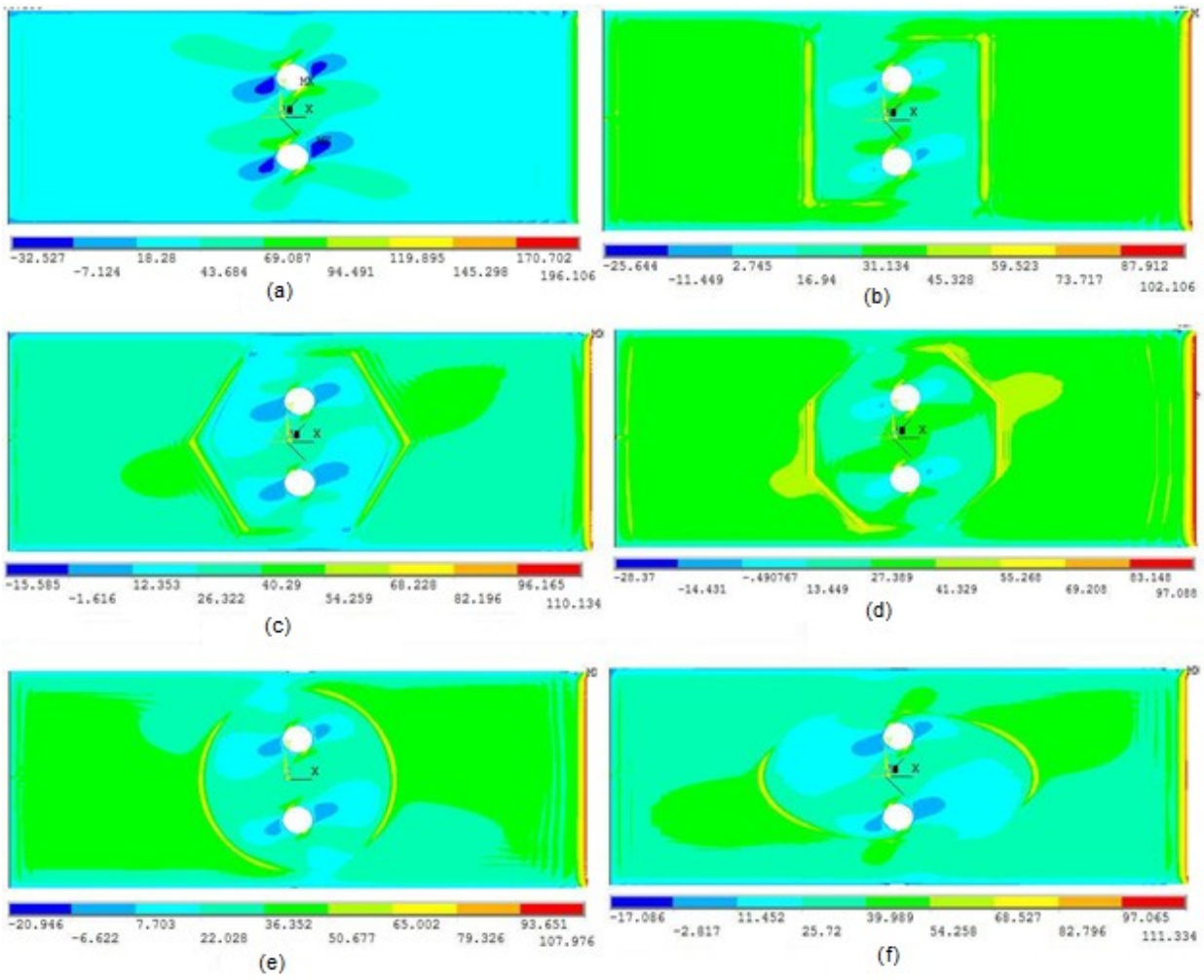

Figure 6.23 Stress contour for 45^0 layer with different patch configuration for SSH pattern at parent and patch interface (a) no patch (b) square (c) hexagonal (d) octagonal (e) circular (f) elliptical

6.4.2 In-plane stresses σ_1. σ_2, τ_{12} for bottom $+45^0$& -45^0ply

The normalized maximum in-plane stresses for $+45^0$ & -45^0 plies are tabulated in Tables 6.8 & 6.9, respectively and comparison of normalized maximum In-plane stresses for $+45^0$ & -45^0 plies for SSH pattern with different patch configurations is shown in the figures 6.24 & 6.25, respectively.

Table 6.8 Normalized maximum in-plane stress for SSH (45^0 ply -bottom) with different patch configurations

Side by Side hole 45^0 ply(bottom)-Normalized in-plane stress			
Configuration	σ_1 / σ_0	σ_2 / σ_0	τ_{12} / σ_0
Without Patch	1.96	1.56	1.66
Square Patch	1.02	0.72	0.73
Hexagonal patch	1.10	0.73	0.75
Octagonal patch	0.97	0.70	0.72
Circular patch	1.08	0.70	0.72
Elliptical patch	1.11	0.75	0.77

Table 6.9 Normalized maximum in-plane stress for SSH (-45^0 ply -bottom) with different patch configurations

Side by Side hole -45^0 ply(bottom)-Normalized in-plane stress			
Configuration	σ_1 / σ_0	σ_2 / σ_0	τ_{12} / σ_0
Without Patch	2.63	2.18	1.50
Square Patch	1.40	1.15	0.81
Hexagonal patch	1.49	1.15	0.80
Octagonal patch	1.38	1.15	0.80
Circular patch	1.40	1.15	0.80
Elliptical patch	1.51	1.25	0.85

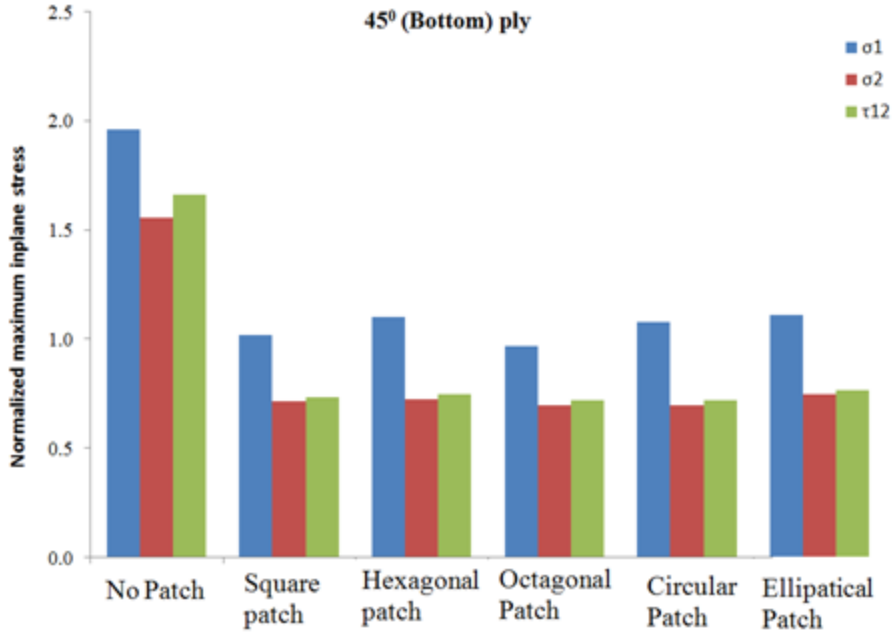

Figure 6.24 Comparison of in-plane stresses (bottom 45^0 layer) for SSH pattern with different patch configurations

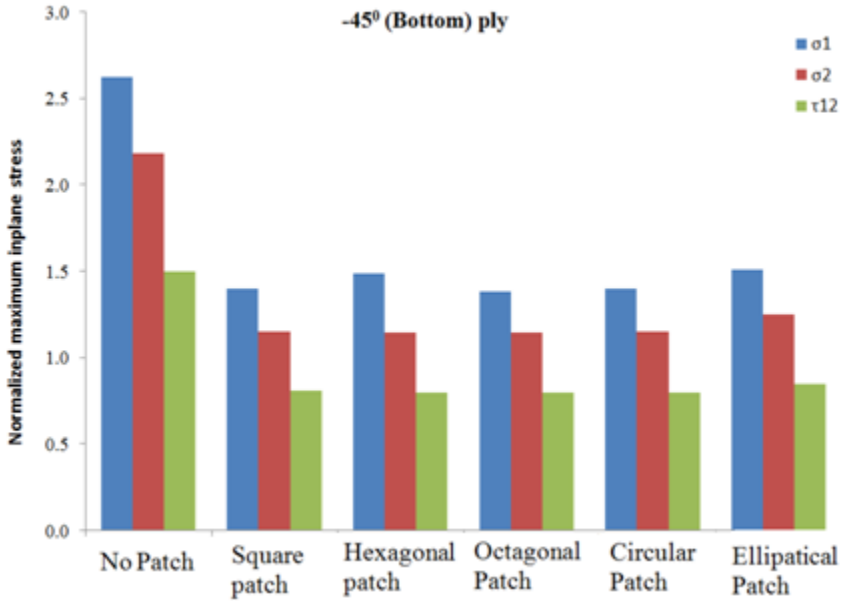

Figure 6.25 Comparison of in-plane stresses (bottom -45^0 layer) for SSH pattern with different patch configurations

6.4.3 Interlaminar stresses σ_3, τ_{23} at the interfaces

There are two interfaces where the interlaminar stresses are critical,

1. Interface between parent laminate and adhesive.
2. Interface between patch laminate and adhesive.

The interlaminar stresses are plotted across the width of the laminate at the center as shown in Figure 6.26. The interlaminar stresses are maximum at the edge of the patch and holes.

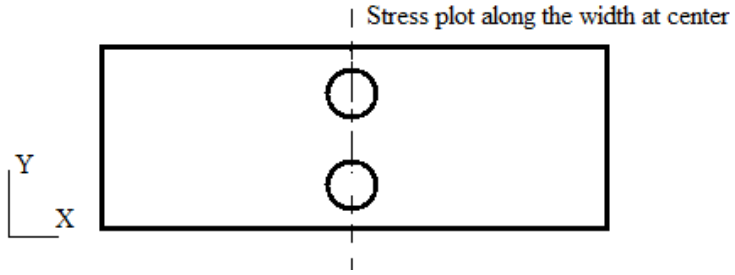

Figure 6.26 Location of stress plot along width of the laminate

The σ_3, τ_{23} distribution is along the width of the laminate at parent and adhesive interface is shown in Figures 6.27 & 6.28.

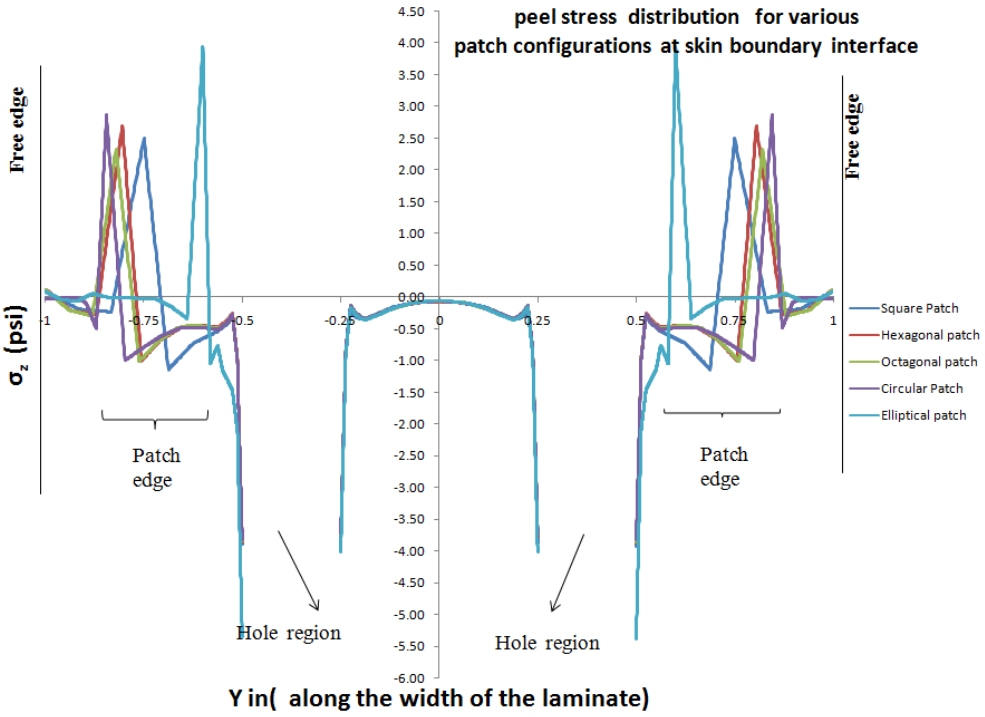

Figure 6.27 σ_3 stress at parent laminate and adhesive interface for all patch configurations

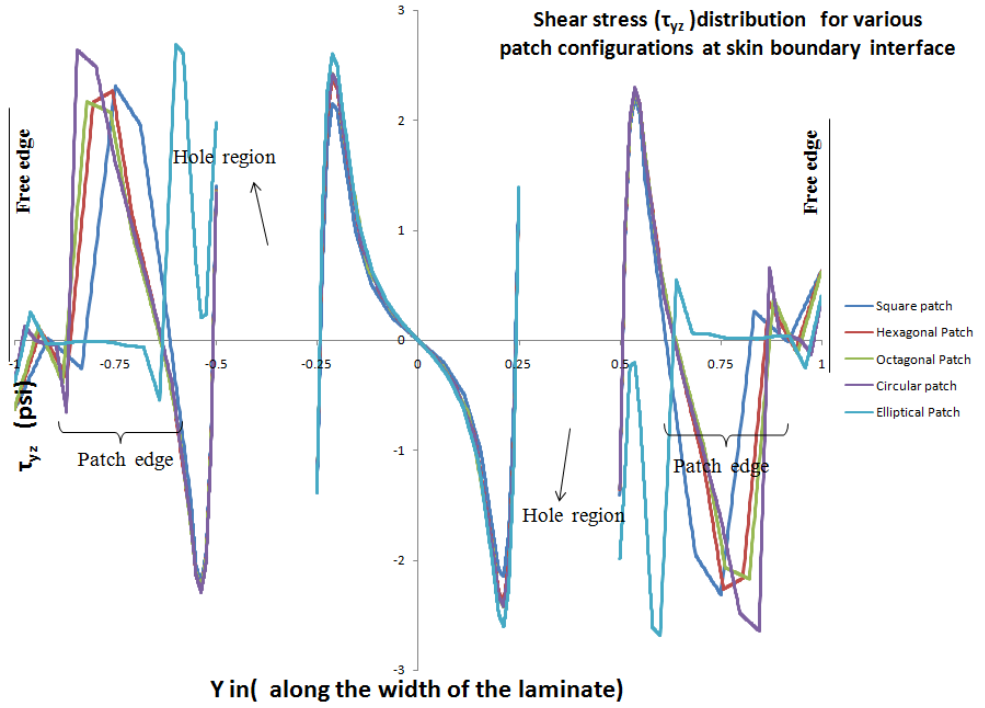

Figure 6.28 τ_{23} stress at parent laminate and adhesive interface for all patch configurations

The σ_3, τ_{23} distribution is along the width of the laminate at patch and adhesive interface is shown in Figures 6.29 & 6.30.

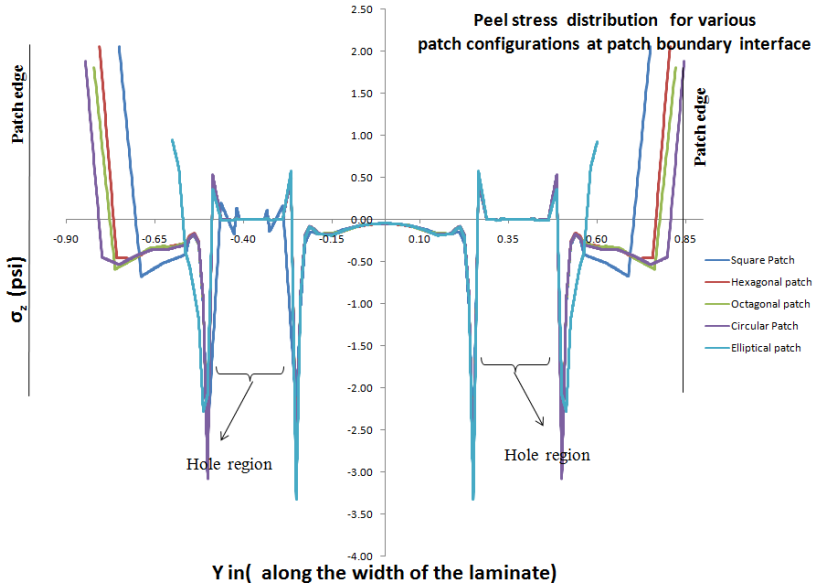

Figure 6.29 σ_3 stress at patch laminate and adhesive interface for all patch configurations

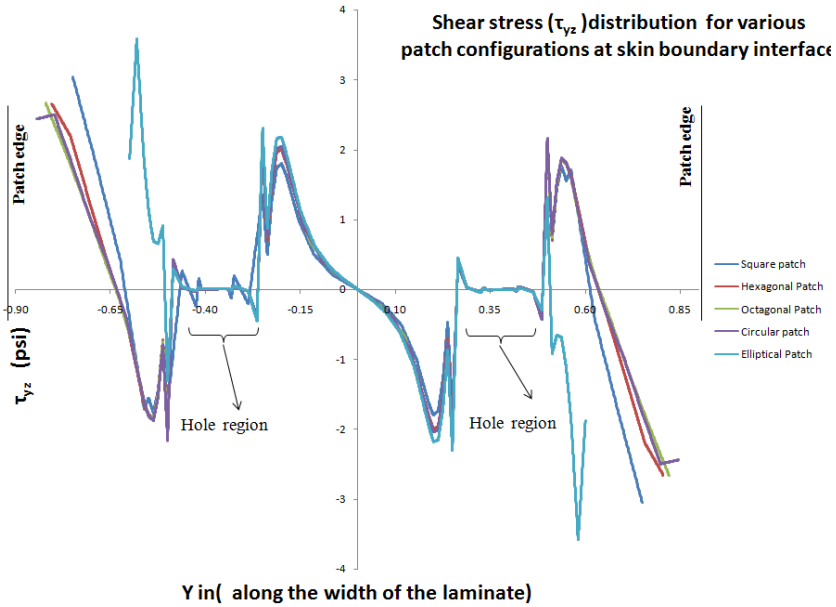

Figure 6.30 τ_{23} stress at patch laminate and adhesive interface for all patch configurations

6.5 Effect of patch configurations with SA pattern on parent laminate

6.5.1 In-plane stresses σ_1. σ_2, τ_{12} for bottom 0^0 ply

The in-plane stress is maximum at bottom 0^0 ply in all configurations. The in-plane stresses are tabulated in Table 6.10 and comparison of normalized maximum in-plane stresses for bottom 0^0 ply for SA pattern with different patch configurations is shown in Figure 6.31.

Table 6.10 Normalized maximum stress for SA (0^0 ply -bottom) with different patch configuration

Square Array-0^0 ply(bottom)-Normalized in-plane stress			
Configuration	σ_1 / σ_0	σ_2 / σ_0	τ_{12} / σ_0
Without Patch	7.62	0.36	0.56
Square Patch	4.69	0.20	0.34
Hexagonal patch	4.93	0.21	0.36
Octagonal patch	4.85	0.20	0.35
Circular patch	4.27	0.18	0.32
Elliptical patch	5.06	0.22	0.38

The peak stress (σ_1) significantly decreases with all patch configurations when compared to No patch in the SA pattern. Among the patch configurations the peak stress (σ_1) is the least for circular patch configuration.

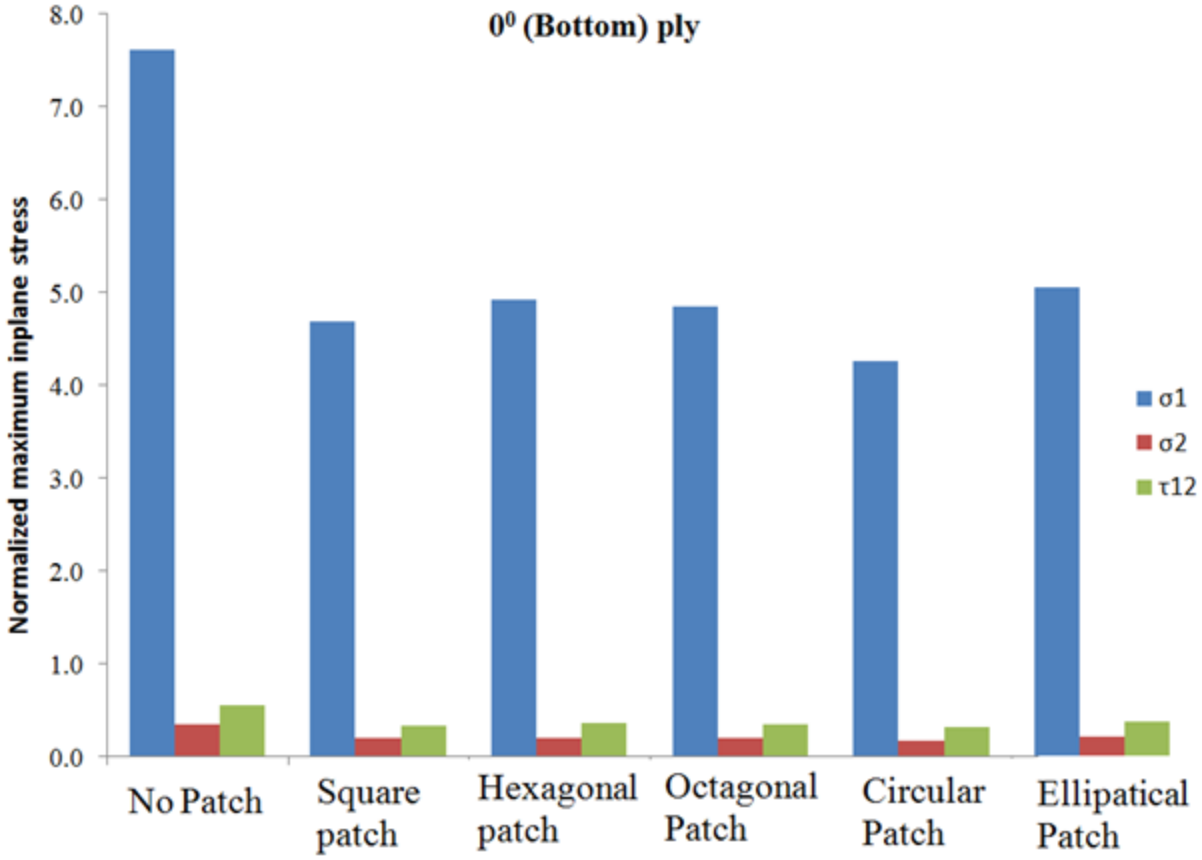

Figure 6.31 Comparison of in-plane stresses (bottom 0^0 layer) for SA pattern with different patch configurations

The stress contour for 0^0 layer with different patch configuration for SA pattern is shown in Figure 6.32,

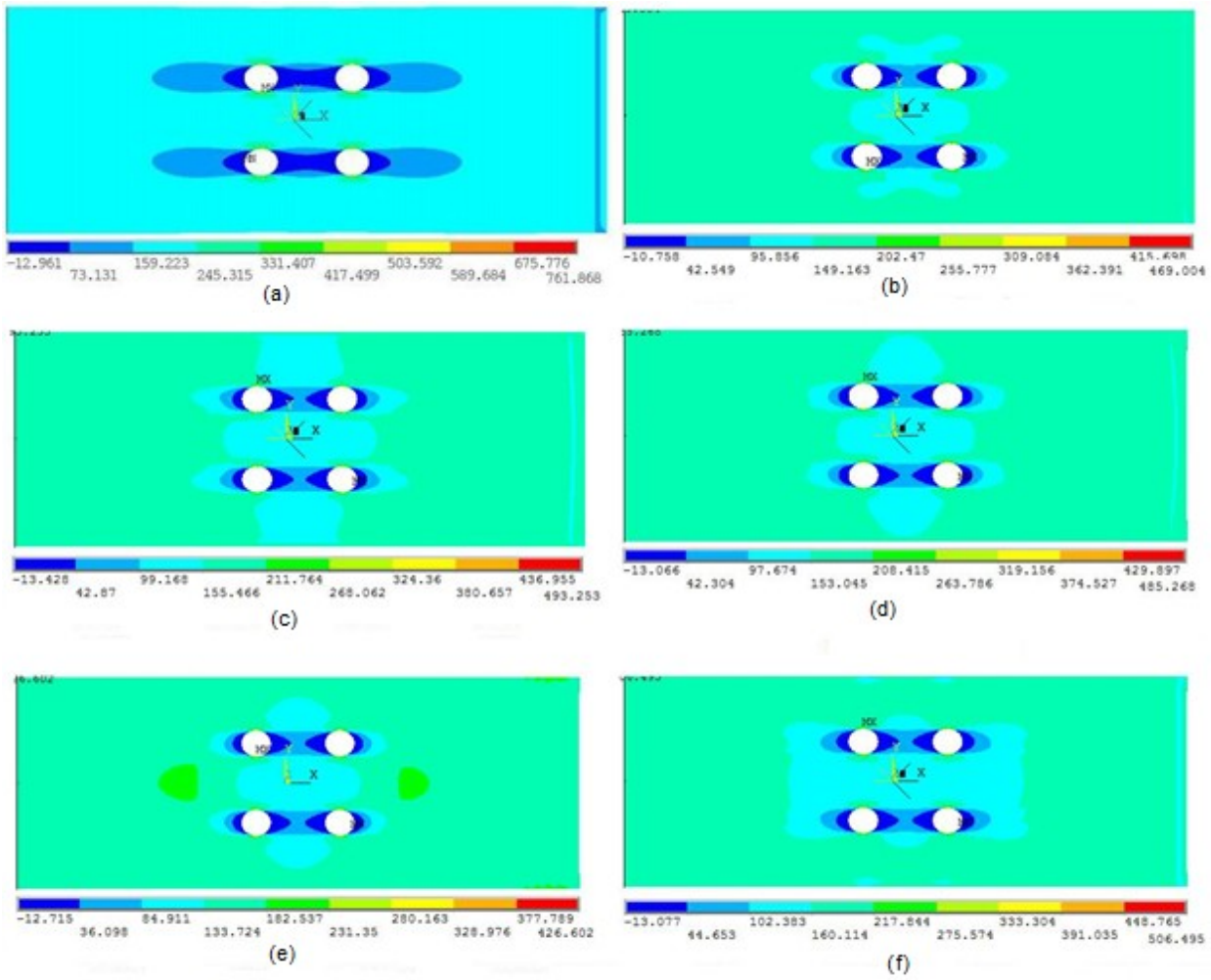

Figure 6.32 Stress contour for 0^0 layer with different patch configuration for SA pattern (a) no patch (b) square (c) hexagonal (d) octagonal (e) circular (f) elliptical

Comparison of the stress contours of the parent laminate (45^0 layer) at the interface between parent and patch laminate for different patch configuration in SA pattern is shown in Figure 6.33,

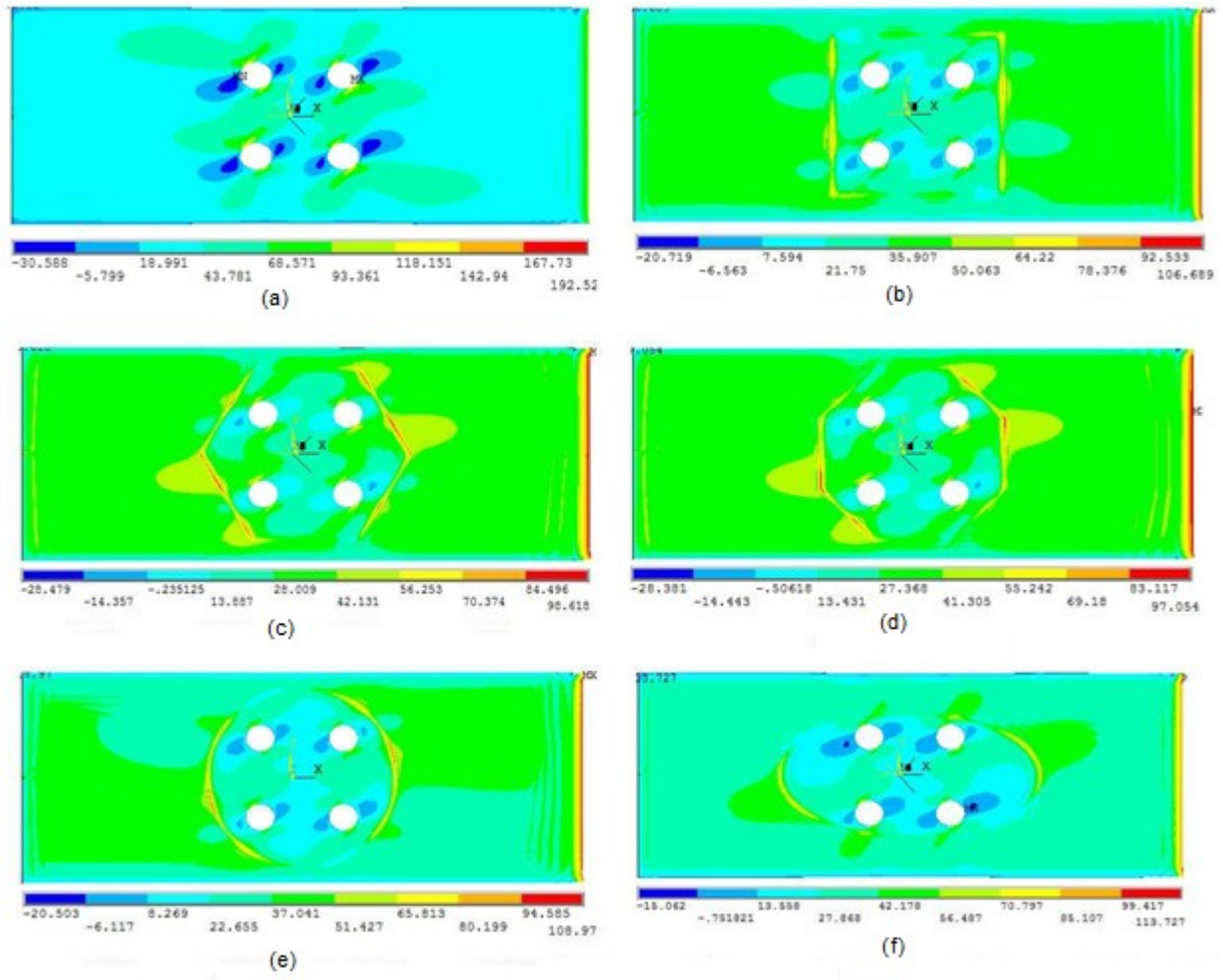

Figure 6.33 Stress contour for 45^0 layer with different patch configuration for SA pattern at parent and patch interface (a) no patch (b) square (c) hexagonal (d) octagonal (e) circular (f) elliptical

6.5.2 In-plane stresses σ_1. σ_2, τ_{12} for bottom $+45^0$& -45^0ply

The normalized maximum in-plane stresses for $+45^0$ & -45^0 plies are tabulated in Tables 6.11 & 6.12, respectively and comparison of normalized maximum in-plane stresses for $+45^0$ & -45^0 plies for SA pattern with different patch configurations is shown in Figures 6.34 & 6.35, respectively.

Table 6.11 Normalized maximum in-plane stress for SA (45^0 ply -bottom) with different patch configurations

Square Array 45^0 ply(bottom)-Normalized in-plane stress			
Configuration	σ_1 / σ_0	σ_2 / σ_0	τ_{12} / σ_0
Without Patch	1.93	1.53	1.64
Square Patch	1.07	0.76	0.78
Hexagonal patch	0.99	0.77	0.80
Octagonal patch	0.97	0.76	0.80
Circular patch	1.09	0.70	0.75
Elliptical patch	1.14	0.77	0.80

Table 6.12 Normalized maximum in-plane stress for SA (-45^0 ply -bottom) with different patch configurations

Square Array -45^0 ply(bottom)-Normalized in-plane stress			
Configuration	σ_1 / σ_0	σ_2 / σ_0	τ_{12} / σ_0
Without Patch	2.56	2.13	1.42
Square Patch	1.46	1.24	0.82
Hexagonal patch	1.45	1.21	0.81
Octagonal patch	1.44	1.21	0.81
Circular patch	1.40	1.09	0.71
Elliptical patch	1.51	1.24	0.85

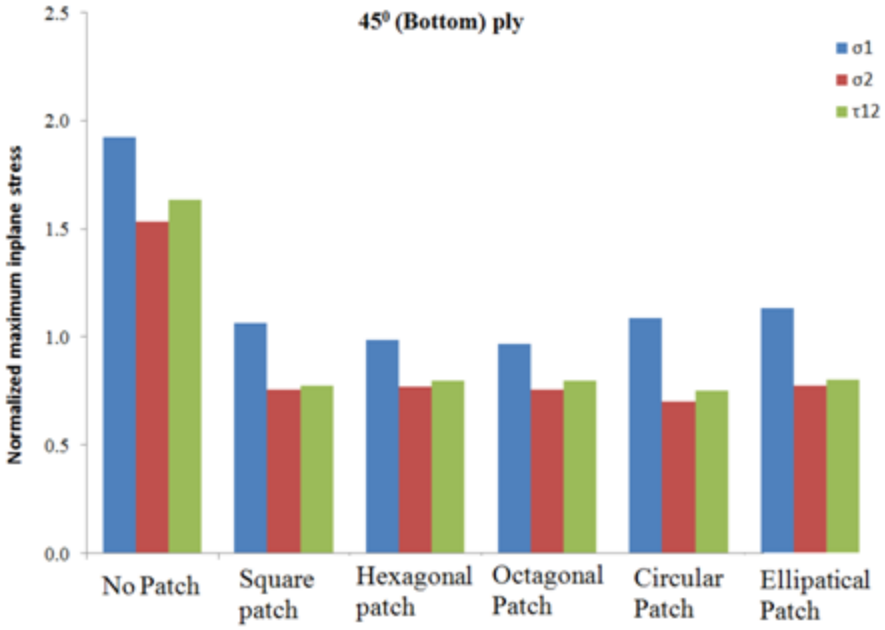

Figure 6.34 Comparison of in-plane stresses (bottom 45^0 layer) for SA pattern with different patch configurations

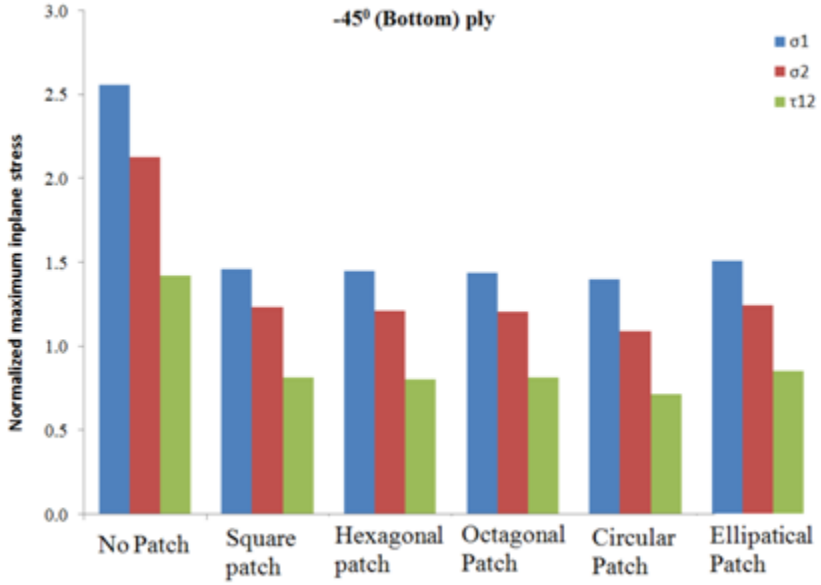

Figure 6.35 Comparison of in-plane stresses (bottom -45^0 layer) for SA pattern with different patch configurations

6.5.3 Interlaminar stresses σ_3, τ_{23} at the interfaces

There are two interfaces where the interlaminar stresses are critical.

1. Interface between parent laminate and adhesive.
2. Interface between patch laminate and adhesive.

The interlaminar stresses are plotted across the width of the laminate at the center as shown in Figure 6.36. The interlaminar stresses are maximum at the edge of the patch and holes.

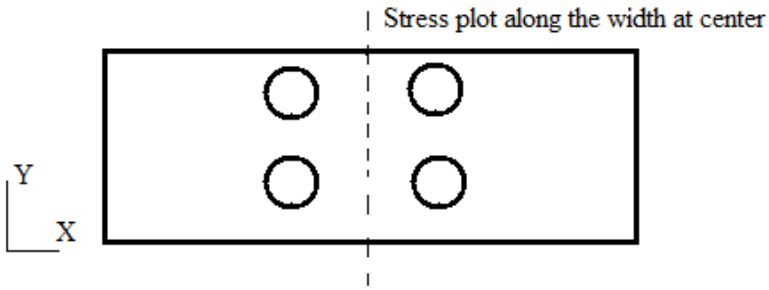

Figure 6.36 Location of stress plot along width of the laminate

The σ_3, τ_{23} distribution is along the width of the laminate at parent and adhesive interface is shown in Figures 6.37& 6.38.

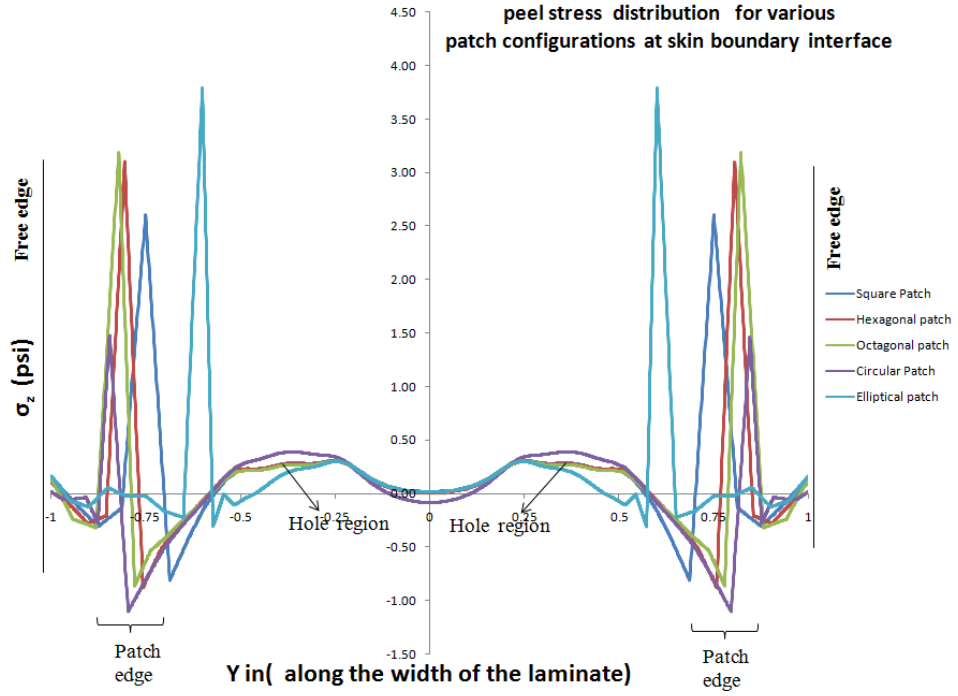

Figure 6.37 σ_3 stresses at parent laminate and adhesive interface for all patch configurations

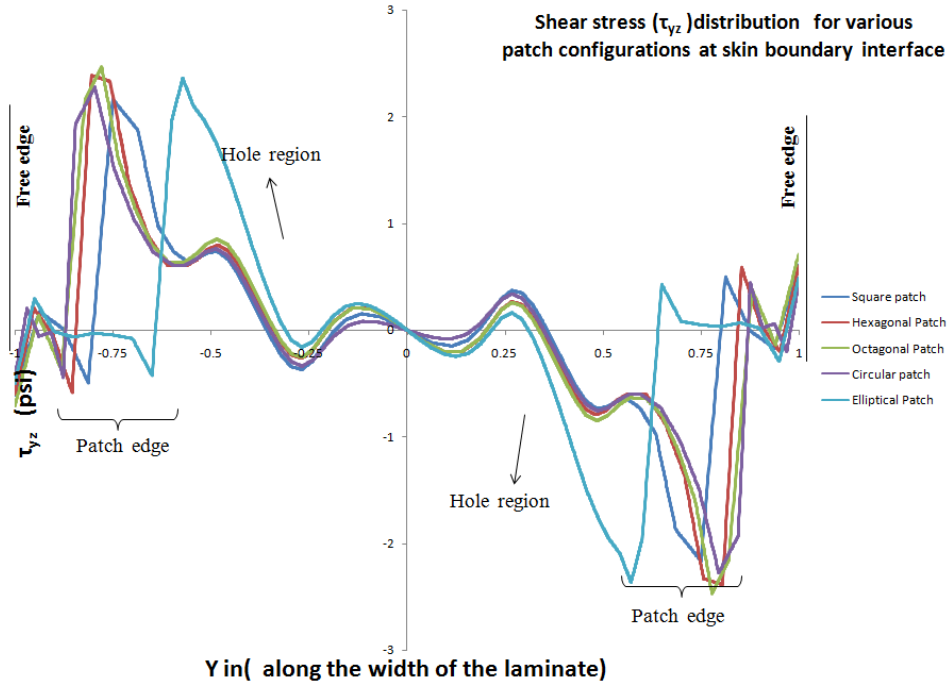

Figure 6.38 τ_{23} stresses at parent laminate and adhesive interface for all patch configurations

The σ_3, τ_{23} distribution is along the width of the laminate at patch and adhesive interface is shown in Figures 6.39 & 6.40.

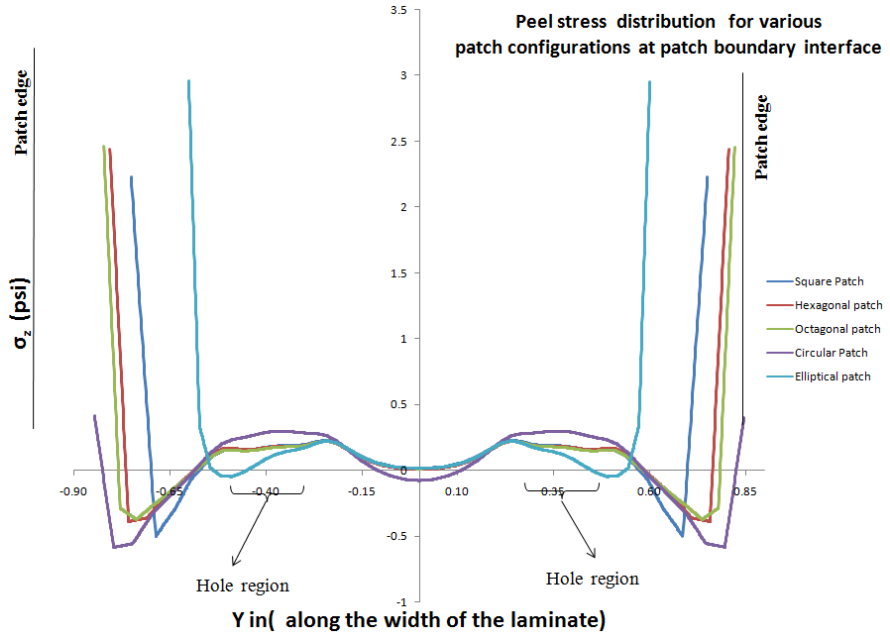

Figure 6.39 σ_3 stresses at patch laminate and adhesive interface for all patch configurations

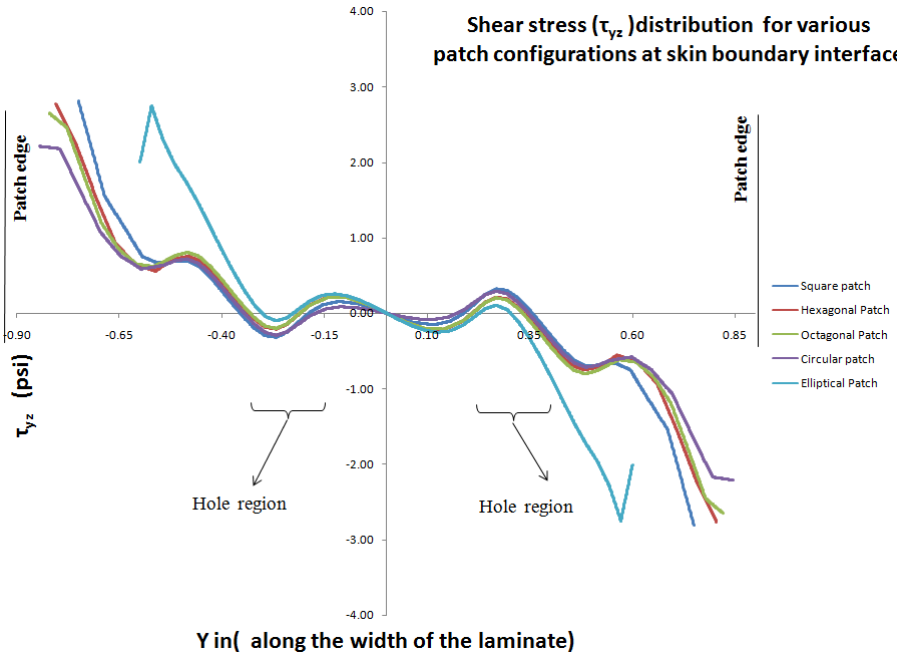

Figure 6.40 τ_{23} stresses at patch laminate and adhesive interface for all patch configurations

6.6 Effect of patch configurations with DA pattern on parent laminate

6.6.1 In-plane stresses σ_1. σ_2, τ_{12} for bottom 0^0 ply

The in-plane stress is maximum at bottom 0^0 ply in all configurations. The in-plane stresses are tabulated in Table 6.13 and comparison of normalized maximum in-plane stresses for bottom 0^0 ply for SA pattern with different patch configurations is shown in Figure 6.41.

Table 6.13 Normalized maximum stress for DA (0^0 ply -bottom) with different patch configuration

Diamond Array-0^0 ply(bottom)-Normalized in-plane stress			
Configuration	σ_1 / σ_0	σ_2 / σ_0	τ_{12} / σ_0
Without Patch	10.25	0.47	0.74
Square Patch	5.24	0.23	0.37
Hexagonal patch	5.30	0.23	0.38
Octagonal patch	4.38	0.19	0.31
Circular patch	4.38	0.19	0.31
Elliptical patch	5.58	0.24	0.40

The peak stress (σ_1) significantly decreases with all patch configurations when compared to No patch in the DA pattern. Among the Patch configurations the peak stress (σ_1) is least for octagonal and circular patch configuration.

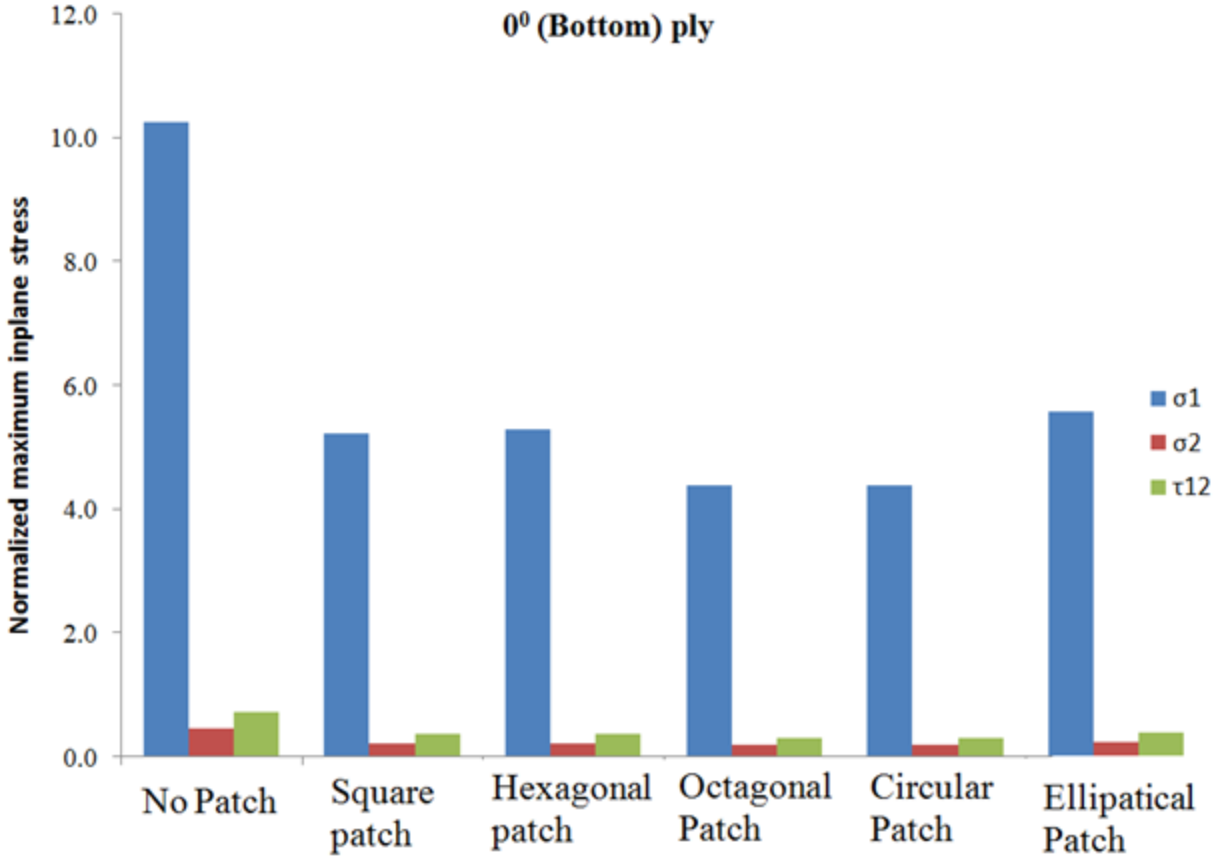

Figure 6.41 Comparison of in-plane stresses (bottom 0^0 layer) for DA pattern with different patch configurations

The stress contour for 0^0 layer with different patch configuration for DA pattern is shown in Figure 6.42,

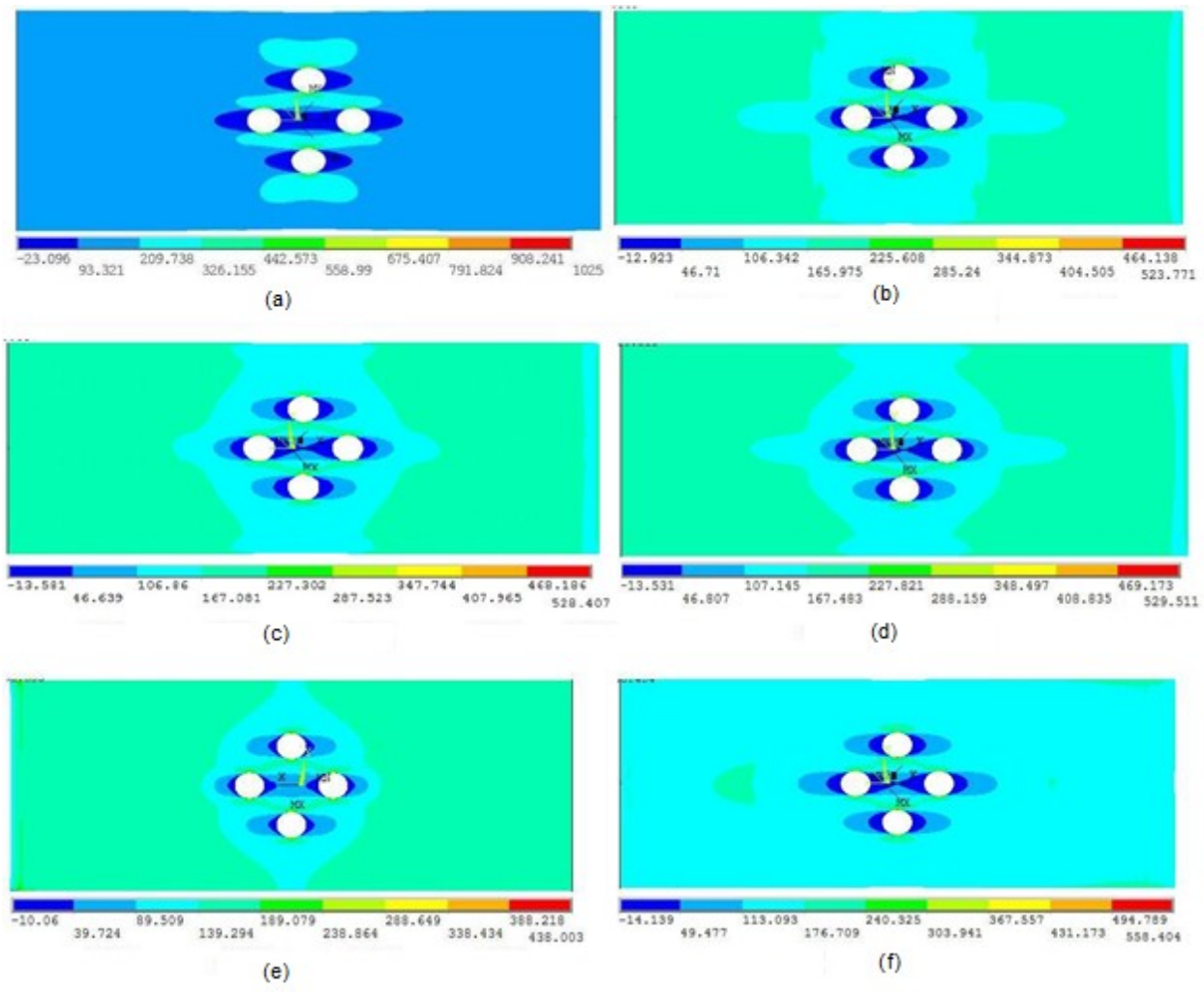

Figure 6.42 Stress contour for 0^0 layer with different patch configuration for DA pattern (a) No patch (b) Square (c) Hexagonal (d) Octagonal (e) Circular (f) Elliptical

Comparison of the stress contours of the parent laminate (45^0 layer) at the interface between parent and patch laminate for different patch configuration in DA pattern is shown in Figure 6.43,

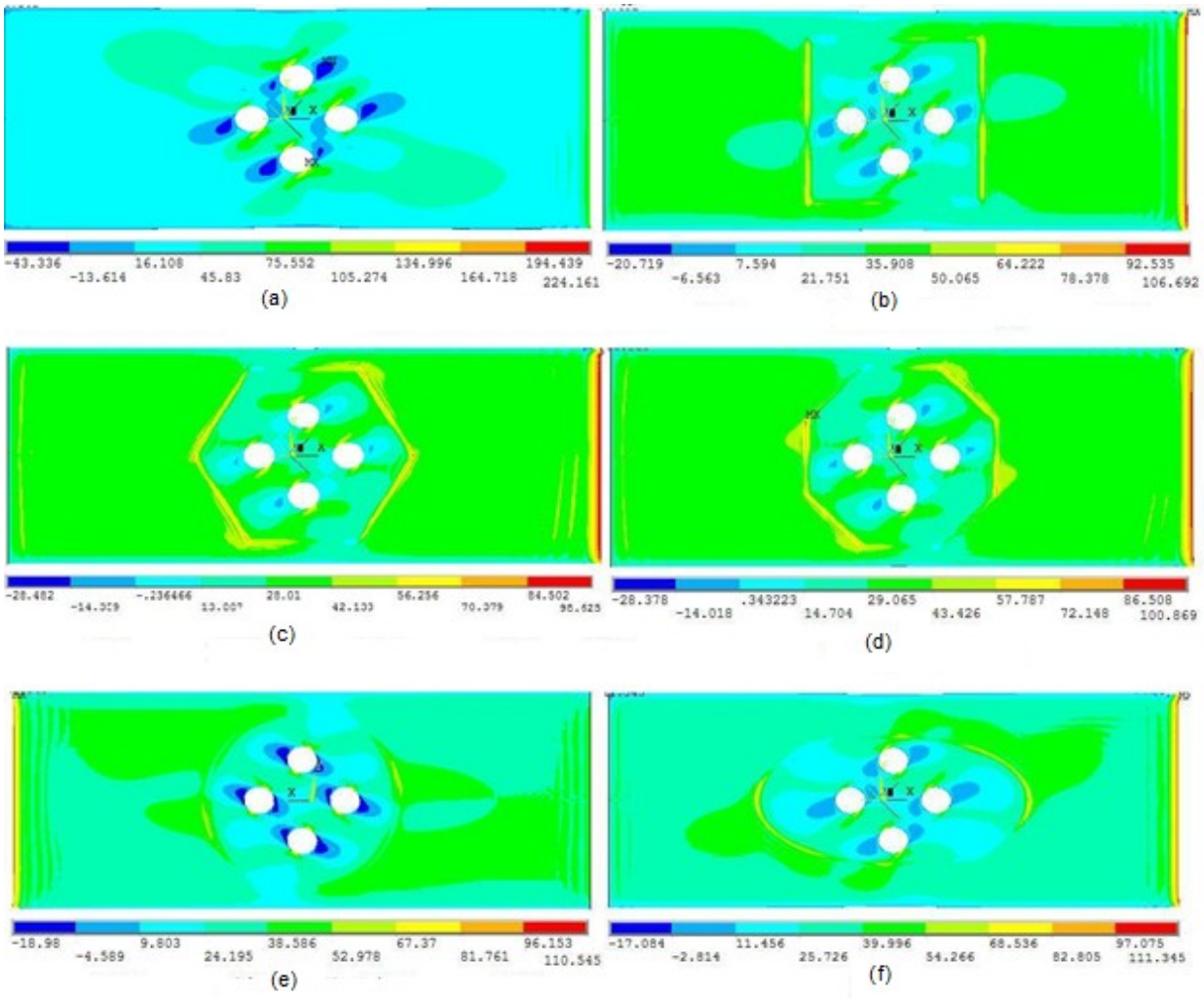

Figure 6.43 Stress contour for 45^0 layer with different patch configuration for DA pattern at parent and patch interface (a) No patch (b) Square (c) Hexagonal (d) Octagonal (e) Circular (f) Elliptical

6.6.2 In-plane stresses σ_1. σ_2, τ_{12} for bottom $+45^0$& -45^0ply

The normalized maximum in-plane stresses for $+45^0$ & -45^0 plies are tabulated in Tables 6.14 & 6.15, respectively and comparison of normalized maximum In-plane stresses for $+45^0$ & -45^0 plies for DA pattern with different patch configurations is shown in Figures 6.44 & 6.45, respectively.

Table 6.14 Normalized maximum in-plane stress for DA (45^0 ply -bottom) with different patch configurations

Diamond Array 45^0 ply(bottom)-Normalized in-plane stress			
Configuration	σ_1 / σ_0	σ_2 / σ_0	τ_{12} / σ_0
Without Patch	2.24	1.74	1.87
Square Patch	1.07	0.75	0.77
Hexagonal patch	1.01	0.74	0.76
Octagonal patch	1.11	0.72	0.66
Circular patch	1.11	0.72	0.66
Elliptical patch	1.11	0.80	0.83

Table 6.15 Normalized maximum in-plane stress for DA (-45^0 ply -bottom) with different patch configurations

Diamond Array -45^0ply(bottom)-Normalized in-plane stress			
Configuration	σ_1 / σ_0	σ_2 / σ_0	τ_{12} / σ_0
Without Patch	3.17	2.58	1.86
Square Patch	1.55	1.27	0.92
Hexagonal patch	1.56	1.26	0.92
Octagonal patch	1.41	1.25	0.93
Circular patch	1.41	1.10	0.77
Elliptical patch	1.67	1.39	0.98

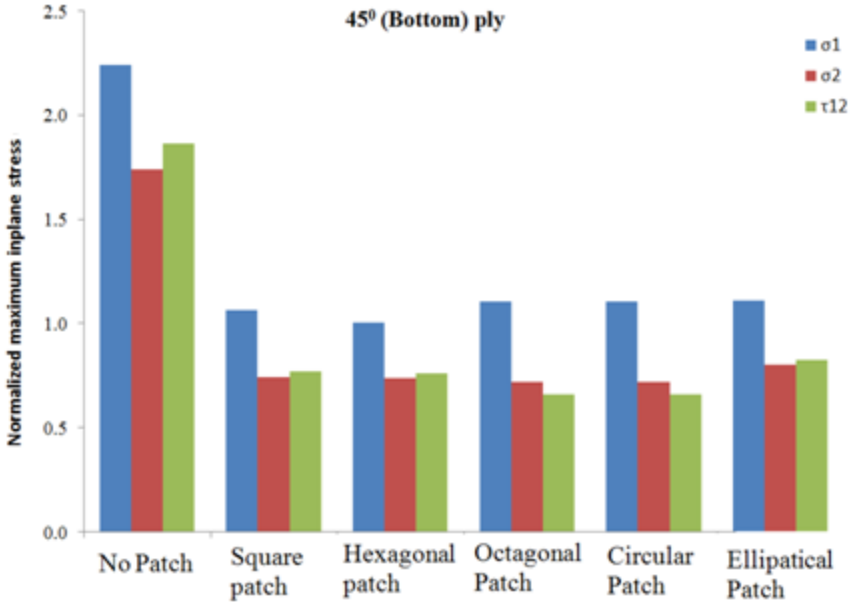

Figure 6.44 Comparison of in-plane stresses (bottom 45^0 layer) for DA pattern with different patch configurations

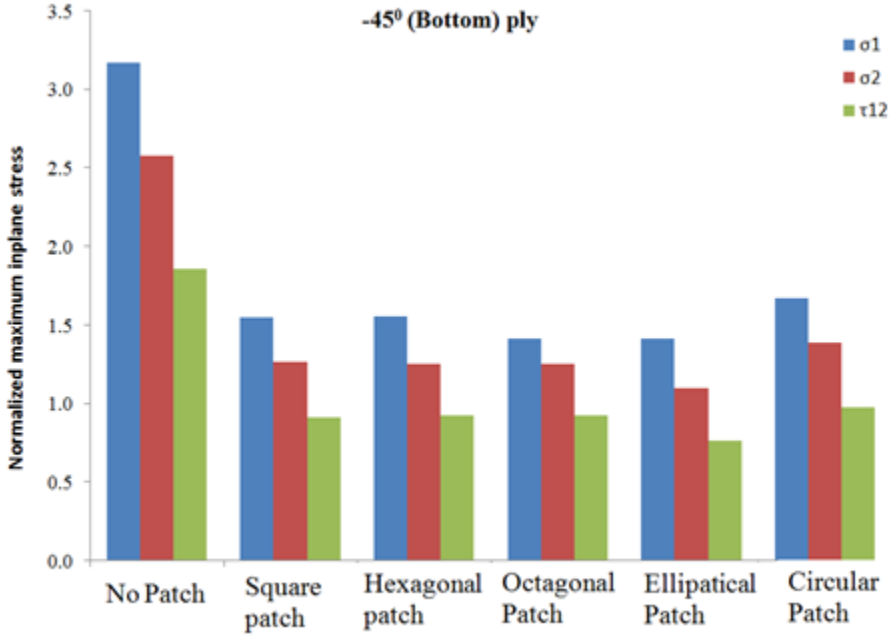

Figure 6.45 Comparison of in-plane stresses (bottom -45^0 layer) for DA pattern with different patch configurations

6.6.3 Interlaminar stresses σ_3, τ_{23} at the interfaces

There are two interfaces where the interlaminar stresses are critical.

1. Interface between parent laminate and adhesive.
2. Interface between patch laminate and adhesive.

The interlaminar stresses are plotted across the width of the laminate at the center as shown in Figure 6.46. The interlaminar stresses are maximum at the edge of the patch and holes.

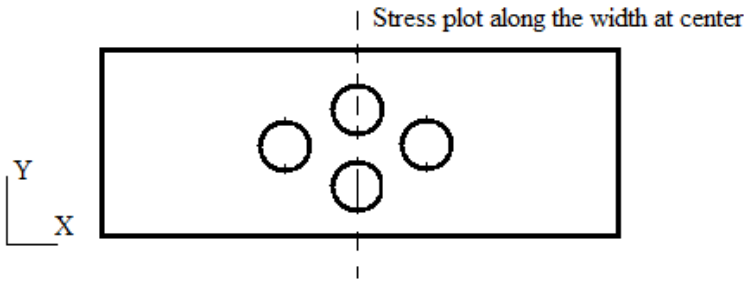

Figure 6.46 Location of stress plot along width of the laminate

The σ_3, τ_{23} distribution is along the width of the laminate at parent and adhesive interface is shown in the Figures 6.47 & 6.48.

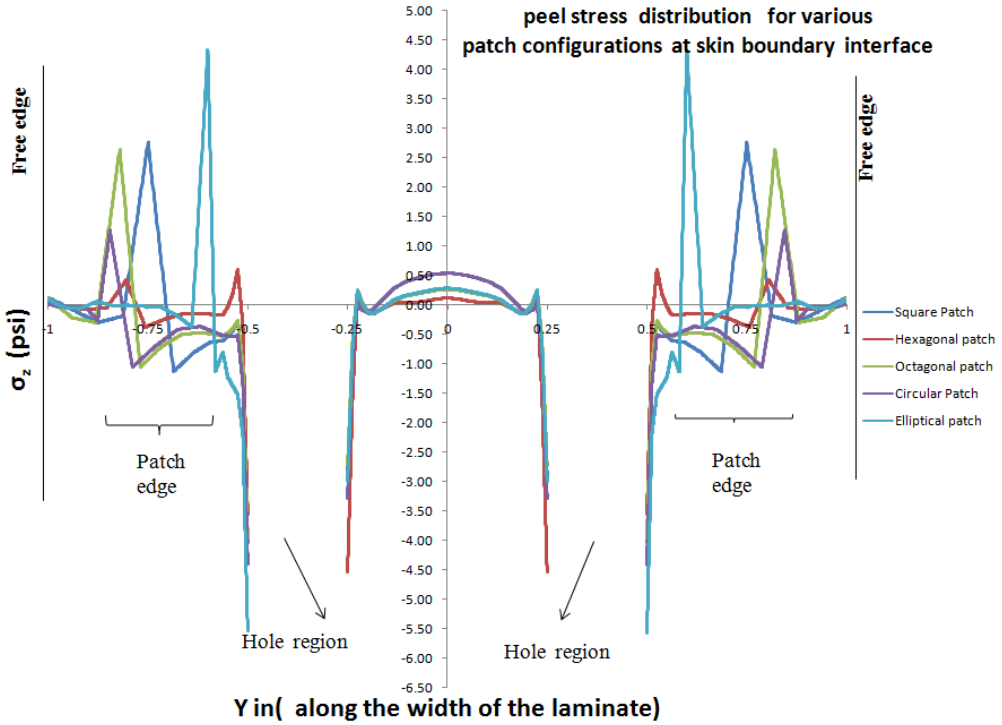

Figure 6.47 σ_3 stress at parent laminate and adhesive interface for all patch configurations

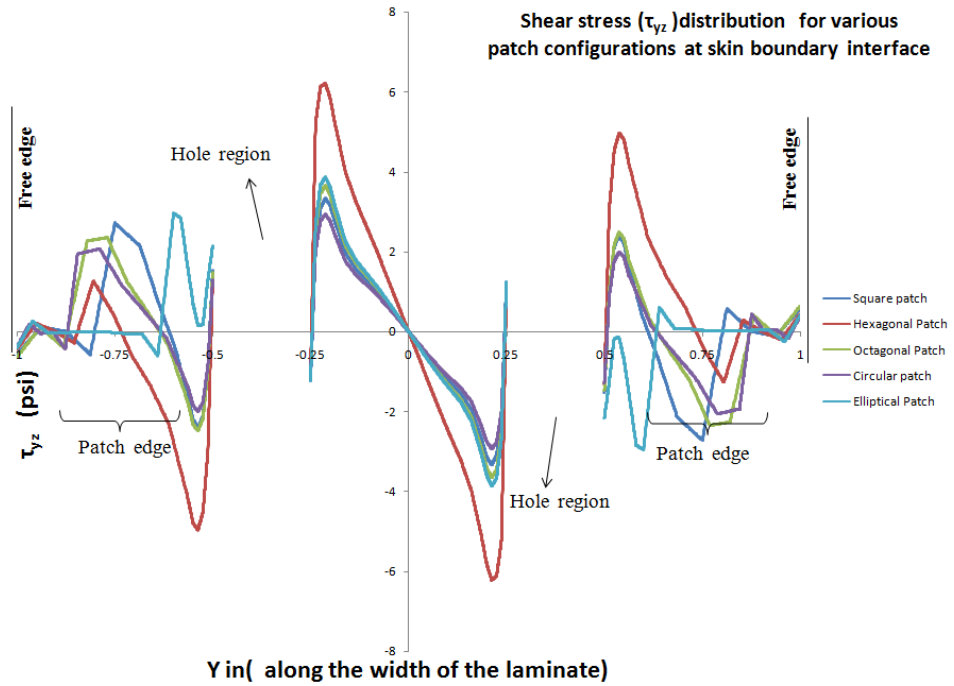

Figure 6.48 τ_{23} stress at parent laminate and adhesive interface for all patch configurations

The σ_3, τ_{23} distribution is along the width of the laminate at patch and adhesive interface is shown in Figures 6.49 & 6.50.

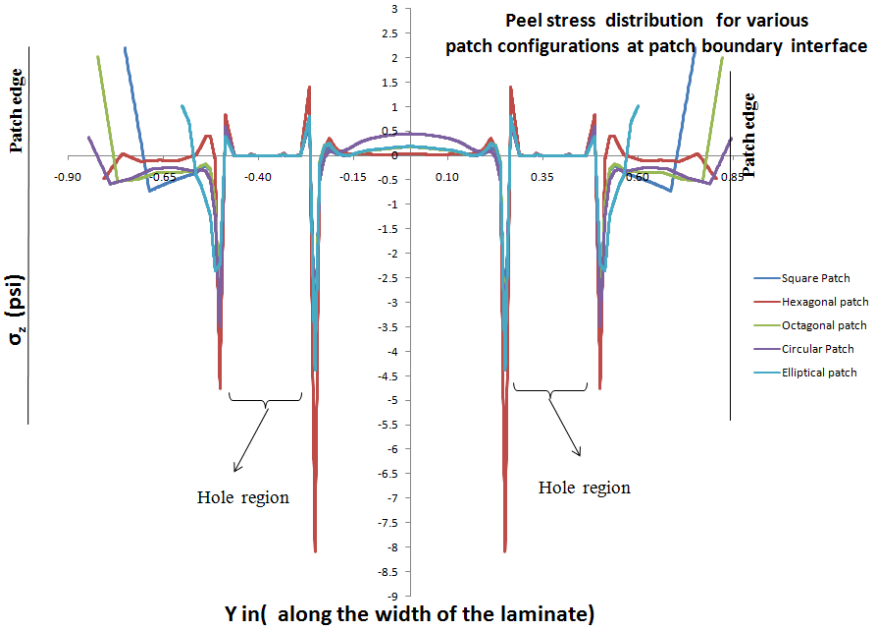

Figure 6.49 σ_3 stress at patch laminate and adhesive interface for all patch configurations

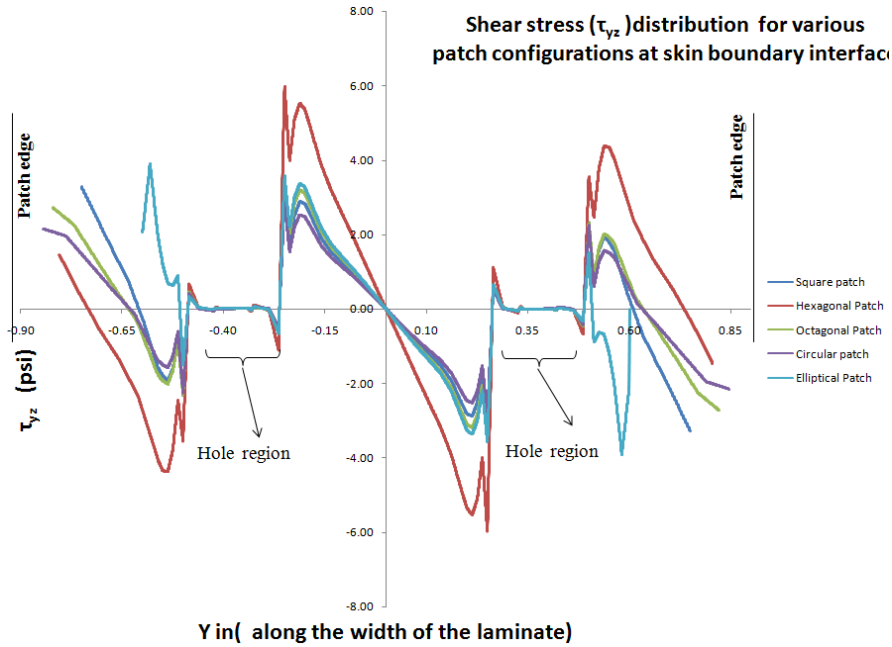

Figure 6.50 τ_{23} stress at patch laminate and adhesive interface for all patch configurations

6.7 Effect of patch configurations with FH pattern on parent laminate

6.7.1 In-plane stresses σ_1. σ_2, τ_{12} for bottom 0^0 ply

The in-plane stress is maximum at bottom 0^0 ply in all configurations. The in-plane stresses are tabulated in Table 6.16 and comparison of normalized maximum in-plane stresses for bottom 0^0 ply for FH pattern with different patch configurations is shown in Figure 6.51.

Table 6.16 Normalized maximum stress for FH (0^0 ply -bottom) with different patch configuration

FH-0^0ply(bottom)-Normalized in-plane stress			
Configuration	σ_1 / σ_0	σ_2 / σ_0	τ_{12} / σ_0
Without Patch	11.20	0.51	0.81
Square Patch	5.52	0.24	0.40
Hexagonal patch	5.67	0.25	0.41
Octagonal patch	5.69	0.25	0.41
Circular patch	4.64	0.20	0.34
Elliptical patch	5.95	0.26	0.43

The peak stress (σ_1) significantly decreases with all patch configurations when compared to No patch in the FH pattern. Among the Patch configurations the peak stress (σ_1) is least for circular patch configuration but not too significant.

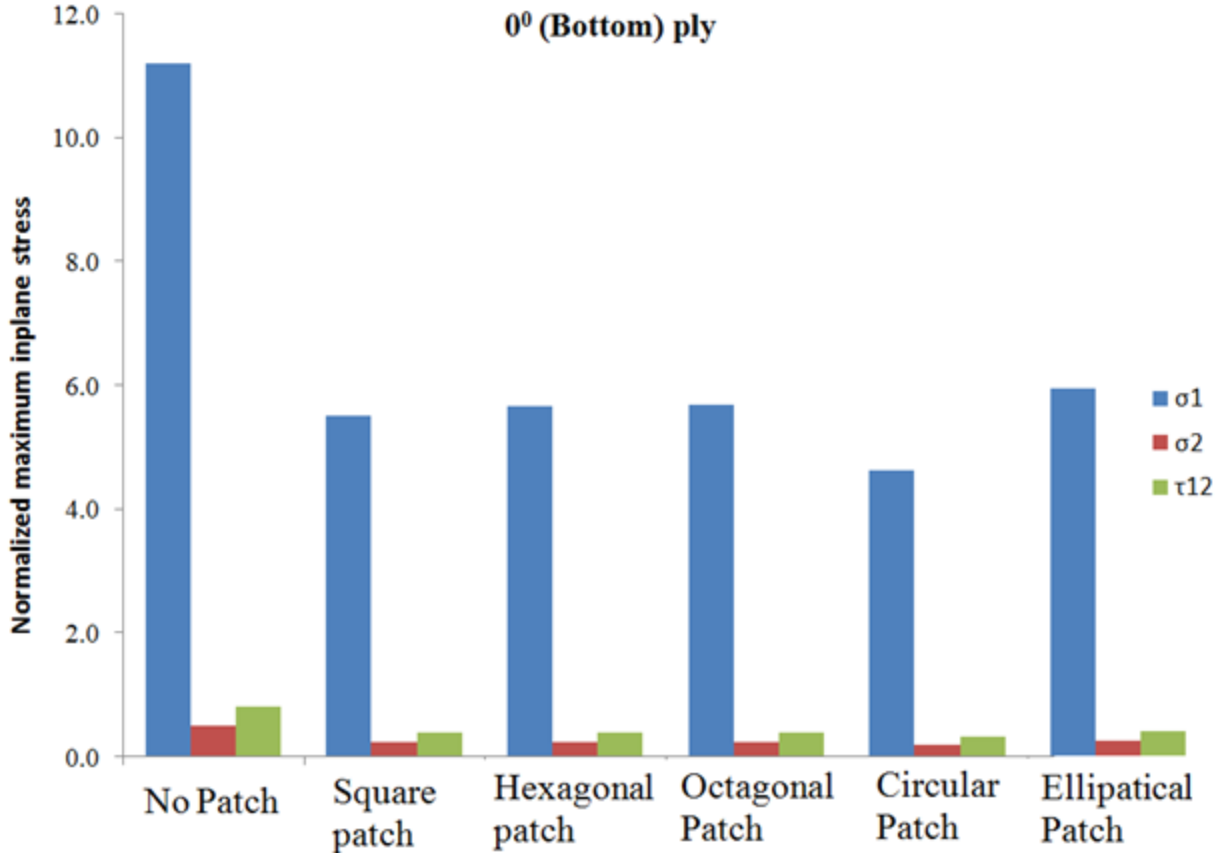

Figure 6.51 Comparison of in-plane stresses (bottom 0^0 layer) for FH pattern with different patch configurations

The stress contour for 0^0 layer with different patch configuration for FH pattern is shown in Figure 6.52,

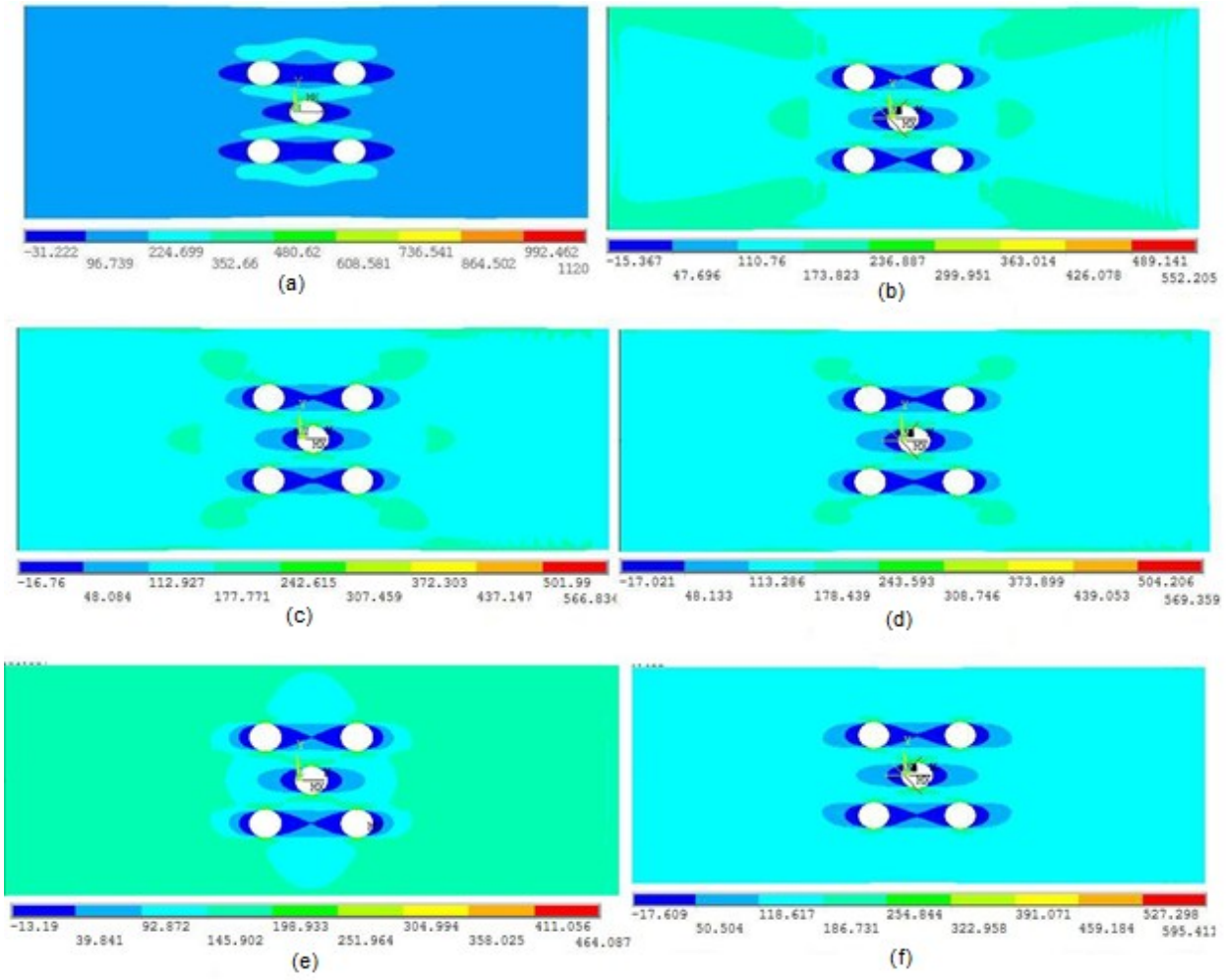

Figure 6.52 Stress contour for 0^0 layer with different patch configuration for FH pattern (a) No patch (b) Square (c) Hexagonal (d) Octagonal (e) Circular (f) Elliptical

Comparison of the stress contours of the parent laminate (45^0 layer) at the interface between parent and patch laminate for different patch configuration in FH pattern is shown in Figure 6.53,

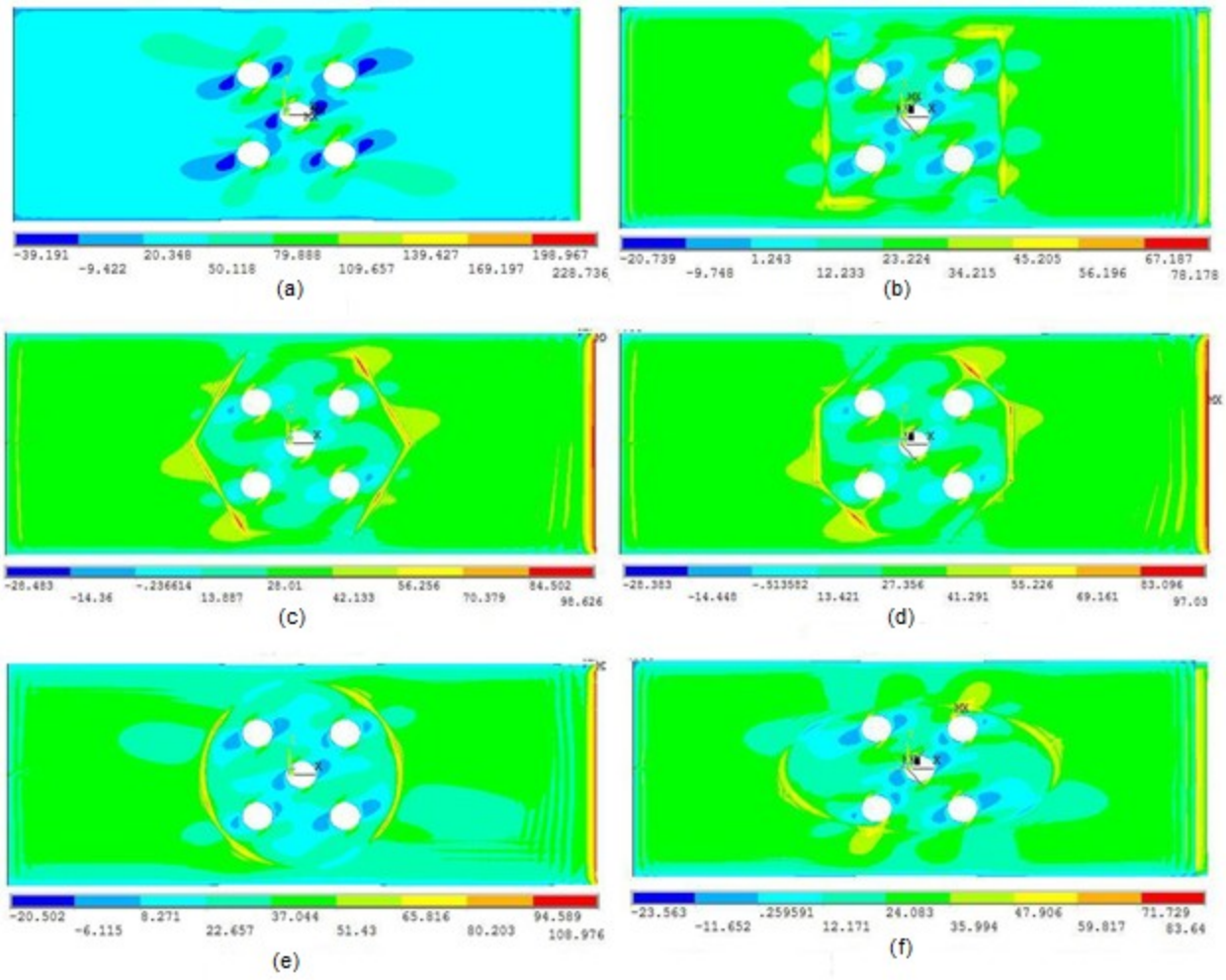

Figure 6.53 Stress contour for 45^0 layer with different patch configuration for DA pattern at parent and patch interface (a) No patch (b) Square (c) Hexagonal (d) Octagonal (e) Circular (f) Elliptical

6.7.2 In-plane stresses σ_1. σ_2, τ_{12} for bottom $+45^0$& -45^0ply

The normalized maximum in-plane stresses for $+45^0$ & -45^0 plies are tabulated in Tables 6.17 & 6.1, respectively and comparison of normalized maximum In-plane stresses for $+45^0$ & -45^0 plies for FH pattern with different patch configurations is shown in Figures 6.54 & 6.55, respectively.

Table 6.17 Normalized maximum in-plane stress for FH (45^0 ply -bottom) with different patch configurations

FH 45^0 ply(bottom)-Normalized in-plane stress			
Configuration	σ_1 / σ_0	σ_2 / σ_0	τ_{12} / σ_0
Without Patch	2.29	1.70	1.90
Square Patch	1.07	0.74	0.78
Hexagonal patch	0.99	0.74	0.79
Octagonal patch	0.97	0.74	0.79
Circular patch	1.09	0.71	0.69
Elliptical patch	1.11	0.82	0.84

Table 6.18 Normalized maximum in-plane stress for FH (-45^0 ply -bottom) with different patch configurations

FH -45^0 ply(bottom)-Normalized in-plane stress			
Configuration	σ_1 / σ_0	σ_2 / σ_0	τ_{12} / σ_0
Without Patch	3.48	2.82	2.04
Square Patch	1.64	1.32	0.97
Hexagonal patch	1.67	1.34	1.00
Octagonal patch	1.68	1.34	1.00
Circular patch	1.40	1.12	0.81
Elliptical patch	1.76	1.41	1.05

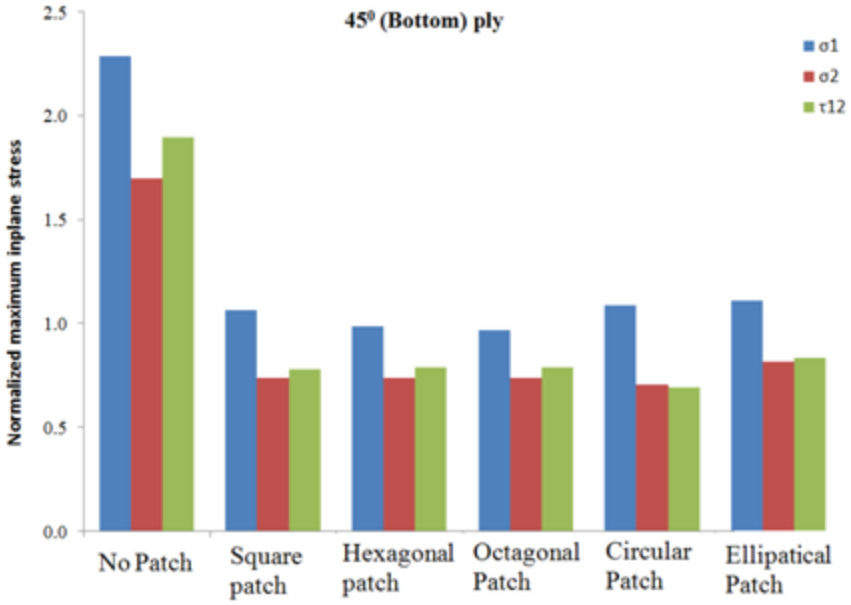

Figure 6.54 Comparison of in-plane stresses (bottom 45^0 layer) for FH pattern with different patch configurations

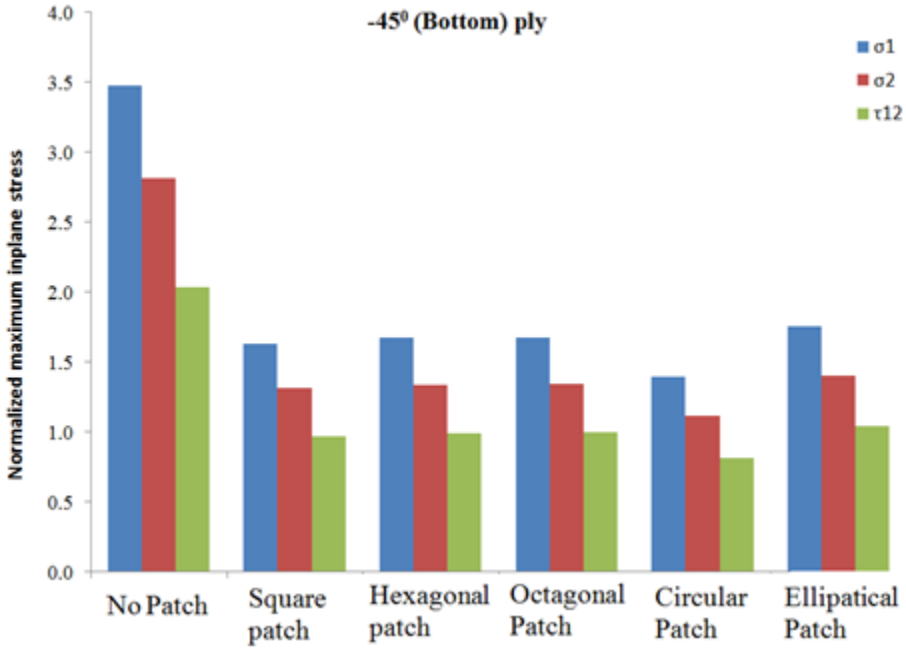

Figure 6.55 Comparison of in-plane stresses (bottom -45^0 layer) for FH pattern with different patch configurations

6.7.3 Interlaminar stresses σ_3, τ_{23} at the interfaces

There are two interfaces where the interlaminar stresses are critical.

1. Interface between parent laminate and adhesive.
2. Interface between patch laminate and adhesive.

The interlaminar stresses are plotted across the width of the laminate at the center as shown in Figure 6.56. The interlaminar stresses are maximum at the edge of the patch and holes.

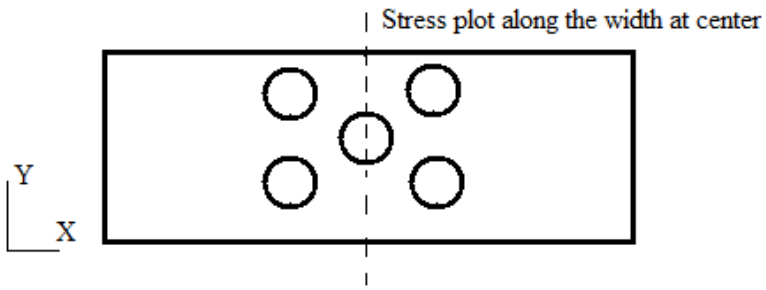

Figure 6.56 Location of stress plot along width of the laminate

The σ_3, τ_{23} distribution is along the width of the laminate at parent and adhesive interface is shown in Figures 6.57 & 6.58.

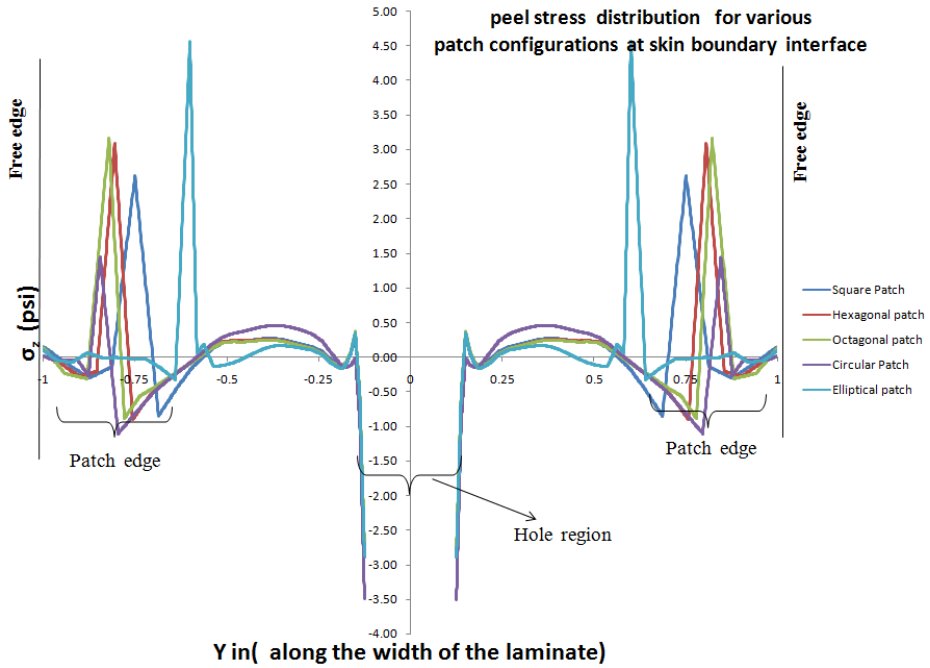

Figure 6.57 σ_3 stress at parent laminate and adhesive interface for all patch configurations

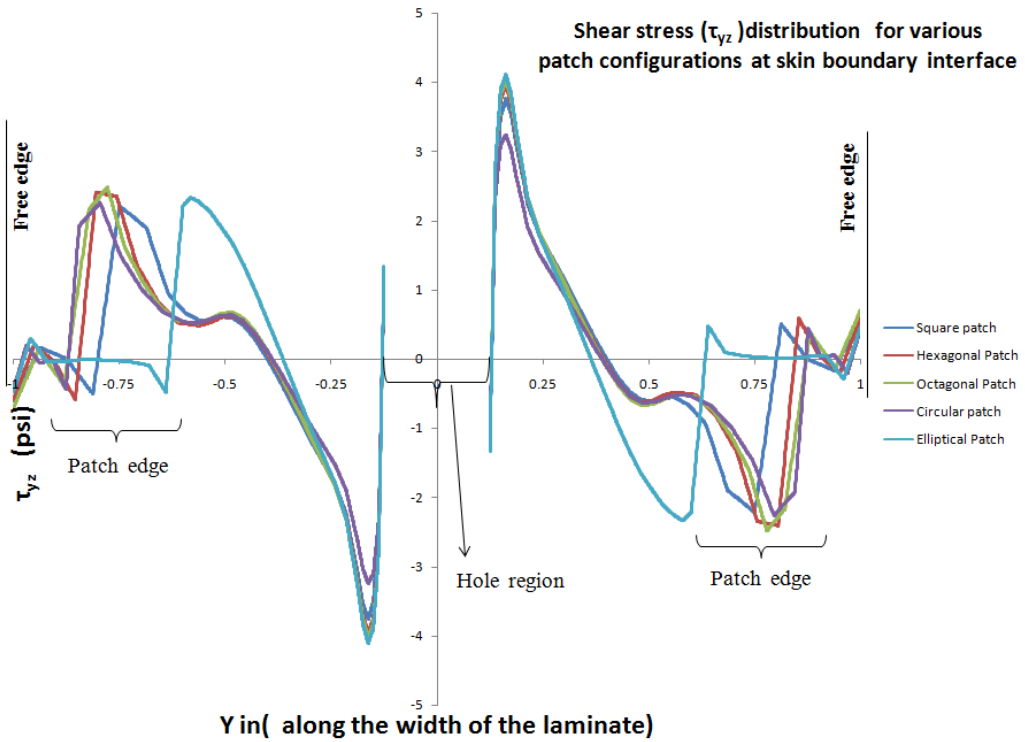

Figure 6.58 τ_{23} stress at parent laminate and adhesive interface for all patch configurations

The σ_3, τ_{23} distribution is along the width of the laminate at patch and adhesive interface is shown in Figures 6.59 & 6.60.

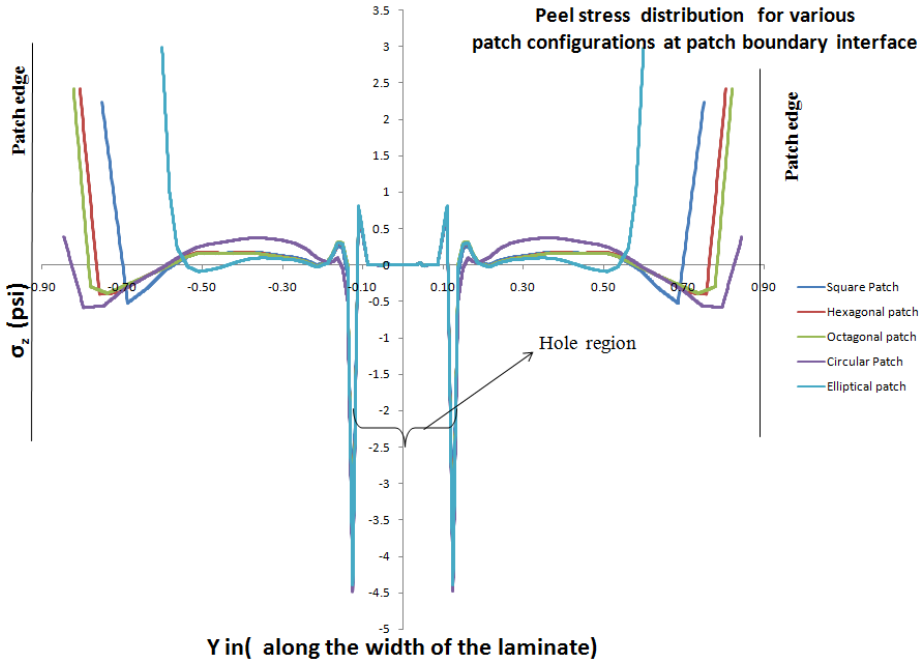

Figure 6.59 σ_3 stress at patch laminate and adhesive interface for all patch configurations

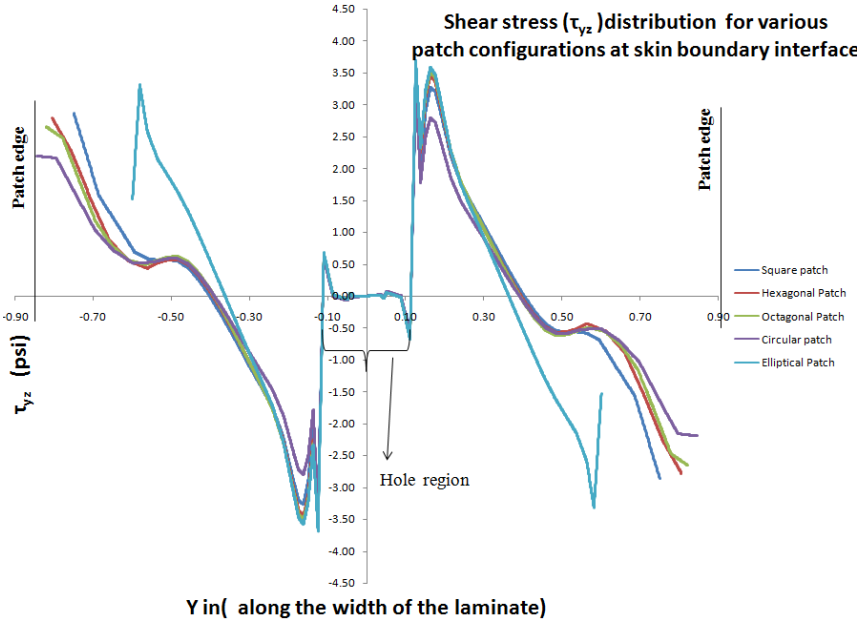

Figure 6.60 τ_{23} stress at patch laminate and adhesive interface for all patch configurations

6.8 Result summary for double patch laminate

1. Out of all configurations circular patch has the least peak stress.

2. The peak stress variation for various patch configuration with different hole patterns is shown in Figure 6.61

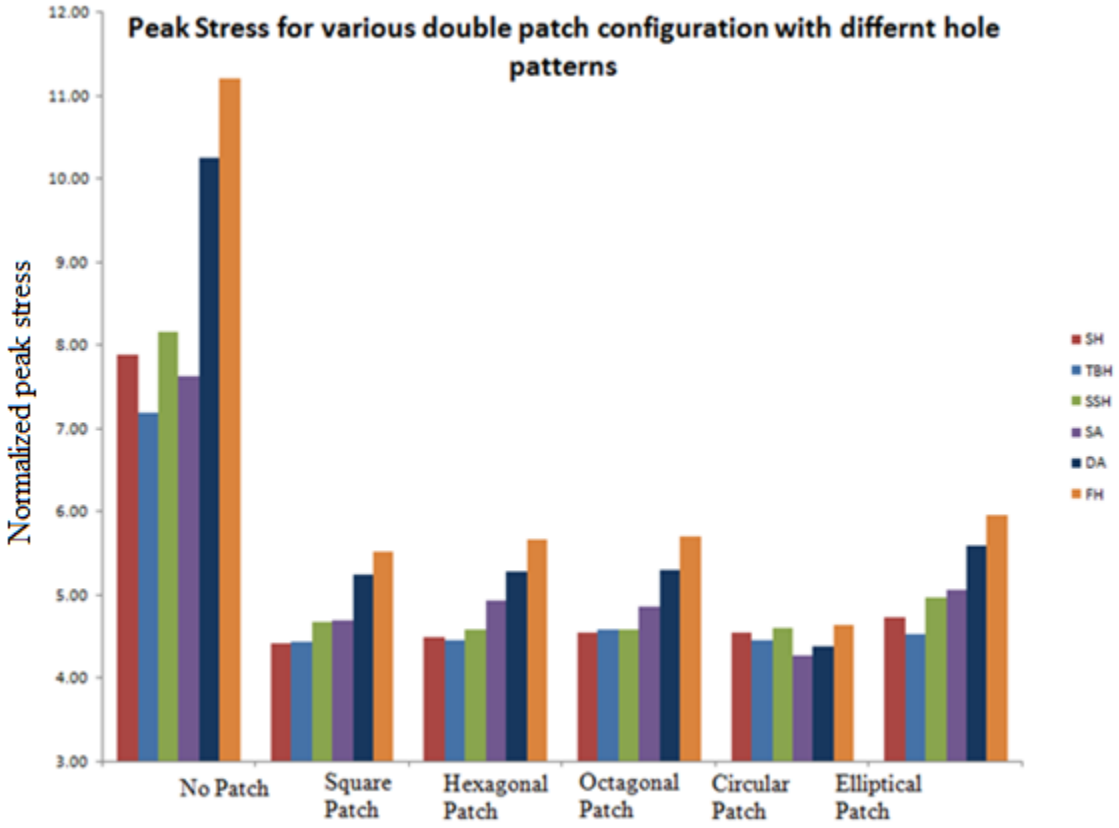

Figure 6.61 Comparison of peak stress for various configurations with different hole patterns

3. The peak stress variation for various patch configuration between single and double patch is shown in Figure 6.62

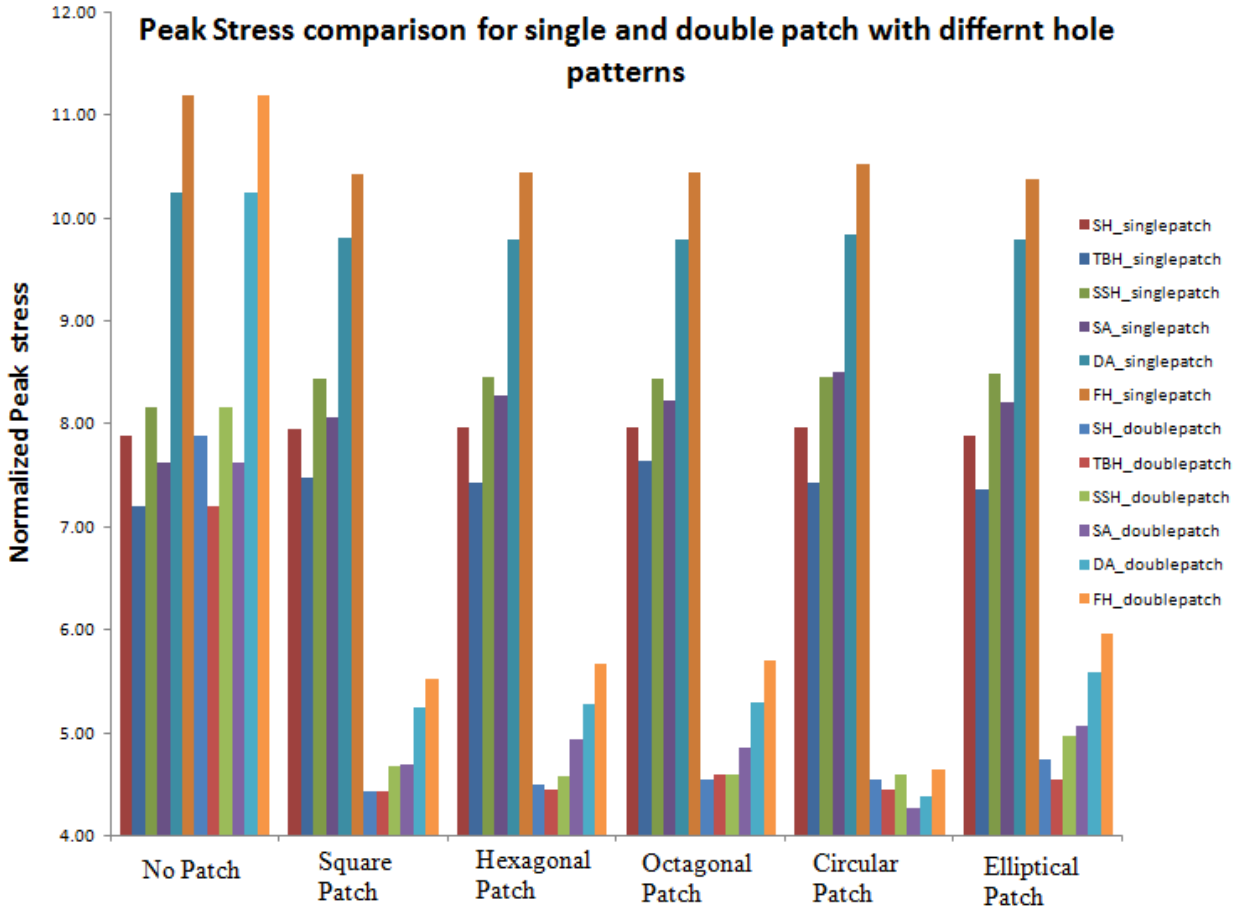

Figure 6.62 Comparison of peak stress for various configurations between single and double patch

4. The circular patch has the least peak stress among different patch configuration. The comparison of peak stresses for various patch configurations for a square array hole pattern is shown in the Figure 6.63

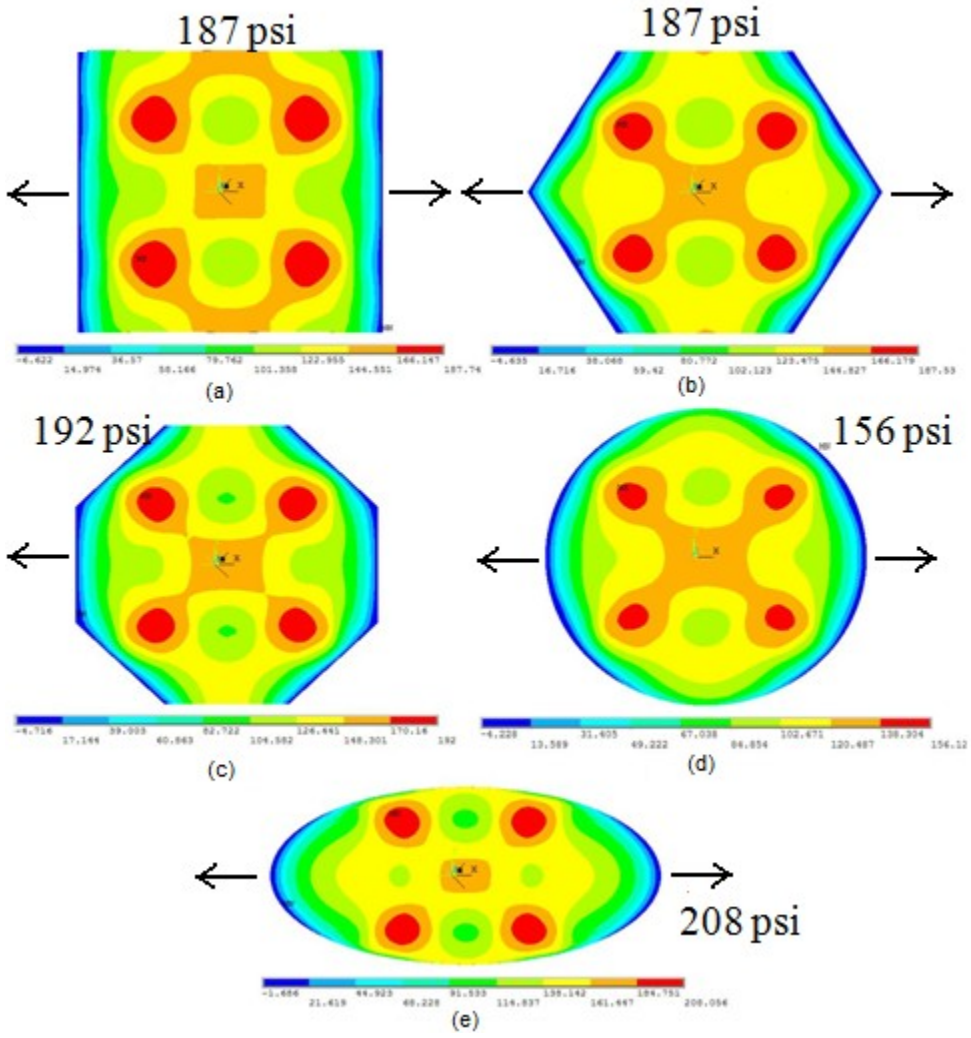

Figure 6.63 Comparison of peak stress at the patch for square array with various patch configurations (a) Square (b) Hexagonal (c) Octagonal (d) Circular (e) Elliptical

CHAPTER 7

CONCLUSION

A study is conducted to investigate the effects of multiple holes on composite laminate strength experimentally and using finite element method. The multiples holes are in analogy with the circular cutouts created on the damaged laminate during composite structural repair. The finite element study is extended to study the effects of different patch configurations on the laminates with multiple holes.

The stress concentrations occurs at the edge of the hole periphery where the fibers are tangent to the hole. The magnitude of stress concentrations in the holes depend on the arrangement of the holes in the laminate. The peak stresses at the hole with multiple hole arrangements is studied.

Two cases of the patch i.e. single and double patch on the parent laminate with different configurations of the patch is studied. The number of patches single and double and shapes of the patches play a major role in determining the peak stresses at the edge of the hole. The peak stresses for the multiple hole arrangements with patch is compared with no patch results and shape of the patch which gives least peak stress is determined.

Among the different patch configuration, the circular patch bonded on the both sides of the laminate exhibited the lowest peak stress. This study contributes to a better understanding in selecting patch configurations or geometries for both composite bonded repairs in order to restore the laminates structural integrity.

Thus from the results we can conclude that,

For a parent laminate without any patch,

- The peak stress occurs at the periphery of the hole in 0^0 ply.
- The arrangement of holes in the laminate plays a significant role is determining the peak stresses.
- Among the different hole pattern laminates without patch, the peak stress of 0^0 ply is

- obtained in the following order TBH (Top and bottom hole) > SH (singlehole) >SA (squared array) > SSH (side-by-side hole)> DA (Diamond array) > FH (five holes). This sequence is in agreement with the test indication where the TBH has the highest strength and FH has the least strength.

For a parent laminate with single patch,

- The peak stresses occur at the periphery of the hole in bottom 0^0 ply of the parent laminate.
- When having a single patch on the parent laminate an additional bending moment is created with the axial load applied due to the eccentricity of the single patch.
- Irrespective to the shape of the patch configuration the peak stresses for Single hole, Top & Bottom hole, Side by Side hole & Square array increases with single patch in comparison with no patch. This is due to prominent effect of additional bending moment caused by the eccentricity of single patch.
- For the Diamond array and Five hole with single patch the peak stress decrease in comparison with no patch. This is because of the prominent interaction of the between the holes in these hole patterns.
- An insignificant effect due to different patch configurations is observed for laminate with a single patch.

For a parent laminate with double patch,

- By having a double patch the additional moments caused by the patches are nullified.
- The peak stresses reduces significantly for all the multiple hole patterns when compared to single patch and no patch cases.
- Of all the different patch configurations circular patch has the least peak stress.

REFERENCES

1. Tomblin J. S., Salah L. , Welch J. M., and Borgma. M. D., “Bonded repair of aircraft composite sandwich structures”, DOT/FAA/AR-03/74, Office of Aviation Research, Washington, D.C. 20591

2. Reis C.A., “Composite repair structure process”, US patent 6174392 B1

3. Composite Repair, Hexcel Composites, Duxford, April 1999, Publication No. UTC 102

4. Fan, W. and Wu, J.,” Stress concentration of a laminate weakened by multiple holes”, Journal of composite structures, Vol. 10, No. 4, 1998, pp303-319.

5. Lekhnitskii, S.G., Anisotropic Plates (translated from second Russian edition by Tsai, S.W. and Cheron, T.) Gordon and Breach Science Publishers, New York, 1968.

6. Ochoa,O.O. and Reddy, J.N., Finite Element Analysis of Composite Laminate, Kluwer Academic Publishers, Netherlands,1992.

7. Xu X.W. , Man H.C., Yue T.M., “Strength prediction of composite laminates with multiple elliptical holes”, International Journal of Solids and Structures 37 (2000) 2887-2900

8. Neelkanthan, H., Shah, D.K. and Chan, W.S., “Effect of stiffener around multiple loaded holes in composite shear panel”, American Institute of Aeronautics and Astronautics, Inc., 38th SDM Conference, 1997.

9. Vendhagiri S. and Chan, W.S., ”Analysis of composite bolted/bonded joints used in repairing”, Journal of composite materials, Vol.35, No.12, 2001, pp 1049-1061.

10. Kheradiya, M., “Stress Concentration of Finite Width Laminated Composite with multiple Holes”, Master Thesis, The University of Texas at Arlington, 2008.

11. SameerH.amoush, Kunigal S., Feras D., Matthew S. and Paul S. “Defective Repairs of Laminated Solid Composites”, Journal of Composite Materials 2005; 39; 2185 originally published online Jun 17, 2005;

12) ANSYS 10.0 software help files.

BIOGRAPHICAL INFORMATION

Sakthivel.S is a MS student from department of Mechanical and Aerospace engineering. His thesis advisor is Dr Wen Chan. He has completed his Bachelor of technology in Aeronautical Engineering from India in may 2005 and worked as an Analysis engineer in a service industry from Feb. 2008-Jul. 2008. Then he came to UTA for MS in Aerospace Engineering in Aug 2008. His thesis work is on composite repair which is a sponsored project from Boeing at Seattle, Washington.